

UNIVERSITY OF SÃO PAULO
SCHOOL OF ANIMAL SCIENCE AND FOOD ENGINEERING

THAIS CARVALHO BRITO OLIVEIRA

**Effect of the incorporation of galactomannans and solid lipid particles stabilized with
different surfactants in the properties and stability of cold-set gels**

Pirassununga

2021

THAIS CARVALHO BRITO OLIVEIRA

Effect of the incorporation of galactomannans and solid lipid particles stabilized with different surfactants in the properties and stability of cold-set gels

CORRECTED VERSION

Thesis presented to the School of Animal Science and Food Engineering, University of São Paulo, as part of the requirements for obtaining the title of Doctor of Science in the Graduate Program in Food Engineering.

Concentration area: Food Engineering Sciences.

Advisor: Prof Dr Samantha Cristina de Pinho

Joint Advisor: Prof Dr Izabel Cristina Freitas Moraes

Pirassununga

2021

Ficha catalográfica elaborada pelo
Serviço de Biblioteca e Informação, FZEA/USP, com
os dados fornecidos pelo(a) autor(a)

Brito-Oliveira, Thais Carvalho

B862e Effect of the incorporation of galactomannans and
solid lipid particles stabilized with different
surfactants in the properties and stability of cold-set
gels

 / Thais Carvalho Brito-Oliveira; orientadora Samantha
Cristina Pinho; coorientadora Izabel Cristina Freitas
Moraes. -- Pirassununga, 2021.

 227 f.

 Tese (Doutorado - Programa de Pós-Graduação em
Engenharia de Alimentos) -- Faculdade de Zootecnia e
Engenharia de Alimentos, Universidade de São Paulo.

 1. Soy protein isolate. 2. Cold-set gelation. 3.
Emulsion-filled gels. 4. Galactomannans. 5. Stability. I.
Pinho, Samantha Cristina, orient. II. Moraes, Izabel
Cristina Freitas, coorient. III. Título.

Data da aprovação: 24/06/2021

Banca Examinadora:

Profª. Drª. Samantha Cristina de Pinho

Instituição: Faculdade de Zootecnia e Engenharia de Alimentos (FZEA/USP)

Presidente da Banca Examinadora

Prof. Dr. Angelo Luiz Fazani Cavallieri

Instituição: Universidade Federal de São Carlos (UFSCar)

Drª Andresa Gomes Brunassi

Instituição: Faculdade de Zootecnia e Engenharia de Alimentos (FZEA/USP)

Profª Drª Carolina Siqueira Franco Picone

Instituição: Universidade Estadual de Campinas (Unicamp)

Profª Drª Flávia Maria Netto

Instituição: Universidade Estadual de Campinas (Unicamp)

Profª Drª Vânia Regina Nicoletti

Instituição: Universidade Estadual Paulista (Unesp)

To my parents ... who showed me the way and conducted me through the whole process.

To my husband Welton ... who gave me the courage to start.

To my brothers ... who gave me the necessary lightness of mind to continue.

And, especially, to my children, Theo, Maria Antônia and Lara, who have been teaching me more about life than anyone. Here is my greatest legacy: my love for science, study, and knowledge.

You guys are, and always will be, my life!

ACKNOWLEDGEMENTS

I am extremely grateful...

To God for all the guidance throughout the hole way that led me to this moment.

To my advisor and great friend Dr Samantha Pinho, who teached me so much during these ten years... in which we shared much more than only work! Thank you so much for all the support and understanding during the construction of my being as a "mother-researcher". It has been great to count on you for everything!

To my parents, Elaine and Brito! This PhD title is also yours. I would NEVER be able to finish this research if it was not for your daily dedication and love for Theo and, consequently, for me. You guys not only encouraged me, gave me the necessary freedom and all the tools to get here, but also walked with me, step by step, up to this point. You both are my strength and my certainty that I will always have someone to count on and someone to return to. I love you with all my heart!

To my husband Welton... for all the respect and incentive so that I could always chase my dreams. Thank you for, even at the times when you could not exactly understand my love and my dedication for this research, you never said one word of discouragement! Thank you for every "yes" you said to me thoroughout this process! Thank you for all the love! Thank you for keeping my wings, so I could fly and get to this point! I love you!

To my son, Theo, who totally took me out of control of my life and my own time, during this PhD, and taught me that this is the best way to live! Thank you, son, for your infinite and unconditional love!

To my brothers, Guilherme, Rafael e Gustavo... you guys were, are and always will be the lightness that I need to keep living, to keep pursuing my dreams and to keep facing challenges!

To the professionals Marcelo Thomazini, Carla Mônaco Lourenço, Ana Mônica Quinta Barbosa Bittante and Rodrigo Lourenço, for their help with the tests carried out at USP / FZEA; to Adriane Cristina Sarti Sprogis for technical assistance with the analysis of scanning electron

microscopy at Unicamp; to all INFABIC/Unicamp professionals who assisted with the laser scanning confocal microscopy assays.

To my good friend Letícia Ferreira, who helped me with sample preparation for microscopy tests during my pregnancy. Lê, your partnership was fundamental to the progress of this project.

To all my friends at LENALIS, and especially to my longtime partners, Nayla, Matheus, Marlucci and Letícia, who started and finished this PhD by my side.

To Camila S. Cazado, Ana Clara M. Cavini and Lorena M.F. Santos who helped me a lot with different experimental parts of this project.

To São Paulo Research Foundation (FAPESP) for the PhD scholarship (FAPESP grant 2017/06224-9) and also to Coordenação de Aperfeiçoamento de Pessoal de Nível Superior (Capes) for all the support to the graduate program.

To all those whom, directly or indirectly, have contributed to my professional or personal growth over these years.

“Human science in no way denies the existence of God. When I consider how many and how wonderful things a man understands, does research and manages to accomplish, then I clearly recognize that the human spirit is the work of God, and the most remarkable.” – Galileu Galilei.

RESUMO

BRITO-OLIVEIRA, T.C. **Efeito da incorporação de galactomananas e partículas lipídicas sólidas estabilizadas com diferentes tensoativos nas propriedades e na estabilidade de géis proteicos obtidos a frio.** 2021. 227 f. Tese (Doutorado) – Faculdade de Zootecnia e Engenharia de Alimentos, Universidade de São Paulo, Pirassununga, 2021.

Géis carregados com emulsão (GC) são sistemas cujas propriedades dependem das características das interações entre as gotículas/partículas lipídicas dispersas e a rede gelificada. Tal rede é geralmente produzida com ingredientes proteicos, como o isolado proteico de soja (IPS), capaz de formar géis a frio. Embora a gelificação a frio de IPS seja abordada na literatura, os estudos raramente utilizam IPS comerciais. Tais isolados proteicos tendem a apresentar características desafiadoras, que podem ser melhoradas a partir da incorporação de polissacarídeos aos sistemas. Nesse contexto, e considerando o interesse da indústria no desenvolvimento de géis com diferentes propriedades, a presente tese de Doutorado teve como principal objetivo investigar o efeito da incorporação de galactomananas (goma locusta - GL e goma guar - GG) e de partículas lipídicas sólidas (PLS) estabilizadas com diferentes tensoativos (isolado proteico de soro de leite – IPSL - e tween 80/span 80), nas propriedades reológicas e estruturais de géis de IPS obtidos a frio, a partir da adição de diferentes sais (CaCl_2 e NaCl), bem como a avaliação da estabilidade físico-química dos sistemas. Para isso, inicialmente, géis com diferentes concentrações de IPS foram produzidos a frio, pela incorporação de diferentes concentrações de CaCl_2 e NaCl , e avaliados quanto aos aspectos visuais, capacidades de retenção de água (CRA) e propriedades reológicas. Verificou-se que o tipo de sal influenciou nas propriedades dos géis, possivelmente devido às ações distintas dos íons no processo de gelificação. A partir dos resultados obtidos, as formulações G_{CaCl_2} (14% IPS, 100 mM CaCl_2) e G_{NaCl} (14% IPS, 300 mM NaCl) foram selecionadas para a produção de géis biopoliméricos mistos, por apresentarem propriedades reológicas e CRA superiores às demais. Assim, diferentes concentrações (0,1 – 0,3%, m/v) de GL e GG foram incorporadas aos géis, que também foram caracterizados. Os resultados revelaram que as incorporações dos polissacarídeos tiveram efeitos distintos nas propriedades dos géis, dependendo do tipo de sal e das características das galactomananas, que influenciaram na extensão do *demixing* nos sistemas. Tal extensão, por sua vez, teve grande efeito nas interações proteína-proteína e, conseqüentemente, nas propriedades reológicas dos géis. Os resultados obtidos permitiram, então, a seleção de duas formulações para a produção de GC: $G_{\text{NaCl}}^{\text{GL}}$ (14% IPS, 300 mM NaCl , 0,1% GL) e $G_{\text{CaCl}_2}^{\text{GL}}$ (14% IPS, 100 mM CaCl_2 , 0,1% GL). PLS estabilizadas com IPSL mostraram-se ativas nos sistemas, que apresentaram aspecto de gel sustentável forte antes da incorporação de sais. Já os GC produzidos com PLS estabilizadas com Tween 80/Span 80, só foram formados após a incorporação de sais. Tais PLS reduziram a força dos géis, porém aumentaram a estabilidade dos sistemas, que puderam ser adequadamente caracterizados durante 20 dias para GC produzidos com CaCl_2 e 30 dias para amostras produzidas com NaCl . GC produzidos com NaCl puderam ser adequadamente utilizados para a encapsulação de beta-caroteno. Em comparação a dispersões de PLS, GC apresentaram uma capacidade superior de proteger o carotenóide, mostrando-se uma alternativa interessante para a indústria para o desenvolvimento de novos alimentos *plant-based* funcionais, com uma textura diferenciada e uma estabilidade satisfatória.

Palavras-chave: Isolado proteico de soja; Gelificação a frio; Géis carregados com emulsões; Galactomananas; Estabilidade.

ABSTRACT

BRITO-OLIVEIRA, T.C. **Effect of the incorporation of galactomannans and solid lipid particles stabilized with different surfactants in the properties and stability of cold-set gels.** 2021. 227 f. Thesis (PhD) – School of Animal Science and Food Engineering, University of São Paulo, Pirassununga, 2021.

Emulsion-filled gels (EFG) are complex systems that present properties highly dependent on the characteristics of the interactions among the dispersed lipid droplets/particles and the gelled network. This network is usually produced with protein ingredients, such as soy protein isolate (SPI), capable of forming cold-set gels. Although studies regarding cold-set gelation of SPI are already found in the literature, they commercial isolates are rarely used. Such ingredients present challenging characteristics, which can be mitigated by the incorporation of polysaccharides to the gels. In this context, and considering the interest of the food industry in the development of gels with different properties, the present PhD thesis aimed to investigate of the effects of incorporating galactomannans (locust bean gum - LBG and gum guar - GG) and solid lipid particles (SLP) stabilized with different surfactants (whey protein isolate - WPI - and tween 80/span 80), in the rheological and microstructural properties of cold-set SPI gels, produced using different salts (CaCl_2 and NaCl), as well as assessing their stability. For this purpose, gels with different concentrations of SPI were produced, by incorporating different concentrations of CaCl_2 and NaCl , and they were evaluated regarding visual aspects, water holding capacities (WHC) and rheological properties. It was found the type of salt affected the properties of the gels, possibly due to the different actions of the ions in the gelation process. From the obtained results, the formulations G_{CaCl_2} (14% SPI, 100 mM CaCl_2) and G_{NaCl} (14% SPI, 300 mM NaCl) were selected to produce mixed gels, as they presented better rheological properties and WHC. Therefore, different concentrations (0.1 – 0.3%, w/v) of LBG and GG were incorporated to the gels, which were also characterized. The incorporations of polysaccharides had distinct effects on the gels' properties, depending on the type of salt and the characteristics of the galactomannans, which influenced on the degree of demixing. Such degree had a significant effect over the protein-protein interactions and, therefore, over the rheological properties of the gels. From the obtained results, two formulations were selected for the production of EFG: $G_{\text{NaCl}}^{\text{LBG}}$ (14% SPI, 300 mM NaCl , 0.1% LBG) and $G_{\text{CaCl}_2}^{\text{LBG}}$ (14% SPI, 100 mM CaCl_2 , 0.1% LBG). SLP stabilized with WPI were active within the systems, which presented aspect of self-supported gels before salt addition. EFG produced with SLP stabilized by Tween 80/Span 80, on the other hand, were only formed after salt incorporation. Such SLP decreased the gels' strength, however, increased the stability of the systems, that could be adequately characterized during 20 days for CaCl_2 -induced EFG and 30 days for NaCl -induced ones. NaCl -induced EFGs were, then, satisfactorily used for encapsulating beta-carotene. In comparison to SLP dispersions, EFG presented a superior ability to protect the carotenoid and it is, therefore, an interesting alternative for the development of new functional plant-based foods, with a unique texture and stability.

Keywords: Soy protein isolate; Cold-set gelation; Emulsion-filled gels; Galactomannans; Stability.

LIST OF TABLES

Table 3.1. Parameters of Power Law model (frequency sweep data), Burger's model (creep/recovery data) and uniaxial compression data of SPI gels produced with different ionic strengths (μ).....	94
Table 3.2. Parameters of Power Law model (frequency sweep data), Burger's model (creep/recovery data) and uniaxial compression obtained from mixed gels produced with different concentrations of locust bean gum (LBG) or guar gum (GG).....	105
Table 4.1. Parameters of Power Law model (frequency sweep data), Burger's model (creep/recovery data) and uniaxial compression data of SPI gels produced with different ionic strengths.....	121
Table 4.2. Parameters of the power law model obtained from frequency sweep data for CaCl_2 -induced gels produced with different concentrations of guar gum (GG) or locust bean gum (LBG)	130
Table 4.3. Burger's model parameters obtained from creep/recovery data for CaCl_2 -induced gels produced with different concentrations of guar gum (GG) or locust bean gum (LBG).	133
Table 4.4. Results of uniaxial compression tests of CaCl_2 -induced gels produced at different guar gum (GG) or locust bean gum (LBG) concentrations.	134
Table 5.1. Formulations used for the production of solid lipid particles (SLP).....	143
Table 5.2. Water holding capacities (WHCs) of non-filled gels and emulsion-filled gels produced at different concentrations of TS-stabilized solid lipid particles (SLP).	148
Table 6.1. Uniaxial compression tests parameters and water holding capacities of non-filled gels and emulsion filled gels produced with different deionized water (DW):solid lipid particles dispersion (SLPD).	175
Table 6.2. Parameters of Power Law model (frequency sweep data), Burger's model (creep/recovery data) and uniaxial compression data of emulsion filled gels (EFG) at different days of storage.	180
Table 7.1 Average particle sizes of solid lipid particles along the storage	196

Table 7.2 Parameters of Burger's model (creep/recovery data) for non-filled and emulsion-filled gels along the storage	201
--	-----

LIST OF FIGURES

Figure 1.1. Action flowchart of the PhD project	31
Figure 2.1. (a) Schematic illustration of native 11S-form glycinin molecule consisting of six acidic (A) and basic (B) polypeptides, with each AB subunit linked by a disulfide bond; (b) illustration for soybean 7S globulin α'	39
Figure 2.2. Schematic overview of an industrial extraction process of soy protein isolate	40
Figure 2.3. Illustrative scheme of heat-induced gelation processes and cold-set gelation processes of protein ingredients.	44
Figure 2.4. Representation of the three possible equilibrium situations for protein and polysaccharide solutions.....	47
Figure 2.5. Possible classification of mixed gels according to their microstructural organizations.....	48
Figure 2.6. Guar gum: (A) pod, (B) seed and (C) powder.	52
Figure 2.7. Locust bean gum: (A) pod, (B) seed and (C) powder.....	52
Figure 2.8. Chemical structure of guar gum (A) and locust bean gum (B) molecules.....	52
Figure 2.9. Schematic representation of the structure of emulsion-filled gels obtained by (a) the gelation of the continuous phase and (b) aggregation of the emulsion droplets.	56
Figure 2.10. Representation of active and inactive particles in emulsion-filled gels.....	59
Figure 3.1. Micrographs obtained by scanning electron microscopy (SEM) of NaCl-induced gels of soy protein isolate produced with different ionic strengths. In Figures A, C and E, the magnification of 500 x was used, and the scale bar corresponds to 200 μm , while in Figures B, D and F, the magnification of 2000 x was used, and the scale bar corresponds to 30 μm	92
Figure 3.2. Results of frequency sweep tests (A, B) and creep/recovery tests (C) of SPI-only gels produced with different ionic strengths.....	96
Figure 3.3. Micrographs of NaCl-induced gels produced with different locust bean gum (LBG) and guar gum (GG) concentrations, obtained by scanning electron microscopy (SEM) (A – D) and confocal laser scanning microscopy (CLSM) (E-H). For the SEM micrographs, the	

magnification of 500 x was used, and the scale bar corresponds to 200 μm . In CLSM micrographs, the Rodamine-B (used to dye the proteins) is identified by red, the FITC (used to dye the polysaccharides) is identified by green and the regions with incomplete demixing present a yellowish color. In CLSM micrographs the scale bar corresponds to 50 μm 98

Figure 3.4. Results of frequency sweep tests (A, B, D, E) and creep/recovery tests (C, F) of NaCl-induced mixed protein/polysaccharide gels with different guar gum (GG) (A, B, C) and locust bean gum (LBG) (D, E, F) concentration 104

Figure 4.1. Scanning electron micrographs of CaCl_2 -induced gels produced with different ionic strengths (100, 200, 300 and 400, which correspond to the CaCl_2 concentrations of 33.3, 66.7, 100 and 133.3 mM). In the micrographs, the magnification of 500 x was used, and the scale bar corresponds to 200 μm 120

Figure 4.2. Results of frequency sweep test (A, B) and creep/recovery tests (C) of gels produced with different with different ionic strengths (100, 200, 300 and 400, which correspond to the CaCl_2 concentrations of 33.3, 66.7, 100 and 133.3 mM). 122

Figure 4.3. Micrographs of CaCl_2 -induced gels produced with 14% soy protein isolate (SPI) and different locust bean gum (LBG) and guar gum (GG) concentrations. In confocal laser scanning micrographs (CLSM) (A-G), the scale bar corresponds to 50 μm . In such micrographs, the colors red and green were used to identify the protein and polysaccharide-rich phases, respectively, and the regions with incomplete demixing present a yellowish color. In scanning electron micrographs (SEM) (H-N), the magnification of 500 x was used, and the scale bar corresponds to 200 μm 127

Figure 4.4. Results of frequency sweep tests of CaCl_2 -induced gels with different guar gum (GG) (A, B) and locust bean gum (LBG) (C, D) concentrations: 0% (\blacksquare \square), 0.1% (\blacklozenge \lozenge); 0.2% (\blacktriangle \triangle) and 0.3% (\bullet \circ). Full (G') and open (G'') symbols. 129

Figure 4.5. Results of creep/recovery tests of CaCl_2 -induced gels with different guar gum (GG) (A) and locust bean gum (LBG) (B) concentrations. 132

Figure 5.1. Visual aspects of the (A) heat-induced emulsion-filled gels produced with different concentrations of WPI-stabilized solid lipid particles (SLP) and (B) NaCl-induced emulsion-filled gels (EFGs) produced with different concentrations of TS-stabilized solid lipid particles (SLP). 147

Figure 5.2. Scanning electron micrographs of emulsion-filled gels produced with different concentrations of solid lipid particles stabilized with Tween 80 and Span 80. For Figures A, D, G and J, the magnification of 100 x was used, and the scale bar corresponds to 1mm. In Figures B, E, H and K, the magnification of 500 x was used, and the scale bar corresponds to 200 μm . In Figures B, D and F, the magnification of 2000 x was used, and the scale bar corresponds to 30 μm	149
Figure 5.3. Confocal laser scanning micrographs of emulsion-filled gels produced with different concentrations of solid lipid particles (SLP) stabilized with Tween 80 and Span 80. In such micrographs, the scale bar corresponds to 33 μm and the colors red, green and purple were used to identify the protein, polysaccharide, and lipid-rich phases of the systems, respectively. Regions with incomplete demixing present a yellowish color.	150
Figure 5.4. Results of uniaxial compression tests of emulsion filled gels (EFG) produced with different concentrations of solid lipid particles stabilized with Tween 80 and Span 80, using different compression speeds.	154
Figure 6.1. Scanning electron micrographs and visual aspects of non-filled gels at days 1(A, B) and 10 (C, D) of storage.	171
Figure 6.2. Visual aspects and micrographs of CaCl_2 -induced gels produced with different deionized water (DW): solid lipid particle dispersion (SLPD) ratios. In scanning electron micrographs, the magnification of 2000 x was used, and the scale bar corresponds to 30 μm . In confocal laser scanning micrographs, the scale bar corresponds to 33 μm and the colors red, green and purple were used to identify the protein, polysaccharide, and lipid-rich phases of the systems, respectively.	174
Figure 6.3. Confocal laser scanning micrographs of CaCl_2 -induced gels produced with different deionized water (DW): solid lipid particle dispersion (SLPD) ratios. In these micrographs, the scale bar corresponds to 33 μm and the colors red, green and purple were used to identify the protein, polysaccharide, and lipid-rich phases of the systems, respectively.	177
Figure 6.4. Visual aspects and scanning electron micrographs of emulsion filled gels at different days of storage.	178
Figure 6.5. Results of frequency sweep tests (A, B) and creep/recovery tests (C) of emulsion filled gels (EFG) in different days of storage.	181

Figure 7.1. Visual aspects of SLP dispersions containing β -carotene after production (A) and retention ratios of β -carotene in SLP dispersions at different days of storage.....	195
Figure 7.2 Scanning electron micrographs of non-filled gels (NFG) and emulsion-filled gels (EFG) at different days of storage, with the magnification of 500 x.....	198
Figure 7.3 Results of frequency sweep tests (A, C) and creep/recovery tests (B, D) of non-filled gels (NFG) (A, B) and emulsion filled gels (EFG) (C, D) at different days of storage.	200
Figure 7.4 Results of uniaxial compression tests of emulsion-filled gels (EFG) at different days of storage.	203
Figure 7.5 Water holding capacities (WHC) of non-filled gels (NFG) and emulsion-filled gels (EFG) along the storage.....	204
Figure 7.6 Concentration of β -carotene in emulsion filled gels (EFG) along the storage.....	205
Figure 8.1. Results obtained from non-filled gels (NFG) and emulsion-filled gels (EFG) induced by NaCl, in different days of storage.....	217
Figure 8.2. Results obtained from non-filled gels (NFG) and emulsion-filled gels (EFG) induced by CaCl ₂ , in different days of storage.....	217

LIST OF ABBREVIATIONS, ACRONYMS AND SYMBOLS

APS: average particle size

BC: beta-carotene

CaCl₂: calcium chloride

CLSM: confocal laser scanning microscopy

EFG: emulsion-filled gel

E_g: Young's modulus obtained from uniaxial compression tests

G': Storage modulus obtained from frequency sweep tests

G'': Loss modulus obtained from frequency sweep tests

GG: guar gum

K' and K'': power law parameters obtained from G' and G'' data, respectively.

LBG: locust bean gum

M/G: mannose-to-galactose ratio

n' and n'': frequency exponents obtained from frequency sweep tests

NaCl: sodium chloride

NFG: non-filled gels

SAXS: small-angle X-ray scattering

SEM: scanning electron microscopy

SLP: solid lipid particle

SLPD: solid lipid particle dispersions

SPI: soy protein isolate

TS: Tween 80/ Span 80

WHC: water holding capacity

WPI: whey protein isolate

XG: xanthan gum

σ_H : rupture strain obtained from uniaxial compression tests

ϵ_H : rupture stress obtained from uniaxial compression tests

ω : angular frequency

J_0 : instantaneous compliance of four-parameter Burger's model obtained from the analysis of creep recovery tests' data

η_0 : viscosity of the Maxwell dashpot of four-parameter Burger's model obtained from the analysis of creep recovery tests' data

J_1 : compliance associated with the Kelvin–Voigt element of four-parameter Burger’s model obtained from the analysis of creep recovery tests’ data

λ_{ret} : retardation time associated with the Kelvin–Voigt element of four-parameter Burger’s model obtained from the analysis of creep recovery tests’ data

t_1 : time when the stress was removed during creep recovery tests

μ : ionic strength

GENERAL INDEX

CHAPTER 1 : GENERAL INTRODUCTION	26
1.1 General Introduction	26
1.2 Objectives	28
1.3 Description of the chapters	29
1.4 Justification of the research	31
CHAPTER 2 : LITERATURE REVIEW	34
2.1 Plant-based foods: importance of the new trends and the challenges for the food industry 35	
2.2 Cold-set gelation of soy protein isolates.....	37
2.2.1 Soy protein isolates: characteristics, functionality and challenges	37
2.2.2 Cold-set gelation methods: properties of salt induced gels.....	42
2.3 Mixed biopolymer gels	46
2.3.1 Gelation of mixed systems of protein and polysaccharides	46
2.3.2 Galactomannans: guar gum and locust bean gum.....	50
2.3.3 Incorporation of galactomannans to protein gels	53
2.4 Emulsion-filled gels (EFG).....	55
2.4.1 Importance of the emulsion filled gels to the food industry	55
2.4.2 Effects of surfactant-matrix interactions on the properties of emulsion filled gels .	58
2.5 Characterization and stability of gelled systems.....	62
2.6 References.....	65

CHAPTER 3 : MICROSTRUCTURAL AND RHEOLOGICAL CHARACTERIZATION OF NaCl-INDUCED GELS OF SOY PROTEIN ISOLATE AND THE EFFECTS OF INCORPORATING DIFFERENT GALACTOMANNANS.....	82
3.1 Abstract.....	84
3.2 Introduction.....	85
3.3 Materials and methods.....	86
3.3.1 Chemicals and reagents.....	86
3.3.2 Production of cold-set gels.....	87
3.3.3 Small strain oscillatory tests.....	87
3.3.4 Creep/recovery tests.....	88
3.3.5 Uniaxial compression tests.....	88
3.3.6 Scanning electron microscopy.....	89
3.3.7 Confocal laser scanning optical microscopy.....	89
3.3.8 Statistical analyses.....	90
3.4 Results and discussion.....	90
3.4.1 Production and characterization of NaCl-induced gels of SPI.....	90
3.4.2 Incorporation of different galactomannans into NaCl-induced gels containing SPI: determination of the critical polysaccharide concentration.....	97
3.4.3 Characterization of NaCl-induced mixed gels of SPI and galactomannans (locust bean gum or guar gum).....	97
3.5 Conclusions.....	106
3.6 References.....	106
CHAPTER 4 : MICROSTRUCTURAL AND RHEOLOGICAL CHARACTERIZATION OF CaCl ₂ -INDUCED GELS OF SOY PROTEIN ISOLATE AND THE EFFECTS OF INCORPORATING DIFFERENT GALACTOMANNANS.....	110

4.1 Abstract	112
4.2 Introduction.....	113
4.3 Materials and methods	114
4.3.1 Chemicals and reagents	114
4.3.2 Production of cold-set SPI gels	114
4.3.3 Small strain oscillatory tests.....	115
4.3.4 Creep/recovery tests	115
4.3.5 Uniaxial compression tests.....	116
4.3.6 Scanning electron microscopy	116
4.3.7 Confocal laser scanning optical microscopy.....	117
4.3.8 Statistical analyses.....	117
4.4 Results and discussion	117
4.4.1 Microstructural organizations of SPI-only gels	117
4.4.2 Rheological properties of SPI-only gels.....	121
4.4.3 Incorporation of galactomannans to the CaCl ₂ -induced gels: microstructural properties.....	125
4.4.4 Incorporation of galactomannans to the CaCl ₂ -induced gels: rheological properties	128
4.5 Conclusions.....	134
4.6 References.....	135
 CHAPTER 5 : INCORPORATION OF SOLID LIPID PARTICLES STABILIZED BY DIFFERENT SURFACTANTS TO COLD-SET GELS OF SOY PROTEIN ISOLATE AND LOCUST BEAN GUM	 138
5.1 Abstract.....	140

5.2 Introduction.....	141
5.3 Materials and methods	142
5.3.1 Chemicals and reagents	142
5.3.2 Production and characterization of SLP stabilized with different surfactants.	142
5.3.3 Production of cold-set EFG.....	143
5.3.4 Water holding capacity.....	143
5.3.5 Uniaxial compression tests.....	144
5.3.6 Scanning electron microscopy	144
5.3.7 Confocal laser scanning optical microscopy.....	145
5.3.8 Statistical analyzes	145
5.4 Results and discussion	145
5.4.1 The visual aspect and WHC	145
5.4.2 Microstructural characterization	148
5.4.3 Uniaxial compression: effect of different compression speeds.....	152
5.5 Conclusions.....	156
5.6 References.....	157

CHAPTER 6 : EFFECTS OF SOLID LIPID PARTICLES INCORPORATION ON THE PROPERTIES AND STABILITY OF $CaCl_2$ -INDUCED GELS OF SOY PROTEIN ISOLATE AND LOCUST BEAN GUM..... 160

6.1 Abstract.....	162
6.2 Introduction.....	163
6.3 Materials and methods	165
6.3.1 Chemicals and reagents	165

6.3.2 Production of cold-set gels.....	165
6.3.3 Characterization of EFG produced with different SLP concentrations.....	166
6.3.4 Evaluation of gels stability.....	166
6.3.5 Confocal laser scanning optical microscopy.....	166
6.3.6 Scanning electron microscopy	166
6.3.7 Water holding capacity.....	167
6.3.8 Uniaxial compression tests.....	167
6.3.9 Small strain oscillatory tests.....	168
6.3.10 Creep/recovery tests	168
6.3.11 Statistical analyses.....	169
6.4 Results and discussion	169
6.4.1 Stability of non-filled gels (NFG).....	169
6.4.2 Incorporation of different SLP concentrations to CaCl ₂ -induced gels.....	173
6.4.3 Stability of emulsion-filled gels (EFG).....	177
6.5 Conclusions.....	181
6.6 References.....	182
 CHAPTER 7 : COLD-SET NA ₂ CO ₃ -INDUCED GELS OF SOY PROTEIN ISOLATE AND LOCUST BEAN GUM: HOW THE AGEING PROCESS AFFECT THEIR MICROSTRUCTURE AND THE STABILITY OF INCORPORATED BETA-CAROTENE	 186
7.1 Abstract.....	188
7.2 Introduction.....	189
7.3 Materials and methods	190
7.3.1 Chemicals and reagents.....	190

7.3.2 Production of solid lipid particles	191
7.3.3 Production of cold-set non-filled gels (NFG) and emulsion-filled gels (EFG)	191
7.3.4 Water holding capacity.....	191
7.3.5 Scanning electron microscopy	192
7.3.6 Uniaxial compression tests.....	192
7.3.7 Small strain oscillatory tests.....	193
7.3.8 Creep/recovery tests	193
7.3.9 Quantification of beta-carotene in solid lipid particles	194
7.3.10 Quantifications of beta-carotene in EFG.....	194
7.3.11 Evaluation of gels stability.....	194
7.3.12 Statistical analyses.....	195
7.4 Results and Discussion	195
7.4.1 Production of solid lipid particles encapsulating beta-carotene and incorporation in emulsion-filled gels EFG	195
7.4.2 Stability of the gelled systems.....	196
7.4.3 Quantification of beta-carotene in EFG	205
7.5 Conclusions.....	206
7.6 References.....	206
CHAPTER 8 : EVALUATING THE STABILITY OF COLD-SET GELS USING SMALL-ANGLE X-RAY SCATTERING (SAXS)	210
8.1 Abstract.....	212
8.2 Introduction.....	213
8.3 Materials and methods	214

8.3.1 Chemicals and reagents	214
8.3.2 Production of cold-set gels	214
8.3.3 Small-angle X-ray scattering (SAXS)	215
8.4 Results and Discussion	215
8.4.1 Small-angle X-ray scattering (SAXS) of non-filled gels and emulsion-filled gels	215
8.5 Conclusions	218
8.6 References	218
GENERAL CONCLUSIONS	221
APPENDICES	223
APPENDIX A – Visual aspects of systems produced with SPI and NaCl	223
APPENDIX B – Visual aspects of systems produced with SPI and CaCl ₂	224
APPENDIX D - Visual aspect of mixed biopolymeric gels produced using formulation G _{CaCl₂} and different galactomannans.	226
ANNEX A – Specification sheet of commercial soy protein isolate, provided by the supplier (Marsul Proteínas LTDA).	227

CHAPTER 1 : GENERAL INTRODUCTION

1.1 General Introduction

Food products are complex systems, whose properties depend on the characteristics and behavior of the constituent macromolecules, including proteins. Protein ingredients are known for presenting very important functional properties and have been focus of research that aim the development of new food formulations. Among these ingredients, the most largely investigated are the whey protein isolates and concentrates, that present good nutritional characteristics and interesting functional properties, including the gelling capacity.

In recent years, however, plant proteins have been considered as alternatives to animal-based ingredients in food formulations, due to the new dietary preferences of many consumers, who are concerned about health, sustainability, and ethical issues related to animal-sourced products. Replacements, however, may be complicated from the technological point of view, as the functionalities of plant proteins are not as explored in the literature as the properties of animal proteins, requiring much more investigation to understand their viability as food ingredients.

Among the most readily available plant protein ingredients are the soy protein isolates, which are known for their nutritional characteristics, low production cost and several functional properties, which include, for example, the ability to form cold-set gels. Cold-set gelation methods have been extensively investigated for allowing the incorporation of thermolabile compounds into food products and reducing the quality losses caused by excessive heat treatments.

They basically consist of two steps: (I) preheating the protein dispersion in non-gelling conditions; and (II) inducing the gelation at low/room temperatures through alterations in the quality of the solvent, for example by the incorporation of different types of salts, such as calcium chloride and sodium chloride, to the systems.

Even though some studies have already investigated the properties of cold-set gels produced with SPI, most part of authors use raw materials extracted in laboratory, under controlled conditions. For this reason, the results of these studies are difficult to reproduce in large scale by the food industry, as commercial ingredients are required in this case. Such ingredients tend to undergo more severe protein denaturation and aggregation processes during their extraction, which significantly change their characteristics and functionality. It is known, for example, that commercial SPI generally present low solubilities in acidic and neutral pHs, making it difficult to exploit their functional properties in foods.

On the other hand, several researchers claim that protein ingredients with limited gelling capacity can be satisfactorily applied in conjunction with polysaccharides, such as galactomannans, which tend to stabilize protein structures, thus improving their functional properties. Galactomannans, including the guar gums (GG) and locust bean gums (LBG), are neutral polysaccharides, consisting of linear chains of 1,4-linked β -D-mannopyranose residues to which varying proportions of α -D-galactopyranosyl residues are randomly attached at position 6 as sidechains.

The distinct galactomannans differ from each other by the mannose-to-galactose (M/G) ratio (also known as *degree of branching*), which influences their interactions with other macromolecules (including proteins) and, therefore, affect in different ways the formation of mixed biopolymeric gels.

Considering the complexity of protein gels and mixed biopolymeric gels, several studies have been developed in order to obtain information regarding the relations among microstructural organizations, rheological and sensory properties of the structures formed. The knowledge obtained from these studies is essential for the food industry, that is constantly seeking to develop new formulations to adapt the products to the new demands of the consumers.

Recently, for example, new preferences of the consumers have led researchers and industry to look for alternatives that allow the production of products with a low lipid content and high sensory quality. Several authors claim that this can be achieved by the combined application of lipids and gelling agents for the production of systems known as emulsion-filled gels (EFG), since a wide variety of structures, with distinct properties, can be obtained from variations in the characteristics of the matrix, dispersed lipids, surfactants applied and the interactions between the various components.

The effects of such variations in the properties of emulsion filled gels may be evaluated by the combined application of several analytical tools, including rheological tests of small and large deformation (uniaxial compression tests, strain and frequency sweep tests and creep/recovery tests), microscopy techniques, and additional analysis, such as small-angle X-ray scattering (SAXS).

All these techniques are fundamental to obtain a complete characterization of the gels, and also for monitoring possible alterations in the gelled structures over time, due to their highly transient and non-linear nature, and its thermodynamically metastable state. Although the structural rearrangements can be subtle, the processes resulting from the aging of the systems

can result in more extreme macroscopic manifestations, such as the collapse of gels, which compromises their possible application as food systems.

1.2 Objectives

Considering the context presented in the General Introduction, the present PhD thesis aimed to study the effect of incorporating different galactomannans (locust gum and guar gum) and solid lipid particles stabilized with different surfactants (whey protein isolate and the combination of tween 80 and span 80), on the rheological and microstructural properties of cold-set soy protein isolate gels, obtained by the incorporation of different salts (CaCl_2 and NaCl), as well as to evaluate the stability of gelled systems over the storage period.

To achieve this main objective, the following specific steps have been determined:

- Characterization of cold-set gels of commercial soy protein isolate, obtained by the incorporation of calcium chloride or sodium chloride, using different protein concentrations and ionic strengths, in order to determine the best conditions/formulations for the production of self-supported (stronger)gels.
- Characterization of cold-set mixed gels of soy protein isolate and different galactomannans (locust gum and guar gum) obtained by the incorporation of calcium chloride or sodium chloride, in order to determine the best operating conditions/formulations for the production of self-supported (stronger)gels.
- Selection of the best formulations of protein gels and/or mixed biopolymeric gels for the production of self-supported (stronger) emulsion filled gels.
- Characterization of emulsion filled gels using different concentrations of solid lipid particles stabilized with different surfactants (whey protein isolate or the combined application of Tween 80/Span 80).
- Selection of the best formulations (self-supported, stronger) of soy protein isolate gels and/or mixed biopolymeric gels, filled and nonfilled with solid lipid particles, for the study of the gelled systems' stability.
- Evaluation of stability of soy protein isolate gels and/or mixed biopolymeric gels, filled and nonfilled with solid lipid particles, through the characterization of such systems on different days of storage.

1.3 Description of the chapters

This PhD thesis is organized in the chapters described below, and the experimental data were obtained according to the action flowchart shown in Figure 1.1.

- ***Chapter 1: General Introduction***
- ***Chapter 2: Literature Review***

In this chapter, the most important theoretical aspects and relevant literature regarding the subjects related to this Thesis are presented and discussed.

- ***Chapter 3: Microstructural and rheological characterization of NaCl-induced gels of soy protein isolate and the effects of incorporating different galactomannans***

In this chapter, the properties of NaCl-induced gels of soy protein isolate (SPI) in the presence and absence of different galactomannans (locust bean gum - LBG and guar gum – GG) at pH 7 were evaluated. Gels produced with different ionic strengths (100 – 400), protein concentrations (10-14%, w/v), and galactomannan concentrations (0 – 0.5%, w/v) were characterized regarding their visual aspects, microstructural organization, and rheological properties.

- ***Chapter 4: Microstructural and rheological characterization of CaCl₂-induced gels of soy protein isolate and the effects of incorporating different galactomannans***

In this chapter, the properties of CaCl₂-induced gels of soy protein isolate (SPI) in the presence and absence of different galactomannans (locust bean gum - LBG and guar gum – GG) at pH 7 were evaluated. Gels were produced with different ionic strengths (100 - 400), protein concentrations (10-14%, w/v), and galactomannan concentrations (0 – 0.3%, w/v) were characterized regarding their visual aspects, microstructural organization, and rheological properties.

- ***Chapter 5: Incorporation of solid lipid particles stabilized by different surfactants to cold-set gels of soy protein isolate and locust bean gum***

In this chapter, the effects of incorporating solid lipid particles (SLP) stabilized by different surfactants (whey protein isolate -WPI and Tween 80/Span 80 - TS) into NaCl-induced cold-set gels of soy protein isolate (SPI) (14%, w/v) and locust bean gum (LBG) (0.1%, w/v) were evaluated. For this purpose, the systems were characterized regarding their visual aspects, water holding capacities, microstructural organizations, and rheological properties.

- ***Chapter 6: Effects of solid lipid particles incorporation on the properties and stability of CaCl₂-induced gels of soy protein isolate and locust bean gum***

In this chapter, the stability of non-filled gels (NFG) produced with 14% soy protein isolate (SPI), 0.1% locust bean gum (LBG) and 100 mM CaCl₂ (100 mM) were evaluated, as well as the effects of incorporating Tween 80/Span 80-stabilized solid lipid particles (SLP) to the system. Non-filled gels and emulsion-filled gels were characterized regarding its water holding capacity (WHC), microstructural organizations and rheological properties in different days of storage.

- ***Chapter 7: Cold-set NaCl-induced gels of soy protein isolate and locust bean gum: how the ageing process affect their microstructure and the stability of incorporated beta-carotene***

In this chapter, the effects of solid lipid particles (SLP) incorporation on the stability of NaCl-induced gels were evaluated, as well as, the feasibility of incorporating β -Carotene (BC) in emulsion-filled gels (EFGs), by comparing the stability of the bioactive in two different systems: SLP and NaCl-induced EFG.

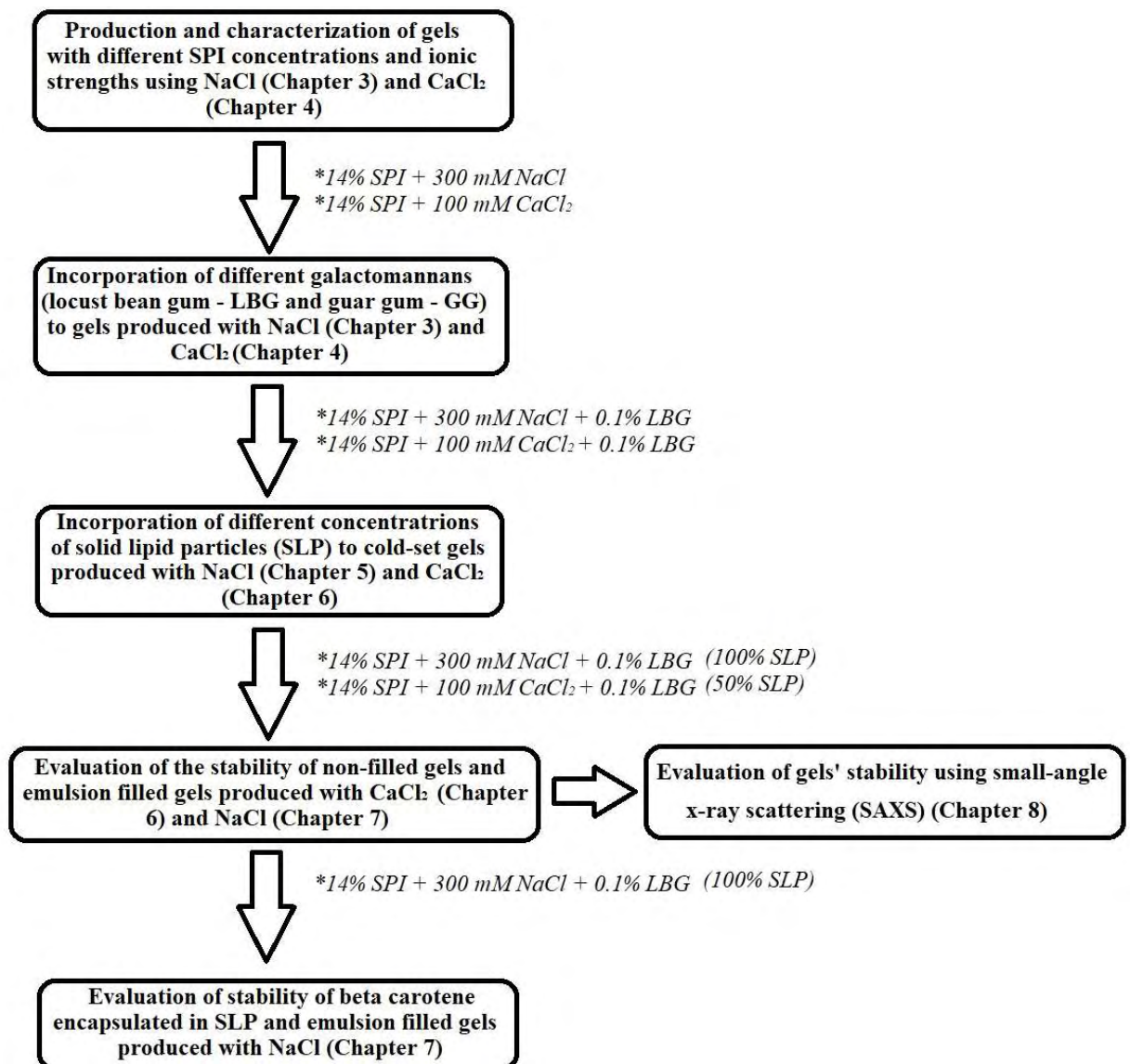
- ***Chapter 8: Evaluating the stability of cold-set gels using small-angle x-ray scattering (SAXS)***

In this chapter, data of small-angle x-ray scattering (SAXS) of non-filled gels and emulsion-filled gels produced with soy protein isolate and locust bean gum, using different salts (NaCl or CaCl₂), at different days of storage, were presented.

- ***Chapter 9: General conclusions***

In this chapter, the main conclusions obtained from the results presented throughout the Thesis were presented and discussed.

Figure 1.1. Action flowchart of the PhD project



1.4 Justification of the research

Gels are systems of very high importance for the food industry, as they provide desirable viscoelastic properties to a series of products. These structures can be formed by the application of protein ingredients, using different gelation methods. Among them are the cold-set gelation processes, which have been drawing the attention of researchers and industry for allowing the obtention of systems with unique properties without the need of a harsh heating step.

Although whey proteins are the ingredients most applied by researchers and the industry in the production of gels, plant proteins, such as soy protein isolates, have been gaining undeniable

importance, due to the new preferences of consumers. On the other hand, it is known that the application of soy protein isolate as a gelling agent on a large scale is limited by the challenging characteristics of commercial ingredients, as low solubility in acidic and neutral pHs.

In some conditions, however, this problem can be reduced by incorporating polysaccharides, such as galactomannans, into protein gels, since the interaction between these different macromolecules can improve SPI properties and originate mixed biopolymeric gels with unique rheological and microstructural characteristics.

The properties of such gels can also be modified through the incorporation of solid lipid particles, whose surface properties, determined by the type of surfactant, directly influence their interactions with the gelled matrix, originating the named *emulsion filled gels* with distinct characteristics.

Although the development of new formulations of gelled systems, with unique structural organizations and textures, is interesting for the industry, it is not a simple process. Given the specificity and complexity of each system, the appropriate development of new formulations requires detailed characterizations, not only right after production, but also throughout the storage period. Such demand arises from the thermodynamically metastable state of the gels, which can lead to changes in the structural organizations through spontaneous processes (known as aging processes) and/or external forces, which affect, therefore, the shelf life of the products.

Considering these problems and hypotheses, the present PhD thesis was justified by the following reasons:

- (i) Need of developing studies to evaluate the functional properties of commercial soy protein isolates, rarely addressed in the literature, in order to understand the real challenges faced by the food industry for the proper application of this type of ingredient.
- (ii) Interest in the development of well-defined protocols and formulations to produce cold-set gels of a commercial SPI, by the application of different salts (CaCl_2 and NaCl), since such gelling methods allow the incorporation of thermolabile compounds into food products and the reduction of quality losses caused by excessive heat treatment.
- (iii) Interest in investigating the influence of the incorporation of galactomannans (locust gum and guar gum) on the properties of cold-set gels of the selected commercial soy protein isolate, in order to understand the effect of different M/G ratios over the

interactions between the biopolymers and also to enable the development of product prototypes with interesting properties to the industry.

- (iv) Interest in obtaining knowledge regarding the influence of the incorporation of solid lipid particles stabilized with different surfactants on the rheological and microstructural properties of cold-set gels produced with commercial soy protein isolate, in the presence and absence of galactomannans, which can be used in the future for the development of new products with different sensory properties.
- (v) Need of developing studies that allow the correlation of results obtained from rheological tests, microscopies and small-angle X-ray scattering, for the proper characterization of complex gelled systems. In addition, SAXS data can be explored to monitor the aging processes of these gels, that can lead to the collapse of structures, making its application unfeasible by the food industry.

CHAPTER 2 : LITERATURE REVIEW

2.1 Plant-based foods: importance of the new trends and the challenges for the food industry

To adapt to new trends and consumer preferences, the food sector needs to be constantly changing. Currently, one of the biggest challenges that the food industry is facing consists in reviewing old formulations and developing new products to the growing group of vegetarians, vegans and, also, flexitarian consumers.

According to the literature, while vegetarians are the ones who do not consume one or more types of foods from animal origin, especially flesh from animals, vegans are people who do not consume any animal foods or by-products of animal husbandry (such as milk, eggs and honey) (DAGNELIE; MARIOT, 2017). “Flexitarian”, on the other hand, a term added to the Oxford English Dictionary in 2014, is a portmanteau of “flexible” and “vegetarian,” referring to an individual who follows a primarily but not strictly vegetarian diet, occasionally eating meat or fish (DERBYSHIRE, 2016; OXFORD ENGLISH DICTIONARY, 2014).

According to The Vegan Society (2021), only in Great Britain, the number of vegans quadrupled between 2014 and 2019. While in 2014 the number of vegans was around 150,000 (0.25% of the population), in 2019 there were over 600,000 vegans (1.16% of the population) (THE VEGAN SOCIETY, 2021). Another important example is the United States, where the number of vegans grew about 600% between 2014 and 2017 (from nearly 4 million to 19.6 million) (THE VEGAN SOCIETY, 2021).

Regarding South America, recent data indicated that about 90% of the region would be interested in consuming plant-based foods (THE VEGAN SOCIETY, 2021). More specifically in Brazil, data provided by *Good Food Institute* revealed that, while in 2018, the percentage of people reducing the consumption of animal products was 29%, in 2020, this percentage increased to 49% (GOOD FOOD INSTITUTE, 2020).

The significant growth of people interested in these types of diets is justified by many different reasons, including nutritional and health issues (MCCLEMENTS, 2020). For many years, the constant growth of the population and the development of a more dynamic lifestyle, have made the consumers to choose a more Western-style diet, which includes high levels foods rich in fat, salt and sugar and a higher consumption of processed meats and animal-based products (DERBYSHIRE, 2016; MCCLEMENTS, 2019, 2020). As a result, many countries have faced a significant increase in the incidences of diet-related chronic diseases (WILLETT et al., 2019; MCCLEMENTS, 2020).

In contrast, research carried out in recent years have shown that the application of a plant-based diet may be a good alternative, not only to avoid, but to prevent the risk of cardiovascular diseases, type 2 diabetes, and certain forms of cancer (BATTAGLIA et al., 2015; DERBYSHIRE, 2016; SATIJA; HU, 2018; MCCLEMENTS, 2020).

Besides these nutritional factors, there is a growing concern regarding the deleterious effects of a high consumption of animal-based products to the environment (POORE; NEMECEK, 2018; WILLETT et al., 2019; MCCLEMENTS, 2019). According to the literature, the global population and the demand for food will continue to increase in a fast pace for at least the next five decades, as well as the competition for land, water, and energy (ONU, 2017; TRIPATHI et al., 2019). For this reason, there is an urgent requirement to reduce the impact of the food production on the environment, to ensure food security for the world population (TRIPATHI et al., 2019).

Considering that raising animals for food production may be much more damaging to the environment (for causing more pollution, increasing land utilization, and depleting water resources) and energetic expensive than directly growing plant foods for humans, reducing the level of animal-based products and ingredients within the industry have been considered very important (MCCLEMENTS, 2020; VAN DER GOOT et al., 2016). Following his idea, in his review, McClements (2020) cited that the results of a comprehensive study on sustainable diets by the EAT-Lancet commission indicated that there should be a considerable reduction in the amount of animal foods consumed globally, which meets the recommendations of the 2030 Agenda for Sustainable Development of the United Nations' Food and Agriculture Organization (FAO).

The replacement of animal-based products in the food industry, however, is not simple, specially considering the protein-based ingredients. According to the literature, there are some important concerns about formulation alterations that need to be considered, specially involving nutritional quality of proteins (e.g. in terms of digestibility and amino acid composition) and functional properties (CHARDIGNY; WALRAND, 2016; LYNCH et al., 2018; LOVEDAY, 2019).

Focusing on the functional aspects of the replacements, the concerns of the food industry are related to the many different technological roles that the animal-based protein ingredients (especially whey protein isolates and concentrates) have in formulated foods, contributing to texture, color, flavor, among other properties (LOVEDAY, 2019).

Considering that the type of protein ingredient strongly affects the characteristics of the food product, and also that the success of new formulations depends on their safety, ordability,

conveniency, shelf-stability, and sensory properties, investigations regarding the functional properties of plant-based ingredients (specially proteins) are fundamental to the satisfactory replacement of animal-based ingredients (NISHINARI et al., 2014; MARTINS et al., 2018; MCCLEMENTS, 2020).

2.2 Cold-set gelation of soy protein isolates

2.2.1 Soy protein isolates: characteristics, functionality and challenges

Proteins are dietary macronutrients recognized by their functional and structural roles in the human body, and by their technological roles in food formulations (LOVEDAY, 2019). Protein-rich ingredients are largely applied by the food industry to alter texture, color and flavor of the products (LOVEDAY, 2019).

In terms of sources, the animal-based protein ingredients, such as the whey protein isolates, are mostly investigated and used in processed foods (CAVALLIERI; CUNHA, 2008; KUHN; CAVALLIERI; CUNHA, 2011; TARHAN et al., 2016). Such fact, however, has been changing due to alterations in the preference of consumers, who are increasingly concerned about the safety and sustainability of animal derived product (GOOD FOOD INSTITUTE, 2020; MCCLEMENTS, 2019, 2020; LOVEDAY, 2019; MONTEIRO et al., 2013).

The sustainability of food ingredients is technically complex, but it can be discussed in terms of footprinting for greenhouse gases, water and energy consumption, for example (LOVEDAY, 2019, MCCLEMENTS, 2019, 2020). Discussions about these factors are fundamental, especially considering the progressive increase of the world's population (MONTEIRO et al., 2013; TRIPATHI et al., 2019).

Considering that the energy necessary for the production of animal-based protein ingredients is higher than that necessary for plant-based alternatives, the application of plant proteins in food formulations has been gaining attention of researchers and industry (GOOD FOOD INSTITUTE, 2020; MCCLEMENTS, 2019, 2020; LOVEDAY, 2019; MONTEIRO et al., 2013; VAN DER GOOT et al., 2016).

Among the most important protein ingredients from vegetable sources, are the soy protein isolates (SPIs). Soybean (*Glycine max* L.) is an important food of great economic importance, known for presenting interesting lipid composition, high nutritional value, high productivity,

low production cost and high protein content (NISHINARI et al. 2014; NISHINARI et al. 2018).

According to Nishinari (2018), in 2014, the top five soybean producing countries were United States (108), Brazil (87), Argentina (53), China (12), and India (10) (million tonnes) (FAOSTAT, 2016; NISHINARI et al., 2018). In the 2019/2020 harvest, on the other hand, the production of soybeans in the world was 337,298 million of tonnes and Brazil was considered the top 1 producing country, being responsible for 124,845 million of tonnes (EMBRAPA, 2021).

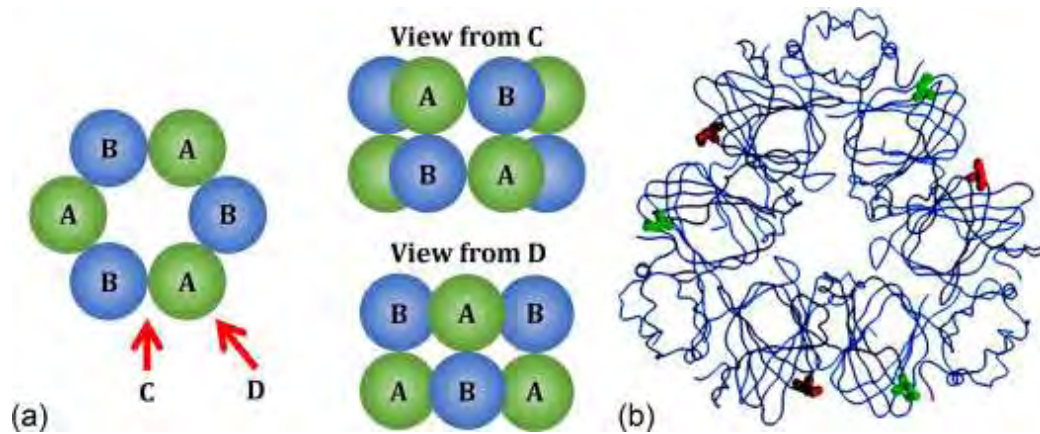
According to Nishinari et al. (2018), soybean contains approximately 40% protein and 20% oil on an average dry matter base and, therefore, is considered an important source of protein, allowing the production of ingredients like the SPIs (NISHINARI et al., 2018). SPIs are known for its high nutritional value and important functional properties, including the emulsifying and gelling capacities (INGRASSIA et al., 2019; LOVEDAY, 2019; MONTEIRO et al., 2013; MONTEIRO; LOPES-DA-SILVA, 2019; MOURE et al., 2006); ZHAO et al., 2021).

According to the literature, the functionality of SPI, is mainly determined by the structure, composition, degree of dissociation, denaturation or aggregation of its globulins, which are classified into four protein categories: 2S, 7S, 11S and 15S, based on their sedimentation coefficients (INGRASSIA et al., 2019; NISHINARI et al., 2014; PUPPO; SORGENTINI; AÑÓN, 2003; UTSUMI; MATSUMURA; MORI, 1997).

Among these proteins, the globulins 7S (β -conglycinin) and 11S (glycinin) represent more than 80% (Figure 2.1) (INGRASSIA et al., 2019; NISHINARI et al., 2014; SAIO; KAMIYA; WATANABE, 1969). While β -Conglycinin is a trimeric glycoprotein consisting of three subunits, α , α' , and β , associated via hydrophobic interactions, glycinin is a hexamer composed of acidic and basic polypeptides linked by disulfide bonds (NISHINARI et al., 2014; WU et al., 2018).

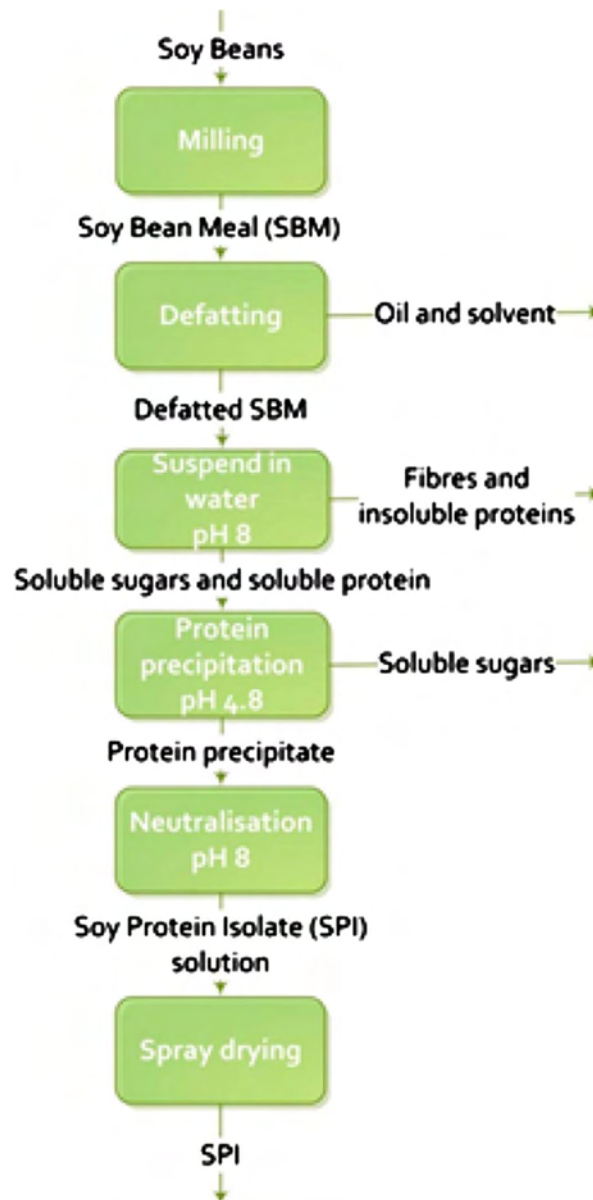
According to the literature, the 7S/11S ration in SPIs generally varies between 0.5 and 1.3 depending on raw materials applied and the extraction process (NISHINARI et al., 2014; SAIO; KAMIYA; WATANABE, 1969). In general, during commercial extraction processes of SPI (schematized in Figure 2.2), defatted soy flour is dispersed in an aqueous medium, at a neutral or alkaline pH (pH 7-10), for the extraction of protein and soluble carbohydrates, centrifuged to remove insoluble residues, and subjected to pH 4.5 (isoelectric point) for the precipitation of proteins, which are then separated by mechanical decanting, washed, neutralized and dried or dehydrated (LIU, 1997; LOVEDAY, 2019; SGARBIERI, 1996).

Figure 2.1. (a) Schematic illustration of native 11S-form glycinin molecule consisting of six acidic (A) and basic (B) polypeptides, with each AB subunit linked by a disulfide bond; (b) illustration for soybean 7S globulin α' .



Source: Tang, C. (2019). Nanostructures of soy proteins for encapsulation of food bioactive ingredients, in *Biopolymer Nanostructures for Food Encapsulation Purposes*, 2019.

Figure 2.2. Schematic overview of an industrial extraction process of soy protein isolate



Source: VAN DER GOOT, A.J. Concepts for further sustainable production of foods. *Journal of Food Engineering*, v. 168, p. 42–51, 2016.

In this process, therefore, soy proteins are subjected to drastic conditions of temperature and pH that alter the composition and characteristics of the constituent globulins previously cited (BRAGA et al., 2006). Possible alterations due to the production process and the complexity of its components make the SPIs available for commercialization in large scale very heterogeneous and, in most of the cases, with challenging properties.

This problematic was very well discussed by Lee et al. (2003), who investigated the solubility of different commercial soy protein products. According to these authors, the

physicochemical properties of food systems are extremely sensitive to past processing history, methods of preparation, and conditions of measurements, and such properties directly affect the functional behavior of the protein products. For this reason, the authors affirm that, even though many reports have investigated the properties of pure proteins, such as protein isolates, 11S protein (glycinin), and 7S protein (conglycinin) prepared carefully in the laboratory, the results are hardly applicable/reproducible for commercial protein products (LEE et al., 2003).

In their study, Lee et al. (2003) verified that the commercial SPI could be separated in three groups from their solubility profiles: (I) SPI with high solubility near the pI; (II) SPI with low solubility near the pI, but high solubility at pH 11 and (III) SPI with low solubility even at pH 11. Considering the importance of the solubility for many other functional properties of protein ingredients, these results evidenced the big challenges faced by the industry for the application of SPI in food products, that generally present acid or neutral pHs.

Such challenges were also discussed in previous studies of our research group (BRITO-OLIVEIRA, 2017; BRITO-OLIVEIRA et al., 2018; BRITO-OLIVEIRA, 2017), in which the commercial SPI obtained from Marsul (also applied in the present study), was fully characterized regarding proximate composition, isoelectric point, solubility profile, thermal behavior by differential scanning calorimetry, surface hydrophobicity, intrinsic tryptophan fluorescence and circular dichroism, at different pHs and after different thermal treatments.

The results indicated the commercial SPI presented very low solubility at acid pH and higher solubilities at pH 7 (32.0%), 9 (51.6%) and 11 (100%), which affected its capacity to form CaCl_2 -induced gels (BRITO-OLIVEIRA, 2017; BRITO-OLIVEIRA et al., 2018). Although self-supported gels could be formed at pH 7 (using a preheating of 80 °C/30 min, 15% SPI and 10 or 15 mM CaCl_2), the systems showed serious instabilities, presenting aspects of non-supported gels after a few minutes at room temperature (BRITO-OLIVEIRA, 2017; BRITO-OLIVEIRA et al., 2018).

The obtained results confirmed that the low solubilities and physicochemical characteristics of the commercial SPI at acid and neutral pH are limiting factors for the application of this ingredient as a gelling agent in food preparations, especially because the pH of food products generally range between 3 and 7 (BRITO-OLIVEIRA, 2017; BRITO-OLIVEIRA et al., 2018).

In fact, several other studies also cite the gelling capacity as a crucial functionality of the SPI but reinforce the poor stability of the protein gels formed may limit its application in certain types of food (GUO et al., 2018; WU et al., 2018; XIAO et al., 2020; ZHAO et al., 2021; ZHENG et al., 2019). However, it has been demonstrated that functional characteristics of the

protein gel can be improved by the incorporation of polysaccharides to the systems, evidencing the importance of the continuous development of studies that investigate the gelling capacity of commercial SPIs to expand their application (GOUZY et al., 2019; ZHOU et al., 2014).

2.2.2 Cold-set gelation methods: properties of salt induced gels

Sensorially pleasant structures and textures in food products are often obtained through the gelation of protein ingredients (CHEN et al., 2019; GUO et al., 2018; LE; RIOUX; TURGEON, 2017; TOTOSAUS et al., 2002). Protein gels can be defined as continuous three-dimensional networks with macroscopic elasticity, that are obtained from a combination of sequential processes that result in the relatively orderly aggregation of denatured molecules (ALTING et al., 2003; CAVALLIERI, 2007; FOEGEDING; DAVIS, 2011; LE; RIOUX; TURGEON, 2017; TOTOSAUS et al. 2002).

Such processes consist, basically, of three main steps: (1) the protein denaturation or unfolding step, which results in the exposure of reactive groups of the proteins and favor intermolecular bonds; (2) the aggregation or coagulation step, in which the formation of molecular aggregates occurs; and (3) the formation of the continuous three-dimensional network, through cross-links among the protein aggregates (CAVALLIERI, 2007; MANGINO, 1984; TOBITANI; ROSS-MURPHY, 1997).

According to the literature, the mechanisms involved in gelation processes are defined by the balance between attractive and repulsive forces established between protein molecules, as well as by protein-solvent interactions (TOTOSAUS et al., 2002). Such interactions (protein-protein and protein-solvent) are influenced by intrinsic factors (e.g. electrostatic interactions, disulfide bonds, molecular weight, amino acid composition, hydrophobicity, etc.) and extrinsic factors (e.g. protein concentration, pH, temperature, ionic strength, pressure, etc.), which determine the final properties of the gels (PHILLIPS; WHITEHEAD; KINSELLA, 1994; TOTOSAUS et al., 2002). In this context, it is evident that the production methods of the gels directly influence the properties of the systems formed (TOTOSAUS et al., 2002).

In the food industry, protein gels are widely produced using thermal induced gelation methods, in which the three steps mentioned above (denaturation, aggregation and gelation) occur simultaneously, under heating, as illustrated in Figure 2.3 (CHEN et al, 2019; BORZOVA et al., 2016; BRYANT; MCCLEMENTS, 2000; LI et al., 2018; TOTOSAUS et al., 2002).

Although such methods are extensively explored in at industrial scale, a well as in most studies found in the literature (BADII; ATRI; DUNSTAN, 2016; CHEN et al, 2019;

BORZOVA et al., 2016; ESTÉVEZ et al., 2017; LI et al., 2018; MONAHAN; GERMAN; KINSELLAT, 1995; TOTOSAUS et al., 2002.; UTSUMI; KINSELLA, 1985), cold-set gelation methods have been identified as interesting alternatives for obtaining products with unique qualities (CAVALLIERI; CUNHA, 2009; CHEN et al., 2019; INGRASSIA et al., 2019; MESSION et al., 2015; RODRIGUES et al., 2020; SADEGHI; MADADLOU; YARMAND, 2014; WIJAYA; VAN DER MEEREN; PATEL, 2017; ZHAO et al., 2021).

According to the literature, such methods can be advantageous over thermal induced gelation methods for allowing the incorporation of thermosensitive compounds to the systems and the introduction of gelled structures to food products, without an excessive heating process (BRITTEN; GIROUX, 2001; CAVALLIERI; CUNHA, 2009; MALTAIS et al., 2009; ZHAO et al., 2021). Such fact happens because during cold-set gelation processes, the partial denaturations and aggregation occur under pre-heating, separately from the gelation step, which is only induced at low/room temperatures (Figure 2.3) (BRYANT; MCCLEMENTS, 2000; CHEN et al., 2019; RODRIGUES et al., 2020; TOTOSAUS et al., 2002; ZHAO et al., 2021).

Therefore, cold-set gelation methods are divided in two consecutive steps: (I) the pre-heating of the protein solution at low ionic strength, pH different than the protein's isoelectric point and a protein concentration lower than the minimum required for gelation; and (II) the alteration of the solvents' quality to induce gelation (CAVALLIERI et al 2007; CAVALLIERI; CUNHA, 2008; CHEN et al., 2019; MALTAIS; REMONDETTO; SUBIRADE, 2008; MALTAIS; REMONDETTO; SUBIRADE, 2009; TOTOSAUS et al., 2002; ZHANG et al., 2016). Such alterations in the solvent's quality are generally performed by the incorporation of salts, acids or enzymes to the protein dispersions (CAVALLIERI; CUNHA, 2008; MESSION et al., 2015; SADEGHI; MADADLOU; YARMAND, 2014; WIJAYA; VAN DER MEEREN; PATEL, 2017).

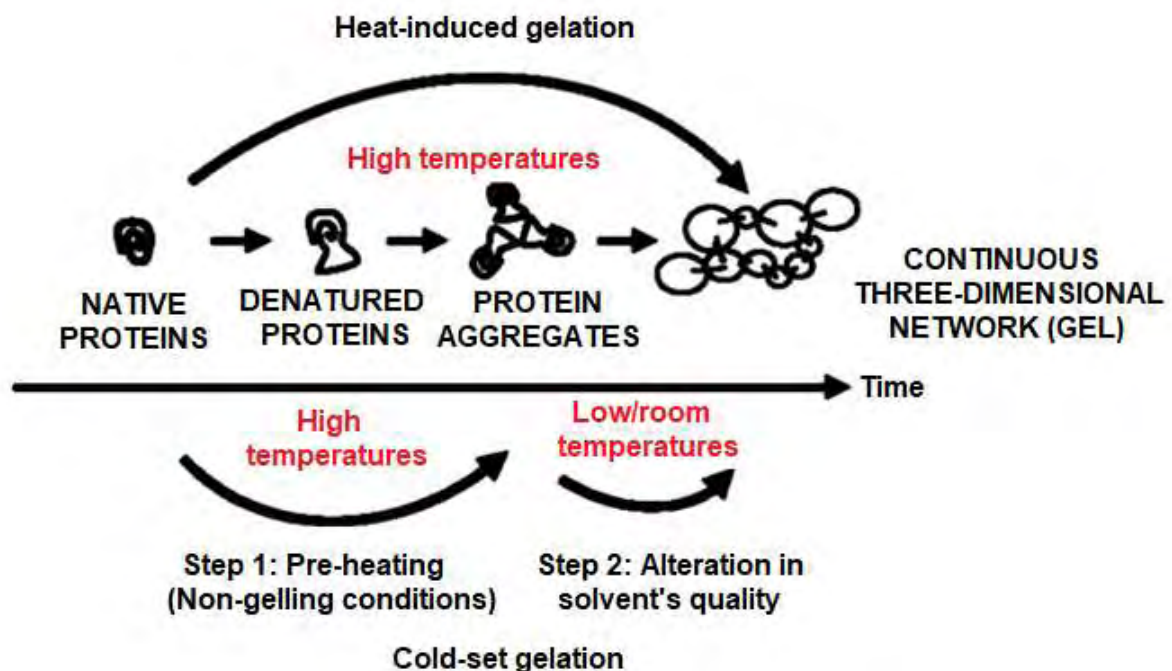
In addition to the previously mentioned advantages, cold gelation methods may originate systems with a wide variety of properties, as the characteristics of the obtained gels are influenced by several factors, including the gelation kinetics, type of induction and properties of aggregates formed during the preheating step (ALTING et al., 2003; RODRIGUES et al., 2020).

For salt-induced gelation methods, for example, the properties of the systems are influenced, not only by the ionic strength, but also by the characteristics of the ions applied (AKO et al., 2010; BRYANT; MCCLEMENTS, 2000; KHARLAMOVA; NICOLAI; CHASSENIEUX, 2018a,b; KHARLAMOVA; NICOLAI; CHASSENIEUX, 2020; KUHN; CAVALLIERI; CUNHA, 2010; KUNDU et al., 2014; MARANGONI et al., 2000; NAVARRA

et al., 2009). Kuhn, Cavallieri e Cunha (2010), for example, investigated the effects of adding different types of salts (sodium chloride and calcium chloride) on the properties of cold-set whey protein isolate gels. These authors verified that the systems formed by the addition of calcium chloride presented greater hardness, elasticity and opacity than the gels obtained by the incorporation of sodium chloride. On the other hand, however, such systems were less deformable and had lower water holding capacities (KUHNS; CAVALLIERI; CUNHA, 2010).

Considering that the different structural organizations influence many characteristics (e.g. opacity, water holding capacity and elastic modulus) of cold-set gels, variations in the quantity and quality of the gelling inducing agent can be investigated and used as interesting tools to obtain systems with desirable and unique properties (ALTING et al 2003; BRYANT; MCCLEMENTS, 2000; CAVALLIERI et al., 2007; CAVALLIERI; CUNHA, 2008; KHARLAMOVA; NICOLAI; CHASSENIEUX, 2018a,b; KHARLAMOVA; NICOLAI; CHASSENIEUX, 2020; TOTOSAUS et al., 2002).

Figure 2.3. Illustrative scheme of heat-induced gelation processes and cold-set gelation processes of protein ingredients.



Source: Adapted from CAVALLIERI, A.L.F. **Cold set gelation of whey proteins: Acidification rate, final pH and polysaccharide addition effects.** Thesis (PhD) Campinas State University, Campinas, Brazil, 2007.

Most of the studies regarding cold-set gelation methods have been developed using whey protein isolates as gelling agents, due to its nutritional value, functional properties and high industrial application (BARBUT, 1995a, b; BRYANT; MCCLEMENTS, 2000; CHEN et al., 2019; CAVALLIERI; CUNHA, 2009; HONGSPRABHAS; BARBUT et al., 1999; KHARLAMOVA; NICOLAI; CHASSENIEUX, 2018a,b; REMONDETTO; SUBIRADE, 2003; RODRIGUES et al., 2020). In recent years, however, plant proteins have been gaining the attention of researchers and industry, due to the new preferences of consumers, who are increasingly concerned with the sustainability and safety of animal-based products (MONTEIRO et al., 2013).

Among the most important plant-based protein ingredients are the soy protein isolates, which present interesting nutritional value and important functional properties, as previously discussed (CHEN ET AL 2017; MALTAIS et al., 2005; MALTAIS; REMONDETTO; SUBIRADE, 2008; MALTAIS; REMONDETTO; SUBIRADE, 2009; MONTEIRO ET AL., 2013; MOURE et al., 2006; NISHINARI et al., 2014; ZHENG et al., 2019; ZHAO et al., 2021).

Like many globular proteins, soy proteins are capable of forming heat induced gels, and the properties of such systems have been widely explored in studies found in the literature (GERMAN; DAMODARAN; KINSELLA, 1982; HERMANSSON, 1986; NICOLAI; CHASSENIEUX, 2019; RENKEMA; GRUPPEN; VAN VLIET, 2002; RENKEMA; KNABBEN; VAN VLIET, 2001; UTSUMI; KINSELLA, 1985; WU et al., 2017; WU et al., 2018). The formation of cold-set SPI gels, on the other hand, is a more recent subject, and has been gaining increasingly attention (CHEN; CHASSENIEUX; NICOLAI, 2018; MALTAIS et al., 2005; MALTAIS; REMONDETTO; SUBIRADE, 2008; MALTAIS; REMONDETTO; SUBIRADE, 2009; ZHAO et al., 2021; ZHENG ET AL. 2019).

It is important to emphasize, however, that in most of the studies regarding SPI gelation, the protein ingredients applied are highly pure and extracted in laboratory, under well controlled conditions (MALTAIS et al., 2005; MALTAIS; REMONDETTO; SUBIRADE, 2008; MALTAIS; REMONDETTO; SUBIRADE, 2009; NISHINARI et al., 2014). As previously discussed, the results obtained in such studies are hardly reproducible in large scale by the food industry, as the commercial SPIs tend to present much more challenging properties, including lower solubilities at acid and neutral pHs (BRITO-OLIVEIRA et al., 2018; LEE; RYUB; RHEEA. 2003).

Such fact only emphasizes the importance and the necessity of the development of investigations about the cold-set gelation of commercial SPIs, for a better comprehension of

the challenges faced by the industry and also for the development of alternatives that allow a wider use of this important ingredient as gelling agent.

2.3 Mixed biopolymer gels

2.3.1 Gelation of mixed systems of protein and polysaccharides

Food matrices are considered complex multicomponent soft materials and have their properties defined by the interactions that occur among the macromolecular components, especially proteins and polysaccharides (LE; RIOUX; TURGEON, 2017; MEZZENGA et al. 2005; MONTEIRO et al., 2013; RAMÍREZ et al. 2002; VAN DER SMAN, 2012). Proteins and polysaccharides are widely applied as functional ingredients in food, both, individually and combined (LE; RIOUX; TURGEON, 2017; LI et al., 2020; MCCLEMENTS, 2006).

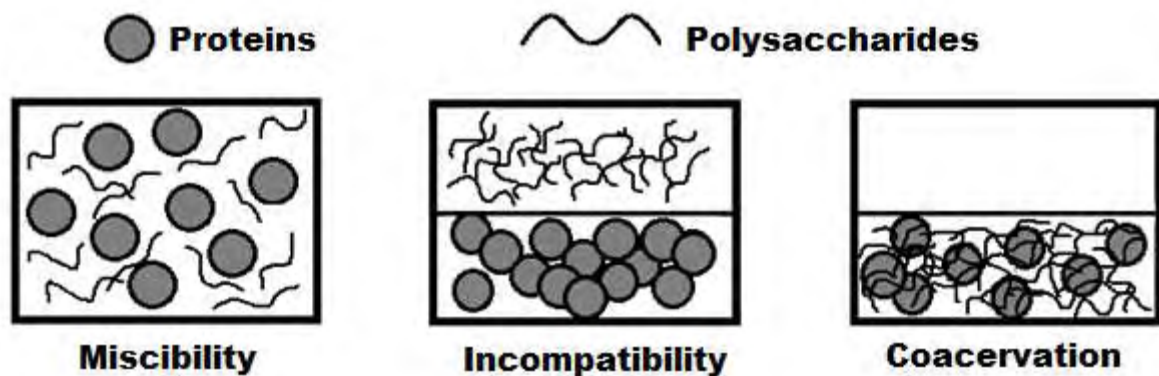
When applied together, these biopolymers can interact in synergistic or antagonistic ways, resulting in major changes in the functional properties of individual ingredients (BENICHO; ASERIN; GARTI, 2002; DE KRUIF; WEINBRECK; DE VRIES, 2004; LE; RIOUX; TURGEON, 2017; MCCLEMENTS, 2006; SCHMITT et al., 1998). For this reason, many studies have been developed aiming the obtation of knowledge regarding the origin and nature of the interactions between proteins and polysaccharides, which can be used for the development of new structures and textures in foods (TURGEON et al., 2003; TURGEON; SCHMITT; SANCHEZ, 2007).

The main non-covalent interactions among proteins and polysaccharides are electrostatic interactions, steric exclusions, hydrophobic interactions and hydrogen bonds (MCCLEMENTS, 2006; WIJAYA et al., 2017). The relative importance of each in a particular system depends on several factors related to the characteristics of the biopolymers (eg molecular mass, charge density, flexibility, hydrophobicity) and the characteristics of the medium (e.g., pH and ionic strength) (MCCLEMENTS, 2006; WIJAYA et al., 2017).

Depending on these factors, proteins and polysaccharides in dispersion can attract or repel each other, originating three possible equilibrium situations, illustrated in Figure 2.4: (I) incompatibility, with strong repulsion (two aqueous phases, immiscible, and each one rich in only one type of biopolymer), (II) coacervation, with strong attraction (two distinct aqueous phases, one rich in both polymers and the other poor in both) or (III) miscibility (interactions between different biopolymers are similar to the interaction between equal biopolymers,

resulting in miscibility) (CAVALLIERI, 2007; DELBEN; TEFANCICH, 1997; SYRBE et al., 1998).

Figure 2.4. Representation of the three possible equilibrium situations for protein and polysaccharide solutions.



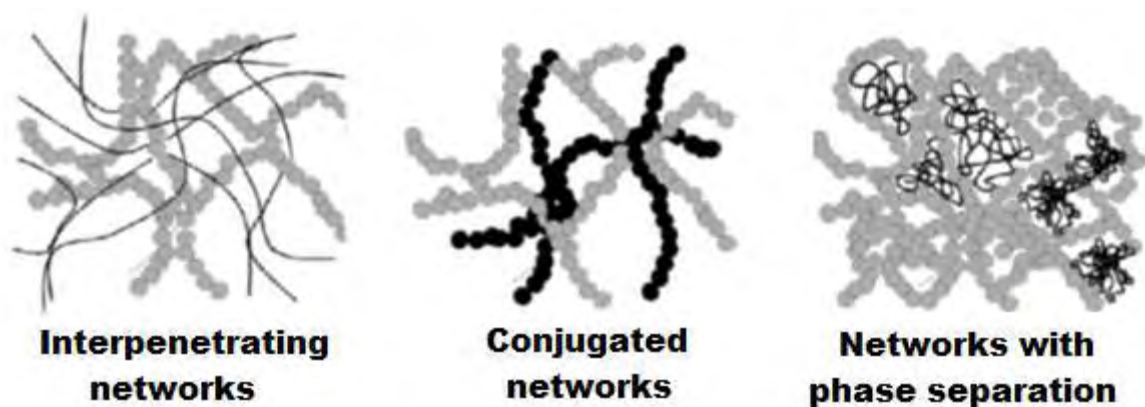
Source: Adapted from CAVALLIERI, A.L.F. **Cold set gelation of whey proteins: Acidification rate, final pH and polysaccharide addition effects.** Thesis (PhD) Campinas State University, Campinas, Brazil, 2007.

It is known that when one or more biopolymers have gelling properties, protein-polysaccharide dispersions can be used to obtain three-dimensional networks with characteristic viscoelastic properties, also known as mixed biopolymeric gels (JONG; VAN DE VELDE, 2007; JONG; JAN KLOK; VAN DE VELDE, 2009; MONTEIRO et al., 2013; RAMÍREZ et al. 2002; TURGEON et al., 2003;).

Such systems have been frequently studied aiming at the development of new products with desirable structural and sensory properties (BI et al., 2017; CHANG ET AL., 2014; DICKINSON, 1993; GEREMIAS-ANDRADE et al., 2017; JONG; VAN DE VELDE, 2007; JONG; JAN KLOK; VAN DE VELDE, 2009; KASRAN; CUI; GOFF, 2013; KUHN; CAVALLIERI; CUNHA, 2011; MONTEIRO et al., 2013; MONTEIRO; LOPES-DA-SILVA, 2017; VAN DE VELDE et al., 2015; VILELA; CAVALLIERI; CUNHA, 2011; WANG et al., 2011; WIJAYA et al., 2017). Under specific conditions, polysaccharides may be able to stabilize the structures formed by proteins, improving the gelling properties of protein ingredients and allowing the obtention of gels with very specific rheological and microstructural properties (KUHN; CAVALLIERI; CUNHA, 2011; JONG; VAN DE VELDE, 2007; MONTEIRO et al., 2013).

Depending on these properties, gelled systems are often classified as: (I) systems with interpenetrating networks, (II) conjugated networks or (III) networks with phase separation, as shown in Figure 2.5 (CAVALLIERI, 2007; JONG; VAN DE VELDE, 2007; MORRIS, 1997). According to the literature, however, most of the food systems are organized as phase separated networks, that generally result from thermodynamic incompatibility (LE; RIOUX; TURGEON, 2017; JONG; VAN DE VELDE, 2007; MORRIS; WILDE, 1997; TURGEON et al., 2003).

Figure 2.5. Possible classification of mixed gels according to their microstructural organizations.



Source: Adapted from CAVALLIERI, A.L.F. **Cold set gelation of whey proteins: Acidification rate, final pH and polysaccharide addition effects.** Thesis (PhD) Campinas State University, Campinas, Brazil, 2007.

The occurrence and extent of phase separation processes are influenced by several factors including the characteristics of the biopolymers (molecular weight, conformation, charge density, etc.), the conditions of the medium (pH, ionic strength, solvent quality, etc.), mixing conditions (proportion, total concentration, etc.) and the processing conditions applied (heat treatment, pressure, shear, etc.) (WIJAYA et al., 2017; TAVARES et al., 2005; TURGEON et al., 2003).

Therefore, the comprehension of the gelation processes and the proper characterization of the mixed gels are fundamental, especially considering that phase separations can be either harmful to the quality of the final product (if macroscopically evident) or beneficial (if they result in desirable changes, resulting in new appearances and textures) (KUHN; CAVALLIERI; CUNHA, 2011).

According to Jong and Van de Velde (2007), the microstructure of phase separated gels result from the competition between a demixing process and gel formation by one or more of the biopolymers. The gelation process generally stops the demixing process before it reaches an equilibrium and becomes macroscopically evident (TURGEON et al., 2003; JONG; VAN DE VELDE, 2007; JONG; JAN KLOK; VAN DE VELDE, 2009). In this context, phase separation in mixed biopolymeric gels are often explained as processes that present a kinetic nature and result from local fluctuations in the concentrations of biopolymers in the total volume of the mixture (TURGEON et al., 2003). Therefore, the gelation method and rate can be considered determinant factors for the microstructure and the rheological properties of the mixed biopolymeric gels (JONG; VAN DE VELDE, 2007; JONG; JAN KLOK; VAN DE VELDE, 2009; TURGEON et al., 2003).

In most of the studies found in the literature regarding the properties of mixed biopolymeric gels, the authors applied heat-induced gelation methods (MONTEIRO et al., 2013; MONTEIRO; LOPES-DA-SILVA, 2017; NISHINARI; ZHANG; IKEDA, 2000; ROCHA et al., 2009; SANCHEZ et al., 1997; TAVARES et al., 2005; TAVARES; LOPES-DA-SILVA, 2003; TURGEON; BEAULIEU, 2001; ZHUANG et al., 2020). On the other hand, some authors have already shown that these systems can be obtained using cold-set gelation methods, by incorporating the polysaccharides to the protein dispersions before the second step of the processes (ie, gelation induction) (BI et al., 2017; CAVALLIERI; CUNHA, 2009; JONG; JAN KLOK; VAN DE VELDE, 2009; KUHN; CAVALLIERI; CUNHA, 2011; VILELA; CAVALLIERI; CUNHA, 2011; ZHAO et al., 2020).

In addition, most of the information available on mixed biopolymeric gels was obtained using whey protein isolates (BEAULIEU; TURGEON; DOUBLIER, 2001; BERTRAND; TURGEON, 2007; CAVALLIERI; CUNHA, 2009; DE JONG; VAN DE VELDE, 2007; VAN DE VELDE et al., 2015; MONTEIRO et al., 2005; ROCHA et al., 2009; TAVARES; LOPES-DA-SILVA, 2003; TAVARES et al., 2005; VILELA; CAVALLIERI; CUNHA, 2011). Much less is known about the behavior of mixed systems produced with plant proteins, such as the SPI (BI et al., 2017; CHANG et al., 2014; MONTEIRO et al., 2013; MONTEIRO; LOPES-DA-SILVA, 2017). Considering the influence of the biopolymer's characteristics on the gel's properties and the growing preference of consumers for vegan foods (MONTEIRO et al., 2013), further studies involving the gelation of mixed systems of polysaccharides and plant proteins are necessary.

2.3.2 Galactomannans: guar gum and locust bean gum

The galactomannans are neutral polysaccharides, obtained from the seeds of some Leguminosae, consisting of linear chains of 1,4-linked β -D-mannopyranose residues to which varying proportions of a α -D-galactopyranosyl residues are randomly attached at position 6 as sidechains (BEMILLER; HUBER, 2010; MANNION et al. 1995; MONTEIRO et al., 2013; MONTEIRO; LOPES-DA-SILVA, 2017; SHARMA et al., 2020; TAVARES et al., 2005).

Such polysaccharides have attracted the attention of researchers and the food industry due to its relative low price and interesting properties, including the ability to retain water and increase the viscosity of aqueous systems (SRIVASTAVA; KAPOOR, 2005; SHARMA et al., 2020). The interest in the application of these polysaccharides is even higher for being classified as “GRAS” (generally recognised as safe) (HALLAGAN et al., 1997; SRIVASTAVA; KAPOOR, 2005).

According to the literature, the different galactomannans present different mannose-to-galactose (M/G) ratios, which depending on the origin of the polysaccharide (BEMILLER; HUBER, 2010; MONTEIRO et al., 2013). Such degree of galactose substitution in the mannose chain influences the behavior and functionality of these compounds (BEMILLER; HUBER, 2010; MCCLEARY et al. 1981; LOPES-DA-SILVA et al., 1996; MONTEIRO et al., 2013; SHARMA et al., 2020).

Among the most exploited galactomannans are the guar gum (GG) (Figure 2.6) and locust bean gum (LBG) (Figure 2.7), which present M/G ratios of 1.8 and 3.5, respectively, and have the chemical structures illustrated in Figure 2.8 (BARAK; MUDGIL, 2014; BEMILLER; HUBER, 2010; DAAS; SCHOLS; DE JONGH, 2000; DEA et al., 1977).

According to Barak and Mudgil (2014), the higher M/G of the LBG makes this polysaccharide less soluble in water at room temperature than the GG. Sánchez, Bartholomai and Pilosof (1995), affirm that the the degree of interactions among adjacent chains of LBG molecules is higher due to the low degree of galactose substitution in the mannose chain, leading to the formation of crystalline regions that hinder the dispersion of this polysaccharide in water at room temperature. However, such crystalline regions are broken when LBG is heated to approximately 80 °C for 30 minutes, allowing an increase in the solubility of this polysaccharide (BARAK; MUDGIL, 2014; SÁNCHEZ; BARTHOLOMAI; PILOSOFF, 1995; SRIVASTAVA; KAPOOR, 2005).

Locust bean gum is considered the first galactomannan to be used as an industrial additive, and, in the case of the food industry, it has gained space for being able to produce very

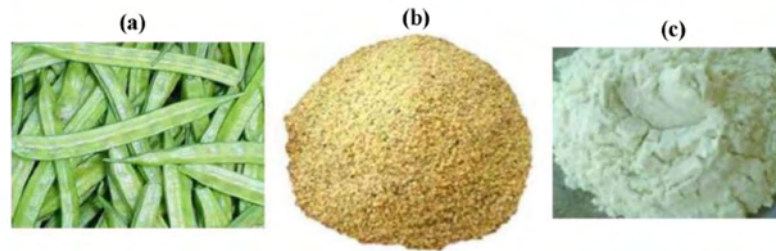
viscous solutions in low concentrations and for being an interesting alternative to stabilize emulsions and replace fats in many products (BARAK; MUDGIL, 2014). Also, according to the literature, LBG can provide a creamy aspect to food products, and, for this reason, it is widely applied in cream cheeses, ice cream, frozen desserts, and yoghurts. (BARAK; MUDGIL, 2014; UNAL; METIN; ISIKLI, 2003).

Guar gum, on the other hand, is commonly applied in ice cream, sauces, and cake mixes (MUDGIL; BARAK; KHATKAR, 2014; PARIJA; MISRA; MOHANTY, 2001). According to Kays, Morris and Kim (2006), this polysaccharide exerts stabilizing, emulsifying and thickening functions in various food products and contributes to the portion of soluble dietary fiber of the original seeds. In addition, some studies claim that GG is interesting to control the release of specific drugs in the gastrointestinal tract and may collaborate in the treatment of colorectal cancer and in the oral rehydration of solutions in the treatment of cholera in adults (CUNHA; PAULA; FEITOSA, 2007; WANG et al., 2010).

GG's ability to retain water is considered one of its most interesting properties. According to Sánchez, Bartholomai and Pilosof (1995), due to the high degree of galactose substitution in the mannose chain, GG has a water retention capacity of approximately 40 mL/g, while for LBG this value is only 11.6 mL/g. On the other hand, these authors found that the hydration time of GG is longer than the hydration time of LBG, probably because the galactose substituents are not uniformly distributed in the main chain but agglomerated in blocks. Thus, macromolecules tend to exhibit regular (or “smooth”) regions of unsubstituted mannose residues, alternating with irregular regions replaced with galactose residues. According to the literature, this structural organization results in the longest hydration times of the GG (SÁNCHEZ; BARTHOLOMAI; PILOSOFF, 1995).

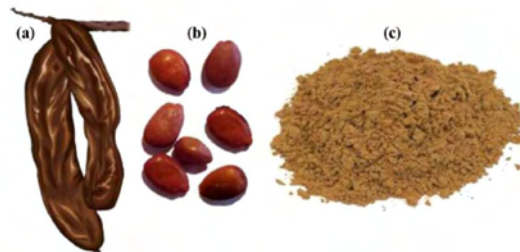
In addition to affecting the water retention capacity, the degree of galactose substitution in the mannose chain interferes in the interactions of galactomannans with other macromolecules present in food systems (BEMILLER; HUBER, 2010). For this reason, many studies have been developed for the comprehension of the behavior and the effect of incorporating these polysaccharides in protein systems, such as gels, or in systems containing other polysaccharides (BEMILLER; HUBER, 2010; HIGIRO et al., 2007; LOPES-DA-SILVA et al., 1996; MCCLEARY et al. 1981; MONTEIRO et al., 2013; MONTEIRO; LOPES-DA-SILVA, 2017; RAMÍREZ et al., 2002; SCHORSCH; GARNIER; DOUBLIER, 1997; TAVARES et al., 2005).

Figure 2.6. Guar gum: (A) pod, (B) seed and (C) powder.



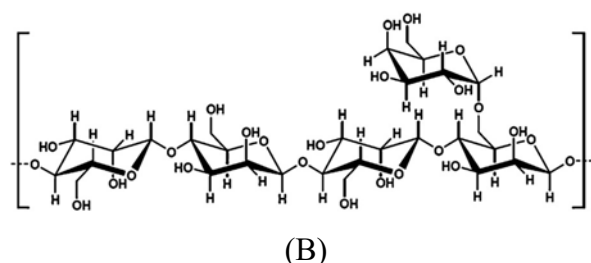
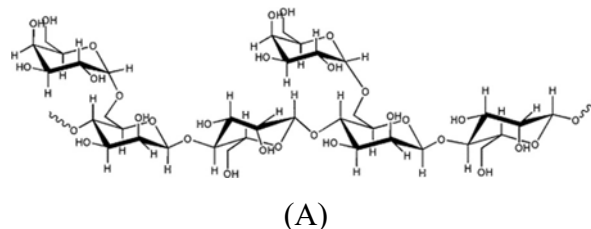
Source: V.D. Prajapati et al. / **International Journal of Biological Macromolecules**,
Nova Iorque, 60 (2013) 83– 92

Figure 2.7. Locust bean gum: (A) pod, (B) seed and (C) powder.



Source: V.D. Prajapati et al. / **International Journal of Biological Macromolecules**,
Nova Iorque, 60 (2013) 83– 92

Figure 2.8. Chemical structure of guar gum (A) and locust bean gum (B) molecules.



Sources: (A) WANG et al. Structure–antioxidant relationships of sulfated galactomannan from guar gum. **International Journal of Biological Macromolecules**, Nova Iorque, v. 46, p. 59-66, 2010. (B) BARAK, S; MUDGIL, D. Locust bean gum: Processing, properties and food applications - A review. **International Journal of Biological Macromolecules**, Nova Iorque, v. 66, p. 74–80, 2014.

2.3.3 Incorporation of galactomannans to protein gels

The behavior of different galactomannans in multicomponent systems have attracted the attention of researchers, who seek to understand the influence of their chemical structures on the interactions of these compounds with other macromolecules (TAVARES et al., 2005; MONTEIRO et al., 2013). The mannose-to-galactose (M/G) ratio of galactomannans plays an important role in the interactions of these polysaccharides with other compounds, like different polysaccharides (LOPES-DA-SILVA et al. 1996; SCHORSCH; GARNIER; DOUBLIER, 1997) and protein ingredients (GONÇALVEZ et al., 2004; MONTEIRO et al., 2005; MONTEIRO et al., 2013; TAVARES; LOPES-DA-SILVA, 2003; TAVARES et al., 2005).

Tavares et al. (2005), for example, was one of the first authors to investigate the influence of the mannose-to-galactose ratio of different galactomannans (guar gum, tara gum and locust gum), in concentrations ranging from 0 to 0.6%, in the gelation of whey protein isolate (13%), at pH 7. The results showed that the presence of galactomannans increased the strength of the gels and reduced the gelation temperatures. According to the study, such effects were more pronounced with the reduction in the degree of branching (substitution of galactose in the mannose chain) of the polysaccharides. The authors also found that mixed gels were organized as two-phase systems. In low concentrations of polysaccharides, the systems presented polysaccharide-rich phases dispersed in the protein matrix, however, in high concentrations of galactomannans (except for guar gum), phase inversions were verified (TAVARES et al., 2005). According to the authors, the higher number of galactose side chains of guar gum (M/G ratio of 1.5) hindered the galactomannan-galactomannan interactions necessary for the occurrence of more severe phase separation.

Fitzsimons, Mulvihill and Morris (2008), on the other hand, studied the effects of the incorporation of guar gum on the heat-induced gelation of WPI (3%), and verified that the incorporation of polysaccharide in concentrations up to 0.05% increased the strength of the systems, however, in higher concentrations, the strength of the gels decreased. In concentrations of 0.5% GG, the samples presented a liquid aspect due to an excessive protein aggregation, caused by the segregative interactions between the different macromolecules, which resulted in the collapse of the cross-links of the gelled networks.

Cavallieri and Cunha (2009) obtained similar results when they studied the incorporation of GG (0-0.5 %) on cold-set WPI gels (5%), induced by acidification. The incompatibility found in WPI systems with high concentrations of GG was related to the mutual exclusion of the accessible volume of the biopolymers mass. Such an effect, known as the

volume exclusion effect (CAVALLIERI; CUNHA, 2009; TOLSTOGUZOV, 2003; ZASYPKIN; BRAUDO; TOLSTOGUZOV, 1997), resulted in the discontinuity of the microstructure of the gels and the formation of non self-supported systems.

Cold-set gelation by acidification was also applied by Sanchez et al. (2000) when they investigated the effects of incorporating locust bean gum on the properties of whey proteins. Like Cavallieri and Cunha (2009), these authors also related the formation of the discontinuous microstructure of systems with high concentrations of polysaccharide, to the formation of regions excessively rich in protein and others in LBG. According to them, as a result of this process, the porosity of the gels was increased in the presence of polysaccharides, due to a localized increase in the density of the casein network in certain regions of the microstructure of the gels.

Differently from Sanchez et al. (2000), Rocha et al. (2009) did not verify the collapse of the whey protein concentrate gels with the increase in the concentration of locust bean gum. However, these authors observed that the incorporation of such galactomannan in concentrations higher than 0.3% reduced the strength of the gels, while the incorporation of 0.1% of polysaccharide significantly increased the strength of the heat-induced systems.

Although several authors have investigated the effects of the incorporation of galactomannans in whey protein gels, a smaller number of studies have reported the behavior of mixed gels produced with these polysaccharides and plant proteins, such as the soy protein isolates (BI et al., 2017; HUA et al. 2003; MONTEIRO et al., 2013; MONTEIRO; LOPES-DA-SILVA, 2017; ZHU et al 2009).

As previously cited, although whey proteins are widely used in the food industry, plant-based ingredients have been gaining the interest of researchers due to the new preferences of the consumers and their concerns regarding the safety of products of animal origin (GOOD FOOD INSTITUTE, 2020; MCCLEMENTS, 2019, 2020; LOVEDAY, 2019; MONTEIRO et al., 2013; VAN DER GOOT et al., 2016). In this context, Monteiro et al. (2013) developed a study to investigate the influence of the incorporation of different galactomannans (locust bean gum, guar gum and tara gum), in concentrations ranging from 0 to 0.5%, on the properties of heat-induced SPI gels, at pH 7. The results revealed that the presence of galactomannans reduced the critical gelling concentration of the proteins, reduced the gelation temperature and increased the strength of the systems. Such effects were more pronounced in more branched polysaccharides.

Since the concentration of galactomannans and the degree of galactose substitution in the mannose chain affect the degree of demixing and phase separation in mixed gels, the

incorporation of these polysaccharides to SPI systems can result in matrices with a wide variety of morphologies, which can be considered extremely useful for the development of new food formulations (BI et al., 2017; HUA et al. 2003; MONTEIRO et al., 2013; MONTEIRO; LOPES-DA-SILVA, 2017; ZHU et al 2009).

In addition, as previously discussed, the incorporation of polysaccharides such as galactomannans into SPI gels may represent an interesting alternative for improving the functional properties of such protein ingredient, which, when extracted at an industrial level, tend to present challenging properties, such as such as low solubilities at acidic and neutral pHs.

In a recent study by our research group (BRITO-OLIVEIRA et al., 2018), the ability of the commercial SPI to form cold-set gels, under different conditions, was evaluated and the results revealed that self-supported gels produced at pH 7 showed relative structural instability. Such instability, however, was minimized with the incorporation of locust bean gum into the systems. The results of the rheological tests revealed that mixed gels produced with SPI and LBG were stronger than systems produced only with the protein ingredient, which was related to the microstructure of the mixed gels, which presented phase separation.

Although these results confirmed the potential of LBG to improve the properties of commercial SPIs, the number of studies regarding the behavior of SPI-galactomannan mixed gels is still limited. Thus, the development of research for the proper understanding of the interactions between such macromolecules is interesting for the development of systems new food systems with unique rheological and microstructural properties.

2.4 Emulsion-filled gels (EFG)

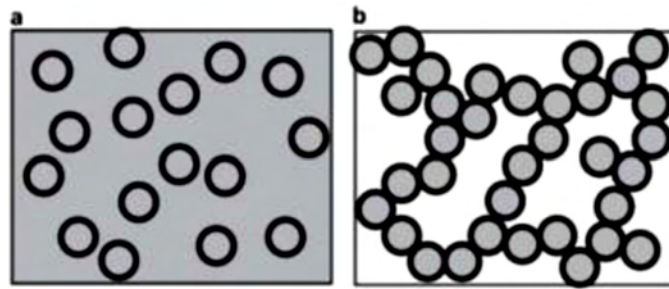
2.4.1 Importance of the emulsion filled gels to the food industry

Filled gels are highly complex systems, consisting of gelled matrices, incorporated with different structures, known as “fillers” (BROWNSEY; MORRIS, 1998). According to Brownsey and Morris (1998), in food systems, fillers can be fibers, gas bubbles, lipid droplets, crystals, fat globules or cellular components.

One of the most important filled gels for the food industry are the emulsion-filled gels, which consist of oil droplets or lipid particles incorporated in the gelled matrices (DICKINSON, 2012; FARJAMI; MADADLOU, 2019; LU et al., 2019; LU et al., 2020; OLIVER; SCHOLTEN; VAN AKEN, 2015; SALA et al., 2009a, b; VAN VLIET, 1988). Such systems

can be obtained from a stable emulsion through the gelation of the continuous phase, or by aggregation of the emulsion droplets caused by some type of operation, such as heat treatment, acidification, and enzymatic treatment, as shown in Figure 2.9 (DICKINSON, 2012; FARJAMI; MADADLOU, 2019; LU et al., 2019; LU et al., 2020).

Figure 2.9. Schematic representation of the structure of emulsion-filled gels obtained by (a) the gelation of the continuous phase and (b) aggregation of the emulsion droplets.



Source: DICKINSON, E. Emulsion gels: The structuring of soft solids with protein-stabilized oil droplets. **Food Hydrocolloids**, Oxford, v. 28, n. 1, p. 224-241, 2012.

Although the application of EFG is already a reality in the food industry, in products like yoghurts, fresh cheeses, gelatines, dairy desserts, puddings and sausages, the development of new formulations has been arousing the interest of researchers (LIU et al., 2015; LU et al., 2019; LU et al., 2020; OLIVER; SCHOLTEN; VAN AKEN, 2015; ROSA et al., 2006; SALA et al., 2009 a, b; SALA et al., 2008). This is because combined applications of lipids and gelling agents may allow, for example, a significant reduction in the lipid content of products, without compromising its sensory quality (LIU et al., 2015; OLIVER; SCHOLTEN; VAN AKEN, 2015).

Alternatives like this are essential for the development of new formulations as consumers have been increasingly concerned with excessive fat intake, often associated with the development of health problems such as obesity, hypertension and heart diseases (LIU et al., 2015; OLIVER; SCHOLTEN; VAN AKEN, 2015; PARADISO et al., 2015; UTZSCHNEIDER et al., 2013).

Although necessary, the reduction of fat content in food formulations represents a major challenge for the industry, as lipids play an important role in the sensory properties of products, such as taste and texture (VAN AKEN; VINGERHOEDS; DE WIJK, 2011; LIU et al., 2015). According to the literature, texture is considered a critical factor in food

acceptability, so changes and/or developments of formulations should involve not only research in the areas of physiology, psychology and sensory analysis, but also in-depth studies on the structural organizations of systems (GUINARD; MAZZUCHELLI, 1996; GWARTNEY; LARICK; FOEGEDING, 2004; SZCZESNIAK, 2002; WILKINSON; DIJKSTERHUIS; MINEKUS, 2000).

Research that investigates the structural aspects of food products (or product prototypes), generally involves mechanical and microstructural characterizations of the systems, which are directly influenced by their composition and the interaction among the components (BELLAMY et al., 2009; DICKINSON, 2012; GWARTNEY; LARICK; FOEGEDING, 2004; HUTCHINGS; LILLFORD, 1988; LIU et al., 2015; STOKES; BOEHM; BAIER, 2013; VAN AKEN; VINGERHOEDS; DE WIJK, 2011; WILKINSON; DIJKSTERHUIS; MINEKUS, 2000).

For this reason, studies involving EFG require rheological tests and microscopy techniques as analytical tools to understand the influence of the characteristics of the gelled matrix (LORENZO; ZARITZKY; CALIFANO, 2013; SALA et al, 2008; SALA et al., 2009a), dispersed lipids (SALA et al., 2009b; VAN AKEN; OLIVER; SCHOLTEN, 2015), and the interactions among the different components (SALA et al., 2007) in the final properties of the systems (DICKINSON, 2012; FARJAMI; MADADLOU, 2019; LU et al., 2019; LU et al., 2020; LORENZO; ZARITZKY; CALIFANO, 2013).

For EFG, rheological tests of high deformation are essential, as they provide information on the apparent elasticity and fracture properties of the systems, which satisfactorily represent their behavior during processing (e.g. mixing, cutting, slicing) and consumption (ROSA et al., 2006; VAN VLIET, 2002). On the other hand, only tests with small deformations (e.g. oscillatory tests), provide some important information regarding the viscoelastic nature of the samples (RAO, 2014; TABILO-MUNIZAGA; BARBOSA-CÁNOVAS, 2005). Thus, it is accepted that only the combined application of small and large deformation techniques allows the complete characterization of systems as complex as EFGs (TABILO-MUNIZAGA; BARBOSA-CÁNOVAS, 2005).

Also, some mathematical models have already been developed a prediction and adequate interpretation of rheological properties of EFG (VAN DER POEL, 1958; VAN VLIET, 1988). However, in most cases, the experimental and theoretical results show considerable deviations, as the models consider samples with homogeneously distributed fillers, which is hardly seen in real systems (CHEN; DICKINSON, 1998; ROSA et al., 2006; VAN VLIET, 1988).

In this context, although the complexity of EFGs makes it difficult to develop accurate models, efforts continue to be made so that the rheological properties of such systems can be predicted based on the properties and quantity of fillers and the presence or absence of interactions between the filler particles/droplets and the gel network (BROWNSEY et al., 1987; GWARTNEY; LARICK; FOEGEDING, 2004; LANGLEY; GREEN, 1989; VAN VLIET, 1988).

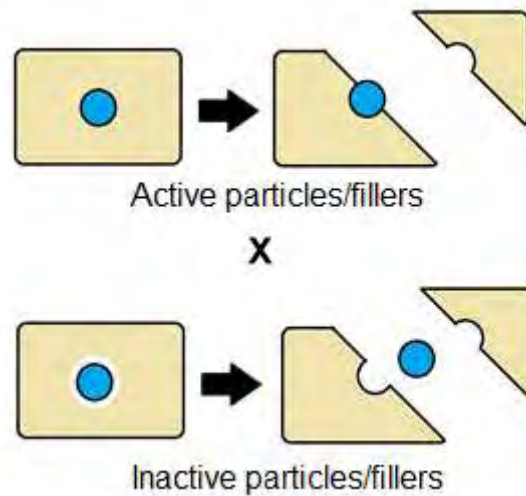
2.4.2 Effects of surfactant-matrix interactions on the properties of emulsion filled gels

Emulsion-filled gels (EFG) are extremely complex systems, whose rheological properties depend on several factors, such as the properties of the gelled matrix, the properties and concentration of the fillers (in this work referred to as particles) and the nature of the interactions among the different components (FARJAMI; MADADLOU, 2019; LU et al., 2019; LU et al., 2020; OLIVER; SCHOLTEN; VAN AKEN, 2015; ROSA et al., 2006; TOLSTOGUZOV; BRAUDO, 1983; VAN VLIET, 1988).

Depending on their effect on the rheology of gels, the particles are usually classified as active (bound) or inactive (unbound) (Figure 2.10) (GEREMIAS-ANDRADE et al., 2016; OLIVER; SCHOLTEN; VAN AKEN, 2015; RING; STAINSBY, 1982; SALA et al., 2007; VAN AKEN; OLIVER; SCHOLTEN, 2015; VAN VLIET, 1988). According to the literature, whereas the active particles interact with the gelled matrix, the inactive particles have little chemical affinity with the molecules that form the gel (GEREMIAS-ANDRADE et al., 2016; RING; STAINSBY, 1982). Consequently, inactive particles tend to reduce the elastic modulus of systems, while active particles can increase or decrease this parameter (GEREMIAS-ANDRADE et al., 2016; OLIVER; SCHOLTEN; VAN AKEN, 2015; RING; STAINSBY, 1982; SALA et al., 2007; VAN AKEN; OLIVER; SCHOLTEN, 2015; VAN VLIET, 1988).

Moreover, incorporations of active and inactive particles have different effects on the rupture properties of the EFG. Whereas the incorporation of inactive particles reduces the rupture stress and can reduce or increase the rupture strain of the systems, the incorporation of active particles tends to increase the rupture stress and reduce the rupture strain of the EFG (OLIVER; SCHOLTEN; VAN AKEN, 2015).

Figure 2.10. Representation of active and inactive particles in emulsion-filled gels.



Source: Own authorship.

Since the interactions between the dispersed lipid phase and the gelled matrix depend on the surface properties of the particles, several studies investigate the influence of the nature of the surfactant applied on the properties of the EFG (DICKINSON; CHEN, 1999; OLIVER; SCHOLTEN; VAN AKEN, 2015; ROSA ET AL 2006; SALA et al., 2007; SALA et al., 2009a, b). In most of them, the authors investigated the properties of whey protein gels, using, basically, two types of surfactants: proteins (usually also represented by whey proteins) and surfactants low molecular weight, such as polysorbates (especially Tween 20) (DICKINSON; CHEN, 1999; YOST; KINSELLA, 1992; MANTOVANI; CAVALLIERI; CUNHA, 2016).

Chen and Dickinson (1998), for example, investigated the viscoelastic properties of gels filled with emulsions stabilized by whey protein isolate, and found that the strength of the gels increased with the incorporation of protein-stabilized emulsions. On the other hand, the results showed that the presence of the Tween 20 surfactant caused a drastic reduction in the strength of the EFG, which was attributed to the displacement of proteins from the oil-water interface. According to the authors, the oil droplets completely covered with Tween 20 are not able to bind to the protein matrix and, therefore, do not contribute to the strengthening of the gel. Therefore, while emulsions stabilized by protein were classified as active in the systems, those stabilized with Tween 20 proved to be inactive.

Sala et al. (2007), on the other hand, investigated the high deformation properties of gelatin gels, whey protein isolate (WPI) or κ -carrageenan, filled with emulsions stabilized by WPI, WPI aggregates, lysozyme or Tween 20. The results obtained showed that, for gelatin

gels, emulsions stabilized by WPI and lysozyme increased the elastic modulus of the systems (active droplets), while those stabilized with Tween 20, reduced this property (inactive droplets). For WPI gels, emulsions stabilized by WPI aggregates, lysozyme and low concentrations of Tween 20 increased the modulus of elasticity (Young's modulus) of the gels (active droplets). According to the authors, variations observed in the Young's modulus of κ -carrageenan gels, were related to the interactions between the matrix and the gelling agents present in the aqueous medium. In general, the results showed that the rupture strain of the systems decreased with the increase of the lipid concentration for the active droplets and remained constant for the inactive ones. In addition, the authors found that theories that describe the effects of incorporating fillers on the rupture properties of the gels failed to predict the results of the experiment. This fact was attributed to the small size of the droplets, which were similar to the structural defects present in the gelled networks.

Unlike these authors, who used heat-induced gelation method, Rosa et al. (2006), used a cold-set gelation method for the production of EFG, using WPI-stabilized emulsion. For this purpose, a suspension of soluble WPI aggregates was mixed with oil in water emulsion to obtain gels with different concentrations of WPI aggregates and oil. The authors verified that, for emulsions stabilized with native WPI, the systems were instable, probably as a result of the differences in size between the droplets and the aggregates. For emulsions stabilized with soluble WPI aggregates, on the other hand, the suspension was stable and the EFG were adequately produced. The results of uniaxial compression of the systems showed the increase in oil concentration resulted in increases in the fracture stress of the gels and reductions in fracture strain (ROSA et al., 2006). As previously mentioned, such effects are obtained in the presence of active particles in EFG.

Ye and Taylor (2009), on the other hand, investigated the cold-set gelation of preheated WPI-stabilized emulsions. The gelation processes were induced by acidification or addition of CaCl_2 , at room temperature. The results revealed that the storage modulus of the gels obtained by acidification increased with the increase of the preheating temperature, with the reduction of the emulsion droplet size and with the increase of the fat content. According to the authors, preheating was the initial step for the formation of the EFG. During this process, the adsorbed proteins were denatured and aggregated on the surfaces of the emulsion droplets, and such droplets, stabilized by WPI, constituted the structural units responsible for the formation of three-dimensional networks.

Geremias-Andrade et al. (2017) also produced EFG using WPI, however, the authors added xanthan gum to the systems, originating mixed biopolymeric gels. Such gels were filled

with solid lipid particles (SLP) encapsulating curcumin. The SLP were produced using babaçu oil and tristearin as lipid phase and mixtures of tween 60 and span 80 as surfactants. The results obtained by the authors revealed that the SLP were homogeneously distributed in the gel matrix and increased the water holding capacity of the systems. Still, according to this study, the interactions between protein and surfactants, as well as the porosity of the gels and the concentration of SLP, affected in different ways the behavior of the EFG when subjected to small and large deformations.

Although the behavior of EFG produced with WPIs has been widely explored in the literature, research regarding the properties of systems produced with SPI (especially obtained by cold-set gelation) is still scarce (KIM; RENKEMA; VAN VLIET, 2001; LI et al., 2012; TANG; LIU, 2013). This number is even more limited when it comes to commercial soy protein isolates, which, as discussed earlier, tend to have challenging properties.

In a recent study by our research group (BRITO-OLIVEIRA et al., 2018), cold-set gels of commercial SPI, in the presence and absence of locust bean gum, were filled with SLP stabilized with Tween 80 and Span 80. For protein gels and for mixed gels, the incorporation of SLP altered the microstructural organization of the systems and increased the values of Young's modulus, storage, and loss moduli. The same formulation of SLP were applied (BRITO-OLIVEIRA et al., 2017) for the production of EFG of commercial SPI and xanthan gum. The comparative study of the properties of non-filled gels and EFG revealed that the SLP stabilized with Tween 80-Span 80 behaved as active fillers in the gel, increasing the Young's modulus, storage, and loss moduli of the systems. In addition, it was found that the incorporation of SLP affected the microstructural organization of the systems, as non-filled gels presented a microstructural organization of interpenetrating networks, while the EFGs presented a microstructure with clear phase separation. In both studies, the incorporation of SLPs resulted in increases of both rupture properties of the gels. As previously cited, increases of E_g and σ_H , are generally associated to incorporations of active fillers in the EFG. On the other hand, such incorporations generally result in decreases of ϵ_H , which was not verified in the studies (BRITO-OLIVEIRA et al., 2017, 2018)

Reductions in rupture strain are associated to the incorporation of active particles in systems, because, in most cases, these structures behave as structural defects/structural breakers within the matrices (LIU et al., 2015; OLIVER; SCHOLTEN; VAN AKEN, 2015). As the rupture processes start in weaker regions of the gelled networks, structural defects or active particles can act as stress concentration points in the matrices, decreasing the ϵ_H of the systems (LIU et al., 2015; OLIVER; SCHOLTEN; VAN AKEN, 2015). On the other hand, it is known

that the extent of this effect depends on many factors, such as the diameter, distribution, and degree of aggregation of the particles in the gels (LIU et al., 2015). Therefore, the increases of ϵ_H verified in the previous studies of our research group (BRITO-OLIVEIRA et al., 2017, 2018) with the incorporation of the active SLP may be justified by the homogeneous distribution of these structures in the gelled matrices, which prevented it to act as structural defects in the systems (BRITO-OLIVEIRA et al., 2017, 2018)

These data reinforce that, although some mathematical models have already been developed for the analysis and prediction of the effects of the incorporation of lipid particles/droplets in EFG, this could only be satisfactorily accomplished if such models and theories considered and quantified effects of the shape, size, distribution and aggregation processes of droplets or lipid particles in the matrices, given the high complexity of the systems (OLIVER; SCHOLTEN; VAN AKEN, 2015).

From the content exposed in this bibliographic review and considering the specificity of each EFG, the study of the effect of the incorporation of SLP in cold-set gels of SPI, in the presence and absence of galactomannans, through rheological and microstructural characterizations can be considered an interesting step for the development of new products with desirable and unique properties.

2.5 Characterization and stability of gelled systems

Ingredients with gelling capacity are extensively used by the food industry to obtain products with desirable texture and sensory characteristics (TOTOSAUS et al., 2002). However, the proper development of gelled systems requires a detailed characterization of the formulations, which tend to be overly complex (BANERJEE; BHATTACHARYA, 2012; TOTOSAUS et al., 2002).

In most of the studies found in the literature, the properties of protein gels, mixed biopolymeric gels and EFG, are evaluated using rheological tests of small and large deformations, such as uniaxial compression tests, strain and frequency sweep tests, and creep/recovery tests (CHANG et al., 2014; MALTAIS; REMONDETTO; SUBIRADE, 2008; OLIVER; SCHOLTEN; VAN AKEN, 2015; SALA et al., 2007; SALA et al., 2009 a,b; TARHAN et al., 2016).

Uniaxial compression tests are used to determine the modulus of elasticity (E_g), or Young's modulus of the systems, as well as the rupture properties. According to the literature, such tests are fundamental for the characterization of food systems, since during processing and

consumption (chewing process), the products are subjected to large deformations, which can result in irreversible deformations and/or ruptures (ROSA et al., 2006; SALA et al., 2007; TABILO-MUNIZAGA; BARBOSA-CÁNOVAS, 2005). Besides, for EFG, the uniaxial compression tests are applied for the classification of the particles as active or inactive (OLIVER; SCHOLTEN; VAN AKEN, 2015; SALA et al., 2007; SALA et al., 2009a,b).

As previously mentioned, it is widely accepted that the incorporation of inactive particles causes reductions in E_g , increases or decreases in rupture strain and decreases in rupture stress (OLIVER; SCHOLTEN; VAN AKEN, 2015). The incorporation of active particles, on the other hand, can lead to increases or decreases in E_g , increases in rupture stress and decreases in rupture strain of the gels. However, it is known that the extent of such effects depends on the characteristics of each emulsified system (LIU et al., 2015; OLIVER; SCHOLTEN; VAN AKEN, 2015).

Although the data obtained from uniaxial compression tests are very important, in some cases, information regarding the interactions among the various components of EFG may not be adequately obtained from rheological tests of large deformation. In these cases, rheological tests of small deformations (provide information without disturbing the 3D structure of materials significantly) tend to be more suitable for detecting effects of small structural differences in the systems (SALA et al., 2007).

Frequency sweep tests (developed within the linear viscoelastic region of the samples), for example, are widely used to evaluate the behavior of the storage (G') and loss (G'') moduli, as well as the loss tangent (ratio between the viscous and elastic moduli) of gelled systems, under constant temperature, in a frequency range. While G' represents the stored deformation energy stored during the test, quantifying its elastic behavior, G'' represents the energy dissipated as heat by the sample, which, therefore, quantifies its viscous behavior. The values of loss tangent (or tangent phase angle) are related to the energy lost per cycle divided by energy stored per cycle. These data are widely discussed in studies found in the literature that evaluate, for example, the effects of the concentrations of different proteins and salts, in cold-set gelation processes, the effects of the addition and concentration of polysaccharides for the production of mixed biopolymeric gels, as well as, the effects of the incorporation of lipid particles or droplets for the production of EFG (CHANG et al., 2014; MALTAIS; REMONDETTO; SUBIRADE, 2008; MONTEIRO et al., 2013; TANG; LI, 2013; TARHAN et al., 2016),)

In addition to these tests, in many studies involving gels, the authors use creep/recovery tests to characterize them (CHANG et al., 2014; TARHAN et al., 2016). Such tests consist in evaluating the deformation of samples subjected to constant stress (usually within the linear

viscoelastic region of the material) over a period of time (creep) and then removing the stress and evaluating the systems' ability to recover after a maximum deformation (recovery) (DOLZ; HERNÁNDEZ; DELEGIDO, 2008). The results obtained from these tests are commonly analyzed using the Burger model, which consists of the association in series of a Maxwell element and a Kelvin-Voigt element (CHANG et al., 2014, DOLZ; HERNÁNDEZ; DELEGIDO, 2008, LORENZO et al., 2011, LORENZO; ZARITZKY; CALIFANO, 2013). However, due to some limitations of such a model (e.g., relatively large number of parameters used, with vague physical meanings and small ability to simultaneously describe creep and recovery data), another method, known as the fractional derivative approach, has recently been introduced for the analysis of the results of food materials (DAVID; KATAYAMA, 2013, SCHAFFTER et al., 2015, TARHAN et al., 2016).

The development of rheological tests is undeniably important for the characterization of gelled systems. However, for the proper understanding of the results obtained from such tests, most authors use microscopy techniques concurrently, such as confocal laser scanning microscopy (CLSM) and scanning electron microscopy (SEM).

According to Abhyankar, Mulvihill e Auty (2011), CLSM is widely explored for the evaluation of the properties of multicomponent systems, as it allows the visualization of individual phases of the samples, from the identification of the components with different fluorescent dyes and the application of laser beams with specific wavelengths, in order to obtain fluorescent signals for each phase, which are then converted into digital images. Although this technique is widely applied, more detailed information regarding gel structures (e.g. pore size, homogeneity or heterogeneity) is generally obtained from SEM images (KUHN; CAVALLIERI; CUNHA, 2011).

In addition to the techniques discussed above, other tests can be used to develop complete characterizations of gelled systems, including small-angle X-ray scattering (SAXS) tests. Although SAXS tests are less applied than rheological and microscopic tests for the characterization of gelled systems, they are important to obtain information regarding the size and characteristics of protein aggregates, the properties and structural organization of gels, as well as to describe the mechanisms involved in the gelling process (ALTING et al., 2004; OCA-ÁVALOS et al., 2016). Besides, according to Alting et al. (2004), SAXS tests can be used to evaluate structural rearrangements of the samples after the gelation process.

It is known that gels have a highly transient and non-linear nature, and due to the thermodynamically metastable state of such systems, their structural organization tends to change over time, due to spontaneous processes (known as aging processes) and/or external

forces (RENARD; VAN DE VELDE; VISSCHERS, 2006; TEECE et al., 2011). Different authors have verified that the aging of gelled systems generally involves a gradual "hardening" of the structures and a change in the firmness of the systems; however, it is known that such behavior can vary according to the specific properties of the gels (CHANG; LEONG, 2014; RENARD; VAN DE VELDE; VISSCHERS, 2006; TEECE et al., 2011). Alting et al. (2003), for example, explained that structures initially formed from the cold-set gelation of whey proteins (induced by acidification), are generally organized in the form of spaced (or open) clusters of protein aggregates, however, such structures tend to be partially stabilized by the formation of additional covalent bonds over time, which result in the formation of denser and opaquer gels.

Although structural rearrangements can be subtle, aging processes can also lead to the collapse of gels (BARTLETT; TEECE; FAERS, 2012; BUSCALL et al. 2009; CHANG; LEONG, 2014; TEECE et al. 2011). Due to the changes throughout the aging process of the gels, the relatively stable networks, capable of supporting their own structures, begin to present clear interfaces, which grow smoothly as the gel shrinks and lead to a rapid collapse, when the phase separation is completed and the interface approaches a final equilibrium "plateau" (TEECE et al., 2011). Considering that such a process is one of the most extreme macroscopic manifestations of aging and that it drastically compromises the structures of the systems, it is fundamental to monitor the stability of the gels, through the application of various characterization techniques (such as rheological tests, microscopies and SAXS), as well as to evaluate possible collapses, in order to adequately develop new food formulations or product prototypes.

2.6 References

ABHYANKAR, A.R.; MULVIHILL, D.M.; AUTY, M.A.E. Combined microscopic and dynamics rheological methods for studying the structural breakdown properties of whey protein gels and emulsion filled gels. *Food Hydrocolloids*, Oxford, v. 25, n. 3, p. 275-282, 2011.

AKO, K; NICOLAI, T.; DURAND, D. Salt-Induced Gelation of Globular Protein Aggregates: Structure and Kinetics. *Biomacromolecules*, Washington, v. 11, p. 864–871, 2010.

ALTING, A.C.; HAMER, R.J.; KRUIF, C.G.; VISSCHERS, R.W. Cold-Set Globular Protein Gels: Interactions, Structure and Rheology as a Function of Protein Concentration. *Journal of Agricultural and Food Chemistry*, Washington, v. 51, p. 3150-3156, 2003.

- ALTING, A.C. ET al. Acid-Induced Cold Gelation of Globular Proteins: Effects of Protein Aggregate Characteristics and Disulfide Bonding on Rheological Properties. *Journal of Agricultural and Food Chemistry*, Washington, v. 52, p. 623-631, 2004.
- BADII, F.; ATRI, H.; DUNSTAN, D.E. The effect of shear on the rheology and structure of heat-induced whey protein gels. *International Journal of Food Science and Technology*, New York, v. 51, p. 1570–1577, 2016.
- BANERJEE, S.; BHATTACHARYA, S. Food Gels: Gelling Process and New Applications. *Critical Reviews in Food Science and Nutrition*, London, v. 52, p. 334–346, 2012.
- BARAK, S; MUDGIL, D. Locust bean gum: Processing, properties and food applications - A review. *International Journal of Biological Macromolecules*, New York, v. 66, p. 74–80, 2014.
- BARBUT, S. Effects of calcium level on the structure of pre-heated whey protein isolate gels. *Lebensmittel-Wissenschaft und -Technologie*, Westport, v. 28, p. 598-603, 1995(a).
- BARBUT, S. Effect of sodium level on the microstructure and texture of whey protein isolate gels. *Food Research International*, Great Britain, v. 28, p. 437- 443, 1995(b).
- BARTLETT, P.; TEECE, L.J.; FAERS, M.A. Sudden collapse of a colloidal gel. *Physical Review E*, Maryland, v. 85, n. 2, p. 021404, 2012.
- BATTAGLIA, R.E. et al. Health risks associated with meat consumption: a review of epidemiological studies. *International Journal for Vitamin and Nutrition Research*, v. 85, n. 1–2, p. 70–78, 2015.
- BEAULIEU, M.; TURGEON, S.L.; DOUBLIER, J.L. Rheology, texture and microstructure of whey proteins/low methoxyl pectins mixed gels with added calcium. *International Dairy Journal*, Great Britain, v. 11, p. 961–967, 2001.
- BELLAMY, M. et al. Influence of emulsion composition on lubrication capacity and texture perception. *International Journal of Food Science and Technology*, New York, v. 44, n. 10, p. 1939-1949, 2009.
- BEMILLER, J.N.; HUBER, K.C. Carbohidratos. In: DAMODARAN, S.; PARKIN, K.L.; FENNEMA, O.R. *Química dos Alimentos de Fennema*. 4.Ed., Porto Alegre: Artmed, 2010. cap. 3.
- BENICHO, A.; ASERIN, A.; GARTI, N. Protein–polysaccharide interactions for stabilization of food emulsions. *Journal of Dispersion Science and Technology*, London, v. 23, n. 1-3, p. 23-93, 2002.
- BERTRAND, M; TURGEON, S.L. Improved gelling properties of whey protein isolate by addition of xanthan gum. *Food Hydrocolloids*, Oxford, v. 21, p. 159–166, 2007.

- BI, C. et al. Effect of LBG on the gel properties of acid-induced SPI gels. *LWT - Food Science and Technology*, Amsterdam, v. 75, p. 1-8., 2017.
- BORZOVA, V.A. et al. Kinetics of thermal denaturation and aggregation of bovine serum albumin. *PLoS One*, v. 11, n. 4, e0153495, 2016.
- BRAGA, A. L. M. et al. Interactions between soy protein isolate and xanthan in heat-induced gels: the effect of salt addition. *Food Hydrocolloids*, Oxford, v. 20, n. 8, p. 1178-1189, 2006.
- BRITO-OLIVEIRA, T.C. Curcumina encapsulada em micropartículas lipídicas incorporadas em géis carregados: um estudo comparativo com géis proteicos e géis biopoliméricos mistos obtidos a frio. 2017. Dissertação (Mestrado), Universidade de São Paulo, Pirassununga, 2017.
- BRITO-OLIVEIRA, T.C. et al. Stability of curcumin encapsulated in solid lipid microparticles incorporated in cold-set emulsion filled gels of soy protein isolate and xanthan gum. *Food Research International*, Great Britain, v. 102, p. 759-767, 2017.
- BRITO-OLIVEIRA, T.C., et al. Cold-Set Gelation of Commercial Soy Protein Isolate: Effects of the Incorporation of Locust Bean Gum and Solid Lipid Microparticles on the Properties of Gels. *Food Biophysics*, New York, p. 1-14, 2018.
- BRITTEN, M.; GIROUX, H. J. Acid-induced gelation of whey protein polymers: effects of pH and calcium concentration during polymerization. *Food Hydrocolloids*, Oxford, v. 15, n. 4-6, p. 609-617, 2001.
- BROWNSEY, G. J.; MORRIS, V. J. Mixed and filled gels: Models for foods. In: BLANSHARD, J. M. V.; MITCHELL, J. R. (Eds.), *Food structure: Its interaction and evaluation*. London: Elsevier Applied Science, 1988, p. 7-23.
- BROWNSEY, G.J. et al. Elasticity and failure in composite gels. *Journal of Rheology*, New York, v. 31, n. 8, p. 635-649, 1987.
- BRYANT, C. M.; McCLEMENTS, D.J. Influence of NaCl and CaCl₂ on cold-set gelation of heat-denatured whey protein. *Journal of Food Science*, Chicago, v. 65, n. 5, p. 801-804, 2000.
- BUSCALL, R. et al. Towards rationalising collapse times for the delayed sedimentation of weakly-aggregated colloidal gels. *Soft Matter*, London, v. 5, p. 1345-1349, 2009.
- CAVALLIERI, A.L.F. Cold set gelation of whey proteins: Acidification rate, final pH and polysaccharide addition effects. Thesis (PhD) Campinas State University, Campinas, Brazil, 2007.
- CAVALLIERI, A.L.F.; CUNHA, R. L. The effects of acidification rate, pH and ageing time on the acidic cold set gelation of whey proteins. *Food Hydrocolloids*, Oxford, v. 22, n. 3, p. 439-448, 2008.

- CAVALLIERI, A. L. F.; CUNHA, R. L. Cold-set whey protein gels with addition of polysaccharides. *Food Biophysics*, New York, v. 4, n. 2, p. 94-105, 2009.
- CAVALLIERI, A.L.F. et al. Whey protein interactions in acidic cold-set gels at different pH values. *Lait*, Copenhagen, v. 87, p. 535–554, 2007.
- CHANG, Y. et al. Effect of gums on the rheological characteristics and microstructure of acid induced SPI-gum mixed gels. *Carbohydrate Polymers*, New York, v. 108, p. 183–191, 2014.
- CHANG, W.; LEONG, Y. Ageing and collapse of bentonite gels—effects of Li, Na, K and Cs ions. *Rheologica Acta*, Berlin, v. 53, p. 109–122, 2014.
- CHARDIGNY, J.; WALRAND, S. Plant protein for food: opportunities and bottlenecks. *OCL*, v. 23, n. 4, D404, 2016.
- CHEN, N.; CHASSENIEUX, C.; NICOLAI, T. Kinetics of NaCl induced gelation of soy protein aggregates: Effects of temperature, aggregate size, and protein concentration. *Food Hydrocolloids*, v. 77, p. 66-74, 2018.
- CHEN, J.; DICKINSON, E. Viscoelastic properties of heat-set whey protein emulsion gels. *Journal of Texture Studies*, Oxford, v. 29, p. 285-304, 1998.
- CHEN, N. et al. The effect of the pH on thermal aggregation and gelation of soy proteins. *Food Hydrocolloids*, Oxford, v. 66, p. 27-36, 2017.
- CHEN, X. et al. Characterization and embedding potential of bovine serum albumin cold-set gel induced by glucono- δ -lactone and sodium chloride. *Food Hydrocolloids*, v. 95, p. 273–282, 2019
- CUNHA, P.L.R.; PAULA, R.C.M.; FEITOSA, J.P.A. Purification of guar gum for biological applications. *International Journal of Biological Macromolecules*, New York, v. 41, n. 3, p. 324-331, 2007.
- DAAS, P.J.H.; SCHOLS, H.A.; DE JONG, H.H.J. On the galactosyl distribution of commercial galactomannans. *Carbohydrate Research*, New York, v.329, p. 609–619, 2000.
- DAGNELIE, P.C.; MARIOT, F. Vegetarian Diets: Definitions and Pitfalls in Interpreting Literature on Health Effects of Vegetarianism (Chap 1). In *Vegetarian and Plant-Based Diets in Health and Disease Prevention*. Academic Press. 2017, Pages 3-10
- DAVID, S. A.; KATAYAMA, A. H. Fractional order for food gums: modeling and simulation. *Applied Mathematics*, Wuhan, v. 4, p. 305-309, 2013.

DE KRUIF, C.G.; WEINBRECK, F.; DE VRIES, R. Complex coacervation of proteins and anionic polysaccharides. *Current Opinion in Colloid and Interface Science*, London, v. 204, n. 9, p.340–349, 2004.

DERBYSHIRE, E.J. Flexitarian Diets and Health: A Review of the Evidence-Based Literature. *Frontiers in Nutrition*, v. 3, p. 55, 2016.

DEA, I. C. M. et al. Associations of like and unlike polysaccharides: mechanism and specificity in galactomannans, interacting bacterial polysaccharides, and related systems. *Carbohydrate Research*, New York, v. 57, p. 249–272, 1977.

DELBEN, F.; STEFANCICH, S. Interaction of Food Proteins with Polysaccharides I: properties upon Mixing. *Journal of Food Engineering*, Oxford, v. 31, n. 3, p. 325-346, 1997.

DICKINSON, E. Emulsion gels: The structuring of soft solids with protein-stabilized oil droplets. *Food Hydrocolloids*, Oxford, v. 28, n. 1, p. 224-241, 2012.

DICKINSON, E.; CHEN, J. Heat-set whey protein emulsion gels: Role of active and inactive filler particles. *Journal of Dispersion Science and Technology*, London, v. 20, n.1-2, p. 197–213, 1999.

DOLZ, M.; HERNÁNDEZ, M.J.; DELEGIDO, J. Creep and recovery experimental investigation of low oil content food emulsions. *Food Hydrocolloids*, Oxford, v. 22, p. 421–427, 2008.

EMBRAPA, 2021. Soja em números (safra 2019/20). Available at: <https://www.embrapa.br/soja/cultivos/soja1/dados-economicos>.

ESTÉVEZ, N. et al. Influence of pH on viscoelastic properties of heat-induced gels obtained with a β -Lactoglobulin fraction isolated from bovine milk whey hydrolysates. *Food Chemistry*, New York, v. 219, p. 169-178, 2017.

FAOSTAT, 2016. Production > Crops > Soybeans > Production of Top 5 Producers. Available from: <http://faostat3.fao.org/>.

FARJAMI, T.; MADADLOU, A. An overview on preparation of emulsion-filled gels and emulsion particulate gels. *Trends in Food Science & Technology*, Amsterdam, v. 86, p. 85–94, 2019.

FITZSIMONS, S.M.; MULVIHILL, D.M.; MORRIS, E.R. Large enhancements in thermogelation of whey protein isolate by incorporation of very low concentrations of guar gum. *Food Hydrocolloids*, Oxford, v. 22, p. 576–586, 2008.

FOEGEDING, E.A.; DAVIS, J.P. Food protein functionality: A comprehensive approach. *Food Hydrocolloids*, Oxford, v. 25, n. 8, p. 1853 - 1864., 2011.

GEREMIAS-ANDRADE et al., 2017; Rheological and mechanical characterization of curcumin-loaded emulsion-filled gels produced with whey protein isolate and xanthan gum. *LWT - Food Science and Technology*, Amsterdam, v. 86, p. 166-173, 2017.

GEREMIAS-ANDRADE et al., 2016. Rheology of Emulsion-Filled Gels Applied to the Development of Food Materials. *Gels*, Basel, v. 2, p. 22 – 40, 2016.

GERMAN, B.; DAMODARAN, S.; KINSELLA, J.E. Thermal Dissociation and Association Behavior of Soy Proteins. *Journal of Agricultural and Food Chemistry*, Washington, v. 30, n. 5, p. 807–811, 1982.

GONÇALVEZ et al. Rheological study of the effect of *Cassia javanica* galactomannans on the heat-set gelation of a whey protein isolate at pH 7. *Food Hydrocolloids*, Oxford, v. 18, n. 2, p. 181-189, 2004.

GOOD FOOD INSTITUTE. O consumidor brasileiro e o mercado plant based. 2020. Available at: <https://gfi.org.br/wp-content/uploads/2021/02/O-consumidor-brasileiro-e-o-mercado-plant-based.pdf>

GOUZY, R. et al. Cellulose microfibril networks in hydrolysed soy protein isolate solutions. *Colloids and Surfaces A: Physicochemical and Engineering Aspects*. v. 568, n. 5, p. 277-283, 2019.

GUINARD, J.X.; MAZZUCHELLI, R. The sensory perception of texture and mouthfeel. *Trends in Food Science and Technology*, New York, v. 7, p. 213–219, 1996.

GUO, Y. et al. Nano-bacterial cellulose/soy protein isolate complex gel as fat substitutes in ice cream model. *Carbohydrate Polymers*, New York, v. 198, p. 620–630, 2018.

GWARTNEY, E.A.; LARICK, D.K.; FOEGEDING, E.A. Sensory Texture and Mechanical Properties of Stranded and Particulate Whey Protein Emulsion Gels. *Journal of Food Science*, Chicago, v. 69, n. 9, p. 333 – 339, 2004.

HALLAGAN, J.B. et al. Assessment of cassia gum. *Food and Chemical Toxicology*, New York, v. 35, n. 6, p. 625, 1997.

HERMANSSON, A.M. Soy protein gelation. *Journal of the American Oil Chemists’ Society*, Champaign, v. 63, n. 5, p.658-666, 1986.

HIGIRO, J. et al. Rheological study of xanthan and locust bean gum interaction in dilute solution: Effect of salt. *Food Research International*, Great Britain, v. 40, n. 4, p. 435–447, 2007.

HONGSPRABHAS, P.; BARBUT, S. Use of cold-set whey protein gelation to improve poultry meat batters. *Poultry Science*, Oxford, v. 78, p. 1074–1078, 1999.

HUA, Y.; CUI, S.W.; WANG, Q. Gelling property of soy protein–gum mixtures. *Food Hydrocolloids*, Oxford, v. 17, n. 6, p. 889–894, 2003.

HUTCHINGS, J.B.; LILLFORD, P.J. The perception of food texture—the philosophy of the breakdown path. *Journal of Texture Studies*, Oxford, v. 19, p. 103–115, 1988.

INGRASSIA, R. et al. Heat treatments of defatted soy flour: Impact on protein structure, aggregation, and cold-set gelation properties. *Food Structure*, v. 22, p. 100130, 2019.

JONG, S.; JAN KLOK, H.; VAN DE VELDE, F. The mechanism behind microstructure formation in mixed whey protein–polysaccharide cold-set gels. *Food Hydrocolloids*, Oxford, v. 23, n. 3, p. 755–764, 2009.

JONG, S.; VAN DE VELDE, F. Charge density of polysaccharide controls microstructure and large deformation properties of mixed gels. *Food Hydrocolloids*, Oxford, v. 21, n. 7, p. 1172–1187, 2007.

KASRAN, M.; CUI, S. W.; GOFF, H. D. Emulsifying properties of soy whey protein isolate–fenugreek gum conjugates in oil-in-water emulsion model system. *Food Hydrocolloids*, Oxford, v. 30 n. 2, p. 691–697, 2013.

KAYS, S.E.; MORRIS, J.B.; KIM, Y. Total and soluble dietary fiber variation in *Cyamopsis tetragonoloba* (L.) Taub. (Guar) genotypes. *Journal of Food Quality*, Nova Jersey, v. 29, p. 383–391, 2006.

KHARLAMOVA, A.; NICOLAI, T.; CHASSENIEUX, C. Mixtures of sodium caseinate and whey protein aggregates: Viscosity and acid- or salt-induced gelation. *International Dairy Journal*, Great Britain, v. 86, p. 110-119, 2018a.

KHARLAMOVA, A.; NICOLAI, T.; CHASSENIEUX, C. Calcium-induced gelation of whey protein aggregates: Kinetics, structure and rheological properties. *Food Hydrocolloids*, Oxford, v. 79, p. 145-157, 2018b.

KHARLAMOVA, A.; NICOLAI, T.; CHASSENIEUX, C. Gelation of whey protein fractal aggregates induced by the interplay between added HCl, CaCl₂ and NaCl. *International Dairy Journal*, Great Britain, v. 111, p. 104824, 2020.

KIM, K.H.; RENKEMA, J.M.S; VAN VLIET, T. Rheological properties of soybean protein isolate gels containing emulsion droplets. *Food Hydrocolloids*, Oxford, v. 15, n. 3, p. 295-302, 2001.

KUHN, K. R.; CAVALLIERI, A.L.F.; CUNHA, R.L. Cold-set whey protein gels induced by calcium or sodium salt addition *International Journal of Food Science and Technology*, New York, v. 45, p. 348–357, 2010.

- KUHN, K.R.; CAVALLIERI, A.L.F; CUNHA, R.L. Cold-set whey protein-flaxseed gum gels induced by mono or divalent salt addition. *Food Hydrocolloids*, Oxford, v. 25, n. 5, p. 1302 – 1310, 2011.
- KUNDU, S. et al. Mono-, di- and tri-valent ion induced protein gelation: Small-angle neutron scattering study. *Chemical Physics Letters*, v. 593, p. 140–144, 2014.
- LANGLEY, K. R.; GREEN, M. L. Compression strength and fracture properties of model particulate food composites in relation to their microstructure and particle-matrix interaction. *Journal of Texture Studies*, Oxford, v. 20, p. 191-207, 1989.
- LE, X.T.; RIOUX, L.; TURGEON, S.L. Formation and functional properties of protein–polysaccharide electrostatic hydrogels in comparison to protein or polysaccharide hydrogels. *Advances in Colloid and Interface Science*, v. 239, p. 127–135, 2017.
- LEE, K.H.; RYUB, H.S.; RHEEA, K.C. Protein Solubility Characteristics of Commercial Soy Protein Products, *JAOCS*, New York, v. 80, n. 1, p. 85-90, 2003.
- LI, Q.; ZHAO, Z. Interaction between lactoferrin and whey proteins and its influence on the heat-induced gelation of whey proteins. *Food Chemistry*, New York, v. 252, p. 92-98, 2018.
- LI, F. et al. Gelation behaviour and rheological properties of acid-induced soy protein-stabilized emulsion gels. *Food Hydrocolloids*, Oxford, v. 29, p. 347-355, 2012.
- LI, X. et al. Formation and functional properties of protein–polysaccharide electrostatic hydrogels in comparison to protein or polysaccharide hydrogels. *Journal of Food Engineering*, v. 274, p. 109851, 2020.
- LIU, K. *Soybeans: Chemistry, Technology and Utilization*. New York: Chapman and Hall, 1997, 532 p.
- LIU, K. et al. Fat droplet characteristics affect rheological, tribological and sensory properties of food gels. *Food Hydrocolloids*, Oxford, v. 44, p. 244-259, 2015.
- LOPES DA SILVA, J. A. et al. Effect of galactomannans on the viscoelastic behaviour of pectin/calcium networks. *Polymer Gels and Networks*, New York, v. 4, p. 65-83, 1996.
- LORENZO, G.; ZARITZKY, N.; CALIFANO, A. Rheological analysis of emulsion-filled gels based on high acyl gellan gum. *Food Hydrocolloids*, Oxford, v. 30, p.672-680, 2013.
- LORENZO, G. et al. Linear viscoelastic assessment of cold gel-like emulsions stabilized with bovine gelatine. *LWT - Food Science and Technology*, Amsterdam, 44, 457-464, 2011.
- LOVEDAY, S.M. Food Proteins: Technological, Nutritional, and Sustainability Attributes of Traditional and Emerging Proteins. *Annual Review of Food Science and Technology*, v. 10, p. 311–339, 2019.

- LU, Y. et al. Development of Emulsion Gels for the Delivery of Functional Food Ingredients: from Structure to Functionality. *Food Engineering Reviews*, v. 11, p. 245–258, 2019.
- LU, Y. et al. Characterization of β -carotene loaded emulsion gels containing denatured and native whey protein. *Food Hydrocolloids*, Oxford, v.102, p. 105600, 2020.
- LYNCH, H.; JOHNSTON, C.; WHARTON, C. Plant-Based Diets: Considerations for Environmental Impact, Protein Quality, and Exercise Performance. *Nutrients*, v. 10, p. 1841, 2018.
- MALTAIS, A. et al. Formation of soy protein isolate cold-set gels: protein and salt effects. *Journal of Food Science*, Chicago, v. 70, n. 1, p. 67-73, 2005.
- MALTAIS, A.; REMONDETTO, G.E.; SUBIRADE, M. Mechanisms involved in the formation and structure of soya protein cold-set gels: A molecular and supramolecular investigation. *Food Hydrocolloids*, Oxford, v. 22, n. 4, p. 550–559, 2008.
- MALTAIS, A.; REMONDETTO, G.E.; SUBIRADE, M. Soy protein cold-set hydrogels as controlled delivery devices for nutraceutical compounds. *Food Hydrocolloids*, Oxford, v. 23, n. 7, p. 1647–1653, 2009.
- MANGINO, M. E. Physicochemical aspects of whey protein functionality. *Journal of Dairy Science*, Savoy, v. 67, n. 11, p. 2711-2722, 1984.
- MANNION, R.O. et al. Mixed gels made from protein and k-carrageenan. *Carbohydrate Polymers*, New York, v. 28, n. 4, p. 337–339, 1995.
- MANTOVANI, R.A.; CAVALLIERI, A.L.F.; CUNHA, R.L. Gelation of oil-in-water emulsions stabilized by whey protein. *Journal of Food Engineering*, Oxford, v. 175, p. 108-116, 2016.
- MARANGONI, A.G. et al. On the structure of particulate gels – the case of salt-induced cold gelation of heat-denatured whey protein isolate *Food Hydrocolloids*, Oxford, v. 14, p. 61–74, 2000.
- MARTINS, J.T. et al. Protein-based structures for food applications: from macro to nanoscale. *Frontiers in Sustainable Food Systems*, v. 2, p. 77, 2018.
- MCCLEARY, B.V. et al. Effect of galactose content on the solution and interaction properties of guar and carob galactomannans. *Carbohydrate Research*, New York, v. 92, p. 269-285, 1981.
- MCCLEMENTS, D. J. Non-covalent interactions between proteins and polysaccharides. *Biotechnology Advances*, New York, v. 24, p. 621–625, 2006.

MCCLEMENTS, D.J. Development of Next-Generation Nutritionally Fortified Plant-Based Milk Substitutes: Structural Design Principles. *Foods*, v. 9, p. 421, 2020.

MCCLEMENTS, D.J. *Future Foods: How Modern Science is Transforming the Way We Eat*; Springer Scientific: New York, NY, USA, 2019.

MESSION et al. Effect of globular pea proteins fractionation on their heat-induced aggregation and acid cold-set gelation. *Food Hydrocolloids*, Oxford, v. 46, p. 233-243, 2015.

MEZZENGA, R. et al. Understanding foods as soft materials. *Nature Materials*, London, v. 4, p. 729-740, 2005.

MONAHAN, F.J.; GERMAN, J.B.; KINSELLAT, J.E. Effect of pH and Temperature on Protein Unfolding and Thiol/ Disulfide Interchange Reactions during Heat-Induced Gelation of Whey Proteins *Journal of Agricultural and Food Chemistry*, Washington, v. 43, p. 46-52, 1995.

MONTEIRO, S. R. ET al. Influence of galactomannans with different molecular weights on the gelation of whey proteins at neutral pH. *Biomacromolecules*, Washington, v. 6, p. 3291-3299, 2005.

MONTEIRO, S.R. et al. The influence of galactomannans with different amount of galactose side chains on the gelation of soy proteins at neutral pH. *Food Hydrocolloids*, Oxford, v. 33, p. 349-360, 2013.

MONTEIRO, S.R.; LOPES-DA-SILVA, J.A. Effect of the molecular weight of a neutral polysaccharide on soy protein gelation. *Food Research International*, Great Britain, v. 102, p. 14–24, 2017.

MONTEIRO, S.R.; LOPES-DA-SILVA, J.A. Critical evaluation of the functionality of soy protein isolates obtained from different raw materials. *European Food Research and Technology*, v. 245, p. 199–212, 2019.

MORRIS, V. J. Gelation of Polysaccharides. *Current Opinion in Colloid and Interface Science*, London, v. 2, n. 6, p. 567-572, 1997.

MORRIS, V. J.; WILDE, P. J. Interaction of food biopolymers. *Current Opinion in Colloid and Interface Science*, London, v. 2, p. 567–572, 1997.

MOURE, A. et al. Functionality of oil seed protein products: a review. *Food Research International*, Great Britain, v. 39, p. 945-963, 2006.

NAVARRA, G. Thermal aggregation and ion-induced cold-gelation of bovine serum albumin. *European Biophysics Journal*, v. 38, p. 437–446, 2009.

NICOLAI, T.; CHASSENIEUX, C. Heat-induced gelation of plant globulins. *Current Opinion in Food Science*, v. 27, p. 18–22, 2019.

- NISHINARI, K. et al. Soy proteins: A review on composition, aggregation and emulsification. *Food Hydrocolloids*, Oxford, v. 39, p. 301-318, 2014.
- NISHINARI, K. et al. Soy as a food ingredient. (Chap 6). In: *Proteins in Food Processing*. Elsevier Ltd., 2018.
- NISHINARI, K.; ZHANG, H.; IKEDA, S. Hydrocolloid gels of polysaccharides and proteins. *Current Opinion in Colloid and Interface Science*, London, v. 5, p. 195-201, 2000.
- OCA-ÁVALOS, J.M.M., et al. Sodium Caseinate/Sunflower Oil Emulsion-Based Gels for Structuring Food. *Food Bioprocess Technology*, Berlin, v. 9, p. 981–992, 2016.
- OLIVER, L; SCHOLTEN, E.; VAN AKEN, G.A. Effect of fat hardness on large deformation rheology of emulsion-filled gels. *Food Hydrocolloids*, Oxford, v. 43, p. 299-310, 2015.
- UNITED NATIONS OF ORGANIZATION (ONU). 2017. Food and Agriculture Organization, United Nations of Organization 2016_2017. World Food Situation. Available at: www.fao.org/worldfoodsituation/csdb/en/.
- OXFORD ENGLISH DICTIONARY. The Definitive Record of the English Language. (2014). Available from: <http://www.oed.com>.
- PARADISO, V.M. et al. Production and characterization of emulsion filled gels based on inulin and extra virgin olive oil. *Food Hydrocolloids*, Oxford, v. 45, p. 30-40, 2015.
- PARIJA, S.; MISRA, M.; MOHANTY, A.K. Studies of natural gum adhesive extracts: an overview. *Polymer Reviews*, v. 41, p. 175–197, 2001.
- PHILLIPS, L. G.; WHITEHEAD, D. M.; KINSELLA, J. E. Structure function properties of food proteins. San Diego. Academic Press, 1994.
- POORE, J.; NEMECEK, T. Reducing food's environmental impacts through producers and consumers. *Science*, v. 360, p. 987–992, 2018.
- PRAJAPATI, V.D. et al. Galactomannan: A versatile biodegradable seed polysaccharide. *International Journal of Biological Macromolecules*, New York, v. 60, p. 83– 92, 2013.
- PUPPO, M. C.; SORGENTINI, D.A.; AÑÓN, M.C. Rheological Properties of Emulsions Containing Modified Soy Protein Isolates. *Journal of the American Oil Chemists' Society*, Champaign, v. 80, n. 6, p. 605-611, 2003.
- RAMÍREZ, J.A. et al. Effect of xanthan and locust bean gums on the gelling properties of myofibrillar protein. *Food Hydrocolloids*, Oxford, v.16, n. 1, p. 11-16, 2002.
- RAO, M.A. Rheology of Fluid, Semisolid, and Solid Foods, Food Engineering Series. New York: Springer Science+Business Media. 2014

- REMONDETTO, G. E.; SUBIRADE, M. Molecular mechanisms of Fe³⁺- induced blactoglobulin cold gelation. *Biopolymers*, Nova Jersey, v. 69, p. 461–469, 2003.
- RENARD, D.; VAN DE VELDE, F.; VISSCHERS, R.W. The gap between food gel structure, texture and perception. *Food Hydrocolloids*, Oxford, v. 20, n.4, p. 423–431, 2006.
- RENKEMA, J. M. S.; GRUPPEN, H.; VLIET, T. Influence of pH and ionic strength on heat-induced formation and rheological properties of soy proteins gels and in relation to denaturation and their protein compositions. *Journal of Agricultural and Food Chemistry*, Washington, v. 50, n. 21, p. 6064-6071, 2002.
- RENKEMA, J. M. S.; KNABBEN, J. H. M.; VAN VLIET, T. Gel formation by α -conglycinin and glycinin and their mixtures. *Food Hydrocolloids*, Oxford, v. 15, p. 407-414, 2001.
- RING, S.; STAINSBY, G. Filler reinforcement of gels. *Progress in Food and Nutrition Science*, Bethesda, v. 6, p. 355-361, 1982.
- ROCHA, C. et al. Rheological and structural characterization of gels from whey protein hydrolysates/locust bean gum mixed systems. *Food Hydrocolloids*, Oxford, v. 23, p. 1734–1745, 2009.
- RODRIGUES, R.M. et al. Effects of moderate electric fields on cold-set gelation of whey proteins – From molecular interactions to functional properties. *Food Hydrocolloids*, Oxford, v. 101, p. 105505, 2020.
- ROSA, P. et al. Cold gelation of whey protein emulsions. *Journal of Texture Studies*, Oxford, v. 37, p. 516–537, 2006.
- SADEGHI, S.; MADADLOU, A.; YARMAND, M. Microemulsification–cold gelation of whey proteins for nanoencapsulation of date palm pit extract. *Food Hydrocolloids*, Oxford, v. 35, p. 590-596, 2014.
- SAIO, K.; KAMIYA, M.; WATANABE, T. Food processing characteristics of soybean 11S and 7S proteins. Part I. Effect of difference of protein components among soybean varieties on formation of tofu-gel. *Agricultural and Biological Chemistry*, v. 33, p. 1301, 1969.
- SALA, G. et al. Effect of droplet–matrix interactions on large deformation properties of emulsion-filled gels. *Journal of Texture Studies*, Oxford, v. 38, n. 4, p. 511–535, 2007.
- SALA, G. et al. Deformation and fracture of emulsion-filled gels: Effect of gelling agent concentration and oil droplet size. *Food Hydrocolloids*, Oxford, v. 23, n. 7, p. 1853–1863, 2009a.
- SALA, G. et al. Deformation and fracture of emulsion-filled gels: Effect of oil content and deformation speed *Food Hydrocolloids*, Oxford, v. 23, n. 7, p. 1381–1393, 2009b.

- SALA, G. et al. Matrix properties affect the sensory perception of emulsion-filled gels. *Food Hydrocolloids*, Oxford, v. 22, n. 3, p. 353–363, 2008.
- SÁNCHEZ, V.E.; BARTHOLOMAI, G.B.; PILOSOFF, A.M.R. Rheological Properties of Food Gums as related to their Water Binding Capacity and to Soy Protein interaction. *LWT – Food Science and Technology*, Amsterdam, v. 28, p. 380-385, 1995.
- SANCHEZ, C. et al. Rheology of whey protein isolate-xanthan mixed solutions and gels, Effect of pH and xanthan concentration. *Food/ Nahrung*, Weinheim, v. 41, n. 6, p.336–343, 1997.
- SANCHEZ, C. et al., Microstructure of acid–induced skim milk–locust bean gum–xanthan gels. *International Dairy Journal*, Great Britain, v. 10, p. 199–212, 2000.
- SATIJA, A. et al. Plant-based dietary patterns and incidence of type 2 diabetes in US men and women: Results from three prospective cohort studies. *PLoS Med.*, v. 13, e1002039, 2016.
- SCHAFFTER, S.; CORVALAN, C. M.; CAMPANELLA, O. H. A creep and recovery model based on fractional calculus for the characterization and design of viscoelastic food materials (internal communication), 2015.
- SCHMITT, C. et al. Structure and techno-functional properties of protein–polysaccharide complexes. *Critical Reviews in Food Science and Nutrition*, London, v. 38, n. 8, p. 689-753, 1998.
- SCHORSCH, C.; GARNIER, C.; DOUBLIER, J. Viscoelastic properties of xanthangalactomannan mixtures: comparison of guar gum with locust bean gum. *Carbohydrate Polymers*, New York, v. 34, n. 3, p. 165-175, 1997.
- SGARBIERI, V.C. Proteínas em Alimentos Protéicos: Propriedades, degradações, modificações. São Paulo: Livraria Varela, 1996. p. 85-109.SCHAFFTER et al., 2015,
- SHARMA, P. et al. A comprehensive review on leguminous galactomannans: structural analysis, functional properties, biosynthesis process and industrial applications. *Critical Reviews in Food Science and Nutrition*, v. 3, p, 1-23, 2020.
- SRIVASTAVA, M.; KAPOOR, V.P. Seed Galactomannans: An Overview. *Chemistry and Biodiversity*, New Jersey, v. 2, p. 295-317, 2005.
- STOKES, J. R.; BOEHM, M. W.; BAIER, S. K. Oral processing, texture and mouthfeel: from rheology to tribology and beyond. *Current Opinion in Colloid and Interface Science*, London, v. 18, n. 4, p. 349-359, 2013.
- SYRBE, A.; BAUER, W. J.; KLOSTERMEYER, H. Polymer science concepts in dairy systems—an overview of milk protein and food hydrocolloid interaction. *International Dairy Journal*, Great Britain, v. 8, n. 3, p. 179–193, 1998.

- SZCZESNIAK, A.S. Texture is a sensory property. *Food Quality and Preference*, New York, v. 13, p. 215–25, 2002.
- TABILO-MUNIZAGA, G.; BARBOSA-CÁNOVAS, G.V. Rheology for the food industry. *Journal of Food Engineering*, Oxford, v. 67, n. 2-3, p. 147–156, 2005.
- TANG, C.; LIU, F. Cold, gel-like soy protein emulsions by microfluidization: Emulsion characteristics, rheological and microstructural properties, and gelling mechanism. *Food Hydrocolloids*, Oxford, v. 30, p.61-72, 2013.
- TARHAN, O. et al. Rheological and structural characterization of whey protein gelation induced by enzymatic hydrolysis. *Food Hydrocolloids*, Oxford, v. 61, p. 211-220, 2016.
- TAVARES, C. et al. Does the branching degree of galactomannans influence their effect on whey protein gelation? *Colloids and Surfaces A: Physicochemical and Engineering Aspects*, Amsterdam, p. 270–271, p. 213–219, 2005.
- TAVARES, C.; LOPES DA SILVA, J.A. Rheology of galactomannan–whey protein mixed systems. *International Dairy Journal*, Great Britain, v. 13, p. 699–706, 2003.
- TEECE, L.J.; FAERS, M.A.; BARTLETT, P. Ageing and collapse in gels with long-range attractions. *Soft Matter*, London, v. 7, p. 1341–1351, 2011.
- THE VEGAN SOCIETY. Worldwide Statistics, 2021. Available at: <https://www.vegansociety.com/news/media/statistics/worldwide>.
- TOBITANI, A.; ROSS-MURPHY, S.B. Heat-Induced Gelation of Globular Proteins. 1. Model for the Effects of Time and Temperature on the Gelation Time of BSA Gels. *Macromolecules*, New York, v. 30, n. 17, p. 4845–4854, 1997.
- TOLSTOGUZOV, V. Some thermodynamic considerations in food formulation. *Food Hydrocolloids*, Oxford, v. 17, p. 1–23, 2003.
- TOLSTOGUZOV, V. B.; BRAUDO, E. E. Fabricated foodstuffs as multicomponent gels. *Journal of Texture Studies*, Oxford, v. 14, p. 183-212, 1983.
- TOTOSAUS, A. et al. A review of physical and chemical protein-gel induction. *International Journal of Food and Technology*, Chester, v. 37, n. 6, p. 589-601, 2002.
- TRIPATHI, A.D. et al. Chapter 1 - Estimates for World Population and Global Food Availability for Global Health. *The Role of Functional Food Security in Global Health*, p. 3-24, 2019.
- TURGEON, S. L. et al. Protein-polysaccharide interactions: phase-ordering kinetics, thermodynamic and structural aspects. *Current Opinion in Colloid and Interface Science*, London, v. 8, p. 401-414, 2003.

TURGEON, S.L.; BEAULIEU, M. Improvement and modification of whey protein gel texture using polysaccharides. *Food Hydrocolloids*, Oxford, v. 15, n. 4–6, p. 583-591, 2001.

TURGEON, S.L.; SCHMITT, C.; SANCHEZ, C. Protein–polysaccharide complexes and coacervates. *Current Opinion in Colloid and Interface Science*, London, v. 12, p. 166–178, 2007.

UNAL, B.; METIN, S.; ISIKLI, N.D. Use of response surface methodology to describe the combined effect of storage time, locust bean gum and dry matter of milk on the physical properties of low-fat set yoghurt. *International Dairy Journal*, Great Britain, v.13, p. 909–916, 2003.

UTSUMI, S.; KINSELLA, J.E. Forces Involved in Soy Protein Gelation: Effects of Various Reagents on the Formation, Hardness and Solubility of Heat-Induced Gels Made from 7S, 11S, and Soy Isolate *Journal of Food Science*, Chicago, v. 50, n. 5, p. 1278-1282, 1985.

UTSUMI, S.; MATSUMURA, Y.; MORI, T. Structure-Function Relationships of Soy Proteins. In: DAMODARAN, S. P. (Ed.), *Food proteins and Their Applications*. New York: Marcel Dekker, Inc., 1997.

UTZSCHNEIDER, K. M. et al. Beneficial effect of a weight-stable, low-fat/low-saturated fat/low-glycaemic index diet to reduce liver fat in older subjects. *The British Journal of Nutrition*, Cambridge, v. 109, n. 6, p. 1096-1104, 2013.

VAN AKEN, G. A.; OLIVER, L.; SCHOLTEN, E. Rheological effect of particle clustering in gelled dispersions. *Food Hydrocolloids*, Oxford, v. 48, p. 102-109, 2015.

VAN AKEN, G. A.; VINGERHOEDS, M. H.; DE WIJK, R. A. Textural perception of liquid emulsions: role of oil content, oil viscosity and emulsion viscosity. *Food Hydrocolloids*, Oxford v. 25, n. 4, p. 789-796, 2011.

VAN DE VELDE, F. et al. Protein-Polysaccharide Interactions to Alter Texture. *Annual Review of Food Science and Technology*, Palo Alto, v. 6, p. 371-388, 2015.

VAN DER GOOT, A.J. Concepts for further sustainable production of foods. *Journal of Food Engineering*, v. 168, p. 42–51, 2016.

VAN DER POEL, C. On the rheology of concentrated dispersion. *Rheologica Acta*, Berlin, v. 1, p. 198-205, 1958.

VAN DER SMAN, R.G.M. Soft matter approaches to food structuring. *Advances in Colloid and Interface Science*, New York, v. 176-177, p. 18-30, 2012.

VAN VLIET, T. On the relation between texture perception and fundamental mechanical parameters for liquids and time dependent solids. *Food Quality and Preference*, New York, v. 13, n. 4, p.227–236, 2002.

- VAN VLIET, T. Rheological properties of filled gels. Influence of filler matrix interaction. *Colloid & Polymer Science*, Darmstadt, v. 266, n.6, p. 518-524, 1988.
- VILELA, J.A.P.; CAVALLIERI, A.L.F.; CUNHA, R.L. The influence of gelation rate on the physical properties/structure of salt-induced gels of soy protein isolate-gellan gum. *Food Hydrocolloids*, Oxford, v. 25, n. 7, p. 1710-1718, 2011.
- WANG et al. Structure–antioxidant relationships of sulfated galactomannan from guar gum. *International Journal of Biological Macromolecules*, New York, v. 46, p. 59-66, 2010
- WANG, Y. et al. The effect of addition of flaxseed gum on the emulsion properties of soybean protein isolate (SPI). *Journal of Food Engineering*, Oxford, v. 104, n.1, p. 56–62, 2011.
- WIJAYA; VAN DER MEEREN; PATEL. Cold-set gelation of whey protein isolate and low-methoxyl pectin at low pH. *Food Hydrocolloids*, Oxford, v. 65, p. 35-45, 2017.
- WU, C. et al. Effect of temperature, ionic strength and 11S ratio on the rheological properties of heat-induced soy protein gels in relation to network proteins content and aggregates size. *Food Hydrocolloids*, Oxford, v. 66, p. 389-395, 2017.
- WU, C. et al. Effects of removal of non-network protein on the rheological properties of heat-induced soy protein gels. *LWT - Food Science and Technology*, Amsterdam, v. 95, p. 193–199, 2018.
- XIAO, Y. et al. Gel properties and formation mechanism of soy protein isolate gels improved by wheat bran cellulose. *Food Chemistry*, New York, v. 324, p. 126876, 2020.
- YE, A.; TAYLOR, S. Characterization of cold-set gels produced from heated emulsions stabilized by whey protein. *International Dairy Journal*, Great Britain, v. 19, p. 721–727, 2009.
- YOST, R.; KINSELLA, J.E. Microstructure of whey protein isolate gels containing emulsified butterfat droplets. *Journal of Food Science*, Chicago, v. 57, p. 892, 1992.
- ZASYPKIN, D.V.; BRAUDO, E.E.; TOLSTOGUZOV, V.B. Multicomponent biopolymer gels. *Food Hydrocolloids*, Oxford, v. 11, p. 159–170, 1997.
- ZHANG. P et al. Effect of high intensity ultrasound on transglutaminase- catalyzed soy protein isolate cold set gel. *Ultrasonics Sonochemistry*, New York, v. 29, p. 380–387, 2016.
- ZHAO, C. et al. Ultrasound heat treatment effects on structure and acid-induced cold set gel properties of soybean protein isolate. *Food Bioscience*, v. 39, p. 100827, 2021.
- ZHENG, L. et al. Addition of Salt Ions before Spraying Improves Heat and Cold-Induced Gel Properties of Soy Protein Isolate (SPI). *Applied Sciences*, v. 9, p. 1076, 2019.

ZHOU, Y. et al. Contribution of three ionic types of polysaccharides to the thermal gelling properties of chicken breast myosin. *Journal of Agricultural and Food Chemistry*, Washington, v. 62, n. 12, p. 2655–2662, 2014.

ZHU, J. H. et al. Effect of guar gum on the rheological, thermal and textural properties of soybean b-conglycinin gel. *International Journal of Food Science and Technology*, New York, v. 44, p. 1314-1322, 2009.

ZHUANG, X. et al. Insight into the mechanism of physicochemical influence by three polysaccharides on myofibrillar protein gelation. *Carbohydrate Polymers*, New York, v. 229, p. 115449, 2020.

**CHAPTER 3 : MICROSTRUCTURAL AND RHEOLOGICAL
CHARACTERIZATION OF NAACL-INDUCED GELS OF SOY PROTEIN ISOLATE
AND THE EFFECTS OF INCORPORATING DIFFERENT GALACTOMANNANS**

(Published in Food Structure)

**Thais C. Brito-Oliveira, Ana Clara M. Cavini, Leticia S. Ferreira, Izabel C.F.
Moraes, and Samantha C. Pinho**

*Brito-Oliveira, T.C.; Cavini, A.C.M.; Ferreira, L.S.; Moraes, I.C.F.; Pinho, S.C.
Microstructural and rheological characterization of NaCl-induced gels of soy protein
isolate and the effects of incorporating different galactomannans. Food Structure, 2020,
26, 100158.*

Microstructural and rheological characterization of NaCl-induced gels of soy protein isolate
and the effects of incorporating different galactomannans

Thais C. Brito-Oliveira, Ana Clara M. Cavini, Leticia S. Ferreira, Izabel C.F. Moraes, and
Samantha C. Pinho*

Department of Food Engineering, School of Animal Science and Food Engineering,
University of São Paulo (USP), Pirassununga, SP, Brazil

* Corresponding author: S.C. Pinho, Department of Food Engineering, School of Animal Science and Food Engineering (FZEA), University of São Paulo (USP), Av. Duque de Caxias Norte 225, Jd. Elite, Pirassununga, SP, Brazil 13635-900. Tel: +55-19-35654288; fax: +55-19-3565-4284.

E-mail address: samantha@usp.br

3.1 Abstract

This study aimed to evaluate the properties of NaCl-induced gels of soy protein isolate (SPI) in the presence and absence of different galactomannans (locust bean gum - LBG and guar gum – GG) at pH 7. For this purpose, systems with different ionic strengths (100 – 400 mM), protein concentrations (10-14%, w/v), and galactomannan concentrations (0 – 0.5%, w/v) were evaluated regarding their visual aspects, microstructural organization, and rheological properties. Among the self-supported protein gels (produced with at least 14% SPI and 200 mM NaCl), those with 300 mM NaCl presented higher G' , G'' , and E_g values and lower compliance values due to their denser microstructural organization. Such formulations were, therefore, selected for mixed (protein+ polysaccharide) gel production. The incorporation of 0.4% and 0.5% galactomannans resulted in heat-induced gels, so only samples with 0.1 - 0.3% galactomannans were characterized. All mixed gels presented incomplete demixing, but the extent of this phenomenon varied with the concentration of galactomannan and its branching degree. LBG demonstrated higher capacity to self-associate, resulting in gels with higher degrees of phase separation; higher G' , G'' , and E_g values; and lower compliance values than GG. Although the galactomannans did not significantly increase the strength of the SPI gels, they increased the stability of the systems at room temperature.

Keywords: Cold-set gelation; Salt-induced; Mixed gels; Locust bean gum; Guar gum; Rheology.

3.2 Introduction

The interest in introducing plant proteins in food formulations has been growing due to consumers' dietary preferences, concerns regarding the safety of animal-based products, issues related to animal welfare, and global awareness of the importance of using environmentally friendly ingredients, especially considering the progressive increase of the world's population (Monteiro et al., 2013; Tripathi et al., 2019).

Among the most popular and abundant plant protein ingredients is soy protein isolate (SPI), which is known for its nutritional value, low cost, physicochemical properties and functional attributes, including the capacity to form cold-set gels (Abaee et al., 2017; Ingrassia et al., 2019). Cold-set gelation methods have received growing attention, as they induce gelation at lower protein concentrations and lower temperatures than other methods, consequently allowing the incorporation of thermolabile compounds to formulations with lower losses (Maltais et al., 2005; Maltais et al., 2010; Zheng et al., 2019). This is possible because, in these methods, denaturation and aggregation occur during an initial preheating step, separate from the gelation process, which may be induced, for example, by salt addition (Bryant & McClements, 2000; Cavallieri & Cunha, 2008; Kuhn et al., 2010).

For example, in a recent study by our group, the ability of SPI to form CaCl_2 -induced gels under different conditions was evaluated, and it was observed that self-supported systems were only formed at neutral or alkaline pH values (Brito-Oliveira et al., 2018). At neutral pH, however, the gels presented structural instability, which was attributed to the relatively low solubility of SPI in such conditions but was improved through the incorporation of locust bean gum (LBG) into the systems, which started to present clear microphase separation (Brito-Oliveira et al., 2018).

In fact, according to the literature, the mixture of galactomannans, such as LBG, with protein ingredients generally leads to phase separation through thermodynamic incompatibility. However, such processes can be significantly reduced with the development of gelation (Jong & Van De Velde, 2007; Monteiro et al., 2013). Therefore, the microstructural organization of such mixed gels is determined by the balance between these two processes, which can be influenced by different factors, including the ionic strength of the system and characteristics of SPI and polysaccharide used (Jong & Van De Velde, 2007; Monteiro et al., 2013; Tavares et al., 2005; Turgeon et al., 2003).

Monteiro et al. (2013), for example, investigated the effect of incorporating different galactomannans in heat-induced gels of soybean proteins at pH 7 and verified that

polysaccharides affected the speed of phase separation in different ways. Consequently, the process resulted in gels with distinct microstructural and rheological properties. According to the authors, such results are related to the different mannose-to-galactose (M/G) ratios of the galactomannans.

Galactomannans are neutral polysaccharides consisting of linear chains of 1,4-linked β -D-mannopyranose randomly attached to different proportions of α -D-galactopyranosyl residues at position 6 as sidechains (Barak & Mudgil, 2014; Monteiro et al., 2013; Mudgil et al., 2014), which differ from each other by the degree of branching, i.e., the mannose-to-galactose ratio. This ratio depends on the origin of the galactomannan and influences its interactions with other ingredients (Monteiro et al., 2013; Tavares et al., 2005).

These interactions between the macromolecular components of food products are recognized as important reasons for the complexity of gelled systems and understanding them is fundamental for the development and optimization of food formulations (Dickinson, 2006; Turgeon, et al., 2007). It is already widely accepted that, with adequate control of the interactions among macromolecules, it is possible to enhance the properties of ingredients with challenging characteristics, such as SPI (Dickinson, 2006; Turgeon, et al., 2007).

In this context, the objectives of this study were to investigate the ability of previously characterized SPI (Brito-Oliveira et al., 2018) to form NaCl-induced gels under different protein concentrations (10-14%, w/v) and ionic strengths (100 – 400 mM) at pH 7, and to evaluate the effects of incorporating different concentrations of two different galactomannans (locust bean gum - LBG and guar gum - GG) into the systems.

3.3 Materials and methods

3.3.1 Chemicals and reagents

SPI (Protimarti M-90) was obtained from Marsul (Montenegro, RS, Brazil). Sodium chloride was obtained from Synth (Diadema, SP, Brazil), GG was obtained from Êxodo Científica (Hortolândia, SP, Brazil), and LBG (Viscogum LBG ®) was donated by Cargill (Campinas, SP, Brazil). Ultrapure water (from a Millipore system Direct Q3®, Billerica, MA, USA) was used throughout the experiments.

3.3.2 Production of cold-set gels

The production of cold-set SPI gels was carried out according to a protocol established in our previous study (Brito-Oliveira et al., 2018), with modifications. For the hydration, deionized water was added to the SPI powder, and the samples were manually mixed using a spatula for 5 min at room temperature. The pH values of the dispersions were adjusted to 7 using a pH meter (UltraBasic Benchtop pH Meter, Denver instrument, New York, NY, USA). The dispersions were then preheated in a water bath at 80°C for 30 min and subsequently cooled to room temperature for the further addition of NaCl. The samples were stored at 10°C for 12 h before characterization. Initially, different SPI concentrations (10–14%, w/v) and ionic strengths (μ : 0–400) were tested to select the best formulation (self-supported and stronger) to produce the mixed (polysaccharide + SPI) gels.

Mixed gels were produced by using the same protocol described above. However, different amounts of LBG or GG (0.1–0.5%, w/v) were added to the SPI powder and hydrated as previously described for the production of SPI-only gels. The protein concentration selected for mixed gels production was 14% (w/v), and the value of μ was 300. The samples were also stored at 10°C for at least 12 h before their characterization. All gels were characterized in terms of their visual aspect, rheological and microstructural properties.

3.3.3 Small strain oscillatory tests

SPI and mixed self-supported gels were characterized via small strain oscillatory tests according to a protocol adapted from Chang et al. (2014), using an AR2000 rheometer (TA Instruments, New Castle, DE, USA) and an aluminum parallel plate geometry (60 mm diameter, 1 mm gap), at 10°C. Initially, a 2 min resting period was used to equilibrate the samples and eliminate stresses created during loading of the sample. Silicone oil was added at the edge of the sample to avoid water evaporation.

Strain sweep tests (data not shown) were performed using a strain sweep in the range of 0.01–100% at a constant frequency of 1 Hz to determine the linear viscoelastic regions (LVRs) of the samples. Frequency sweep tests were also carried out using a strain amplitude of 2% (within the LVRs) over an angular frequency range of 0.016–1.6 Hz. The dependence of the viscoelastic moduli (G' and G'') on angular frequency was described by a power law model (Equations 3.1 and 3.2) using the nonlinear regression feature in Excel (Microsoft, Seattle, WA, USA) (Chang et al., 2014):

$$G' = K' \cdot \omega^{n'} \quad (3.1)$$

$$G'' = K'' \cdot \omega^{n''} \quad (3.2)$$

where K' and K'' are power law parameters, n' and n'' are frequency exponents, and ω is the angular frequency.

3.3.4 Creep/recovery tests

SPI and mixed self-supported gels were characterized via creep/recovery tests using an AR2000 rheometer (TA Instruments, New Castle, PN, EUA) and an aluminum parallel plate geometry (60 mm diameter, 2 mm gap) at 10°C. For the creep step, a constant stress of 5 Pa was applied for 15 min and then removed for the evaluation of the recovery behavior of the samples for 15 min. To eliminate loading effects, a resting time of 10 minutes was applied before the tests. To avoid evaporation, silicone oil was added on the edges of the samples. Creep and recovery data were analyzed using the four-parameter Burger's model, consisting of a Maxwell element and a Kelvin–Voigt element connected in series, which, according to the Boltzmann superposition principle, is represented by Equation 3.3 (Chang et al., 2014).

$$J(t) = \begin{cases} J_0 + J_1 \left(1 - \exp\left(\frac{-t}{\lambda_{ret}}\right) \right) + \frac{t}{\eta_0}, & t \leq t_1 \\ J_1 \left(\exp\left(\frac{t_1-t}{\lambda_{ret}}\right) - \exp\left(\frac{-t}{\lambda_{ret}}\right) \right) + \frac{t_1}{\eta_0}, & t > t_1 \end{cases} \quad (3.3)$$

where J_0 is the instantaneous compliance in Pa^{-1} , η_0 is the viscosity of the Maxwell dashpot in $\text{Pa}\cdot\text{s}$, J_1 is the compliance associated with the Kelvin–Voigt element in Pa^{-1} , λ_{ret} is the retardation time associated with the Kelvin–Voigt element in s, and t_1 is the time when the stress was removed.

The recovery rates were calculated using Equation 3.4, where ε_{max} is the maximum strain at the end of the creep test and ε_f is the final strain (Chang et al., 2014).

$$Recovery (\%) = \frac{\varepsilon_{max} - \varepsilon_f}{\varepsilon_{max}} \quad (3.4)$$

3.3.5 Uniaxial compression tests

SPI and mixed self-supported gels were analyzed via uniaxial compression tests using a texturometer (TA-XT.plus Texture Analyser, Godalming, Surrey, UK) according to a protocol adapted from Oliver et al. (2015). Samples had a cylindrical shape of 30 mm height and 20 mm diameter and were compressed to 80% of their original height using an aluminum probe

lubricated with silicone oil to minimize friction at a deformation speed of 1 mm/s. Each formulation was tested using five replicates. The values of Hencky stress (σ_H) and Hencky strain (ε_H) were obtained from the force-deformation data according to Equations (3.5) and (3.6), respectively:

$$\sigma_H = F(t) \cdot \frac{H(t)}{H_0 \cdot A_0} \quad (3.5)$$

$$\varepsilon_H = \ln \frac{H(t)}{H_0} \quad (3.6)$$

where $F(t)$ is the force at time t , A_0 is the initial area, H_0 is the initial height, and $H(t)$ is the height at time t . The rupture parameters were associated with the maximum value of the stress-strain curve. The values of the apparent Young's modulus (E_g) of the systems were determined by the slope of the first linear interval in the Hencky stress (σ_H) versus Hencky strain (ε_H) curves, up to rupture.

3.3.6 Scanning electron microscopy

SPI and mixed self-supported gels were also analyzed using scanning electron microscopy (SEM). Samples were prepared for this purpose according to a protocol described by Picone et al. (2011). Initially, gels (rectangular shapes $1.0 \times 0.5 \times 0.5$ cm) were fixed at 2.5 g/100 g of glutaraldehyde in a cacodylate buffer (16 g/L) at pH 7.2 and stored at 7°C for 24 h. Subsequently, they were rinsed twice in a cacodylate sodium buffer (16 g/L, pH 7.2) and fractured in liquid nitrogen. The samples were then subjected to postfixation using osmium tetroxide 1 g/100 g in a cacodylate buffer (16 g/L, pH 7.2) for 120 min and rinsed twice in deionized water. Following this, they were dehydrated in a graded ethanol series (30, 50, 70, and 90 mL/100 mL) for 20 min in each. Dehydration was continued in 100% ethanol (three changes in 1 h) and then completed by critical point drying (CPD03 Balzers Critical Point Dryer, Alzenau, Germany). The dried samples were fractured, placed in aluminum stubs and coated with gold (200 s/40 mA) in a Balzers SCD 050 Sputter Coater (Alzenau, Germany). SEM observations were performed using a TM 3000 tabletop microscope (Hitachi, Tokyo, Japan).

3.3.7 Confocal laser scanning optical microscopy

Confocal laser scanning microscopy (CLSM) (Confocal Upright Microscope LSM 780 NLO-Zeiss, Zeiss, Germany) was performed for the evaluation of mixed self-supported gels

using simultaneous dual-channel imaging according to a protocol adapted from Abhyankar et al. (2011). The protein phase was visualized by exciting rhodamine B at a wavelength of 543 nm with an emission wavelength range of 551–655 nm. For this purpose, a rhodamine B solution (0.2%, w/v, in deionized water) was added to the gels (10 μ L solution/mL of gel). The polysaccharides were visualized by exciting the dye fluorescein isothiocyanate (FITC) at an excitation wavelength of 488 nm and an emission wavelength range of 493–543 nm. For this purpose, a solution of FITC (1 mg/mL dimethyl sulfoxide, DMSO) was prepared and added to the gels (0.05 mL of solution/mL of gel).

3.3.8 Statistical analyses

All measurements and experimental samples were performed/produced at least in triplicate, and mean values and corresponding errors were calculated. For the statistical treatment of data, an analysis of variance (ANOVA) was conducted, followed by Tukey's tests with a 5% significance level using SAS software version 9.2 (SAS Institute Inc, Cary, NC).

3.4 Results and discussion

3.4.1 Production and characterization of NaCl-induced gels of SPI

To select conditions for producing self-supported gels, different SPI concentrations and μ were tested (μ 100, 200, 300 and 400, obtained in NaCl concentrations of 100 mM, 200 mM, 300 mM and 400 mM, respectively). The visual aspects of the samples revealed that self-supported gels were only formed from formulations with at least 14% SPI and μ of 200 (200 mM NaCl). At lower protein and salt concentrations, the systems could be classified as viscous dispersions or nonsupported gels. The patterns used for visual classification of the samples were determined in a previous study of our group (Brito-Oliveira et al., 2017).

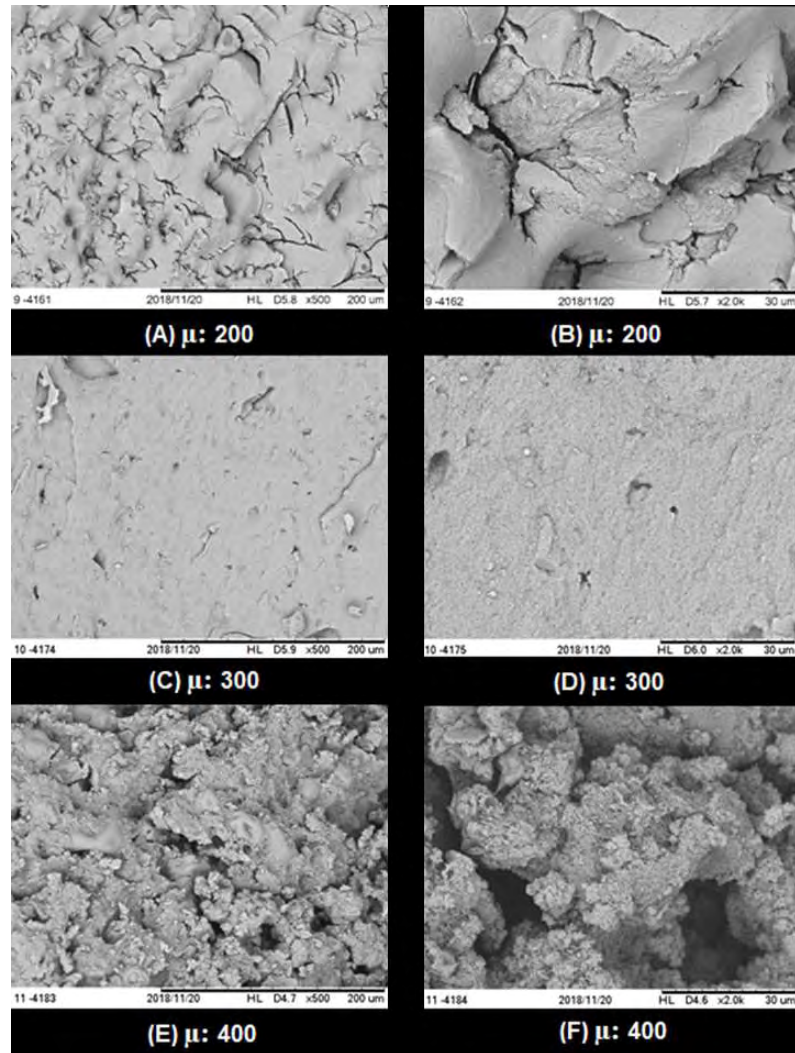
Control of the protein concentration and μ to produce cold-set gels is important to avoid the immediate overaggregation of protein molecules during preheating and, consequently, the formation of heat-induced gels instead (Maltais et al., 2005). The SPI concentration (14%) applied here was higher than those generally used for the production of cold-set gels (Maltais et al., 2005; Maltais et al., 2008), because protein aggregation during the preheating step was

not enough to induce gelation. Such behavior is probably related to the relatively low solubility of SPI at pH 7 (32%), already reported by Brito-Oliveira et al. (2018).

In that investigation, it was verified that the SPI used was not able to form heat-induced gels using the same preheating conditions (80 °C/30 min), even at higher protein concentrations (15% SPI), as self-supported gels were only formed after CaCl₂ incorporation. These results highlighted one of the most interesting features of cold-set gelation methods, i.e., the formation of gelled systems using lower protein concentrations than those required to produce heat-induced gels (Bryant & McClements, 2000; Maltais et al., 2005).

To understand the effects of the different μ values in the microstructural organizations of the NaCl-induced gels, the self-supported systems were characterized by SEM, and the micrographs are shown in Figure 3.1.

Figure 3.1. Micrographs obtained by scanning electron microscopy (SEM) of NaCl-induced gels of soy protein isolate produced with different ionic strengths. In Figures A, C and E, the magnification of 500 x was used, and the scale bar corresponds to 200 μm , while in Figures B, D and F, the magnification of 2000 x was used, and the scale bar corresponds to 30 μm .



According to the images, the gels produced with μ of 200 (Fig 3.1A and 3.1B) presented homogeneous microstructures with well distributed pores, similar to small cracks in the network, whereas the gels produced with μ of 300 (Fig 3.1C and 3.1D) presented less porous, more compact, and denser organization. According to the literature, monovalent ions can only neutralize negatively charged residues in biopolymers, promoting indirect crosslinking in double helices or other linkages by shielding the electrostatic repulsion of the carboxylate groups (Vilela et al., 2011). Therefore, it is possible to state that the denser microstructures verified in gels produced with μ of 300 (300 mM NaCl) resulted from the more effective

reduction of electrostatic repulsions among the protein groups, leading to higher protein-protein interactions (Abhyankar et al., 2011).

The increase in μ to 400 (400 mM NaCl) (Figure 3.1E and 3.1F), on the other hand, resulted in systems with less dense and more disordered and porous networks due to the excessively fast reduction of the electrostatic repulsions (Abhyankar et al., 2011; Marangoni et al., 2000). According to the literature, lower salt concentrations result in slower gelation processes, leading to the formation of stronger and ordered gels, whereas higher salt concentrations result in faster processes, causing the formation of weaker, less ordered structures with particulate microstructures, as verified in the present study (Kuhn et al., 2010; Marangoni et al., 2000). The addition of 400 mM NaCl may have caused faster aggregation of the groups, increasing the interactions within the aggregates at the expense of interactions among the aggregates that formed the gels, resulting in a particulate and porous structure.

The consequences of such microstructural organization in the rheological properties of the gels were assessed, starting with frequency sweep tests. The results shown in Figure 3.2A revealed that the increase in μ from 200 to 300 caused increases in G' and G'' and, consequently, K' and K'' (Table 3.1). Such results confirmed that the more effective reduction of electrostatic repulsions between the protein groups in systems with 300 NaCl allowed an increase in protein-protein interactions, causing the strengthening of the structures.

Table 3.1. Parameters of Power Law model (frequency sweep data), Burger's model (creep/recovery data) and uniaxial compression data of SPI gels produced with different ionic strengths (μ).

Analysis	Parameter	Ionic strength (NaCl concentration)		
		200 (200 mM)	300 (300 mM)	400 (400 mM)
Frequency sweep test	K' (Pa)	805.6 ^b ± 26.7	1122.6 ^a ± 182.2	937.0 ^{ab} ± 112.5
	n'	0.115 ^a ± 0.001	0.114 ^a ± 0.001	0.120 ^a ± 0.001
	R ²	0.99	0.99	0.99
	K'' (Pa)	145.6 ^b ± 4.3	203.0 ^a ± 33.7	176.0 ^{ab} ± 17.8
	n''	0.106 ^a ± 0.002	0.107 ^a ± 0.001	0.094 ^b ± 0.001
	R ²	0.94	0.95	0.94
Creep/recovery test	J ₀ (Pa ⁻¹)	0.6019 ^a ± 0.0298	0.3455 ^c ± 0.0233	0.4861 ^b ± 0.0194
	J ₁ (Pa ⁻¹)	0.2982 ^a ± 0.0087	0.1799 ^c ± 0.0086	0.2545 ^b ± 0.0004
	λ _{ret} (s)	29.04 ^a ± 2.28	33.72 ^a ± 2.02	31.37 ^a ± 1.74
	η ₀ (Pa.s)	2023.36 ^b ± 370.2	3422.91 ^a ± 177.23	2227.72 ^b ± 291.39
	R ²	0.81	0.81	0.82
	Recovery (%)	72.04 ^a ± 5.07	72.33 ^a ± 2.02	70.02 ^a ± 4.10
Uniaxial compression test	E _g (Pa)	1085.3 ^{ab} ± 248.8	1402.7 ^a ± 189.7	977.3 ^b ± 60.7
	σ _H (Pa)	290.5 ^a ± 22.2	417.6 ^a ± 46.8	296.7 ^a ± 18.81
	ε _H	0.187 ^a ± 0.028	0.187 ^a ± 0.042	0.233 ^a ± 0.049

Averages followed by different lowercase letters in the same line are statistically different ($p < 0.05$) for gels with different μ .

The increase from 300 to 400, on the other hand, decreased these parameters, indicating that the more porous, disorganized protein networks and thicker aggregates caused a reduction in gel strength. These results provided evidence that, at such salt concentrations, the protein interactions were probably increased within the aggregates and therefore diminished in the network, leading to the weakening of the gels. In addition, the gels produced with μ of 400 (400 mM NaCl) presented smaller elastic responses in comparison to the other values of μ tested, as verified through the higher values of $\tan \delta$ (Figure 3.2B), indicating that the effectiveness of the interactions among the protein aggregates in the network were compromised by the excessively fast reduction of the electrostatic repulsions, as previously cited.

As verified in Table 3.1, all NaCl-induced systems presented low values of n' and n'' , indicating a small dependency of G' and G'' on frequency. According to Stading and Hermansson (1990), the dependence of G' and G'' on frequency reveals the type of gel formed. For protein gels, G' and G'' depend on the frequency, but this dependence is minimal (approximately 0.1), as verified in the present study, indicating that covalent and noncovalent bonds were involved in the network formation process (Rocha et al., 2009).

The results obtained from creep/recovery tests (Figure 3.2C) were in complete agreement with the behavior observed in the frequency sweep tests. As verified in Figure 3.2C, the gels with μ of 300 presented lower compliance values than those with μ of 200, indicating a higher resistance to deformation with the constant stress applied during the creep step. However, the increase in μ to 400 decreased such resistance, providing evidence for the weakening of the gels, as previously cited.

For a better understanding of the obtained results, the data were reasonably well modeled ($R^2 > 0.81$) using Burger's model, and the parameters obtained are presented in Table 3.1. It was verified that for all formulations, the values of J_0 were higher than those of J_1 , which, according to the literature, indicates that the instantaneous elastic strain is larger than the retarded elastic and viscous flow deformation (Chang et al., 2014).

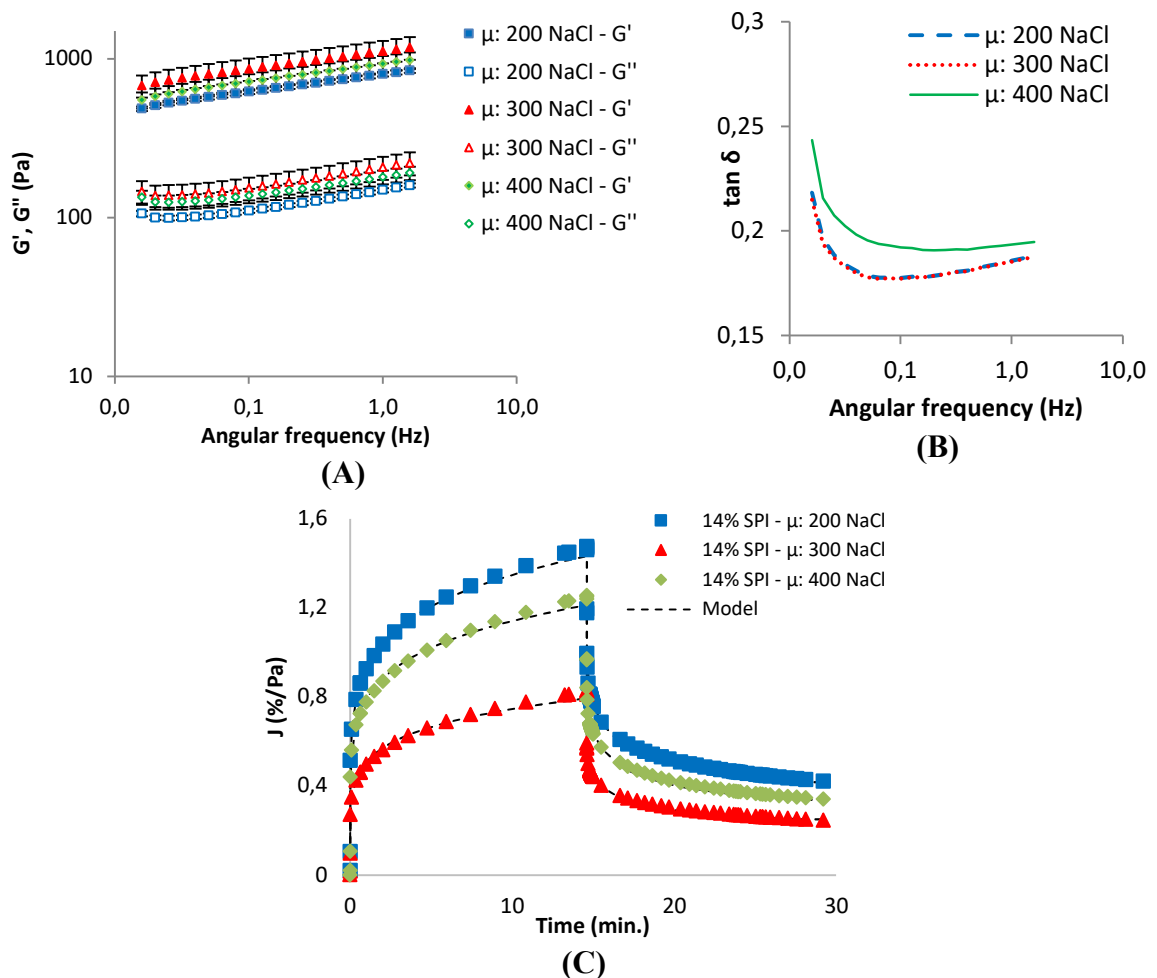
As expected, the variation in μ from 200 to 300 decreased the values of J_0 and J_1 and increased η_0 , reflecting the increase in the systems' resistance to deformation. The variation in μ from 300 to 400, however, increased J_0 and J_1 and decreased η_0 . For all systems, the values of λ_{ret} were not affected.

In addition, the obtained results revealed that variation in μ did not significantly alter the recovery percentage (\mathcal{E}) of NaCl-induced gels, which ranged between 70 and 73%, indicating that approximately 30% of the gels' deformation during the creep step was permanent and, therefore, not recoverable during the recovery step.

The results of uniaxial compression tests, also shown in Table 3.1, revealed similar effects of the variation in salt concentration on the large deformation properties of the systems. It was verified that, whereas the increase in μ from 200 to 300 increased the E_g of NaCl-induced gels, the increase from 300 to 400 decreased this parameter. All these systems, however, presented statistically the same ($p>0.05$) rupture properties.

Even though the systems characterized here were classified as self-supported gels, their strength and stability were not satisfactory, presenting aspects of weak self-supported systems after approximately 10 minutes at room temperature (Supplementary material). Such results indicated the importance of investigating alternatives to change the properties of SPI-containing cold-set gels, including the incorporation of polysaccharides into the systems. In this context and considering the higher strength of the gels produced with μ of 300 (300 mM NaCl), this ionic strength was selected to produce cold-set mixed gels with different galactomannans.

Figure 3.2. Results of frequency sweep tests (A, B) and creep/recovery tests (C) of SPI-only gels produced with different ionic strengths.



3.4.2 Incorporation of different galactomannans into NaCl-induced gels containing SPI: determination of the critical polysaccharide concentration

It is known that in cold-set methods, gelation should only occur after alteration of the quality of the solvent at low temperatures, and therefore, the protein dispersion subjected to the preheating process must have a concentration lower than the minimum required for the formation of heat-induced gels (Cavallieri & Cunha, 2008; Liu et al., 2017; Maltais et al., 2008).

Even though all self-supported gels previously characterized were only formed after salt incorporation (i.e., were all cold-set gels), there is a concern regarding the decrease in the minimal protein concentration necessary for heat-induced gel formation after the incorporation of galactomannans (Monteiro et al., 2013). According to the literature, microphase separations in mixed systems may increase the local biopolymer concentration at each phase, leading to more extensive polymer self-association and, therefore, decreasing the critical protein concentration previously cited (Maltais et al., 2008; Oliveira et al., 2015; Turgeon et al., 2003).

In this context and considering the aim of this research in characterizing cold-set mixed gels, the second step of this study consisted of incorporating different concentrations of GG and LBG between 0.1% and 0.5% into the dispersions of SPI at the concentration previously selected (14%) and determining whether the systems were self-supported gels immediately after the preheating process.

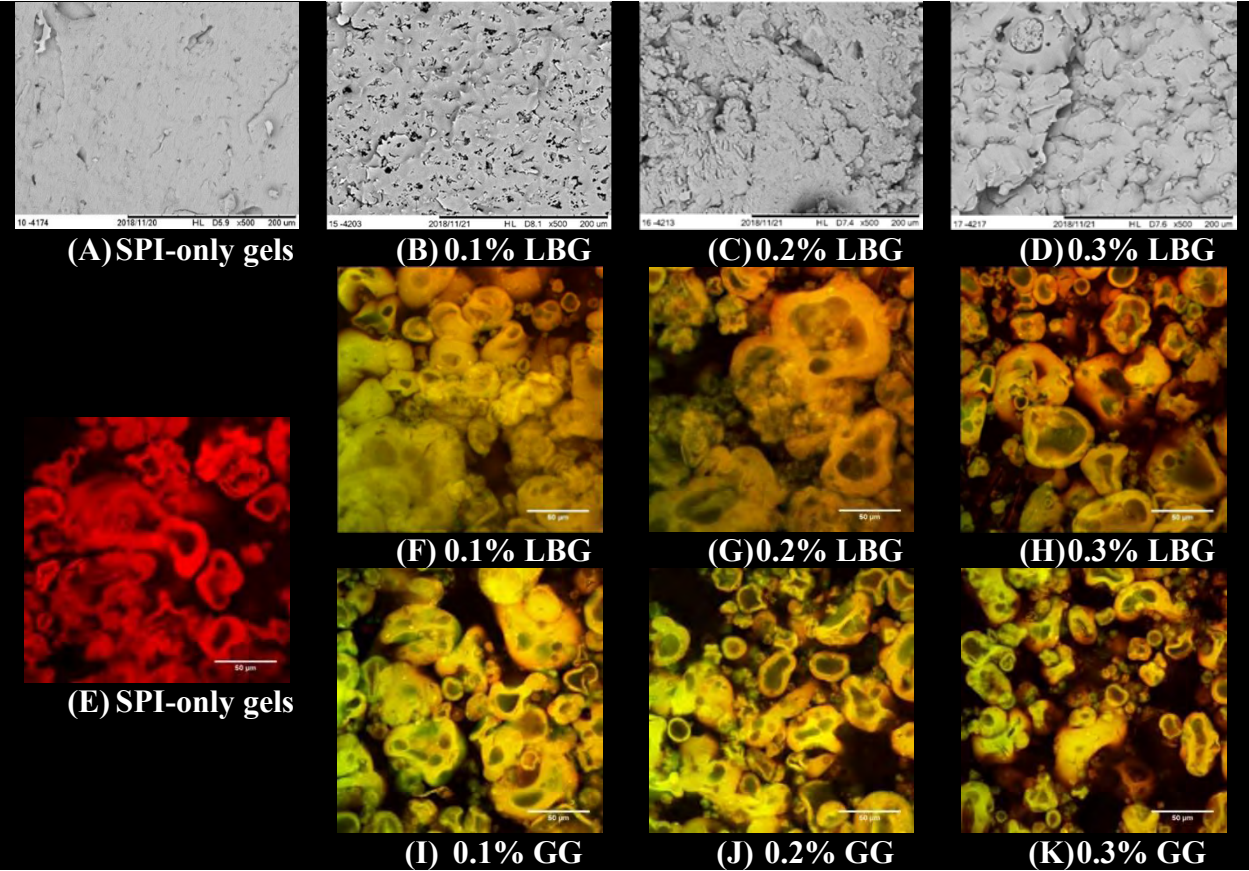
According to the visual aspects of the samples, it was verified that only the incorporation of 0.1 - 0.3% of each polysaccharide allowed the production of cold-set gels. Samples produced with 0.4% and 0.5% GG or LBG, on the other hand, were strong self-supported gels before the addition of salt (i.e., the systems were, in fact, heat-induced gels). For this reason, only concentrations of between 0.1% and 0.3% polysaccharides were selected for further evaluations.

3.4.3 Characterization of NaCl-induced mixed gels of SPI and galactomannans (locust bean gum or guar gum)

Different concentrations of the two galactomannans were incorporated into the protein gels, and the resulting systems were evaluated in terms of their microstructural organization and rheological properties.

Initially, the effect of LBG incorporation was evaluated by microscopy techniques (CLSM and SEM), and the micrographs obtained are shown in Figure 3.3.

Figure 3.3. Micrographs of NaCl-induced gels produced with different locust bean gum (LBG) and guar gum (GG) concentrations, obtained by scanning electron microscopy (SEM) (A – D) and confocal laser scanning microscopy (CLSM) (E-H). For the SEM micrographs, the magnification of 500 x was used, and the scale bar corresponds to 200 μ m. In CLSM micrographs, the Rodamine-B (used to dye the proteins) is identified by red, the FITC (used to dye the polysaccharides) is identified by green and the regions with incomplete demixing present a yellowish color. In CLSM micrographs the scale bar corresponds to 50 μ m.



The images showed that the gels with 0.1% LBG presented smaller pores (Figure 3.3B), with no clear phase separation (Figure 3.3F), which is probably related to the gelation method applied. According to the literature, the direct addition of salt results in faster gelation (Vilela et al., 2011). In the present study, this means that salt addition probably interrupted the phase separation before gel development, thereby causing incomplete demixing of the gelled systems.

The micrographs also revealed that the increase in LBG concentration from 0.1% (Figures 3.3B and 3.3F) to 0.2% (Figures 3.3C and 3.3G) increased the heterogeneity of the systems, but phase separations were not verified yet. It is possible that this increase in polysaccharide concentration increased the effects of incomplete demixing, causing a decrease in protein-protein interaction intensity, which led to a more heterogeneous and porous microstructure.

The increase in LBG concentration from 0.2% (Figures 3.3C and 3.3G) to 0.3% (Figures 3.3D and 3.3H), on the other hand, caused a small increase in the extension of the phase separation, as verified by the more evident greenish and reddish regions in the systems with higher LBG concentrations. Even though the demixing was still incomplete, this increased extension of phase separation in systems with 0.3% LBG may have allowed an increase in protein-protein interactions, resulting in a more homogeneous microstructure, with a smaller and more homogeneously distributed pore network.

As shown in Figure 3.4 and Table 3.2, the incorporation of LBG decreased the values of G' and G'' and, consequently, K' and K'' for the gels, indicating a weakening of the structures, probably due to the incomplete demixing previously explained. Among the mixed systems produced with LBG, those produced with 0.2% presented lower values of K' and K'' , followed by the gels produced with 0.1% LBG and 0.3% LBG. For all of these systems, the incorporation of polysaccharide did not affect the frequency dependency of G' and G'' , as seen by n' and n'' values (Table 3.2), nor the $\tan \delta$ values of the gels and their frequency dependence.

A decrease in the strength of SPI gels with the incorporation of LBG was also found by Hua et al. (2003), who investigated the properties of heat-induced gels. This weakening was also attributed by the authors to the incomplete demixing of the systems. The explanation given was that during heat treatment, incompatible biopolymers tend to form a single-phase solution, while during cooling, the reduction in temperature favors phase separation by reducing the contribution of the entropy of mixing to thermodynamic stability. According to these authors, cooling may also cause the formation of ordered structures, aggregation and/or gelation (in the case of heat-induced gels) of the biopolymer mixture. They stated that, for some biopolymer mixtures, a critical amount of ordering is required to induce phase separation. Due to the structural properties of LBG (which has an extended random coil conformation in dispersion),

cooling of the mixture would not induce the significant formation of ordered structures in the LBG, allowing the aggregation of soybean proteins and formation of the gelled network to take place more quickly than the phase separation process and resulting in systems with incomplete demixing.

This effect may have been even more pronounced for the systems analyzed in the present study, considering that the direct addition of salt causes fast reductions in the electrostatic repulsion between protein groups and accelerates the processes of aggregation and gelling (Vilela et al., 2011), possibly leaving even less time for the phase separation process.

The results of creep/recovery tests (Figures 3.4C and 3.4F), however, indicated the incorporation of LBG at the three concentrations tested (0.1-0.3%) resulted in decreases in compliance, with a higher resistance of the mixed systems in terms of deformation with the application of constant stress during the creep step.

Even though the presence of LBG has reduced protein-protein interactions, resulting in lower values of G' and G'' , as previously cited, it has probably stabilized the existing bounds and interactions between the protein groups, increasing the resistance of the systems to deformation when subjected to the constant stress of 5 Pa for 15 minutes. As previously cited, the interactions between the protein groups in the SPI-only gels were relatively unstable, resulting in systems with reduced ability to resist deformation (i.e., higher compliance values).

These results were also verified through the Burger model parameters (Table 3.2), which showed the incorporation of LBG decreased the values of J_0 and J_1 and increased the values of η_0 . On the other hand, all systems (in the presence and absence of LBG) presented the same recovery capacities ($p > 0.05$).

Similarly, the results of uniaxial compression tests revealed that the incorporation of 0.1% and 0.3% LBG increased the values of E_g and rupture stress in comparison to those of the protein gels, but these differences were not statistically significant ($p > 0.05$) for gels with 0.2% LBG. The incorporation of 0.1% LBG resulted in increases in rupture strain, whereas the incorporation of 0.2% and 0.3% LBG did not cause significant alterations ($p > 0.05$). These data confirmed the hypothesis previously discussed from the results of creep/recovery tests. Therefore, the presence of this polysaccharide probably stabilized the bonds and interactions among the molecules, increasing the E_g of the systems in comparison to protein gels.

The lower E_g values for gels with 0.2% LBG in comparison to those of the other concentrations tested were probably related to the extension of incomplete demixing of the systems. As previously cited, it is possible that the increase in LBG concentration from 0.1% to 0.2% caused an increase in the effects of incomplete demixing, as the higher concentration

of polysaccharides may have reduced the protein-protein interactions even more. On the other hand, with the increase from 0.2% to 0.3% LBG, the polysaccharide molecules probably started to self-associate, increasing the demixing/phase separation processes, which were still incomplete but became more intense, allowing a small increase in protein-protein interactions. In addition, as previously described, the structures were more homogeneous for gels with 0.1% and 0.3% LBG.

For systems produced with GG, microstructural characterizations were only performed using CLSM (Figure 3.3), as the strengths of the gels were not enough to resist the sample preparation process necessary for SEM. The micrographs (Figure 3.3I, 3.3J and 3.3K) show that the incorporation of this polysaccharide into the systems increased the heterogeneity of the microstructures, which did not show evident phase separation. These results also indicated the incomplete demixing of the gels, which led to lower protein-protein interactions and resulted in more discontinuous and porous and weaker systems, as also shown by the results of the frequency sweep tests (Figure 3.4 and Table 3.2).

Our results showed the incorporation of GG decreased the values of G' and G'' for the protein gels, but the variation in polysaccharide concentration from 0.1% to 0.3% did not significantly affect ($p > 0.05$) the values of K' and K'' . It was also verified that increasing the GG concentration beyond 0.2% resulted in increases in n' and n'' , indicating a higher frequency dependence of G' and G'' (Table 3.3). According to Monteiro et al. (2013), these increases in n' and n'' indicate that higher molecular rearrangements were allowed within the mixed gels during the test.

In terms of $\tan \delta$, the results shown in Figure 3.4B shows that the incorporation of GG (especially at 0.2%) increased both this parameter and its frequency dependence, indicating a decrease in the elastic responses of the systems.

Regarding the creep/recovery tests results (Figure 3.4), the incorporation of 0.1% GG into the protein systems resulted in decreases in compliance, whereas the incorporation of higher concentrations of this polysaccharide increased this parameter. This behavior was also verified through the Burger model parameters (Table 3.2), which revealed that, whereas the incorporation of 0.1% GG decreased the values of J_0 and J_1 and increased the values of η_0 , the incorporation of higher concentrations increased the values of J_0 and J_1 and decreased the values of η_0 . Additionally, in this case, the incorporation of GG did not significantly alter the recovery capacity of the systems (Table 3.2).

The different types of behavior verified here with the incorporation of distinct concentrations of GG are possibly related to rearrangements and molecular interactions in

systems. It is probable that, during the test, structural rearrangements reduced the effect of incomplete demixing in systems with 0.1% GG, allowing an increase in interactions among protein molecules and, consequently, increasing the resistance of the systems to deformation.

On the other hand, it seems that in the gels produced with higher GG concentrations (0.2 and 0.3%), the application of constant stress probably resulted in less pronounced structural rearrangements. Therefore, the incomplete demixing verified in the micrographs decreased the interactions among the protein groups, which may have reduced the resistance of the systems to deformation.

It should be noted that gels produced with GG were not strong enough to undergo uniaxial compression tests, and these results are, therefore, not available.

Finally, the properties of the gels produced with the same concentrations of the different polysaccharides were compared. The different microstructures formed (Figure 3.3) were related to the higher capacity of the LBG to self-associate due to its lower degree of branching. For this reason, the phase separation processes in systems containing LBG were faster than those in systems containing GG. According to Monteiro et al. (2013), the more pronounced phase separations in mixed systems of SPI and galactomannans are caused by increases in galactomannan concentration and reductions in the branching degree. These authors affirm that less branched galactomannans are prone to autoassociate and to be part of more extensive molecular interactions, as shown in the present study.

These different capacities and microstructural organizations also affected the rheological properties of the gels. It was noticed that gels with LBG showed higher values of G' and G'' and, consequently, K' and K'' , than those with GG. In addition, at polysaccharide concentrations of 0.2% and 0.3%, gels with GG showed more frequency-dependent moduli, as indicated by the values of n' and n'' .

Additionally, from the creep/recovery tests (Figure 3.4), it was verified that the LBG-SPI mixed gels presented lower compliance values and, consequently, lower values of J_0 and J_1 and higher values of η_0 than GG-SPI mixed gels. The recovery capacities (Table 3.2), however, were statistically the same for gels produced with the two galactomannans.

According to Monteiro et al. (2013), the stronger forces in gels produced with LBG in comparison to those produced with GG are related to the lower degree of branching of the LBG molecules. For galactomannans, intermolecular interactions tend to occur mainly via hydrogen bonds between the nonsubstituted mannan regions of the structures. Thus, for polysaccharides with a higher mannose-to-galactose (M/G) ratio, the length of the unsubstituted mannan

backbone available for intermolecular associations is higher, which contributes to the formation of stronger systems (Monteiro et al., 2013).

From the gels analyzed here, those with GG showed higher values of $\tan \delta$ than those with LBG, indicating that the incorporation of the polysaccharide with the higher M/G ratio resulted in the formation of systems with higher elastic contributions, probably due to the stronger intermolecular interactions, as previously explained.

Even though the incorporation of galactomannans did not increase the SPI gel strength, the presence of LBG increased the stability of the systems at room temperature, possibly by stabilizing the protein-protein interactions within the matrices, as the mixed systems were still self-supported after a longer period than the SPI-only gels (Supplementary material). According to the literature, non-ionic polysaccharides may, in fact, exert a stabilizing effect through electrostatic interactions with soy proteins (Giancone, Torrieri, Masi, & Michon, 2009; Monteiro et al., 2013), depending mainly on polymer concentration, as verified in the present study.

Figure 3.4. Results of frequency sweep tests (A, B, D, E) and creep/recovery tests (C, F) of NaCl-induced mixed protein/polysaccharide gels with different guar gum (GG) (A, B, C) and locust bean gum (LBG) (D, E, F) concentration

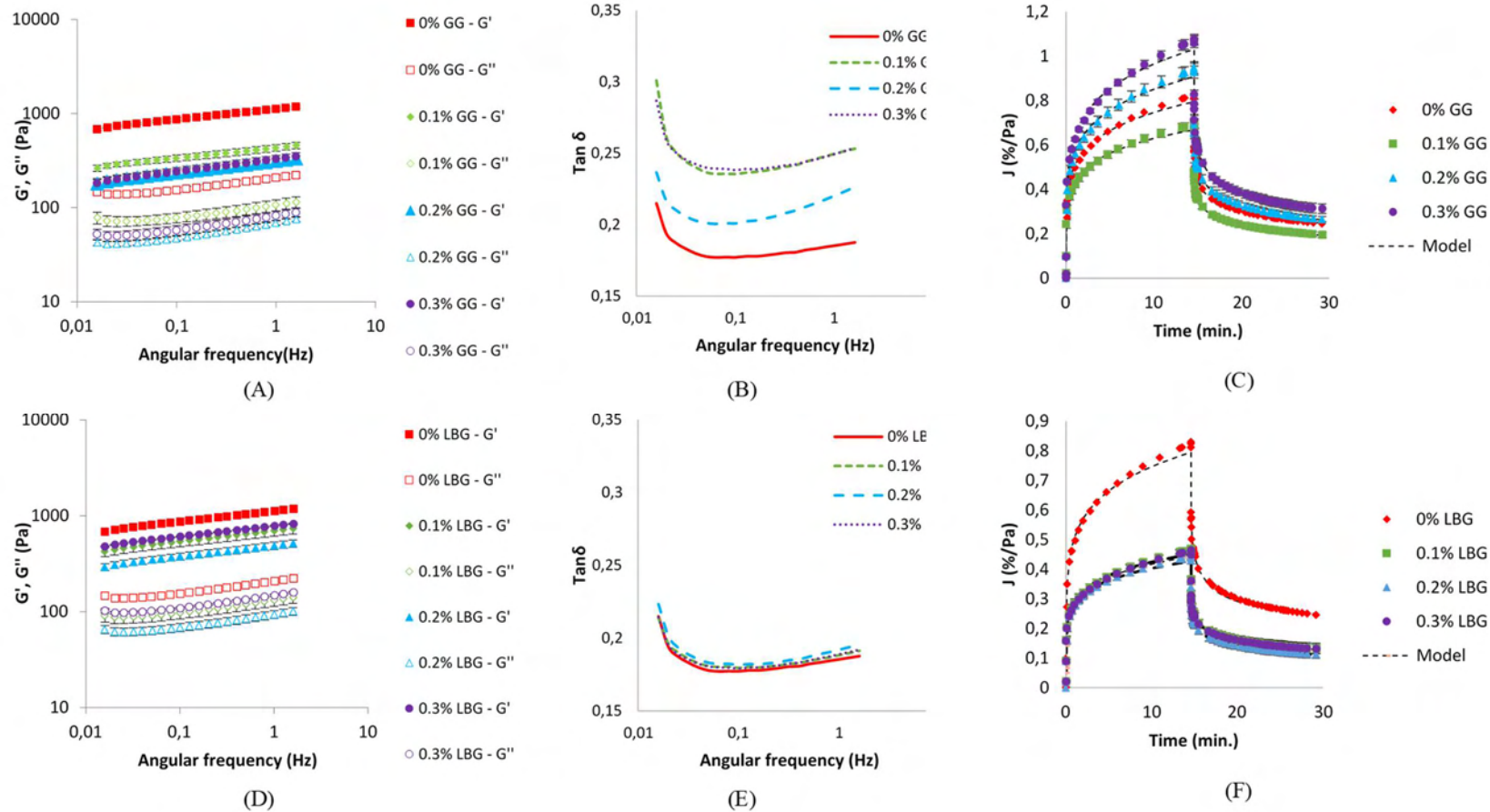


Table 3.2. Parameters of Power Law model (frequency sweep data), Burger's model (creep/recovery data) and uniaxial compression obtained from mixed gels produced with different concentrations of locust bean gum (LBG) or guar gum (GG).

Analysis	Parameter	Formulation						
		SPI-only	0.1% LBG	0.2% LBG	0.3% LBG	0.1% GG	0.2% GG	0.3GG
Frequency sweep test	K' (Pa)	1123 ^a ± 182	704 ^{bcA} ± 90	490 ^{cA} ± 43	783 ^{bA} ± 4	433 ^{bb} ± 36	313 ^{bb} ± 21	329 ^{bb} ± 31
	n'	0.114 ^a ± 0.001	0.115 ^{aA} ± 0.001	0.117 ^{aA} ± 0.002	0.114 ^{ab} ± 0.002	0.113 ^{ba} ± 0.005	0.128 ^{abA} ± 0.011	0.137 ^{aA} ± 0.005
	R ²	0.998	0.998	0.997	0.998	0.996	0.998	0.998
	K'' (Pa)	203 ^a ± 34	129 ^{bcA} ± 18	91 ^{cA} ± 9	144 ^{bA} ± 3	103 ^{bA} ± 14	67 ^{bb} ± 4	80 ^{bb} ± 9
	n''	0.107 ^a ± 0.002	0.109 ^{aA} ± 0.001	0.110 ^{ab} ± 0.001	0.110 ^{ab} ± 0.002	0.103 ^{ba} ± 0.006	0.137 ^{aA} ± 0.014	0.130 ^{aA} ± 0.005
	R ²	0.950	0.910	0.960	0.966	0.910	0.960	0.966
Creep/recovery test	J ₀ (Pa ⁻¹)	0.3455 ^a ± 0.0233	0.1890 ^{bb} ± 0.0110	0.1877 ^{bb} ± 0.0085	0.1846 ^{bb} ± 0.0054	0.2809 ^{cA} ± 0.0158	0.362 ^{abA} ± 0.0238	0.3987 ^{aA} ± 0.0071
	J ₁ (Pa ⁻¹)	0.1799 ^a ± 0.0086	0.0954 ^{bb} ± 0.0046	0.0883 ^{bb} ± 0.0045	0.0938 ^{bb} ± 0.0044	0.1415 ^{dA} ± 0.0018	0.2032 ^{ba} ± 0.0107	0.2322 ^{aA} ± 0.0016
	λ _{ret} (s)	33.72 ^a ± 2.02	32.28 ^{aA} ± 0.81	30.59 ^{aA} ± 1.26	32.42 ^{aA} ± 0.60	32.96 ^{aA} ± 0.93	34.08 ^{aA} ± 2.59	33.69 ^{aA} ± 0.78
	η ₀ (Pa.s)	3422.91 ^b ± 177.23	6213.7 ^{aA} ± 686.31	7154.07 ^{aA} ± 839.15	6087.94 ^{aA} ± 496.76	4183.24 ^{ab} ± 223.72	3066.07 ^{bcB} ± 140.91	2616.62 ^{cB} ± 143.13
	R ²	0.81	0.83	0.82	0.83	0.81	0.82	0.83
	Recovery (%)	72.33 ^a ± 2.02	71.68 ^{aA} ± 3.93	74.27 ^{aA} ± 3.36	71.58 ^{aA} ± 3.79	71.84 ^{aA} ± 1.37	71.75 ^{aA} ± 1.60	70.79 ^{aA} ± 1.47
Uniaxial compression test	E _g (Pa)	1403 ^b ± 190	1978 ^a ± 21	1074 ^b ± 82	2083 ^a ± 215	-	-	-
	σ _H (Pa)	418 ^b ± 47	766 ^a ± 24	531 ^{ab} ± 75	737 ^a ± 70	-	-	-
	ε _H	0.187 ^b ± 0.042	0.264 ^a ± 0.013	0.258 ^{ab} ± 0.072	0.235 ^{ab} ± 0.041	-	-	-

Averages followed by different lowercase letters, in the same line, are statistically different (p<0.05) for gels with different concentrations of the same polysaccharide. Averages followed by different capital letters, in the same line, are statistically different (p<0.05) for gels with the same concentration of different polysaccharides.

3.5 Conclusions

The results obtained here showed the ability of SPI to form self-supported gels from systems with at least 14% SPI and μ of 200 (200 mM NaCl). Such a relatively high protein concentration is related to the solubility profile of the commercial ingredient applied. Due to the relatively low solubility of SPI at pH 7, the protein gels were relatively unstable, indicating features of weak self-supported gels after a few minutes at room temperature. The systems' stability increased with the incorporation of LBG and GG, even though such additions did not increase the gel strength. The decrease in the gel strength with galactomannan incorporation was caused by the incomplete demixing of the systems, whose extension varied with the concentration and branching degree of the galactomannans. Due to the higher capacity of LBG to self-associate, its incorporation resulted in stronger gels, with higher microstructural phase separation and higher stability. Even though LBG incorporation did not satisfactorily increase the strength of the SPI gels, it increased the stability of the gels, increasing, therefore, the possibility of future applications for the formulations characterized here, especially those with 14% SPI and 0.1% LBG. In our next study, for example, such formulations will be applied to produce emulsion-filled gels, which are important and promising systems for the food industry.

Acknowledgments

This study was funded by Fundação de Amparo à Pesquisa do Estado de São Paulo (FAPESP) (grant number 2017/06224-9). We also thank the access to equipment and assistance provided by the Electron Microscope Laboratory (LME/UNICAMP).

Conflict of Interest: The authors declare that they have no conflict of interest.

3.6 References

- Abae, A., Mohammadian, M., & Jafari, S.M. (2017). Whey and soy protein-based hydrogels and nano-hydrogels as bioactive delivery systems. *Trends in Food Science and Technology*, 70, 69–81.
- Abhyankar, A.R., Mulvihill, D.M., & Auty, M.A.E. (2011). Combined microscopic and dynamics rheological methods for studying the structural breakdown properties of whey protein gels and emulsion filled gels. *Food Hydrocolloids*, 25 (3), 275-282.

- Barak, S., & Mudgil, D. (2014). Locust bean gum: Processing, properties and food applications - A review. *International Journal of Biological Macromolecules*, 66, 74–80.
- Brito-Oliveira, T.C., Bispo, M., Moraes, I.C.F., Campanella, O.H. & Pinho, S.C. (2017). Stability of curcumin encapsulated in solid lipid microparticles incorporated in cold-set emulsion filled gels of soy protein isolate and xanthan gum. *Food Research International*, 102, 759–767.
- Brito-Oliveira, T.C., Bispo, M., Moraes, I.C.F., Campanella, O.H. & Pinho, S.C. (2018). Cold-Set Gelation of Commercial Soy Protein Isolate: Effects of the Incorporation of Locust Bean Gum and Solid Lipid Microparticles on the Properties of Gels. *Food Biophysics*, 13(3), 226–239.
- Bryant, C.M. & McClements, D.J. (2000). Influence of NaCl and CaCl₂ on cold-set gelation of heat-denatured whey protein. *Journal of Food Science*, 65(5), 801–804.
- Cavallieri, A.L.F, & Cunha, R.L. (2008). The effects of acidification rate, pH and ageing time on the acidic cold set gelation of whey proteins, *Food Hydrocolloids*, 22(3), 439–448.
- Chang, Y., Li, D., Wang, L., Bi, C. & Adhikari, B. (2014). Effect of gums on the rheological characteristics and microstructure of acid-induced SPI-gum mixed gels. *Carbohydrate Polymers*, 108, 183–191.
- Dickinson, E. (2006). Colloid science of mixed ingredients. *Soft Matter*, 2, 642–652.
- Giancone, T., Torrieri, E., Masi, P., & Michon, C. (2009). Proteine-polysaccharide interactions: phase behaviour of pectine-soy flour mixture. *Food Hydrocolloids*, 23, 1263–1269.
- Hua, Y., Cui, S.W. , & Wang, Q. (2003). Gelling property of soy protein–gum mixtures. *Food Hydrocolloids*, 17(6), 889–894.
- Ingrassia, R., Bea, L.L., Hidalgo, M.E., & Risso, P.H. (2019). Microstructural and textural characteristics of soy protein isolate and tara gum cold-set gels. *LWT - Food Science and Technology*. 113 (2019) 108286.
- Jong, S., & Van De Velde, F. (2007). Charge density of polysaccharide controls microstructure and large deformation properties of mixed gels. *Food Hydrocolloids*, 21(7), 1172–1187.

- Kuhn, K. R., Cavallieri, A.L.F., & Cunha, R.L. (2010). Cold-set whey protein gels induced by calcium or sodium salt addition. *International Journal of Food Science and Technology*, 45, 348–357
- Liu, B., Wang, H., Hu, T., Zhang, P., Zhang, Z., Pan, S. & Hu, H. (2017). Ball-milling changed the physicochemical properties of SPI and its cold-set gels. *Journal of Food Engineering*, 195, 158–165.
- Maltais, A., Remondetto, G.E., Gonzalez, R., & Subirade, M (2005). Formation of soy protein isolate cold-set gels: protein and salt effects. *Journal of Food Science*, 70(1), 67–73.
- Maltais, A, Remondetto, G.E., & Subirade, M. (2008). Mechanisms involved in the formation and structure of soya protein cold-set gels: A molecular and supramolecular investigation, *Food Hydrocolloids*. 22(4), 550–559.
- Marangoni, A.G., Barbut, S., McGauley, S.E., Marcone, M., & Narine, S.S. (2000). On the structure of particulate gels – the case of salt-induced cold gelation of heat-denatured whey protein isolate, *Food Hydrocolloids*., 14, 61–74.
- Monteiro, S.R., Rebelo, S., Silva, O.A.B.C., & Lopes-da-Silva J.A. (2013). The influence of galactomannans with different amount of galactose side chains on the gelation of soy proteins at neutral pH. *Food Hydrocolloids*, 33, 349-360.
- Mudgil, D, Barak, S., & Khatkar, B.S. (2014). Guar gum: processing, properties and food applications—A Review. *Journal of Food Science and Technology*, 51(3), 409–418.
- Oliver, L, Scholten, E., & Van Aken, G.A. (2015). Effect of fat hardness on large deformation rheology of emulsion-filled gels. *Food Hydrocolloids*, 43, 299-310.
- Picone, C. S. F., Takeuchi, K. P., & Cunha, R. L. (2011). Heat-induced whey protein gels: Effects of pH and the addition of sodium caseinate. *Food Biophysics*, 6, 77-83.
- Rocha, C., Teixeira, J.A., Hilliou, L., Sampaio, P., & Gonçalves, M.P. (2009). Rheological and structural characterization of gels from whey protein hydrolysates/locust bean gum mixed systems. *Food Hydrocolloids*, 23, 1734–1745.
- Stading, M., & Hermansson, M.A. (1990). Viscoelastic behaviour of b-lactoglobulin structures. *Food Hydrocolloids*. 4(2), 121–135.

Tavares, C., Monteiro, S.R., Moreno, N. & Lopes da Silva, J.A. (2005). Does the branching degree of galactomannans influence their effect on whey protein gelation? *Colloids and Surfaces A: Physicochem. Eng. Aspects*, 270–271, 213–219.

Tolstoguzov, V. (2003). Some thermodynamic considerations in food formulation. *Food Hydrocolloids*, 17, 1–23.

Tripathi, A.D., Mishra, R., Maurya, K.K., Singh, R.B., & Wilson, D.W. - Estimates for world population and global food availability for global health in Singh, R.B., Watson, R.R., & Takahashi, T. (Eds.), *The role of functional food security in global health*, Academic Press (2019)

Turgeon, S.L., Beaulieu, M., Schmitt, C. & Sanchez, C. (2003). Protein-polysaccharide interactions: phase-ordering kinetics, thermodynamic and structural aspects. *Current Opinion in Colloid and Interface Science*, 8, 401-414.

Vilela, J.A.P., Cavallieri, A.L.F., & Cunha, R.L. (2011). The influence of gelation rate on the physical properties/structure of salt-induced gels of soy protein isolate-gellan gum. *Food Hydrocolloids*, 25(7), 1710-1718.

Zheng, L, Teng, F, Wang, N., Zhang, X., Regenstein, J.M., Liu, J., Li, Y. & Wang, Z. (2019). Addition of Salt Ions before Spraying Improves Heat and Cold-Induced Gel Properties of Soy Protein Isolate (SPI). *Applied Sciences*, 9, 1076.

**CHAPTER 4 : MICROSTRUCTURAL AND RHEOLOGICAL
CHARACTERIZATION OF CaCl_2 -INDUCED GELS OF SOY PROTEIN ISOLATE
AND THE EFFECTS OF INCORPORATING DIFFERENT GALACTOMANNANS**

(Edited for submission to: Journal of Molecular Liquids)

**Thais C. Brito-Oliveira, Ana Clara M. Cavini, Leticia S. Ferreira, Izabel C.F.
Moraes, and Samantha C. Pinho**

Microstructural and rheological characterization of CaCl₂-induced gels of soy protein isolate
and the effects of incorporating different galactomannans

Thais C. Brito-Oliveira¹, Ana Clara M. Cavini¹, Leticia S. Ferreira¹, Izabel C.F. Moraes¹, and
Samantha C. Pinho^{1*}

¹Department of Food Engineering, School of Animal Science and Food Engineering,
University of São Paulo (USP), Pirassununga, SP, Brazil

* Corresponding author: S.C. Pinho, Department of Food Engineering, School of Animal Science and Food Engineering (FZEA), University of São Paulo (USP), Av. Duque de Caxias Norte 225, Jd. Elite, Pirassununga, SP, Brazil 13635-900. Tel: +55-19-35654288; fax: +55-19-3565-4284.

E-mail address: samantha@usp.br

4.1 Abstract

This study aimed to evaluate the microstructural organizations and rheological properties of CaCl_2 -induced gels of soy protein isolate (SPI) (14%, w/v) produced with different ionic strengths (μ : 100 – 400), and also investigate the effects of incorporating guar gum (GG) and locust bean gum (LBG) (0.1 – 0.3%, w/v) to the systems. The results revealed that, the higher the salt concentration the higher the gels' heterogeneity, coarseness and porosity. Systems with 100 mM CaCl_2 presented higher G' , G'' , and E_g and lower compliance values, being, therefore, chosen for producing mixed (protein + galactomannans) gels. Mixed gels presented different degrees of phase separation, which decreased with the increase of galactomannans' concentrations. GG demonstrated a lower capacity to self-associate, resulting in gels with lower G' , G'' , and E_g , and higher compliance values than LBG. Galactomannan's incorporation was interesting to modify the gels' microstructure, increasing their strength, especially at low concentrations, with more pronounced microphase separations.

Keywords: Soy protein isolate; Cold-set gelation; Galactomannans; Salt-induced

4.2 Introduction

Protein gelation is an important process used to obtain interesting texture attributes in many food products. Such process involves three steps: unfold of native protein structure, aggregation, and formation of the continuous protein matrix¹. These steps, however, may be carried out using different methods, including heat-induction¹. Even though heat-induced gelation methods are the most common, a great effort has been made for the development and characterization of cold-set gels²⁻⁸. In cold-set gelation, the denaturation and aggregation occur during a preheating step, and the gelation process is induced at lower temperatures, by alterations of solvent quality, by incorporating salts, for example²⁻⁸.

The properties of salt-induced gels depend mostly on the ionic strength and the type of salt applied^{5,7}. According to Bryant and McClements⁵, who produced cold-set gels of whey-protein isolate (WPI) using different concentrations of NaCl (0 to 400 mM) and CaCl₂ (0 to 15 mM), systems induced by divalent ions tend to present higher strength due to the higher capacity of such salts to screen electrostatic interactions and its ability to form salt bridges between the negatively charged carboxylic groups on neighboring protein molecules. For such capacities, CaCl₂ can form gels at lower ionic strengths than NaCl.

The same NaCl concentrations applied by Bryant and McClements⁵ were used in the last study of our group for producing cold-set gels of soy protein isolate (SPI)². In such study, however, the NaCl-induced gels were highly unstable, due to the relatively low solubility of the protein ingredient at pH 7 (applied throughout the experiments)^{2,9,10}. Due to such drawback, galactomannans (locust bean gum - LBG and guar gum – GG) were incorporated to the systems, as a strategy to possibly improve protein functionality, altering the structure and stability of the gels^{2,11,12}. In fact, after the incorporation of the polysaccharides, especially of LBG, the gels had their stability increased, and protein matrices with unique microstructural and rheological properties were obtained².

SPIs are important plant protein ingredients, known for its nutritional value, low cost and functional properties, including the capacity to form cold-set gels^{2,13,14}. The growing interest in introducing such plant proteins in food formulations is justified by the new dietary preferences of many consumers, who are concerned with the safety and sustainability of animal-based products and also with issues related to animal welfare^{2,11,13-15}.

Considering the importance of continuing the investigation of the properties of cold-set SPI gels, the present study aimed to characterize CaCl₂-induced gels produced using the same SPI concentration (14%) and same ionic strengths (100 – 400) than the ones previously applied for

producing NaCl-induced gels ². In addition, the effects of incorporating two distinct galactomannans (LBG and GG) to the systems were also evaluated. The CaCl₂ concentrations tested here (33.3 mM – 133.3 mM) were calculated to obtain the same ionic strengths used in our previous study ².

4.3 Materials and methods

4.3.1 Chemicals and reagents

SPI (Protimarti M-90, 84.3% protein) was obtained from Marsul (Montenegro, RS, Brazil) and has been previously characterized ¹⁰. Calcium chloride dihydrate was purchased from Kyma (Americana, SP, Brazil), guar gum (M/G: 1.5) was obtained from Êxodo Científica (Hortolândia, SP, Brazil) and locust bean gum (M/G: 3.8) (Viscogum LBG ®) was donated by Cargill (Campinas, SP, Brazil). Ultrapure water (from a Millipore system Direct Q3®, Billerica, MA, USA) was used throughout the experiments.

4.3.2 Production of cold-set SPI gels

Cold-set SPI gels were produced according to protocol applied in our previous study ². For this purpose, the SPI powder was hydrated using deionized water up to 14% (w/v) and the samples were manually mixed for 5 min at room temperature. Afterwards, the pH of the dispersions was adjusted to 7 (UltraBasic Benchtop pH Meter, Denver instrument, New York, NY, USA), and the systems were preheated in a water bath at 80°C for 30 min. Then, the samples were cooled to room temperature for the addition of CaCl₂. The samples were stored at 10°C for 12 h before the characterizations. Different ionic strength were tested (μ : 100, 200, 300 and 400, obtained with the incorporation of 33.3 mM, 66.7 mM, 100 mM and 133.3 mM of CaCl₂, respectively) and the best formulation (which resulted in self-supported and stronger gels) was selected to produce the mixed (polysaccharide + SPI) gels.

For mixed gels production the same protocol described above was applied, however different amounts of LBG or GG (0.1–0.3%, w/v) added to the SPI powder before hydration. The ionic strength selected for mixed gels production was 300 (100 mM CaCl₂). The samples were also stored at 10°C for 12 h before the characterizations.

4.3.3 Small strain oscillatory tests

Small strain oscillatory tests were performed according to a protocol adapted from Chang et al.¹⁶, in an AR2000 rheometer (TA Instruments, New Castle, DE, USA), using an aluminum parallel plate geometry (60 mm diameter, 1 mm gap), at 10°C. To avoid water evaporation, silicone oil was added at the edge of the samples and before the experiments, a 2 min resting period was respected. Strain sweep tests (data not shown) were developed in the range 0.01–100%, at a constant frequency of 1 Hz, for the determination of the linear viscoelastic regions (LVRs) of the samples. Frequency sweep tests were carried out over an angular frequency range of 0.016–1.6 Hz, using a strain amplitude of 2% (within the LVRs). The dependence of both viscoelastic moduli (G' and G'') on angular frequency was described by a power law model (Equations 4.1 and 4.2), using the nonlinear regression feature in Excel (Microsoft, Seattle, WA, USA)¹⁶:

$$G' = K' \cdot \omega^{n'} \quad (4.1)$$

$$G'' = K'' \cdot \omega^{n''} \quad (4.2)$$

where K' and K'' are power law parameters, n' and n'' are frequency exponents, and ω is the angular frequency.

4.3.4 Creep/recovery tests

Creep/recovery tests were developed according to Brito-Oliveira et al.² in an AR2000 rheometer (TA Instruments, New Castle, PN, EUA), using an aluminum parallel plate geometry (60 mm diameter, 2 mm gap), at 10°C. For this purpose, a resting time of 10 minutes was applied for the elimination of loading effects. Afterwards, a constant stress of 5 Pa was applied for 15 min (creep) and then removed for the evaluation of the recovery behavior of the samples for more 15 min. Silicone oil was added on the edges of the samples in order to avoid water evaporation. Creep and recovery data were analyzed using the four-parameter Burger's model represented by Equation 4.3¹⁶.

$$J(t) = \begin{cases} J_0 + J_1 \left(1 - \exp \left(\frac{-t}{\lambda_{ret}} \right) \right) + \frac{t}{\eta_0}, & t \leq t_1 \\ J_1 \left(\exp \left(\frac{t_1-t}{\lambda_{ret}} \right) - \exp \left(\frac{-t}{\lambda_{ret}} \right) \right) + \frac{t_1}{\eta_0}, & t > t_1 \end{cases} \quad (4.3)$$

where J_0 is the instantaneous compliance in Pa^{-1} , η_0 is the viscosity of the Maxwell dashpot in $\text{Pa}\cdot\text{s}$, J_1 is the compliance associated with the Kelvin–Voigt element in Pa^{-1} , λ_{ret} is the retardation

time associated with the Kelvin–Voigt element in s, and t_1 is the time when the stress was removed.

The recovery rates were calculated using Equation 4.4, where ε_{\max} is the maximum strain at the end of the creep test and ε_f is the final strain ¹⁶.

$$\text{Recovery (\%)} = \frac{\varepsilon_{\max} - \varepsilon_f}{\varepsilon_{\max}} \quad (4.4)$$

4.3.5 Uniaxial compression tests

Uniaxial compression tests were performed in a texturometer (TA-XT.plus Texture Analyser, Godalming, Surrey, UK) according to a protocol adapted from Oliver et al.¹⁷. All samples had a cylindrical shape of 30 mm height and 20 mm diameter and were compressed to 80% of their original height using an aluminum probe, at a crosshead speed of 1 mm/s. The probe was lubricated with silicone oil to minimize friction. All formulations were tested using five replicates. The values of Hencky stress (σ_H) and Hencky strain (ε_H) were calculated using Equations (4.5) and (4.6), respectively:

$$\sigma_H = F(t) \cdot \frac{H(t)}{H_0 \cdot A_0} \quad (4.5)$$

$$\varepsilon_H = \ln \frac{H(t)}{H_0} \quad (4.6)$$

where $F(t)$ is the force at time t , A_0 is the initial area, H_0 is the initial height, and $H(t)$ is the height at time t . The rupture parameters were associated with the maximum value of the stress–strain curve. The values of the apparent Young’s modulus (E_g) of the systems were calculated by the slope of the first linear interval in the Hencky stress (σ_H) versus Hencky strain (ε_H) curves, up to rupture.

4.3.6 Scanning electron microscopy

Samples were prepared before scanning electron microscopy (SEM), following protocol described by Picone et al.¹⁸. The gels ($1.0 \times 0.5 \times 0.5$ cm) were initially fixed in 2.5 g/100 g glutaraldehyde in a cacodylate buffer (16 g/L) at pH 7.2 and stored at 7°C for 24 h. Afterwards, they were rinsed twice in a cacodylate sodium buffer (16 g/L, pH 7.2) and fractured in liquid nitrogen. Subsequently, the gels were subjected to post-fixation using osmium tetroxide 1 g/100 g in a cacodylate buffer (16 g/L, pH 7.2) for 120 min, rinsed twice in deionized water, and dehydrated in a graded ethanol series (30, 50, 70, and 90 mL/100 mL) for 20 min in each. Dehydration was continued in 100% ethanol (three changes in 1 h), and then completed by

critical point drying (CPD03 Balzers Critical Point Dryer, Alzenau, Germany). The samples were fractured, placed in aluminum stubs and coated with gold (200 s/40 mA) in a Balzers SCD 050 Sputter Coater (Alzenau, Germany). SEM observations were performed using a TM 3000 tabletop microscope (Hitachi, Tokyo, Japan).

4.3.7 Confocal laser scanning optical microscopy

Confocal laser scanning microscopy (CLSM) (Confocal Upright Microscope LSM 780 NLO-Zeiss, Zeiss, Germany) was developed using simultaneous dual-channel imaging, according to Brito-Oliveira et al.⁹. Two different solutions were prepared and incorporated to the gels: (I) rhodamine B solution (0.2 %, w/v, in deionized water - 10 μ L solution/mL of gel) and (II) fluorescein isothiocyanate (FITC) solution (1 mg/mL dimethyl sulfoxide, DMSO - 0.05 mL solution/mL of gel). The protein phase was visualized by exciting rhodamine B at a wavelength of 543 nm and at an emission wavelength range of 551–655 nm, and the polysaccharides were visualized by exciting the dye fluorescein isothiocyanate (FITC) at an excitation wavelength of 488 nm and an emission wavelength range of 493–543 nm.

4.3.8 Statistical analyses

All measurements and experimental samples were performed/produced at least in triplicate and mean values and corresponding errors were calculated. For the statistical treatment of data, an analysis of variance (ANOVA) was conducted, followed by Tukey's tests with a 5% significance level using SAS software version 9.2 (SAS Institute Inc, Cary, NC).

4.4 Results and discussion

4.4.1 Microstructural organizations of SPI-only gels

From the visual aspects of the samples produced with different ionic strengths (Figure 4.1), it was verified that all systems were self-supported gels. Even though the protein concentration applied is higher than the ones generally used for cold-set gelation processes, the results of our last study showed it was lower than the critical concentration necessary for heat-induced gelation². In that case, NaCl-induced gels were only formed using a ionic strength of, at least, 200, as at lower ionic strengths, the concentrations of NaCl were not enough to produce

self-supported gels². As verified in the present study, however, the incorporation of CaCl₂ allowed the formation of gels at a lower ionic strength (μ of 100, obtained using a CaCl₂ concentration of 33.3 mM).

According to the literature, the ability of CaCl₂ to induce the formation of self-supported gels at lower ionic strengths is related to the distinct capacities of the different ions. Although both, monovalent and divalent salts, are able to screen electrostatic interactions between charged protein molecules, resulting in decreases of electrostatic repulsions and protein aggregation, only the divalent cations can act as bridges between the negatively charged carboxylic groups on neighboring protein molecules, directly stabilizing the interactions between them^{5,7}.

From the SEM micrographs, shown in Figure 4.1, it was verified that all gels presented coarse and heterogeneous microstructures, and they varied with the salt concentration. Gels produced with μ of 100 (33.3 mM CaCl₂ - Figure 4.1B) presented more continuous and less porous matrices than the others with some structures similar to “capsules” in some of their regions (highlighted in the micrograph).

The continuous increase of ionic strength from 100 to 300 (i.e. 33.3 to 100 mM CaCl₂, increased the porosity and coarseness of the systems. Figures 4.1(D) to 4.1(F) indicated that gels with μ of 200 and 300 (66.7 and 100 mM CaCl₂) were mainly composed by capsule-like structures, which varied in size and proximity to each other, depending on the salt concentration. In systems produced with μ of 300 (100 mM CaCl₂), such structures were bigger and closer to each other, making the matrices more continuous and compact. In gels produced with μ of 400 (133.3 mM CaCl₂), on the other hand, the microstructures were mainly formed by the small protein particles/aggregates, presenting a “sandy” and very particulate aspect.

The formation of these microstructures is probably related to the different aggregation processes that occurred from preheating and subsequent salt incorporation. According to Guo et al.¹⁹, when β -conglycinin and the glycinin (both present in the SPI) are heated together at pH 7, the hydrophilic groups from β -conglycinin may occupy the surface of the complex aggregates formed mainly by glycinin. Possibly, such aggregation process led to an initial formation of the “capsule-like” structures previously cited. As the protein concentration used was below the critical concentration for the formation of heat-induced gels², such aggregates were still dispersed and were not able to form a continuous matrix during preheating.

After the incorporation of 33.3 mM of CaCl₂ (μ of 100), however, the interactions inside and among the protein aggregates increased due to the reduction of electrostatic repulsion between protein chains and the formation of salt bridges among the charged carboxylic groups.

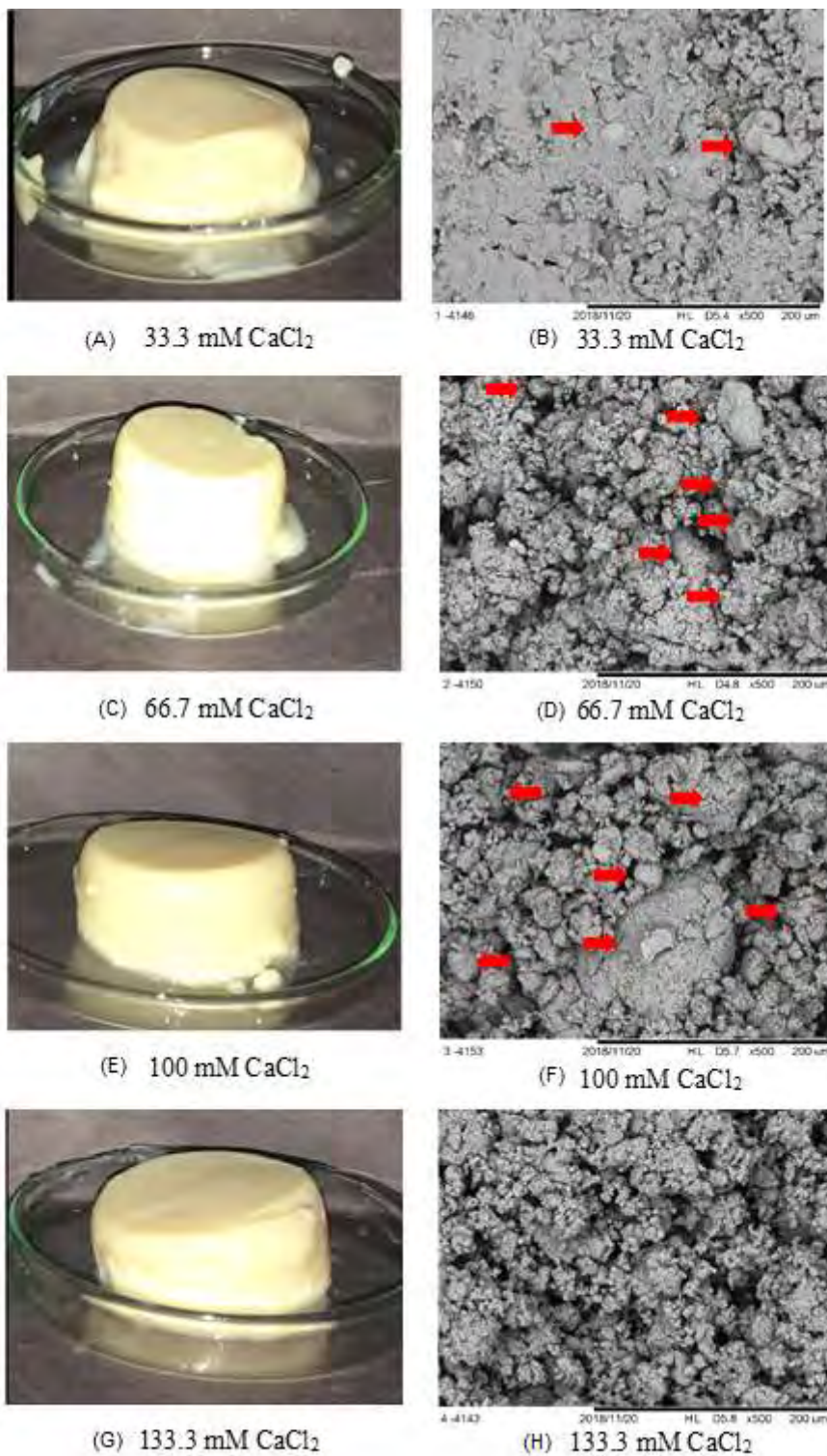
At such salt concentration, the speed of gelation allowed a slower and more effective approximation of the aggregates and, therefore, the formation of a more continuous and homogeneous microstructure. At some specific points, where the intra-aggregate interactions were more effective than the inter-aggregate, the capsule-like structures were then formed.

In systems with μ of 200 and 300 (containing 66.7 and 100 mM of CaCl_2), the gelation was faster than at lower salt concentrations, resulting in the more coarse and particulate microstructures (Fig. 4.1F). In such concentrations, the increase in protein interactions were higher and faster inside the protein aggregates, resulting in a faster and more effective formation of the “capsules”, possibly composed mainly by glycinin groups inside and β -conglycinin outside (“covering” the aggregates formed by the glycinin), as described by Guo et al.¹⁹.

Such microstructural organizations resemble the microstructures of systems called microgels by some authors²⁰. According to Nicolai and Durand²⁰, during primary protein aggregation a finite size aggregates are formed with, basically, two distinct morphologies: thin elongated aggregates and roughly spherical aggregates, which have also been called as microgels (fractal, self-similar, branched aggregates, or clusters)²⁰. The authors stated that such expression implies that the particle (here referred as capsule) is formed by a crosslinked network and contains a relatively large fraction of solvent²⁰.

At μ of 400 (133.3 mM CaCl_2 - Figure 4.1H), on the other hand, the decrease of electrostatic repulsion was excessively fast due to the high salt concentration, resulting in the heterogeneous and porous microstructure. In fact, according to the literature, lower salt concentrations generally result in slower gelation and, consequently, the formation of stronger gels, with a more ordered microstructure, while at higher salt concentration, the gelation is faster, leading to the formation of weaker gels, with a less ordered and more particulate microstructure^{7,21}.

Figure 4.1. Scanning electron micrographs of CaCl_2 -induced gels produced with different ionic strengths (100, 200, 300 and 400, which correspond to the CaCl_2 concentrations of 33.3, 66.7, 100 and 133.3 mM). In the micrographs, the magnification of 500 x was used, and the scale bar corresponds to 200 μm .



4.4.2 Rheological properties of SPI-only gels

Frequency sweep tests, shown in Figure 4.2 and Table 4.1, showed that the increase of ionic strength from 100 to 300 (33.3 mM to 100 mM CaCl₂) increased the gels strength, as indicated by the values of G', G'', K' and K''. On the other hand, gels produced with 133.3 mM were weaker than the systems produced with 100 mM. Such behavior reflected the effects of the microstructural organizations previously explained. The first increase of gels' strength from μ of 100 to 300 was related to the higher decrease of electrostatic repulsion and higher formation of salt bridges between protein groups, whereas the decrease of gels' strength between μ of 300 and 400 is related to the disorganized, particulate, and "sandy" microstructure of the systems produced with the higher salt concentration.

The variations in ionic strengths, however, had only a small effect over the frequency dependence of G' and G'', as verified by the values of n' and n'', which were all around 0.1 (Table 4.1). According to the literature, protein gels tend to present small values of n' and n'', such as the ones verified in the present study, due to the presence of covalent and non-covalent bonds in the network formation process²³.

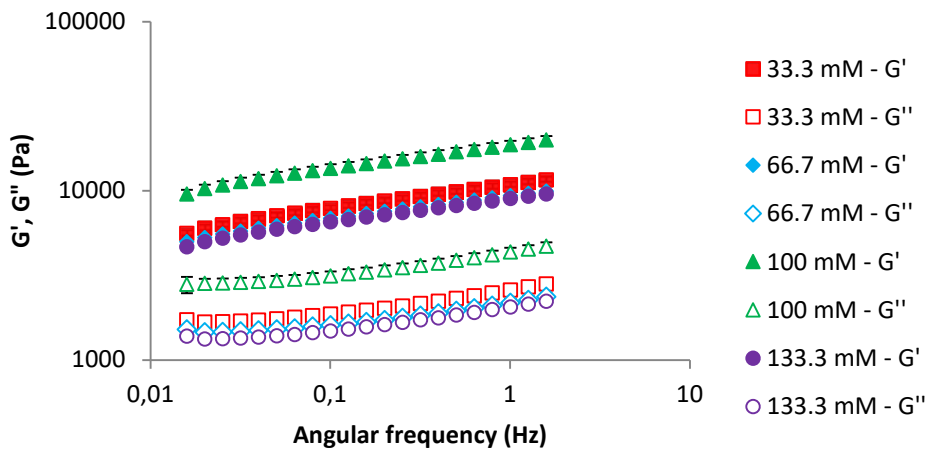
Table 4.1. Parameters of Power Law model (frequency sweep data), Burger's model (creep/recovery data) and uniaxial compression data of SPI gels produced with different ionic strengths.

Analysis	Parameter	Ionic strengths (CaCl ₂ concentrations)			
		100 (33.3 mM)	200 (66.7 mM)	300 (100 mM)	400 (133.3 mM)
Frequency sweep test	K' (Pa)	10948.3 ^b ± 561.8	9444.5 ^b ± 656.7	18881.0 ^a ± 1109.3	9079.3 ^b ± 848.2
	n'	0.149 ^a ± 0.001	0.143 ^b ± 0.002	0.150 ^a ± 0.003	0.148 ^{ab} ± 0.001
	R ²	0.99	0.99	0.99	0.99
	K'' (Pa)	2521.7 ^b ± 114.6	2117.2 ^{bc} ± 110.2	4233.3 ^a ± 248.3	2005.9 ^c ± 184.5
	n''	0.115 ^a ± 0.002	0.105 ^b ± 0.004	0.115 ^a ± 0.004	0.115 ^a ± 0.002
	R ²	0.95	0.94	0.96	0.95
Creep/recovery test	J ₀ (Pa ⁻¹)	0.040 ^b ± 0.002	0.046 ^a ± 0.002	0.031 ^c ± 0.001	0.045 ^{ab} ± 0.002
	J ₁ (Pa ⁻¹)	0.028 ^a ± 0.001	0.031 ^a ± 0.003	0.021 ^b ± 0.001	0.028 ^a ± 0.001
	λ_{ret} (s)	40.46 ^a ± 1.20	37.33 ^{ab} ± 2.01	39.58 ^a ± 1.32	34.79 ^b ± 2.42
	η_0 (Pa.s)	22027 ^b ± 1037	18989 ^c ± 295	27865 ^a ± 1232	21475 ^{bc} ± 1130
	R ²	0.88	0.88	0.88	0.87
	Recovery (%)	69.0 ^a ± 2.2	70.0 ^a ± 1.5	68.0 ^a ± 1.9	70.1 ^a ± 2.0
Uniaxial compression test	E _g (Pa)	3478 ^b ± 450	3576 ^b ± 351	4469 ^a ± 97	3902 ^{ab} ± 128
	σ_H (Pa)	960 ^a ± 122	924 ^a ± 105.7	1301 ^a ± 333.9	1195 ^a ± 91.8
	ϵ_H	0.235 ^a ± 0.055	0.241 ^a ± 0.040	0.288 ^a ± 0.046	0.260 ^a ± 0.018

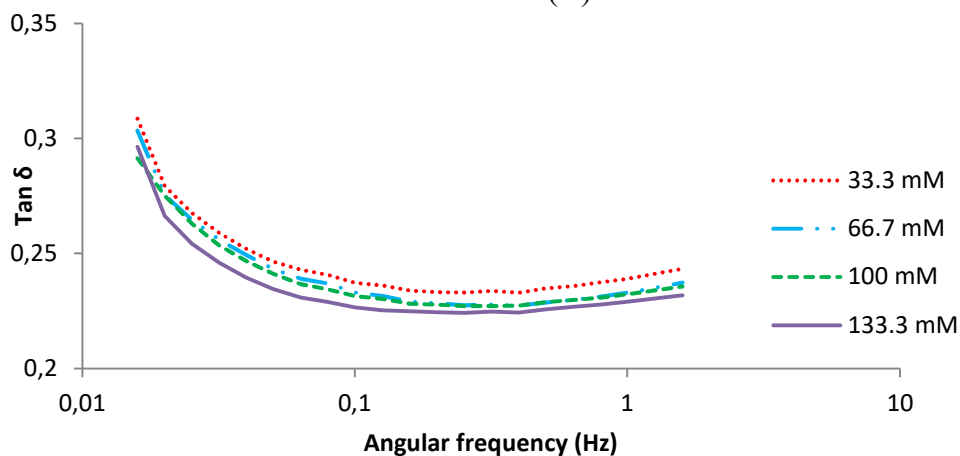
Averages followed by different lowercase letters in the same line are statistically different (p < 0.05) for gels

with different ionic strengths.

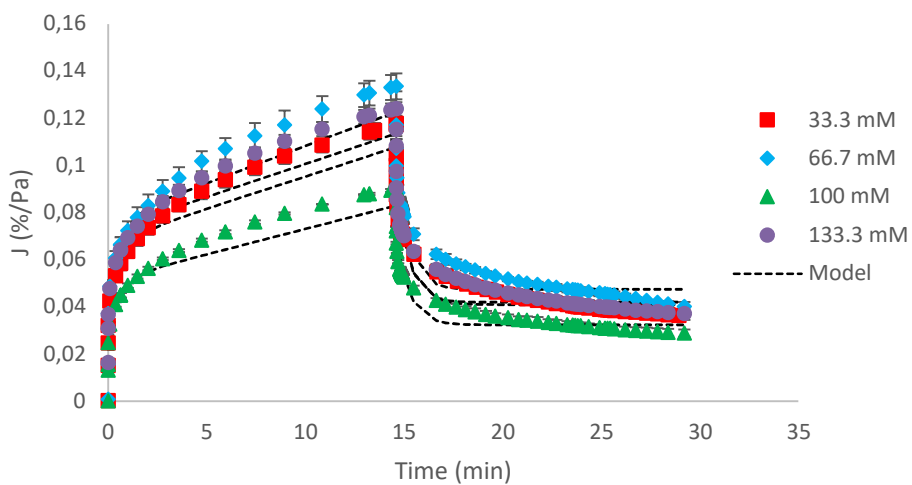
Figure 4.2. Results of frequency sweep test (A, B) and creep/recovery tests (C) of gels produced with different with different ionic strengths (100, 200, 300 and 400, which correspond to the CaCl_2 concentrations of 33.3, 66.7, 100 and 133.3 mM).



(A)



(B)



(C)

The results shown in Figure 4.2B revealed that increases of ionic strength resulted in decreases of $\tan \delta$, indicating increases in the elastic character of the systems. Although the higher ionic strength led to the formation of the most disorganized network, the higher number of salt bridges favored the elasticity of the systems under such small deformations.

The behavior of the gels during creep/recovery tests (Figure 4.2C and Table 4.1) led to similar conclusions, as gels produced with μ of 300 (i.e 100 mM CaCl₂) presented higher strength in comparison to the other salt concentrations tested, with lower compliance, J_0 and J_1 , and higher η_0 . Besides, the values of λ_{ret} were lower for systems produced with μ of 400 (133.3 mM CaCl₂).

For all gels, J_0 was higher than J_1 , indicating that the instantaneous elastic strain was larger than the retarded elastic and viscous flow deformation¹⁶. According to the literature, J_1 value reflects the magnitude of the retarded elastic deformation and the resistance to deformation caused by the three-dimensional network structure, therefore, higher values of such parameter indicate a simpler and less resistant structure¹⁶. Thus, the lower values for such parameter obtained from systems produced with μ of 300 indicated a higher complexity and resistance for deformation, in comparison to the other formulations.

The parameter η_0 , on the other hand, reflects the viscous behavior of the gels. According to the literature, the higher values of η_0 for gels produced with μ of 400 (133.3 mM CaCl₂) indicates that, during the test, the viscous component of such systems were higher in comparison to the other formulations¹⁶. Such conclusions are different than the ones obtained from $\tan \delta$ values, according to which the gels produced with higher ionic strength have shown to be more elastic. Such apparently contradictory behavior reflects the complexity of the systems formed with μ of 400 (133.3 mM of CaCl₂). Even though the higher number of salt bridges formed under these conditions increased the elastic character of the systems during the oscillatory test, when subjected to 5 Pa for 15 min during creep the systems acquired a more viscous behavior, possibly due to structural rearrangements resulted from the weaker and more disorganized microstructure.

On the other hand, the lower values for λ_{ret} verified for systems produced with μ of 400 (133.3 mM CaCl₂) indicated that these systems required a lower time for the structural elements to decrease to approximately 63% of their maximum strain¹⁶, indicating that after the removal of the stress, the recovery process was faster to these systems, possibly due to the higher number of salt bridges within the aggregates.

As shown in Table 4.1, the final recovery capacities of the systems were not significantly affected by variations of ionic strength, as all systems presented recovery rates around 68 and 70%.

Similarly, results of uniaxial compression tests showed the increase ionic strength from 100 to 300 (33.3 to 100 mM CaCl_2) increased the Young's modulus of the systems, whereas the increase from 300 to 400 (100 to 133.3 mM) reduced such parameter, for the same reasons previously cited. In addition, the variation of ionic strength did not significantly affect ($p > 0.05$) the rupture properties of the gels.

The behavior verified and discussed here are similar than behavior verified in NaCl-induced gels using the same ionic strengths². For such gels, the system produced with the ionic strength of 300 were stronger than the other ionic strengths tested, indicating that this was an “optimum” condition for the production of stronger gels.

The comparison of systems produced with different salts, however, revealed that NaCl-induced gels² were weaker than CaCl_2 -induced ones (Table 4.1), presenting smaller values of G' , G'' , K' and K'' . In addition, CaCl_2 -induced gels presented higher n' and n'' . The higher strength of CaCl_2 -induced gels is probably related to its higher screening power and ability to form bonds between charged carboxyl groups^{5,7}. Possibly due to the formation of these salt bridges, CaCl_2 -induced gels presented higher dependence of G' and G'' with frequency, indicating a higher contribution of physical interactions in these systems. It has also affected the $\tan \delta$ values, which were higher and more frequency dependent for these gels than NaCl-induced ones, indicating lower elastic contributions.

Therefore, even though the CaCl_2 -induced gels were stronger, they were less elastic under small and oscillatory deformations. Such results are possibly related to the more particulate microstructure verified in these gels, in comparison to NaCl-induced ones². From the addition of CaCl_2 , the interactions among the aggregates were much faster and effective, due to the screening of the electrical charges and cross-linking among negatively charged carboxyl groups induced by the presence of salt²². As previously cited, fast gelation processes lead to less ordered structures with more particulate microstructures, as verified in Figure 4.1.

Results of creep/recovery tests confirmed such conclusions. Besides, the higher stiffness and lower elasticity of CaCl_2 -induced gels also affected the recovery capacity of the samples, which were higher for NaCl-induced gels. For CaCl_2 -induced gels, the stress application possibly resulted in disruptions of the salt bridges between the charged carboxylic groups, which caused greater reductions in the systems' ability to recover when the stress was removed, in comparison to NaCl-induced systems. The comparison of gels produced with different salts indicated that

CaCl₂-induced gels presented higher Young's modulus and rupture stress. Rupture strain, on the other hand, was less affected. Significant differences ($p < 0.05$) were only verified for systems with 14% SPI at ionic strength of 300 (100 mM CaCl₂), in which the incorporation of CaCl₂ resulted in the formation of structures with higher rupture strains.

From such results, the formulation produced with μ of 300 (100 mM CaCl₂) was selected for the incorporation of galactomannans and production of mixed gels.

4.4.3 Incorporation of galactomannans to the CaCl₂-induced gels: microstructural properties

Mixed gels produced using different concentration of GG and LBG were analyzed using CLSM and SEM and the micrographs obtained are shown in Figure 4.3. Such images showed that the incorporation of GG increased the porosity and the heterogeneity of the gels, which presented a more particulate aspect in comparison to the SPI-only systems. GG-SPI mixed gels did not present the structures similar to capsules, but were formed by small and numerous protein aggregates, similar to small microgels.

From SEM micrographs it was not possible to identify significant differences among the mixed gels produced with different concentrations of GG, however, CLSM images indicated that these matrices presented different degrees of phase separation. According to the literature, the most common phenomena observed in protein-neutral polysaccharide aqueous mixtures are incompatibility and phase separation, which, are segregative and related to volume excluded effects between both biopolymers¹¹. For systems containing galactomannans, that consist of linear chains of 1,4-linked β -D-mannopyranose randomly attached to different proportions of α -D-galactopyranosyl residues at position 6 as sidechains, the phase separation is also influenced by the degree of branching, i.e., the mannose-to-galactose ratio of the polysaccharide^{2, 11}.

According to the literature, intermolecular interactions of galactomannans tend to occur mainly via hydrogen bonds between the non-substituted mannan regions of the structures¹¹. For this reason, polysaccharides with higher M/G ratio, which present higher length of unsubstituted mannan backbone available, tend to present higher intermolecular associations which may accelerate the phase separation process¹¹.

As verified in Figure 4.3, whereas the incorporation of 0.1% of GG resulted in systems with microphase separation, higher concentrations of such polysaccharide resulted in

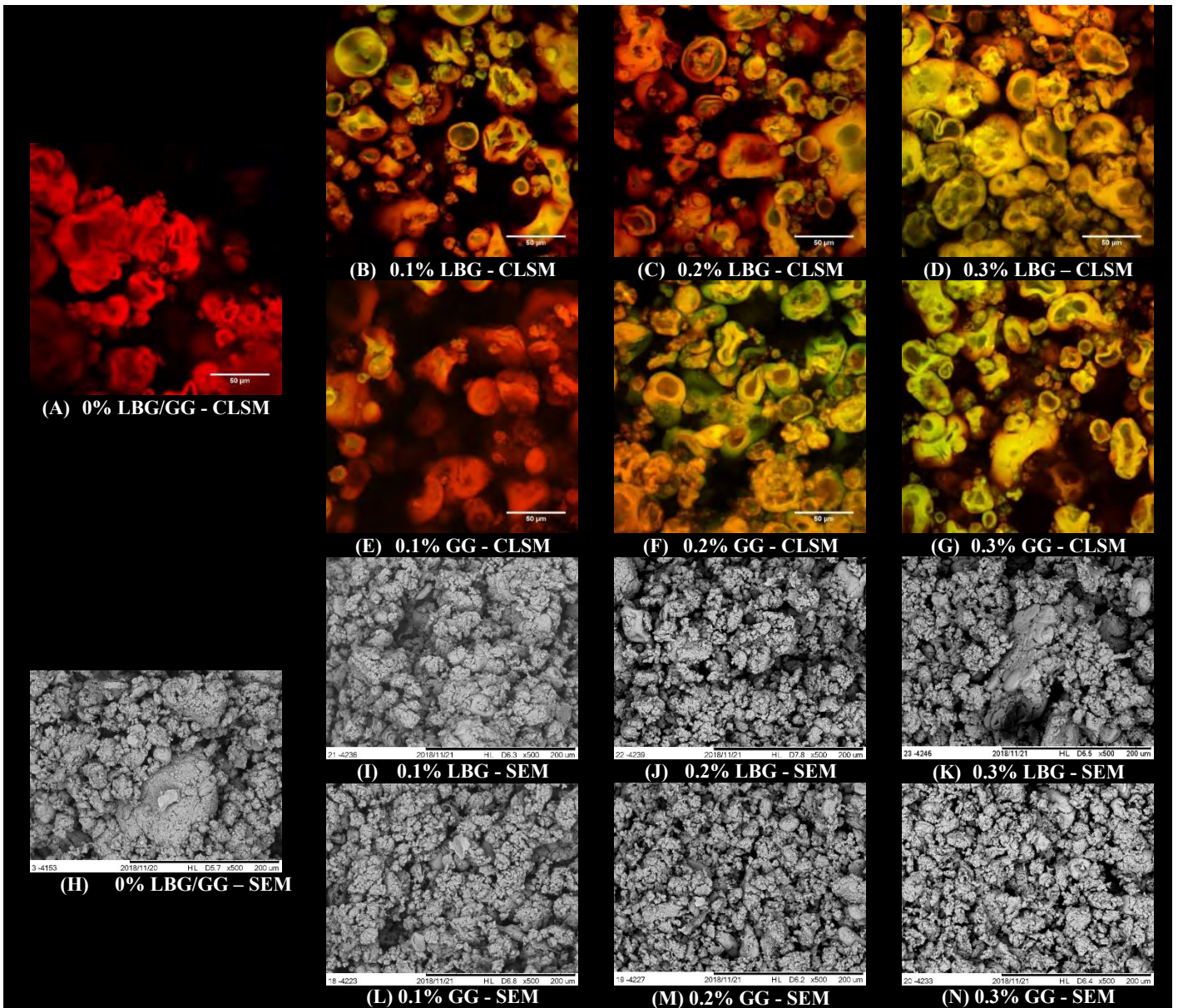
microstructures with incomplete demixing, due to the reduced mobility of the polysaccharide and its small capacity for self-association¹¹.

Regarding the incorporation of LBG, there was an increase in the heterogeneity of the systems, as shown in Figures 4.3I to 4.3K. SEM images showed that the higher the LBG content, the smaller and more separated are the gels' aggregates. For gels produced with 0.3% LBG, on the other hand, some regions presented more compact matrices, formed by microgel-like structures, as shown in Figure 4.3K.

CLSM evidenced that the gels produced with 0.1% (Fig 4.3B) and 0.2% LBG (Fig 4.3C) presented a certain degree of phase separation, with some reddish and others greenish regions, however, the increase of LBG concentration to 0.3% LBG decreased the extension of such phenomenon, as verified in Figure 4.3D.

The higher degree of phase separation verified in systems with LBG in comparison to the ones with GG (especially for 0.1 and 0.2%) is related to the reduced capacity of GG molecules to self-associate due to its lower M/G ratio, as previously explained^{2, 11}.

Figure 4.3. Micrographs of CaCl_2 -induced gels produced with 14% soy protein isolate (SPI) and different locust bean gum (LBG) and guar gum (GG) concentrations. In confocal laser scanning micrographs (CLSM) (A-G), the scale bar corresponds to 50 μm . In such micrographs, the colors red and green were used to identify the protein and polysaccharide-rich phases, respectively, and the regions with incomplete demixing present a yellowish color. In scanning electron micrographs (SEM) (H-N), the magnification of 500 x was used, and the scale bar corresponds to 200 μm .



4.4.4 Incorporation of galactomannans to the CaCl₂-induced gels: rheological properties

From frequency sweep data (Figure 4.4 and Table 4.2), it was verified that the incorporation of 0.1% GG increased G' , G'' , K' and K'' . On the other hand, the incorporation of higher concentrations of such polysaccharide decreased these parameters. The strengthening of the gels with 0.1% GG is related to the microstructural organization with clear phase separation, previously discussed. According to Monteiro et al.¹¹, increases of gels strength in mixed systems with microphase separations may be justified by the increases of local biopolymer concentration, which favours a reduction of the excluded volume and a more extensive polymer self-association within each phase. For systems with higher polysaccharide concentration (0.2 and 0.3% GG), on the other hand, the incomplete demixing led to decreases of protein-protein interactions, causing the weakening of the gels.

Figure 4.4. Results of frequency sweep tests of CaCl₂-induced gels with different guar gum (GG) (A, B) and locust bean gum (LBG) (C, D) concentrations: 0% (■□), 0.1% (◆◇); 0.2% (▲△) and 0.3% (●○). Full (G') and open (G'') symbols.

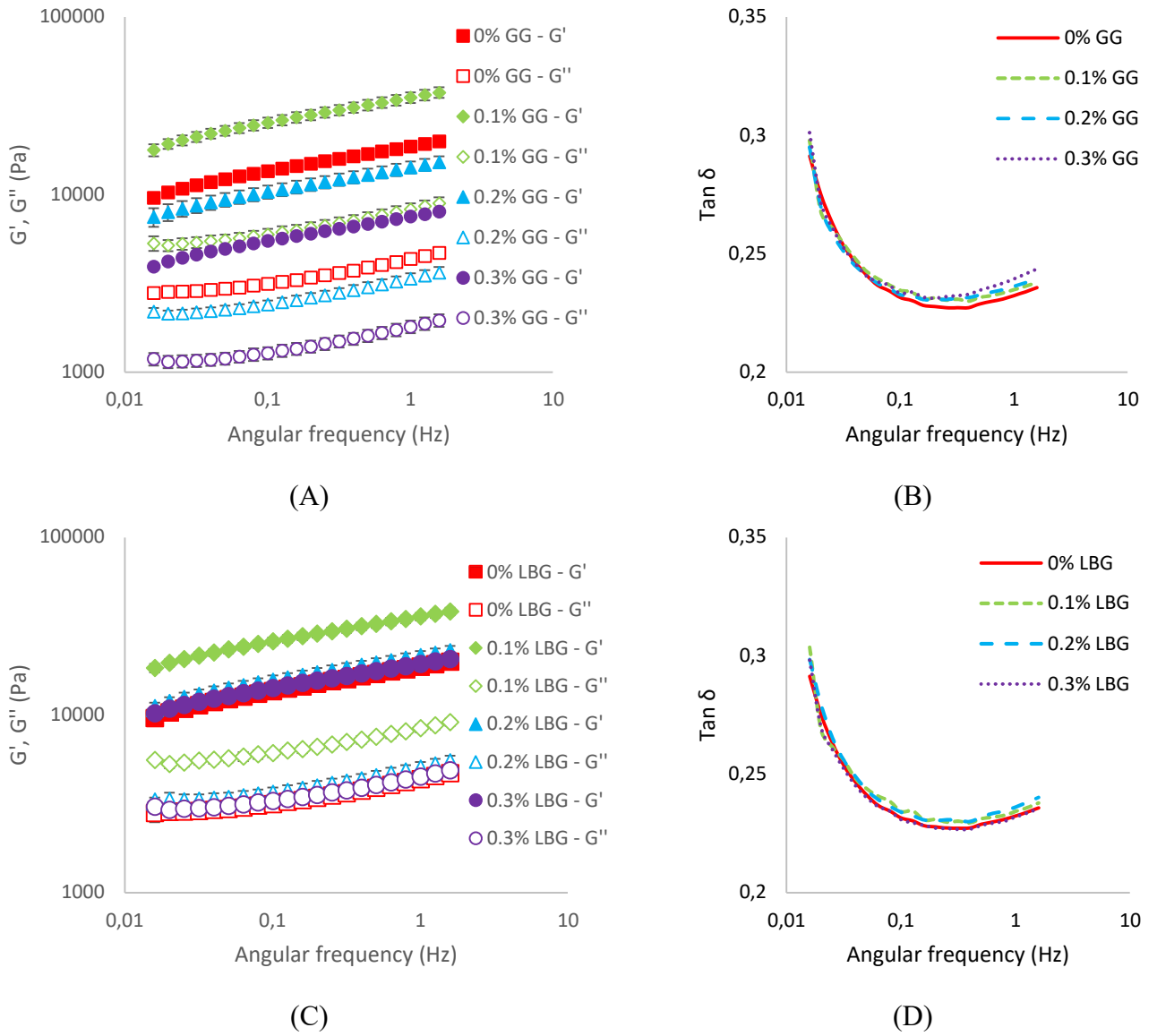


Table 4.2. Parameters of the power law model obtained from frequency sweep data for CaCl₂-induced gels produced with different concentrations of guar gum (GG) or locust bean gum (LBG)

Formulation	K' (Pa)	n'	R ²	K'' (Pa)	n''	R ²
0% GG	18881 ^b ± 1109	0.150 ^a ± 0.003	0.994	4233 ^b ± 248	0.115 ^a ± 0.004	0.960
0.1% GG	35615 ^{aA} ± 2435	0.152 ^{aA} ± 0.001	0.993	8098 ^{aA} ± 614	0.120 ^{aA} ± 0.001	0.973
0.2% GG	14371 ^{cB} ± 2435	0.147 ^{aA} ± 0.009	0.996	3285 ^{cB} ± 228	0.119 ^{aA} ± 0.008	0.963
0.3% GG	7595 ^{dB} ± 591	0.147 ^{aA} ± 0.002	0.995	1753 ^{dB} ± 140	0.119 ^{aA} ± 0.002	0.953
0% LBG	18881 ^b ± 1109	0.150 ^a ± 0.003	0.994	4233 ^b ± 248	0.115 ^a ± 0.004	0.960
0.1% LBG	36225 ^{aA} ± 1750	0.151 ^{aA} ± 0.002	0.994	8208 ^{aA} ± 401	0.117 ^{aB} ± 0.001	0.964
0.2% LBG	21322 ^{bA} ± 1865	0.149 ^{aA} ± 0.002	0.994	4852 ^{bA} ± 433	0.115 ^{aA} ± 0.003	0.953
0.3% LBG	19550 ^{bA} ± 1072	0.146 ^{aA} ± 0.002	0.995	4376 ^{bA} ± 263	0.112 ^{aB} ± 0.002	0.953

Averages followed by different lowercase letters are statistically different ($p < 0.05$) for gels with different concentrations of the same polysaccharide. Averages followed by different capital letters are statistically different ($p < 0.05$) for gels with the same concentration of different polysaccharides.

Similarly, the addition of 0.1% LBG increased G' , G'' and, consequently, K' , and K'' . However, the incorporation of 0.2 and 0.3% did not significantly change ($p > 0.05$) the values of K' and K'' in comparison to SPI only gels. For all formulations (SPI-only gels and mixed systems), on the other hand, the values of $\tan \delta$ (Figures 4B and 4D), n' and n'' (Table 4.2) were similar.

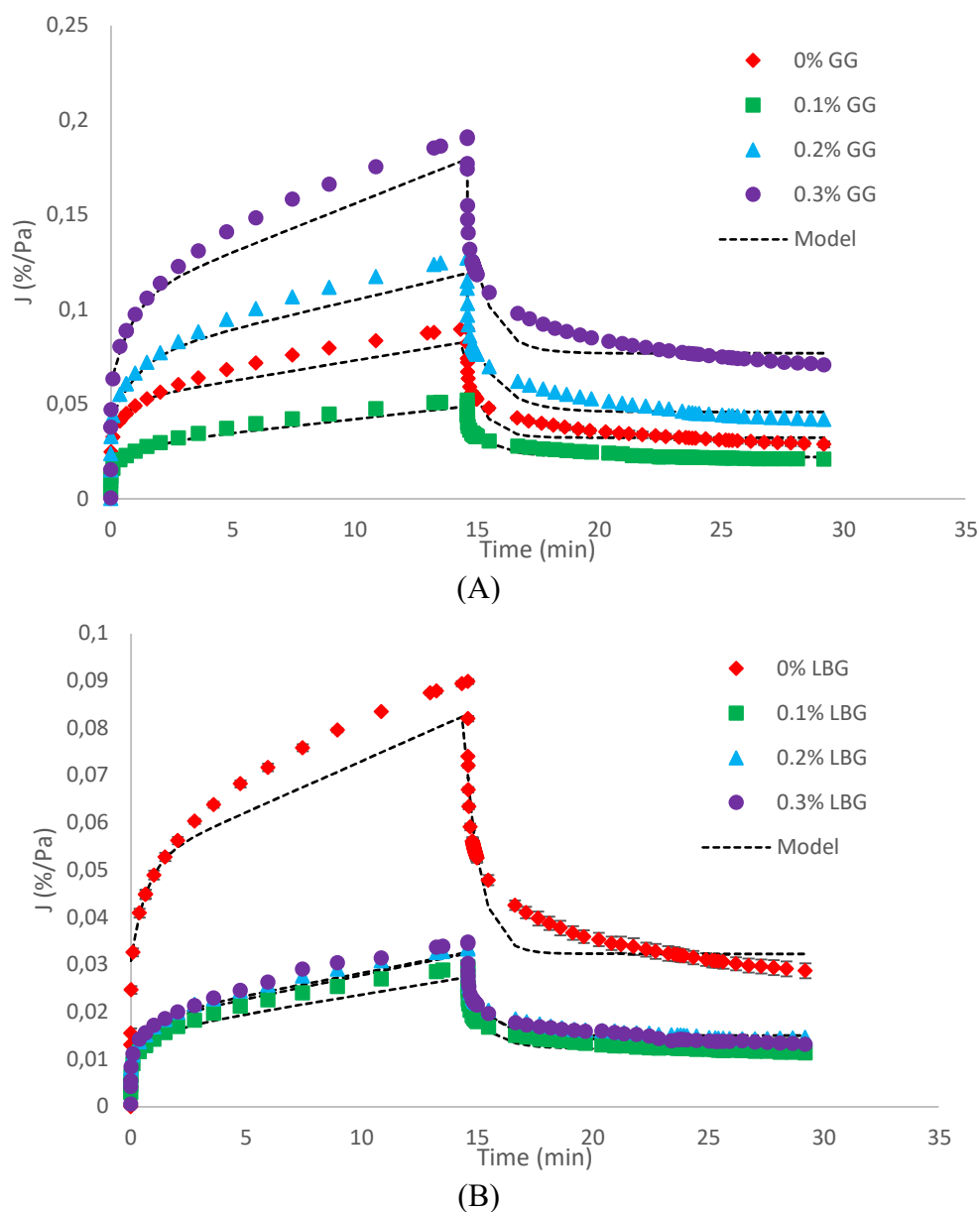
In addition, gels produced with LBG were stronger than the ones produced with GG, presenting higher G' and G'' . According to Monteiro et al.¹¹, mixed gels containing LBG tend to be stronger than gels produced with GG, due to its lower degree of branching. As previously cited, the polysaccharides with a higher M/G ratio tend to form stronger systems for presenting higher length of the unsubstituted mannan backbone available for intermolecular associations¹¹.

As verified in Figure 4.5, the results of creep/recovery tests led to similar conclusions. Whereas the incorporation of 0.1% GG decreased the compliance values of the gels, the incorporation of 0.2 and 0.3% of such polysaccharide increased this parameter. As expected such behavior influenced on the values of Burger's model parameters, shown in Table 4.3. Gels with 0.1% GG presented lower values of J_0 and J_1 , and higher values of η_0 , in comparison

to the SPI-only gels and to the systems with higher concentrations of the same galactomannan. Such mixed gels, however, presented higher J_0 and J_1 , and lower η_0 in comparison to the SPI-only systems. From η_0 values it was verified that the viscous component of gels produced with 0.1% GG were higher than the other formulations, while in higher concentrations the contribution of such component was lower ¹⁶.

For all concentrations tested, however, the presence of GG increased λ_{ret} , indicating that they required a higher time for the structural elements to decrease to approximately 63% of their maximum strain ¹⁶.

Figure 4.5. Results of creep/recovery tests of CaCl_2 -induced gels with different guar gum (GG) (A) and locust bean gum (LBG) (B) concentrations.



The incorporation of LBG, on the other hand, decreased the compliance values in all three concentrations tested. Even though the strengthening of the gels was only verified from the incorporation of 0.1% LBG during frequency sweep tests, the presence of this galactomannan in all concentrations tested increased the resistance of the samples to deform with the application of the constant stress during the creep step. Such fact reflected over the values of J_0 and J_1 , which were lower for systems containing LBG. Besides, LBG-SPI mixed gels presented higher η_0 . λ_{ret} , on the other hand, was not significantly affected.

Table 4.3. Burger's model parameters obtained from creep/recovery data for CaCl₂-induced gels produced with different concentrations of guar gum (GG) or locust bean gum (LBG).

Formulation	J_0 (Pa ⁻¹)	J_1 (Pa ⁻¹)	λ_{ret} (s)	η_0 (Pa.s)	R ²	Recovery (%)
0% GG	0.031 ^c ± 0.001	0.021 ^c ± 0.001	39.58 ^b ± 1.32	27865 ^b ± 1232	0.88	68.0 ^a ± 1.9
0.1% GG	0.016 ^{dA} ± 0.001	0.012 ^{dA} ± 0.001	66.23 ^{aA} ± 11.68	40947 ^{aB} ± 337	0.90	59.9 ^{cA} ± 1.6
0.2% GG	0.042 ^{bA} ± 0.001	0.033 ^{bA} ± 0.001	66.68 ^{aA} ± 10.56	19698 ^{cB} ± 1762	0.91	67.1 ^{abA} ± 2.1
0.3% GG	0.061 ^{aA} ± 0.001	0.044 ^{aA} ± 0.001	51.91 ^{abA} ± 3.99	11705 ^{dB} ± 141	0.90	62.8 ^{bcA} ± 0.7
0% LBG	0.031 ^a ± 0.001	0.021 ^a ± 0.001	39.58 ^a ± 1.32	27865 ^b ± 1232	0.88	68.0 ^a ± 1.9
0.1% LBG	0.009 ^{bB} ± 0.002	0.006 ^{bB} ± 0.002	58.61 ^{aA} ± 31.97	76547 ^{aA} ± 17173	0.90	61.7 ^{aA} ± 8.6
0.2% LBG	0.010 ^{bB} ± 0.001	0.007 ^{bB} ± 0.001	55.52 ^{aA} ± 5.93	5995 ^{aA} ± 2398	0.91	56.3 ^{aB} ± 1.9
0.3% LBG	0.011 ^{bB} ± 0.002	0.008 ^{bB} ± 0.001	66.05 ^{aA} ± 9.72	63553 ^{aA} ± 7003	0.91	62.1 ^{aA} ± 2.8

Averages followed by different lowercase letters are statistically different ($p < 0.05$) for gels with different concentrations of the same polysaccharide. Averages followed by different capital letters are statistically different ($p < 0.05$) for gels with the same concentration of different polysaccharides.

Such strengthening with the incorporation of LBG is related to the increase of protein-protein interactions (mainly through saline bridges between charged carboxylic groups) and the higher self-association of polysaccharides, which possibly reduced the effects of incomplete demixing, and resulted in the more evident microphase separations previously discussed. However, the increase of the viscous contribution verified from the η_0 values. On the other hand, also due to this more pronounced microphase separation, the incorporation of LBG increased the viscous contribution of this systems, verified from the values of η_0 , possibly leading to more effective permanent structural changes.

Regarding the recovery capacity of the systems (Table 4.3), it was verified that, whereas the incorporation of 0.1 and 0.3% GG decreased the ability of the gels to recover, the incorporation of 0.2% GG did not significantly alter such parameter. For LBG, on the other hand, the presence of the polysaccharide did not significantly affect the ability of the gels to recover.

The comparison of systems produced with the different galactomannans has also confirmed that gels produced with LBG presented lower values of J_0 and J_1 , and higher values of η_0 .

On the other hand, uniaxial compression tests results, shown in Table 4.4, indicated the incorporation of GG decreased the values of E_g , but it did not affect the rupture parameters of the gels. Similarly, the incorporation of LBG has also decreased E_g of the gels, but, in this case,

the presence of concentrations equal or higher than 0.2% of polysaccharide decreased the rupture parameters of the systems. Such results indicated that, even though the presence of the galactomannans, especially LBG, has increased the gels strength under oscillatory/small deformations, it compromised the strength of the gels under large deformation (lower E_g), possibly due to the heterogeneous and more porous microstructures verified for mixed systems in the SEM micrographs.

According to the literature, microphase separations can increase interactions among biopolymers within each phase and increase the elastic response of systems if the connectivity between protein aggregates is not affected ²³. In fact, the fragility of connectivity within the systems with a higher LBG concentrations (0.2 and 0.3%) resulted in the lowest rupture parameters previously verified. However, they did not compromised the strength of the systems under smaller deformations, as verified from frequency sweep tests and creep/recovery tests.

Table 4.4. Results of uniaxial compression tests of CaCl₂-induced gels produced at different guar gum (GG) or locust bean gum (LBG) concentrations.

Formulation	E_g (Pa)	σ_H (Pa)	ϵ_H
0% GG	4469 ^a ± 97	1301 ^a ± 334	0.288 ^a ± 0.046
0.1% GG	3455 ^{bB} ± 316	1102 ^{aB} ± 120	0.285 ^{aA} ± 0.029
0.2% GG	2403 ^{cA} ± 433	836 ^{aA} ± 69	0.238 ^{aA} ± 0.052
0.3% GG	2951 ^{bcA} ± 251	808 ^{aA} ± 179	0.219 ^{aA} ± 0.030
0% LBG	4469 ^a ± 97	1301 ^{ab} ± 334	0.288 ^{ab} ± 0.046
0.1% LBG	4064 ^{bA} ± 82	1519 ^{aA} ± 199	0.346 ^{aA} ± 0.056
0.2% LBG	2877 ^{cA} ± 248	845 ^{bA} ± 82	0.212 ^{bA} ± 0.031
0.3% LBG	2868 ^{cA} ± 102	859 ^{bA} ± 93	0.225 ^{bA} ± 0.014

Averages followed by different lowercase letters are statistically different ($p < 0.05$) for gels with different concentrations of the same polysaccharide. Averages followed by different capital letters are statistically different ($p < 0.05$) for gels with the same concentration of different polysaccharides.

4.5 Conclusions

CaCl₂-induced SPI gels were formed using all the four ionic strengths tested. All protein gels presented heterogeneous microstructure; however, it was verified that increases of salt concentrations led to increases of porosity and coarseness. Rheological data indicated the existence of an “optimum” ionic strength for the production of stronger SPI gels, as systems produced with μ of 300 (100 mM CaCl₂) presented higher G' , G'' , and E_g and lower compliance values, in comparison to the other ionic strengths tested. At lower ionic strengths, the formation

of salt bridges was probably less effective, meanwhile at μ of 400 (133.3 mM CaCl_2) the microstructure was too disorganized, possibly due to an excessively fast aggregation process. This “optimum” formulation (14% SPI + 100 mM CaCl_2) was incorporated with different galactomannans, resulting in gels with different degrees of phase separation. For both, GG and LBG, the extension of the phase separation processes decreased with the increase of polysaccharide concentration. Gels produced with GG presented lower G' , G'' , and E_g values; and higher compliance values in comparison to LBG, due to its lower capacity to self-associate. From the obtained results, it was verified that galactomannans' incorporation was an interesting strategy to alter the systems microstructure and improve the gels' strength (especially at low concentrations).

Acknowledgments

This study was funded by Fundação de Amparo à Pesquisa do Estado de São Paulo (FAPESP) (grant number 2017/06224-9). We also thank the access to equipment and assistance provided by the Electron Microscope Laboratory (LME/UNICAMP).

Conflict of Interest: The authors declare that they have no conflict of interest.

4.6 References

- [1] Totosaus, A.; Montejano, J.G.; Salazar, J.A.; Guerrero, I. A review of physical and chemical protein-gel induction. *Int. J. Food Sci. Technol.* 2002, 37(6), 589–601.
- [2] Brito-Oliveira, T.C.; Cavini, A.C.M.; Ferreira, L.S.; Moraes, I.C.F.; Pinho, S.C. Microstructural and rheological characterization of NaCl-induced gels of soy protein isolate and the effects of incorporating different galactomannans. *Food Struct.* 2020, 26, 100158.
- [3] Luo, K.; Liu, S.; Miao, S.; Adhikari, B.; Wang, X.; Chen, J. Effects of transglutaminase pre-crosslinking on salt-induced gelation of soy protein isolate emulsion. *J. Food Eng.* 2019, 263, 280 – 287.
- [4] Rodrigues, R.M.; Fasolin, L.H.; Avelar, Z.; Petersen, S.B.; Vicente, A.A.; Pereira, R.N. Effects of moderate electric fields on cold-set gelation of whey proteins – From molecular interactions to functional properties. *Food Hydrocoll.* 2020, 101,105505
- [5] Bryant, C.M.; McClements, D.J. Influence of NaCl and CaCl_2 on cold-set gelation of heat-denatured whey protein. *J. Food Sci.* 2000, 65(5), 801–804.
- [6] Cavallieri, A.L.F; Cunha, R.L. The effects of acidification rate, pH and ageing time on the acidic cold set gelation of whey proteins. *Food Hydrocoll.* 2008, 22(3), 439–448.

- [7] Kuhn, K. R.; Cavallieri, A.L.F.; Cunha, R.L. Cold-set whey protein gels induced by calcium or sodium salt addition. *Int. J. Food Sci. Technol.* 2010, 45, 348–357.
- [8] Maltais, A.; Remondetto, G.E.; Subirade, M. Soy protein cold-set hydrogels as controlled delivery devices for nutraceutical compounds. *Food Hydrocoll.* 2009, 23(7), 1647–1653.
- [9] Brito-Oliveira, T.C.; Bispo, M.; Moraes, I.C.F.; Campanella, O.H.; Pinho, S.C. Stability of curcumin encapsulated in solid lipid microparticles incorporated in cold-set emulsion filled gels of soy protein isolate and xanthan gum. *Food Res. Int.* 2017, 102, 759–767.
- [10] Brito-Oliveira, T.C.; Bispo, M.; Moraes, I.C.F.; Campanella, O.H.; Pinho, S.C. Cold-Set Gelation of Commercial Soy Protein Isolate: Effects of the Incorporation of Locust Bean Gum and Solid Lipid Microparticles on the Properties of Gels. *Food Biophys.* 2018, 13(3), 226–239.
- [11] Monteiro, S.R.; Rebelo, S.; Silva, O.A.B.C.; Lopes-da-Silva J.A. The influence of galactomannans with different amount of galactose side chains on the gelation of soy proteins at neutral pH. *Food Hydrocoll.* 2013, 33, 349–360.
- [12] Turgeon, S.L.; Beaulieu, M.; Schmitt, C.; Sanchez, C. Protein-polysaccharide interactions: phase-ordering kinetics, thermodynamic and structural aspects. *Curr. Opin. Colloid Interface Sci.* 2013, 8, 401–414.
- [13] Abaee, A.; Mohammadian, M.; Jafari, S.M. Whey and soy protein-based hydrogels and nano-hydrogels as bioactive delivery systems. *Trends Food Sci Technol*, 2017, 70, 69–81.
- [14] Ingrassia, R.; Bea, L.L.; Hidalgo, M.E.; Risso, P.H. Microstructural and textural characteristics of soy protein isolate and tara gum cold-set gels. *LWT - Food Sci. Technol.*, 2019, 113, 108286.
- [15] Tripathi, A.D., Mishra, R., Maurya, K.K., Singh, R.B., & Wilson, D.W. - Estimates for world population and global food availability for global health in Singh, R.B., Watson, R.R., & Takahashi, T. (Eds.), *The role of functional food security in global health*, Academic Press (2019)
- [16] Chang, Y.; Li, D.; Wang, L.; Bi, C.; Adhikari, B. Effect of gums on the rheological characteristics and microstructure of acid-induced SPI-gum mixed gels. *Carbohydr. Polym.* 2014, 108, 183–191.
- [17] Oliver, L; Scholten, E.; Van Aken, G.A. Effect of fat hardness on large deformation rheology of emulsion-filled gels. *Food Hydrocoll.* 2015, 43, 299–310.
- [18] Picone, C. S. F.; Takeuchi, K. P.; Cunha, R. L. Heat-induced whey protein gels: Effects of pH and the addition of sodium caseinate. *Food Biophys.* 2011, 6, 77–83.

- [19] Guo, J.; Yang, X.; He, X.; Wu, N.; Wang, J.; Gu, W.; Zhang, Y. Limited Aggregation Behavior of β -Conglycinin and Its Terminating Effect on Glycinin Aggregation during Heating at pH 7.0. *J. Agric. Food Chem.* 2012, 60, 3782–3791.
- [20] Nicolai, T.; Durand, D. Controlled food protein aggregation for new functionality. *Curr. Opin. Colloid Interface Sci.* 2013, 18, 249–256.
- [21] Marangoni, A.G.; Barbut, S.; McGauley, S.E.; Marcone, M.; Narine, S.S. On the structure of particulate gels – the case of salt-induced cold gelation of heat-denatured whey protein isolate. *Food Hydrocoll.* 2000, 14, 61–74.
- [22] Bryant, C.M.; McClements, D.J. Molecular basis of protein functionality with special consideration of cold-set gels derived from heat-denatured whey. *Trends Food Sci. Technol.* 1998, 9, 143–151.
- [23] Rocha, C.; Teixeira, J.A.; Hilliou, L.; Sampaio, P.; Gonçalves, M.P. Rheological and structural characterization of gels from whey protein hydrolysates/locust bean gum mixed systems. *Food Hydrocoll.* 2009, 23, 1734–1745.

**CHAPTER 5 : INCORPORATION OF SOLID LIPID PARTICLES STABILIZED BY
DIFFERENT SURFACTANTS TO COLD-SET GELS OF SOY PROTEIN ISOLATE
AND LOCUST BEAN GUM**

(Edited for submission to: Journal of Food Engineering)

**Thais C. Brito-Oliveira, Camila S. Cazado, Ana Clara M. Cavini, Lorena M.F. Santos,
Izabel C.F. Moraes, and Samantha C. Pinho**

Incorporation of solid lipid particles stabilized by different surfactants to cold-set gels of soy protein isolate and locust bean gum

Thais C. Brito-Oliveira¹, Camila S. Cazado¹, Ana Clara M. Cavini¹, Lorena M.F. Santos¹,
Izabel C.F. Moraes¹, and Samantha C. Pinho^{1*}

¹Department of Food Engineering, School of Animal Science and Food Engineering,
University of São Paulo (USP), Pirassununga, SP, Brazil

* Corresponding author: S.C. Pinho, Department of Food Engineering, School of Animal Science and Food Engineering (FZEA), University of São Paulo (USP), Av. Duque de Caxias Norte 225, Jd. Elite, Pirassununga, SP, Brazil 13635-900. Tel: +55-19-35654288; fax: +55-19-3565-4284.

E-mail address: samantha@usp.br

5.1 Abstract

This study investigates the effects of incorporating solid lipid particles (SLP) stabilized by different surfactants (whey protein isolate -WPI and Tween 80/Span 80 - TS) into NaCl-induced cold-set gels of soy protein isolate (SPI) (14%, w/v) and locust bean gum (LBG) (0.1%, w/v). While WPI-stabilized SLP were active fillers and formed heat-induced gels, systems containing TS-stabilized SLP were formed only after incorporating the salt. TS-stabilized SLP reduced water holding capacities and altered the gel microstructures, presented as “microgel-like” organization. Besides, the incorporation of SLP decreased E_g , σ_H , and ϵ_H , as compared to non-filled gels. The increased SLP content had induced various effects on uniaxial compression parameters due to the heterogeneous distribution of SLP in the gelled matrix. These findings suggested that while TS-stabilized SLP were “unbound” to the matrix due to the low chemical affinity to surfactant/proteins, they were “active” by affecting the aggregation patterns and microstructural organizations.

Keywords: Plant protein; Galactomannan; Emulsion-filled gels; Cold-set gelation; Microstructure; Salt-induced gelation.

5.2 Introduction

Many food products, such as yogurt, fresh cheeses, dairy desserts, and puddings, can be categorized as emulsion-filled gels (EFGs) (Sala et al., 2008). The importance of EFGs to the food industry is attributed to their complex structural properties, which are highly dependent on the characteristics of gelling agents, dispersed fillers, and interactions between them (Dickinson, 2012; Geremias-Andrade et al., 2016; Sala et al., 2007).

With such complexity, the creation of new formulations involves in-depth studies of their microstructural organizations and the rheological properties of systems. For example, rheological assays, particularly uniaxial compression tests, are often used to classify fillers as active or inactive in the gel matrices (Sala et al., 2007). Researchers have shown that active fillers are stabilized by surfactants that have a strong chemical affinity with gelling agents, resulting in an increase or decrease of modulus of elasticity of gels (Geremias-Andrade et al., 2016; Oliver et al., 2015; Sala et al., 2007). In contrast, inactive fillers are stabilized by surfactants with poor chemical affinity to the gelling agents, and the modulus of elasticity of the systems are often decreased, as indicated in the recent literature (Geremias-Andrade et al., 2016; Oliver et al., 2015; Sala et al., 2007).

While these observations are true, the complexity of EFG does not allow us to predict the effect of adding fillers solely based on the chemical affinity between their components. In our previous studies, we had shown that solid lipid particles (SLP) were stabilized by Tween 80 and Span 80, and then incorporated into CaCl₂-induced soy protein isolate (SPI) gels, in the presence or absence of locust bean gum (LBG) or xanthan gum (XG), which causes an increase in Young's moduli (Brito-Oliveira et al., 2017, 2018). These results suggested that SLP was active in gels, although the fillers stabilized by nonionic surfactants were supposed to behave as inactive due to the formation of chemical affinity matrix (Chen et al. 2000; Sala et al., 2007). However, this may have occurred due to physical interactions between SLP and gelled matrices, allowing protein/polysaccharides to be anchored on the surface of the SLP formed by different sizes of polar heads of synthetic surfactants (Brito-Oliveira et al., 2017, 2018).

The production of EFG by SPI is not as diverse as whey proteins. Nevertheless, the use of plant proteins in food products has been increased due to the rising concerns about the sustainability of animal-based products and the preferences for healthy, cruelty-free, and environmentally friendly ingredients (Monteiro et al., 2013). In this context, the objective of this research was to evaluate the effects of the introduction of SLP, stabilized by different surfactants (whey protein isolate and Tween 80/Span 80) in NaCl-induced SPI and LBG gels based on our previous studies of non-filled gels (Brito-Oliveira et al., 2020).

5.3 Materials and methods

5.3.1 Chemicals and reagents

SPI (Protimarti M-90, 84.3% protein) was obtained from Marsul (Montenegro, RS, Brazil), whereas sodium chloride was procured from Synth (Diadema, SP, Brazil), and LBG (Viscogum LBG®) was donated by Cargill (Campinas, SP, Brazil). For the production of SLP, palm stearin (PS) (melting point 50.1°C) was donated by Agropalma (Belém, PA, Brazil), and Tween 80 and Span 80 were procured from Sigma-Aldrich (St. Louis, MO, USA). Ultrapure water (Millipore system Direct Q3®, Billerica, MA, USA) was used throughout the experiments.

5.3.2 Production and characterization of SLP stabilized with different surfactants.

Table 5.1 presents the two formulations (TS and WPI) used to develop SLP. For both formulations, the lipid phases were initially fixed at 80°C for 30 min to eliminate the thermal memory. Subsequently, the SLP was produced by dispersing the aqueous phases in the lipid phases using a rotor-stator device (IKA T25, IKA, Staufen, Germany) at 80°C. For WPI, the lipid phase consisted of PS, while the aqueous phase existed of a WPI dispersion prepared by Cazado & Pinho (2016). For this formulation, XG was added to the systems by magnetic stirring after the production (Cazado & Pinho, 2016). For TS, the lipid phase consisted of PS and Span 80, and the aqueous phase consisted of Tween 80 and deionized water (Brito-Oliveira et al., 2017, 2018). Both formulations were produced in triplicate and stored at 10°C. Sodium benzoate (0.02%, w/w) was added to the samples to prevent microbiological contamination. The average particle size of the SLPs was determined by laser diffraction (SALD-201 V, Shimadzu, Kyoto, Japan).

Table 5.1. Formulations used for the production of solid lipid particles (SLP).

Formulation	Surfactant	Xanthan gum (%, w/w)	Palm stearin (%, w/w)	Production parameters
TS	Tween 80 (1.8%, w/v) and Span 80 (2.7%, w/w)	-	4.5%	18,000 rpm for 5 min
WPI	Whey protein isolate (2%, w/w)	0.2%	4.5%	12,000 rpm for 5 min

5.3.3 Production of cold-set EFG

The cold-set gelation of the systems was carried out using the protocol described by Brito-Oliveira et al. (2020). In this study, non-filled gels were formed by the initial hydration of SPI powder (14%, w/v) with LBG (0.1%, w/v) at pH 7, followed by a preheating process in a water bath at 80°C for 30 min and by the addition of NaCl (300 mM) at room temperature. For EFGs production, different proportions of deionized water were used to hydrate SPI/LBG samples and were replaced by solid lipid particles dispersions (SLPD). The different ratios of deionized water and SLPD were calculated as 25:75, 50:50, 75:25, and 0:100. The samples were then stored at 10°C for 12 h prior to characterization. All gels were characterized by visual appearance, water holding capacity, microstructural properties, and uniaxial compression parameters.

5.3.4 Water holding capacity

Water holding capacities (WHCs) of the systems were determined, followed by the protocol mentioned in Beuschel et al. (1992). The samples were first weighed on Whatman filter paper Grade 1, placed in Falcon tubes, and centrifuged at a speed of 2500 rpm for 10 min at 6°C (Hermle centrifuge Labortechnik GmbH, Z-216 MK, Wehingen, Germany). Subsequently, the gels were extracted by the filters and determined the weight of the papers. WHCs can be calculated using the following Equation 5.1.

$$\text{WHC (\%)} = \left(1 - \left(\frac{m_f - m_i}{m_s} \right) \right) * 100 \quad (5.1)$$

Where m_f refers to the weight of the wet filter (g); m_i is the initial weight of the dry filter (g); m_s is the weight of the SPI sample (1–2 g). Experiments were performed in triplicate and repeated three times with similar results.

5.3.5 Uniaxial compression tests

Uniaxial compression tests were carried out using texturometer (TA-Xt.plus Texture Analyser, Godalming, Surrey, UK), followed by a protocol adapted from Oliver et al.(2015). Samples with cylindrical shapes were compressed to 80% of their original height using a silicon oil-lubricated aluminum probe to reduce friction at four different speeds of deformation: 0.05, 1, 2, and 4 mm/s. Five replicates were used to test the formulations. The values of Hencky stress (σ_H) and Hencky strain (ϵ_H) were derived from the force-deformation data using Equations (5.2) and (5.3), respectively:

$$\sigma_H = F(t) \cdot \frac{H(t)}{H_0 \cdot A_0} \quad (5.2)$$

$$\epsilon_H = \ln \frac{H(t)}{H_0} \quad (5.3)$$

Where $F(t)$ is the force at time t ; A_0 is the initial area; H_0 is the initial height; $H(t)$ is the height at time t . The rupture parameters were associated with the maximum value of the stress-strain curve. The values of the apparent Young's modulus (E_g) of the systems were calculated by the slope of the first linear interval in the Hencky stress (σ_H) versus Hencky strain (ϵ_H) curves, up to rupture.

5.3.6 Scanning electron microscopy

Samples were prepared following the procedure described in Picone et al. (2011). The samples (1.0 cm × 0.5 cm × 0.5 cm) were initially fixed in 2.5 g/100 g glutaraldehyde with cacodylate buffer (16 g/L) at pH 7.2 of 7°C for 24 h. After rinsing twice in cacodylate sodium buffer (16 g/L, pH 7.2), the samples were fractured in liquid nitrogen. The samples were then subjected to post-fixation using osmium tetroxide 1 g/100 g in cacodylate buffer (16 g/L, pH 7.2) for 120 min, and rinsed twice in deionized water. Subsequently, they were dehydrated in graded ethanol series (30, 50, 70, and 90 mL/100 mL) for 20 min. Dehydration was continued in 100% ethanol (three adjustments during 1 h) followed by critical point drying (CPD03 Balzers Critical Point Dryer, Alzenau, Germany). Then the dried samples were fractured, mounted on aluminum stubs, and coated with gold (200 s/40 mA) in a Balzers SCD 050 Sputter

Coater (Alzenau, Germany), and analyzed using a TM 3000 tabletop microscope (Hitachi, Tokyo, Japan).

5.3.7 Confocal laser scanning optical microscopy

Confocal laser scanning microscopy (CLSM) (Confocal Upright Microscope LSM 780 NLO-Zeiss, Zeiss, Germany) images were taken using simultaneous dual-channel imaging following the procedure mentioned in Brito-Oliveira et al. (2017). Here, three different solutions were prepared and incorporated to the gels: (I) rhodamine B solution (0.2%, w/v in deionized water-10 μ L solution/mL of gel); (II) fluorescein isothiocyanate (FITC) solution (1 mg/mL dimethyl sulfoxide, DMSO-0.05 mL solution/mL of gel); (III) Nile Red solution (0.1 g/100 mL of methanol-10 μ L solution/g of lipid). The protein phase was observed by exciting rhodamine B at a wavelength of 543 nm and an emission wavelength range of 551–655 nm; however, the polysaccharides were observed by exciting the FITC at an excitation wavelength of 488 nm, and an emission wavelength range of 493–543 nm and the SLP were visualized by exciting the Nile Red dye at 488 nm of excitation wavelength and an emission wavelength range of 500–580 nm.

5.3.8 Statistical analyzes

All measurements were carried out at least in triplicate, and mean values and corresponding errors were calculated. For statistical data processing, an analysis of variance was performed, followed by Tukey's tests with a 5% significance level using SAS software version 9.2 (SAS Institute Inc, Cary, NC).

5.4 Results and discussion

5.4.1 The visual aspect and WHC

The average particle sizes (APS) of dispersions produced with WPI and TS formulations have initially been monitored for 30 days (data not shown) because EFG can only be produced from stable emulsions or SLPD (Dickinson, 2012). Both formulations had good stability over the entire period (with APS approximately 600 nm for TS and 1 μ m for WPI), thus suitable for producing cold-set EFGs.

Cold-set gelation methods essentially consist of two steps: (I) preheating of protein dispersions under non-gelling conditions; (II) altering the quality of solvents at low temperatures in order to induce gelation of the systems (Bryant & McClements, 2000; Cavallieri & Cunha, 2008; Kuhn et al., 2010). Therefore, one of the most critical aspects to be regulated in such processes is the preheating conditions to prevent the over-aggregation of macromolecules (Maltais et al., 2005). For this purpose, it is important to check the visual aspects of the samples immediately before preheating to ensure that heat-induced gels have not already been created.

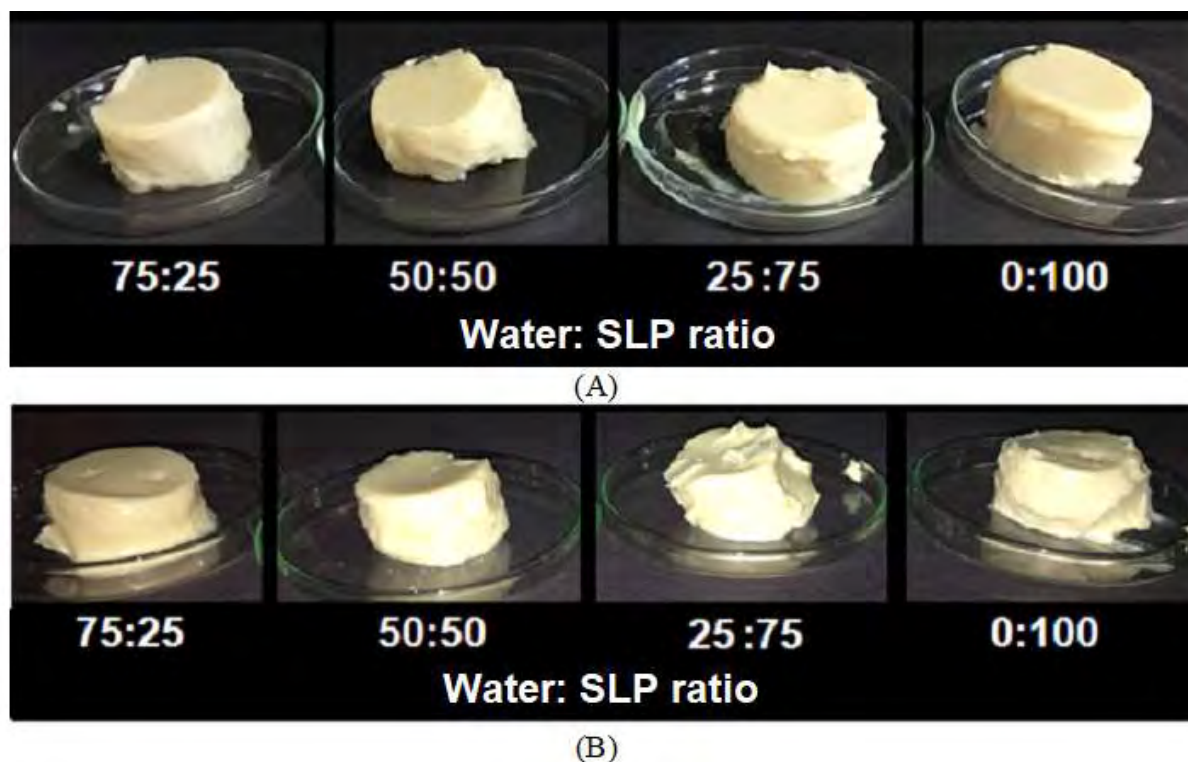
This evaluation was carried out in our previous study for non-filled gels developed with the same formulation used in the present research (Brito-Oliveira et al., 2020). It has been verified that the heating at 80°C for 30 min in samples with 14% SPI and 0.1% LBG, at pH 7, was not enough to form gels. Self-supported systems were obtained only after the incorporation of NaCl, thus classifying the structures as cold-set gels (Brito-Oliveira et al., 2020).

While the concentrations of SPI, LBG, pH, and preheating used in this study are the same as that previously used, the dispersion medium was different due to the presence of SLPs. The effects of replacing water with SLP dispersions for producing cold-set gels are not extensively discussed in the literature (Brito-Oliveira et al., 2017, 2018). Thus, it is still uncertain whether such structures can reduce the protein concentrations required for heat-induced gels formation.

In this sense, all systems containing the SLP produced with both formulations were evaluated regarding its visual aspects in two different moments of the process: after the preheating and after the salt incorporation, in order to guarantee that cold-set gels were being produced before further characterizations.

The presence of WPI-stabilized SLP, in all concentrations tested, decreased the protein concentration required for the formation of heat-induced gels, as strong self-supported systems were formed immediately after the preheating process, as presented in Figure 5.1A. These results suggested that these SLPs could interact with the matrices (active fillers), and caused an over-aggregation of molecules, leading to the formation of gel before adding salt. Researchers have shown the behavior of protein-stabilized emulsions as active fillers in protein gels. However, most of their studies analyzed using whey protein isolates/concentrates and heat-induced gelation (Chen et al. 2000; Sala et al., 2007).

Figure 5.1. Visual aspects of the (A) heat-induced emulsion-filled gels produced with different concentrations of WPI-stabilized solid lipid particles (SLP) and (B) NaCl-induced emulsion-filled gels (EFGs) produced with different concentrations of TS-stabilized solid lipid particles (SLP).



Based on these results, it was confirmed that even at low concentrations, it is not possible to produce cold-set EFG using the conditions applied by incorporating WPI-stabilized SLP. Thus, such systems were not characterized further.

In contrast, the formation of self-supporting gels in SLP-containing TS formulation systems was confirmed only after adding NaCl (Figure 5.1B). These systems were then labeled as cold-set gels and analyzed for WHC, and the results are shown in Table 5.2. Experimental data showed that the replacement of 25, 50, and 75% of the water by solid lipid particles dispersion (SLPD) reduced the WHC of gels; however, the total replacement is not influenced by this parameter. The decrease in WHC of gels by adding emulsions/SLP may be attributed due to alterations in microstructures and/or decreases in gel strength, which can only be examined from uniaxial compression data and SEM/CLSM micrographs.

Table 5.2. Water holding capacities (WHCs) of non-filled gels and emulsion-filled gels produced at different concentrations of TS-stabilized solid lipid particles (SLP).

Water:Solid lipid particles dispersion (SLPD) Ratio	WHC (%)
Non-filled gels	81.1 ^a ± 3.5
75:25	59.0 ^c ± 0.8
50:50	72.8 ^b ± 3.0
25:75	71.5 ^b ± 1.6
0:100	77.1 ^{ab} ± 1.8

Averages followed by different lowercase letters are statistically different ($p < 0.05$) for gels with different Water:SLPD ratios

5.4.2 Microstructural characterization

The results of microstructural organizations of EFG produced with different ratios of water and SLPD are shown in Figures 5.2 and 5.3 in which all EFG presented porous matrices, with “puzzle-like” patterns. Such microstructures are quite different from those obtained through non-filled gels (NFG), which were more compact, homogeneous with small pores (Brito-Oliveira et al., 2020).

The size and number of pores of the gelled systems have a direct effect on WHC of the system, as stated in the earlier report. Gels with lower pores and denser networks tend to retain more water due to stronger capillary forces (Maltais et al., 2005).

These differences between the non-filled gel micrographs and EFG showed that the presence of SLP influenced the aggregation and gelling behavior of the SPI/LBG system. As presented in Figure 5.2, the EFG matrices are composed of gelled “pieces,” placed relatively close to each other in which the SLP were located. Such organizations resemble systems called microgels (Vincent & Saunders, 2011; Schmitt et al., 2009). According to the literature microgels are deformable polymer-based particles possessing a porous internal structure, resulting from a self-limited aggregation controlled by the protein net charge and hydrophobic regions exposed to heat denaturation (Schmitt et al., 2009).

Figure 5.2. Scanning electron micrographs of emulsion-filled gels produced with different concentrations of solid lipid particles stabilized with Tween 80 and Span 80. For Figures A, D, G and J, the magnification of 100 x was used, and the scale bar corresponds to 1mm. In Figures B, E, H and K, the magnification of 500 x was used, and the scale bar corresponds to 200 μm . In Figures B, D and F, the magnification of 2000 x was used, and the scale bar corresponds to 30 μm .

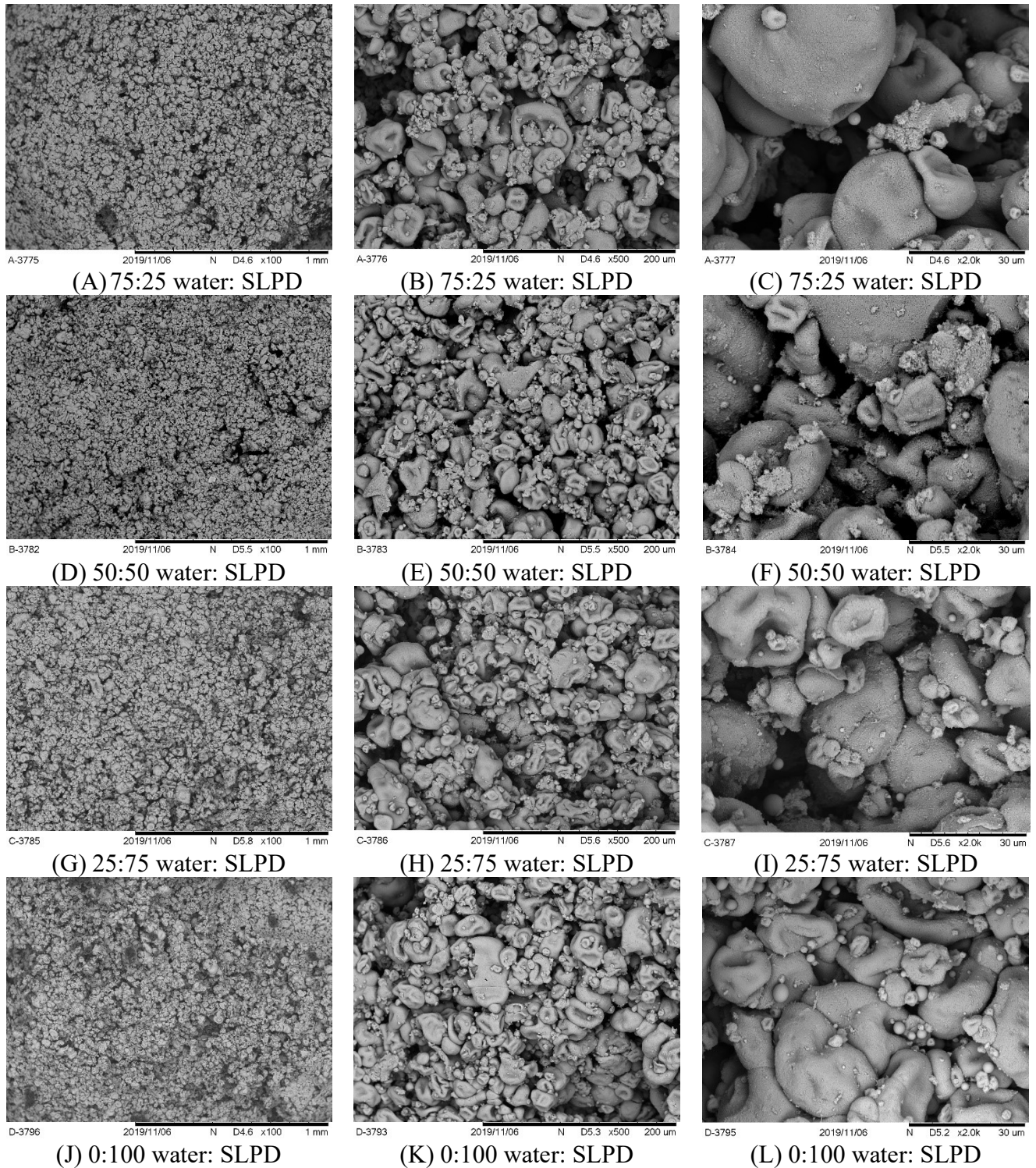
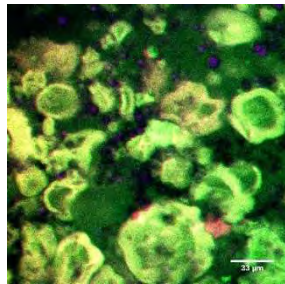
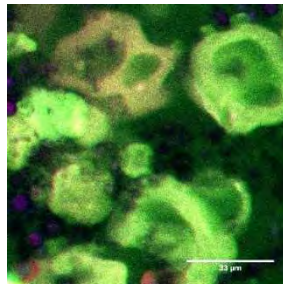


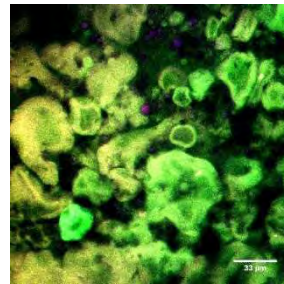
Figure 5.3. Confocal laser scanning micrographs of emulsion-filled gels produced with different concentrations of solid lipid particles (SLP) stabilized with Tween 80 and Span 80. In such micrographs, the scale bar corresponds to 33 μm and the colors red, green and purple were used to identify the protein, polysaccharide, and lipid-rich phases of the systems, respectively. Regions with incomplete demixing present a yellowish color.



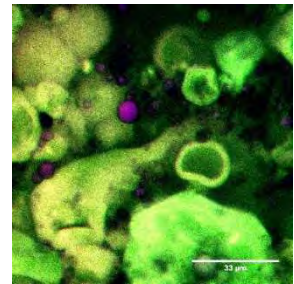
(A) 75:25 water:
SLPD



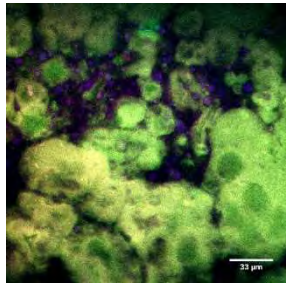
(B) 75:25 water:
SLPD



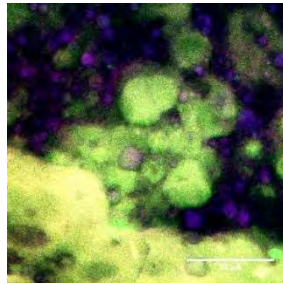
(C) 75:25 water:
SLPD



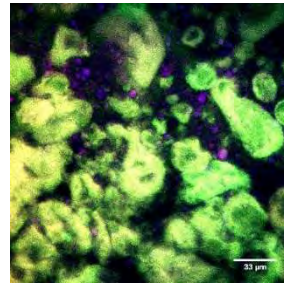
(D) 75:25 water:
SLPD



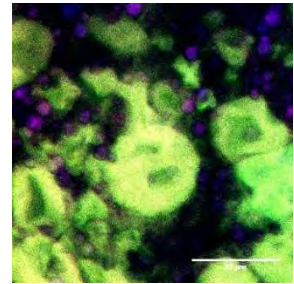
(E) 50:50 water:
SLPD



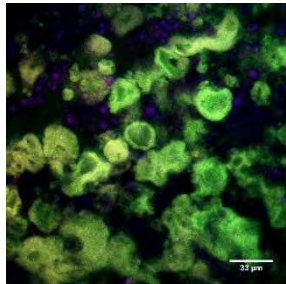
(F) 50:50 water:
SLPD



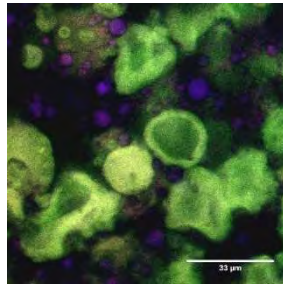
(G) 50:50 water:
SLPD



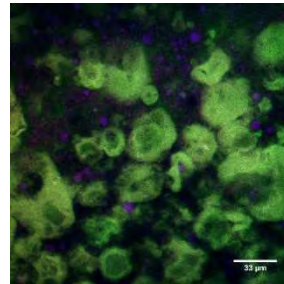
(H) 50:50 water:
SLPD



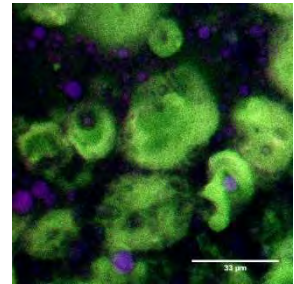
(I) 25:75 water:
SLPD



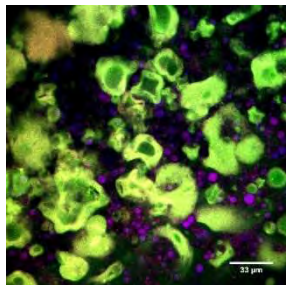
(J) 25:75 water:
SLPD



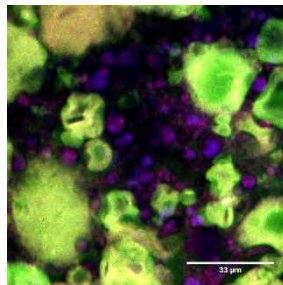
(K) 25:75 water:
SLPD



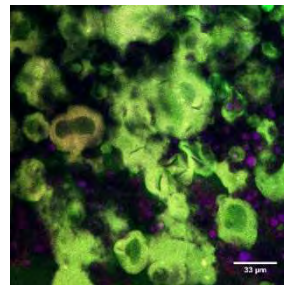
(L) 25:75 water:
SLPD



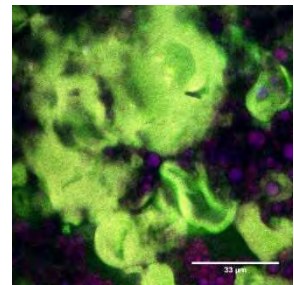
(M) 0:100 water:
SLPD



(N) 0:100 water:
SLPD



(O) 0:100 water:
SLPD



(P) 0:100 water:
SLPD

By comparing the microstructures of the NFG (Brito-Oliveira et al., 2020) and the EFG (Figure 5.2), it is evident that SLP has affected interactions between the biopolymers, restricted their continuous aggregation necessary to form a homogeneous network, and enabled the proteins to interact locally with closer molecules by forming the “particles”/microgels, as shown in Figure 5.2.

The increase in the SLP concentration took these microgels closer, as the gap between the structures was much smaller for systems with water and SLPD ratio of 0:100. Such effects were even more evident in the CLSM micrographs shown in Figure 5.3, locating the position of SLP (identified by purple color) among the microgels. However, these structures were clustered in certain regions of systems with 50, 75, and 100% SLP, bringing the microgels closer to each other and possibly increasing protein-protein interactions between them.

The interaction between a pair of microgel particles may be determined by steric effects of a similar nature to those present between solid particles and carrying a layer of adsorbed polymer chains (Vincent & Saunders, 2011). While the presence of low concentrations of TS-stabilized SLP (25:75 water: SLPD ratio) restricted the aggregation of the structures, leading to microgel-like organizations, the increase in the SLP concentration affected the balance of “particles”/microgels interactions by decreasing the repulsive interactions between them.

In order to understand the presented results, it is important to know the mechanisms involved in the formation of NaCl-induced gels, and also the properties of the surfactants and the gelling agents used. According to Vilela et al. (2011), monovalent ions, such as NaCl, neutralizes negatively charged residues in biopolymers, facilitate indirect cross-linking in double helices or other linkages by shielding the electrostatic repulsion of the carboxylate groups. Thus, the approximation of the protein groups is essential for establishing the protein-protein interactions. In this context, structures that hinder such approximation may reduce molecular interactions, compromise the process of aggregation/gelation processes, and consequently, the microstructural organization of the systems.

The presence of TS-stabilized SLP has physically restricted the aggregation of protein groups due to the presence of NaCl, resulting in the formation of microstructures, as shown in Figures 5.2 and 5.3.

In higher SLP concentrations, however, the presence of such structures decreased the distance among the microgels possibly by affecting the charge distribution around them. It is known that oil droplets or SLP stabilized with Tween/Span tend to present a negative net charge, so, these structures attract anions in the dispersion media to their interfaces. For this reason, it is possible that the SLP helped to decrease the electrostatic repulsion among the

microgels for removing part of the anions, bringing them closer together, as seen in the micrographs.

Besides, at higher concentrations, certain groups of protein and/or polysaccharide chains anchored to spaces in the particle interface, which resulted from the different sizes of polar heads of Tween 80 and Span 80 molecules (Brito-Oliveira et al., 2017, 2018), leading to the SLP as “junction” zones/points in the structures.

Notably, no phase separation between SPI and LBG has been observed, whereas structures formed by galactomannans and protein ingredients appear to present microphase separations due to the thermodynamic incompatibility between biopolymers (Turgeon et al., 2003). However, phase separation may be less intense with the initiation of gelation; hence, the resulting microstructures depend on the balance between these two processes (Turgeon et al., 2003; Jong & Van De Velde, 2007).

In our earlier study (Brito-Oliveira et al., 2020), it was confirmed that the non-filled gel developed with the same formulation used here did not show a consistent phase separation. Such a fact has been attributed to the applied gelation method as the direct addition of NaCl may cause excessively fast gelation, kinetically preventing phase separation (Vilela et al., 2011). Figure 5.3 presents an incomplete demixing of EFG as the gelled structures in the micrographs had only one prominent color (greenish). Thus, the presence of SLP altered the microstructural organization of the gel but did not interfere significantly with the phase separation.

5.4.3 Uniaxial compression: effect of different compression speeds

In our previous research, gels produced with 14% SPI, 0.1% LBG, and 300 mM NaCl were subjected to uniaxial compression tests at a compression speed of 1 mm/s, and the results showed E_g , σ_H , and ϵ_H as 1978 (± 12) Pa, 766 (± 24) Pa and 0.264 (± 0.013), respectively (Brito-Oliveira et al., 2020). In order to understand the impacts of SLP to the rheological properties of gels with the same formulation, the systems previously characterized by SEM and CLSM were initially subjected to uniaxial compression tests using the same compression speed (1 mm/s), and the results are shown in Figure 5.4.

According to the obtained data, it was found that the incorporation of SLP significantly decreased the values of three parameters, indicating that a weakening of structures, likely to be associated with more heterogeneous and porous organizations. Besides, the reduction of the

rupture properties suggests that the SLP within the gelled matrix possibly reflected structural defects that acted as stress concentrates within the system (Sala et al., 2009).

The classification of SLP as active or inactive in EFG usually depends on the rheological properties of the systems of large deformations (Liu et al., 2015; Oliver et al., 2015; Sala et al., 2009). In general, SLP/droplets are active when they interact with the gelled matrix, either causing an increase or decrease in the Young's modulus of the systems. However, such structures appear to increase the rupture stress and reduce the rupture strain of EFG (Oliver et al., 2015). Furthermore, inactive SLP/droplets form the gel due to their small chemical affinity with the molecules; however, they reduce the Young's modulus and the rupture stress of the systems and may either decrease or increase their rupture strain (Geremias-Andrade et al., 2016).

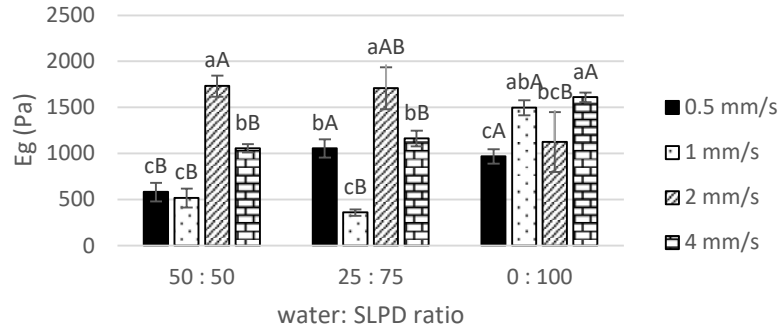
By comparing the results presented in Figure 5.4 with the data of NFG discussed in our previous study (Brito-Oliveira et al., 2020), we conclude that SLP was inactive in the gels and expected to stabilize by Tween 80 and Span 80. Based on the properties of the surfactants used, the effect of lipid particles/oil droplets incorporated into EFG shows that other factors may influence the behavior of the different structures within the gelled matrix.

The same TS-stabilized SLP had been incorporated into CaCl_2 -induced gels of SPI in our earlier research in the presence and absence of LBG or XG, and the results showed an increase in Young's modulus of the gels (Brito-Oliveira et al., 2017, 2018). Although both the gels produced here and in these studies are similar in terms of the characteristics of the gelling agent and the SLP used, the systems were produced using different ionic strengths and different salts.

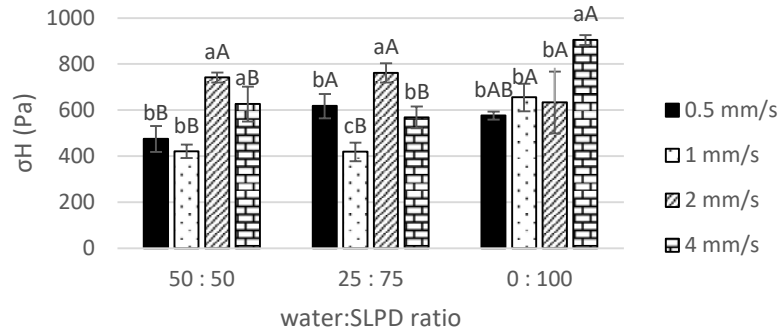
Researchers have shown that CaCl_2 can form bonds between protein groups, while NaCl only reduces electrostatic repulsion between them, enabling an increase in protein-protein interactions, which explains the ability of CaCl_2 to form gels of lower ionic strengths (Bryant & McClements, 2000).

In the case of CaCl_2 -induced gels, the ions could form bonds between the protein groups, possibly by trapping SLP, which would then increase the strength of the structures, acting as "hooks" in the network (Brito-Oliveira et al., 2017, 2018). For the NaCl-induced system, the SLP hindered the approximation between protein groups, thus reducing the strength of the structures, as cited earlier.

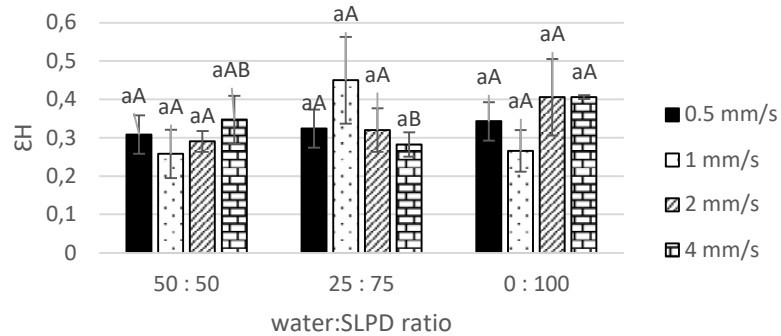
Figure 5.4. Results of uniaxial compression tests of emulsion filled gels (EFG) produced with different concentrations of solid lipid particles stabilized with Tween 80 and Span 80, using different compression speeds.



(A)



(B)



(C)

Averages followed by different lowercase letters are statistically different ($p < 0.05$) for gels with different Water:SLPD Ratios, using the same compression speed. Averages followed by different capital letters are statistically different ($p < 0.05$) for gels with the same Water:SLPD Ratios, using different compression speeds.

With these results, it is evident that the classification of SLP/droplets as active or inactive based only on the properties of the surfactant used can be very imprecise, if other factors, such as ionic strength and the gelation method are not considered, given the complexity of the EFG.

Earlier, Sala et al. (2009) also discussed the complexity of the above system using uniaxial compression tests and examined the effects of compression speed on EFG properties stabilized by different surfactants. The authors explained the results of the compression speed on E_g and fracture properties of the gels based on five mechanisms related to energy dissipation: viscoelastic behavior, induced viscous flow of the matrix, unzipping of physical bonding, friction between structural components, and stress concentration.

Following Sala et al. (2009), in the present study, EFGs have also been characterized using three other compression speeds (0.5 mm/s, 2 mm/s, and 4 mm/s), and the results are shown in Figure 5.4.

For gels produced with water and SLPD had a ratio of 50:50 in which an increase in E_g and σ_H was observed with the rise of compression speed from 0.5 mm/s to 2 mm/s. However, this increase in compression speed reduced the values of such parameters. In contrast, the values of ϵ_H were not affected by the variation in compression speed.

The viscoelastic behavior of the system could explain the first increases of E_g and σ_H from 0.5 mm/s to 2 mm/s. Sala et al. (2009) showed that the elastic behavior of the gels allows storing the energy supplied during deformation and for recovering its original shape when the force is removed. Thus, no energy dissipation occurs here, and thus, E_g is not dependent on the compression speed. In contrast, for viscoelastic gels, energy dissipation occurs in the linear region, causing the E_g to increase with compression speed. However, the authors also stated that in absolute terms, energy dissipation is typically high at high-speed deformation, leading to an increase in fracture stress.

The decrease in E_g and σ_H from 2 mm/s to 4 mm/s suggests that the stress concentration mechanism is more intense in the SLP and overcomes the effect of the viscoelastic nature of the systems. Both phenomena are present in the samples during the compression; however, at lower compression speeds, microstructural rearrangements require a longer period of time by preventing bonds/interactions between the macromolecules from damages and ruptures. Thus, the effects of viscoelasticity play a crucial role in the analysis. At higher compression speeds, however, the interactions and microstructural organizations were more influenced by a decrease in the energy storage capacity of the system, as confirmed by the decrease of E_g .

For gels with a ratio of 25:75 of water and SLP, the reduction of E_g from 0.5 to 1 mm/s and σ_H from 2 to 4 mm/s indicates a prevalence of the effect of stress concentration mechanism. In

contrast, the process relating to the viscoelastic activity of the system was stronger from 1 to 2 mm/s. These results suggest the possible existence of an “optimal” compression speed for the storage of maximum energy in the systems and subsequent return of samples to their original shapes. At this speed (2 mm/s), structural rearrangements and interactions between protein groups during the test favor their viscoelastic behavior and a more homogeneous distribution of the forces and stress within the sample.

A continuous increase of E_g and σ_H with a rise in compression speed from 0.5 to 4 mm/s were confirmed for systems with a ratio of 0:100 of water and SLP. The “agglomeration” of the particles between the microgels and the decrease in distance between them was confirmed by an increase in the SLP concentration. This could possibly increase the interactions between the microgels and their elastic responses. Besides, the higher concentrations of SLP are likely to increase the friction between the structural components. In this context, Sala et al. (2009) showed that the energy dissipation due to friction between structural elements increases with the rise in compression speed. These authors confirm that the inhomogeneous deformation of the gels induces a displacement of gel matrices on the surfaces of the SLP. As a result, the friction between these elements will increase compared to unfilled gels or gels containing less SLP, causing an increase of σ_H .

Systems were developed with different SLP concentrations at the same compression speed and did not reveal any specific trends, possibly due to the heterogeneity of the systems.

The results obtained by uniaxial compression tests showed that even though the fillers applied could be classified as unbound due to the chemical affinity of the components of the samples, they have interacted with the gelled matrices by changing their aggregation patterns and microstructural organizations, especially at a higher particle concentration. From these results, it is possible to propose a new application for the terms active/inactive or bound/unbound systematically used as synonyms in EFG studies (Oliver et al., 2015; Sala et al., 2007). Thus, although the fillers were probably not bound to the gelled matrices, particularly at lower concentrations, due to the properties of the surfactants (low chemical affinity), they were active in the microstructure, interacting and affecting the aggregation/gelling process and consequently, the properties of the systems.

5.5 Conclusions

The results showed that WPI-stabilized SLP were active fillers in the matrices, increasing protein-protein interactions, and decreasing the critical concentration of protein needed for

heat-induced gelation. Besides, EFG containing SLP, which had been stabilized by Tween 80 and Span 80, was developed only after incorporating NaCl. Owing to the low chemical affinity between surfactants and gelled matrix (unbound fillers), the presence of such structures reduced WHC, altered the microstructures of the gels (resulting in “microgel-like” organizations), and decreased E_g , σ_H , and ϵ_H , as compared to NFG. However, increases in the SLP content caused different effects over E_g , σ_H , and ϵ_H , possibly due to the heterogeneity of the samples. These results suggested that, even though TS-stabilized SLP were “unbound” to the matrix, they were “active” by interacting with the gelled matrices, which changed their aggregation patterns and microstructural organizations.

Acknowledgments

This study was funded by Fundação de Amparo à Pesquisa do Estado de São Paulo (FAPESP) (grant number 2017/06224–9). We also thank the access to equipment and assistance provided by the Electron Microscope Laboratory (LME/UNICAMP).

Conflict of Interest: The authors declare that they have no conflict of interest.

5.6 References

- Beuschel, B. C., Culbertson, J.D., Partridge, P.A., & Smith, D. M. (1992). Gelation and emulsification properties of partially insolubilized whey protein concentrates. *Journal of Food Science*, 57, 605–609.
- Brito-Oliveira, T.C., Bispo, M., Moraes, I.C.F., Campanella, O.H., & Pinho, S.C. (2017). Stability of curcumin encapsulated in solid lipid microparticles incorporated in cold-set emulsion filled gels of soy protein isolate and xanthan gum. *Food Research International*, 102, 759–767.
- Brito-Oliveira, T.C., Bispo, M., Moraes, I.C.F., Campanella, O.H., & Pinho, S.C. (2018). Cold-set gelation of commercial soy protein isolate: effects of the incorporation of locust bean gum and solid lipid microparticles on the properties of gels. *Food Biophysics*, 13, 226–239.
- Brito-Oliveira, Cavini, Ferreira, Moraes & Pinho (2020). Microstructural and rheological characterization of NaCl-induced gels of soy protein isolate and the effects of incorporating different galactomannans. *Food Structure*, 26, 100158.
- Bryant, C.M., & McClements, D.J. (2000). Influence of NaCl and CaCl₂ on Cold-Set Gelation of Heat-denatured Whey Protein. *Journal of Food Science*, 65(5), 801–804.

- Cavallieri, A.L.F. & Cunha, R. L. (2008). The effects of acidification rate, pH and aging time on the acidic cold set gelation of whey proteins. *Food Hydrocolloids*, 22(3), 439–448.
- Cazado, C.P.S. & Pinho, S.C. (2016). Effect of different stress conditions on the stability of quercetin-loaded lipid microparticles produced with babaçu (*Orbignya speciosa*) oil: evaluation of their potential use in food applications. *Food Science and Technology (Campinas)*, 36(1), 9–17.
- Chen, J., Dickinson, E., Langton, M., & Hermansson, A.M. (2000). Mechanical properties and microstructure of heat-set whey protein gels: Effect of emulsifiers. *LTW–Food Science and Technology*, 33, 299–307.
- Dickinson, E. (2012). Emulsion gels: The structuring of soft solids with protein-stabilized oil droplets. *Food Hydrocolloids*, 28(1), 224–241.
- Geremias-Andrade, I.M., Souki, N.P.B.G., Moraes, I.C.F. & Pinho, S.C. (2016). Rheology of emulsion-filled gels applied to the development of food materials. *Gels*, 2, 22.
- Jong, S. & Van De Velde, F. (2007). Charge density of polysaccharide controls microstructure and large deformation properties of mixed gels. *Food Hydrocolloids*, 21(7), 1172–1187.
- Kuhn, K. R., Cavallieri, A.L.F., & Cunha, R.L. (2010). Cold-set whey protein gels induced by calcium or sodium salt addition *International Journal of Food Science and Technology*, 45, 348–357.
- Liu, K., Stieger, M., van der Linden, E., & van de Velde, F. (2015). Fat droplet characteristics affect rheological, tribological and sensory properties of food gels. *Food Hydrocolloids*, 44, 244–259.
- Maltais, A., Remondetto, G.E., Gonzalez, R. & Subirade, M. (2005). Formation of soy protein isolate cold-set gels: protein and salt effects. *Journal of Food Science*, 70(1), 67–73.
- Monteiro, S.R., Rebelo, S., Silva, O.A.B.C., & Lopes-da-Silva, J.A. (2013). The influence of galactomannans with different amount of galactose side chains on the gelation of soy proteins at neutral pH. *Food Hydrocolloids*, 33, 349–360.
- Oliver, L., Scholten, E., & van Aken, G.A. (2015). Effect of fat hardness on large deformation rheology of emulsion-filled gels. *Food Hydrocolloids*, 43, 299–310.
- Picone, C. S. F., Takeuchi, K. P. & Cunha, R. L. (2011). Heat-induced whey protein gels: Effects of pH and the addition of sodium caseinate. *Food Biophysics*, 6, 77–83.
- Sala, G., van Aken, G.A., Stuart, M.A.C., & van de Velde, F. (2007). Effect of droplet–matrix interactions on large deformation properties of emulsion-filled gels. *Journal of Texture Studies*, 38, 511–535.

- Sala, G., Wijk, R.A., van de Velde, F. & van Aken, G.A. (2008). Matrix properties affect the sensory perception of emulsion-filled gels. *Food Hydrocolloids*, 22(3), 353–363.
- Sala, G., van Vliet, T., Stuart, M.A.C., van Aken, G.A., & van de Velde, F. (2009) Deformation and fracture of emulsion-filled gels: Effect of oil content and deformation speed. *Food Hydrocolloids*, 23, 1381–1393.
- Schmitt, C., Bovay, C., Vuillomenet, A.-M., Rouvet, M., Bovetto, L., Barbar, R., et al. (2009). Multiscale characterization of individualized b-lactoglobulin microgels formed upon heat treatment under narrow pH range conditions. *Langmuir*, 25, 7899–7909.
- Turgeon, S. L., Beaulieu, M., Schmitt, C., & Sanchez, C. (2003). Proteinepolysaccharide interactions: phase-ordering kinetics, thermodynamic and structural aspects. *Current Opinion in Colloid and Interface Science*, 8, 401–414.
- Vincent, B. & Saunders, B. R. (2011). Interactions and colloid stability of microgel particles. In A. Fernandez-Nieves, H. Wyss, J. Mattsson, & D. A. Weitz (Eds.), *Microgel suspensions*. Weinheim: WileyVCH, Chap. 6.
- Vilela, J.A.P., Cavallieri, A.L.F., & Cunha, R.L. (2011). The influence of gelation rate on the physical properties/structure of salt-induced gels of soy protein isolate-gellan gum. *Food Hydrocolloids*, 25, 1710–1718.

**CHAPTER 6 : EFFECTS OF SOLID LIPID PARTICLES INCORPORATION ON
THE PROPERTIES AND STABILITY OF CaCl_2 -INDUCED GELS OF SOY
PROTEIN ISOLATE AND LOCUST BEAN GUM**

(Edited for submission to: LWT - Food Science and Technology)

**Thais C. Brito-Oliveira, Camila S. Cazado, Ana Clara M. Cavini, Lorena M.F. Santos,
Izabel C.F. Moraes, and Samantha C. Pinho**

Effects of solid lipid particles incorporation on the properties and stability of CaCl₂-induced gels of soy protein isolate and locust bean gum

Thais C. Brito-Oliveira¹, Camila S. Cazado¹, Ana Clara M. Cavini¹, Lorena M.F. Santos¹,
Izabel C.F. Moraes¹, and Samantha C. Pinho^{1*}

¹Department of Food Engineering, School of Animal Science and Food Engineering,
University of São Paulo (USP), Pirassununga, SP, Brazil

* Corresponding author: S.C. Pinho, Department of Food Engineering, School of Animal Science and Food Engineering (FZEA), University of São Paulo (USP), Av. Duque de Caxias Norte 225, Jd. Elite, Pirassununga, SP, Brazil 13635-900. Tel: +55-19-35654288; fax: +55-19-3565-4284.

E-mail address: samantha@usp.br

6.1 Abstract

This study evaluated the stability of non-filled gels (NFG) produced with 14% soy protein isolate (SPI), 0.1% locust bean gum (LBG) and 100 mM CaCl₂, and also the effects of incorporating Tween 80/Span 80-stabilized solid lipid particles (SLP) to the system. The gels were characterized regarding its water holding capacity (WHC), microstructural organizations and rheological properties. NFG presented low WHC (46.5%) at the 1st day, mainly due to its particulate and porous microstructure. After 10 days, the matrices presented a great microstructural compaction and extensive syneresis, which prevented the analyzes on subsequent days. The incorporation of SLP to the NFG originated emulsion-filled gels (EFG) with microgel-composed matrices. Such systems were more stable than NFG and could be evaluated for 20 days. During this period, the EFG presented a more subtle microstructural compaction and a constant WHC (around 65%). Such compaction resulted from the formation of new bonds among the biopolymers molecules, which approximate the microgels, leading to increases of G' , G'' , E_g and rupture parameters and decreases of compliance values. Such results confirmed that the SLPs incorporation was beneficial to the gels stability, especially for decreasing the microstructural alterations and reducing the water loss verified in NFG.

Keywords: Soy protein isolate; Cold-set gelation; Solid lipid particles; Emulsion filled gels; Stability

6.2 Introduction

Soy protein isolates (SPIs) are important ingredients obtained from the abundant byproducts of soybean oil industry, that have been receiving a great attention from researchers due to the growing necessity of the food industry in replacing animal-based ingredients by plant-based ones (Monteiro, Rebelo, Cruz e Silva & Lopes-da-Silva, 2013; Nicolai & Chassenieux, 2019). This necessity is mainly justified by the new dietary preferences of many consumers, that are concerned about animal welfare and issues related to the safety and sustainability of animal-based products (Monteiro et al., 2013; Tripathi, Mishra, Maurya, Singh & Wilson, 2019).

Such replacement, however, represents a big challenge for the industry, especially because the desirable textural properties of many food products are obtained from the gelation of whey protein isolates (WPIs) (Monteiro et al., 2013; Spotti, Tarhan, Schaffter, Corvalan & Campanella, 2016). According to the literature, gels formed by WPI present quite distinct properties than SPI gels, due to the different protein compositions and past processing history (Lee, Ryu, & Rhee, 2003; Monteiro et al., 2013; Monteiro & Lopes-da-Silva, 2017; Brito-Oliveira, Bispo, Moraes, Campanella & Pinho, 2017, 2018). During the commercial extraction processes soy proteins may experience different degrees of denaturation, impacting the solubility profile of the resulting SPIs (Lee et al., 2013). According to the literature, most of these ingredient present low solubilities at acid and neutral pHs, and, therefore, a limiting gelling capacity (Lee et al., 2003; Brito-Oliveira et al., 2017, 2018).

There are, however, different strategies that may be applied to alter and improve the properties of gels formed by such protein ingredients, including the incorporation of polysaccharides (Monteiro et al., 2013; Monteiro & Lopes-da-Silva, 2017; Brito-Oliveira et al., 2017, 2018; Brito-Oliveira, Cavini, Ferreira, Moraes & Pinho, 2020) and lipid fillers (Brito-Oliveira et al., 2017, 2018) to the systems.

The incorporation of polysaccharides has been appointed as an advantageous strategy to improve gelling properties of protein ingredients, especially by stabilizing the structures formed by the proteins (Monteiro & Lopes-da-Silva, 2017; Le, Rioux & Turgeon, 2017). Such fact was verified in a recent study of our research group, in which the ability of the SPI to form CaCl_2 -induced gels was analyzed (Chapter 4). The results revealed that, even though the SPI applied presented a relatively low solubility at neutral pH (37%) (Brito-Oliveira et al., 2018), self-supported gels could be formed using a protein concentration of 14%. Such concentration is much higher than the concentrations necessary for producing cold-set whey protein gels (5-10 %) (Cavallieri & Cunha, 2008; Kuhn, Cavallieri & Cunha., 2011; Spotti et al., 2016),

evidencing the limited gelling capacity of the SPI applied. For this reason, different galactomannans were added to the CaCl₂-induced gels and it was verified that the incorporation low concentrations of locust bean gum (0.1%) had a positive effect, strengthening the matrices (Chapter 4).

The strengthening of protein gels with the incorporation of polysaccharides is not always verified, because the properties of the mixed systems depend on many factors including biopolymer concentration, characteristics of the ingredients used and the environmental conditions (Le et al., 2017; Monteiro et al., 2017). In general, three distinct microstructural organizations are verified in mixed gels: (I) interpenetrating networks, (II) coupled gels and (III) phase-separated networks, being the last one the most common (Le et al., 2017).

Such organizations may also be affected by the addition of lipid fillers (e.g. emulsion or solid lipid particles) to the matrices, originating “emulsion filled gels” (EFG). The properties of such complex systems depend on the characteristics of the gelled matrix, lipid fillers and interactions between such components (Lorenzo, Zaritzky & Califano, 2013; Brito-Oliveira et al., 2017, 2018). Therefore, the adequate manipulation of formulation and production method may allow the development of systems with interesting properties and satisfactory stability.

Investigations regarding the stability of gelled systems are fundamental considering its highly transient and non-linear nature (Teece, Faers & Bartlett, 2011). Due to the thermodynamically metastable state of such systems, its structural organization tends to change over time, due to spontaneous processes (known as aging processes) and/or external forces (Renard, van de Velde & Visschers., 2006; Teece et al., 2011). Although structural rearrangements can be subtle, aging processes can also lead to the collapse of gels, and, for food formulations, the consequences of such processes may affect the shelf life and acceptability of the systems (Buscall et al. 2009; Teece et al. 2011; Bartlett, Teece, & Faers, 2012; Chang & Leong, 2014).

Considering that the quantitative prediction of stability of gelled systems is a critically important issue in the formulation and manufacture of commercial food products (Barlett et al., 2012), the objective of the present study was to evaluate the stability of the non-filled cold-set gels produced and characterized in our last study using SPI (14%), LBG (0.1%) and CaCl₂ (100 mM) (Chapter 4) and also to evaluate the effects of incorporating solid lipid particles stabilized with Tween 80 and Span 80 on the properties and stability of such gelled system.

6.3 Materials and methods

6.3.1 Chemicals and reagents

SPI (Protimarti M-90, 84.3% protein) was obtained from Marsul (Montenegro, RS, Brazil). Calcium chloride dihydrate was purchased from Kyma (Americana, SP, Brazil), and locust bean gum (Viscogum LBG®) was donated by Cargill (Campinas, SP, Brazil). For SLP production, palm stearin (PS) (melting point 50.1°C) was donated by Agropalma (Belém, PA, Brazil) and Tween 80 and Span 80 were obtained from Sigma-Aldrich (St. Louis, MO, USA). Ultrapure water (from a Millipore system Direct Q3®, Billerica, MA, USA) was used throughout the experiments.

6.3.2 Production of cold-set gels

6.3.2.1 Production of solid lipid particles (SLP)

SLP were produced according to Brito-Oliveira et al. (2017). For this purpose, the lipid phase, composed by palm stearin (4.5% w/w) and Span 80 (2.7%, w/w), was kept at 80°C for 30 min to eliminate the thermal memory. Subsequently, the aqueous phase, composed by Tween 80 (1.8 %, w/v) and deionized water, was dispersed in the lipid phase, at 80°C, using a rotor–stator device (IKA T25, IKA, Staufen, Germany) at 18.000 rpm for 5 min. Sodium benzoate (0.02%, w/w) was added to the samples to avoid microbiological contamination. The solid lipid particles dispersions (SLPD) were kept overnight at 10 °C before its application to produce EFGs.

6.3.2.2 Production of cold-set gels: non-filled gels and emulsion filled gels

Non-filled gels were produced according to Brito-Oliveira et al. (Chapter 4). For this purpose, SPI powder (14%, w/v) with LBG (0.1 %, w/v) was hydrated using deionized water at pH 7, and the systems were preheated in a water bath at 80 °C for 30 min. Subsequently, CaCl₂ (100 mM) was incorporated to the systems at room temperature. For EFGs production, the same protocol was applied, however, different proportions of deionized water used to hydrate the SPI/LBG were replaced by solid lipid particles dispersions (SLPD). The ratios of deionized water (DW) and SLPD tested were 25:75, 50:50, 75:25 and 0:100. The samples were stored at 10°C for 12 h before any characterization.

6.3.3 Characterization of EFG produced with different SLP concentrations.

EFG produced with different SLP: DW ratios were characterized in terms of their visual aspects, water holding capacities (WHCs), microstructural properties (scanning electron microscopy and confocal laser scanning microscopy) and uniaxial compression parameters.

6.3.4 Evaluation of gels stability

Gelled systems were characterized in terms of their visual aspects, WHCs, microstructural properties (scanning electron microscopy) and rheological parameters (uniaxial compression tests, small strain oscillatory tests and creep/recovery tests) in different days of storage in order to investigate the stability of the systems.

6.3.5 Confocal laser scanning optical microscopy

Confocal laser scanning microscopy (CLSM) (Confocal Upright Microscope LSM 780 NLO-Zeiss, Zeiss, Germany) was developed using simultaneous dual-channel imaging, according to Brito-Oliveira et al. (2018). For this purpose, three different solutions were prepared and incorporated to the gels: (I) rhodamine B solution (0.2 %, w/v, in deionized water - 10 μ L solution/mL of gel), (II) fluorescein isothiocyanate (FITC) solution (1 mg/mL dimethyl sulfoxide, DMSO - 0.05 mL solution/mL of gel) and (III) Nile Red solution (0.1 g/100 mL of methanol - 10 μ L solution/g of lipid). The protein phase was visualized by exciting rhodamine B at a wavelength of 543 nm and at an emission wavelength range of 551–655 nm, the polysaccharides were visualized by exciting the dye fluorescein isothiocyanate (FITC) at an excitation wavelength of 488 nm and an emission wavelength range of 493–543 nm and the SLP were visualized by exciting the Nile Red dye at 488 nm of excitation wavelength and an emission wavelength range of 500–580 nm.

6.3.6 Scanning electron microscopy

For scanning electron microscopy (SEM), the samples were prepared according to Picone, Takeuchi & Cunha (2011). Initially, the samples (1.0 \times 0.5 \times 0.5 cm) were fixed in 2.5 g/100 g glutaraldehyde in a cacodylate buffer (16 g/L) at pH 7.2 and stored at 7°C for 24 h. Afterwards, they were rinsed twice in a cacodylate sodium buffer (16 g/L, pH 7.2), fractured in liquid

nitrogen, subjected to post-fixation using osmium tetroxide 1 g/100 g in a cacodylate buffer (16 g/L, pH 7.2) for 120 min, and rinsed twice in deionized water. Subsequently, they were dehydrated in a graded ethanol series (30, 50, 70, and 90 mL/100 mL) for 20 min in each. Dehydration was continued in 100% ethanol (three changes in 1 h), and completed by critical point drying (CPD03 Balzers Critical Point Dryer, Alzenau, Germany). The samples were fractured, placed in aluminum stubs, coated with gold (200 s/40 mA) in a Balzers SCD 050 Sputter Coater (Alzenau, Germany), and analyzed using a TM 3000 tabletop microscope (Hitachi, Tokyo, Japan).

6.3.7 Water holding capacity

Water-holding capacities (WHCs) of the systems were determined according to Beuschel, Culbertson, Partridge & Smith (1992). For this purpose, the samples were weighed on Whatman paper No. 1, placed in Falcon tubes, and centrifuged at 2500 rpm for 10 min at 6°C (Hermle centrifuge Labortechnik GmbH, model Z-216 MK, Wehingen, Germany). Subsequently, the gels were removed from the filters and the papers weights were determined. WHCs calculated using Equation 6.1.

$$\text{WHC (\%)} = \left(1 - \left(\frac{m_f - m_i}{m_s} \right) \right) * 100 \quad (6.1)$$

where m_f is the weight of the wet filter (g), m_i is the initial weight of the dry filter (g), and m_s is the weight of the SPI sample (1–2 g). Each experiment was performed in triplicate.

6.3.8 Uniaxial compression tests

Uniaxial compression tests were performed in a texturometer (TA-XT.plus Texture Analyser, Godalming, Surrey, UK), using protocol adapted from Oliver, Scholten & van Aken (2015). The samples with cylindrical shape were compressed to 80% of their original height using an aluminum probe lubricated with silicone oil to minimize friction, with a deformation speed of 1 mm/s. The formulations were tested using five replicates. The values of Hencky stress (σ_H) and Hencky strain (ϵ_H) were obtained from the force-deformation data according to Equations (6.2) and (6.3), respectively:

$$\sigma_H = F(t) \cdot \frac{H(t)}{H_0 \cdot A_0} \quad (6.2)$$

$$\varepsilon_H = \ln \frac{H(t)}{H_0} \quad (6.3)$$

where $F(t)$ is the force at time t , A_0 is the initial area, H_0 is the initial height, and $H(t)$ is the height at time t . The rupture parameters were associated with the maximum value of the stress–strain curve. The values of the apparent Young’s modulus (E_g) of the systems were determined by the slope of the first linear interval in the Hencky stress (σ_H) versus Hencky strain (ε_H) curves, up to rupture.

6.3.9 Small strain oscillatory tests

Small strain oscillatory tests were performed according to a protocol adapted from Chang, Li, Wang, Bi & Adhikari (2014), in an AR2000 rheometer (TA Instruments, New Castle, DE, USA), using an aluminum parallel plate geometry (60 mm diameter, 1 mm gap), at 10°C. To avoid water evaporation, silicone oil was added at the edge of the samples and before the experiments, a 2 min resting period was respected. Strain sweep tests (data not shown) were developed in the range 0.01–100%, at a constant frequency of 1 Hz, for the determination of the linear viscoelastic regions (LVRs) of the samples. Frequency sweep tests were carried out over an angular frequency range of 0.016–1.6 Hz, using a strain amplitude of 2% (within the LVRs). The dependence of both viscoelastic moduli (G' and G'') on angular frequency was described by a power law model (Equations 6.4 and 6.5), using the nonlinear regression feature in Excel (Microsoft, Seattle, WA, USA) (Chang et al., 2014):

$$G' = K' \cdot \omega^{n'} \quad (6.4)$$

$$G'' = K'' \cdot \omega^{n''} \quad (6.5)$$

where K' and K'' are power law parameters, n' and n'' are frequency exponents, and ω is the angular frequency.

6.3.10 Creep/recovery tests

Creep/recovery tests were developed according to Brito-Oliveira et al. (2020) in an AR2000 rheometer (TA Instruments, New Castle, PN, EUA), using an aluminum parallel plate geometry (60 mm diameter, 2 mm gap), at 10°C. For this purpose, a resting time of 10 minutes was applied for the elimination of loading effects. Afterwards, a constant stress of 5 Pa was applied for 15 min (creep) and then removed for the evaluation of the recovery behavior of the

samples for more 15 min. Silicone oil was added on the edges of the samples in order to avoid water evaporation. Creep and recovery data were analyzed using the four-parameter Burger's model represented by Equation 6.6 (Chang et al., 2014).

$$J(t) = \begin{cases} J_0 + J_1 \left(1 - \exp \left(\frac{-t}{\lambda_{ret}} \right) \right) + \frac{t}{\eta_0}, & t \leq t_1 \\ J_1 \left(\exp \left(\frac{t_1-t}{\lambda_{ret}} \right) - \exp \left(\frac{-t}{\lambda_{ret}} \right) \right) + \frac{t_1}{\eta_0}, & t > t_1 \end{cases} \quad (6.6)$$

where J_0 is the instantaneous compliance in %/Pa, η_0 is the viscosity of the Maxwell dashpot in Pa.s/%, J_1 is the compliance associated with the Kelvin–Voigt element in %/Pa, λ_{ret} is the retardation time associated with the Kelvin–Voigt element in s, and t_1 is the time when the stress was removed.

The recovery rates were calculated using Equation 6.7, where ε_{max} is the maximum strain at the end of the creep test and ε_f is the final strain (Chang et al., 2014).

$$Recovery (\%) = \left(\frac{\varepsilon_{max} - \varepsilon_f}{\varepsilon_{max}} \right) * 100 \quad (6.7)$$

6.3.11 Statistical analyses

All measurements were performed at least in triplicate, and mean values and corresponding errors were calculated. For the statistical treatment of data, an analysis of variance (ANOVA) was conducted, followed by Tukey's tests with a 5% significance level using SAS software version 9.2 (SAS Institute Inc, Cary, NC).

6.4 Results and discussion

6.4.1 Stability of non-filled gels (NFG)

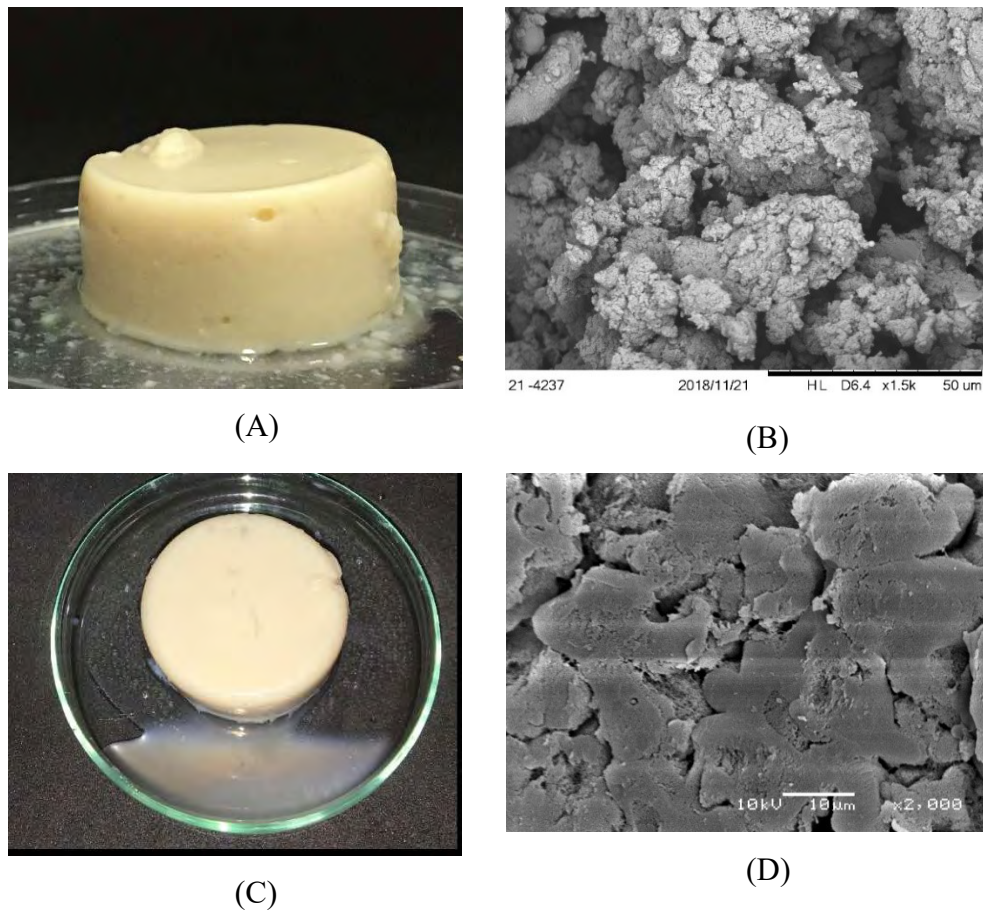
NFG were evaluated in different days of storage regarding its visual aspects and microstructural organizations. As expected, in the first day of storage, the systems presented the same properties verified in our previous study, in which CaCl₂-induced gels were produced using different protein, salt and galactomannans concentrations (Chapter 4). In such research, the formulation applied here (i.e. 14% SPI, 0.1% LBG and 100 mM CaCl₂) revealed to be the

most interesting in terms of strength (evaluated through frequency sweep tests, creep/recovery tests and uniaxial compression tests) and short-term stability (the systems were evaluated during 10 minutes at room temperature) (Chapter 4).

As verified in Figure 6.1(A), at the first day of storage the NFG were self-supported and opaque. According to the literature, evaluations of the visual aspect of gelled systems are important for giving information regarding the nature of protein aggregates, being a good indicator of the type of matrix formed (Bryant & McClements, 1998; Kuhn, Cavallieri, Cunha, 2010). Opaque gels, such as the NFG produced in the present study, are formed by aggregated particles resulted from a large and random aggregation process (Bryant & McClements, 1998; Kuhn et al., 2010). Such fact was confirmed in the SEM micrograph available in Figure 6.1(B), in which it is possible to see that NFG presented a very particulate, disorganized, and porous microstructure.

This organization is justified mainly by two factors: (I) the gelation method involving direct salt addition and (II) the type of salt applied. According to the literature, the direct salt addition may cause an excessively fast gelation process, leading to random aggregations and resulting in weaker systems, with less ordered microstructures, such as the one verified in Figure 6.1(B) (Vilela, Cavallieri & Cunha, 2011; Marangoni, Barbut, McGauley, Marcone & Narine, 2000). Regarding the type of salt used, it is known that divalent salts cause much faster and effective interactions among protein aggregates than monovalent salts, due to its higher capacity to screen electrical charges and to cross-link negatively charged carboxyl groups (Bryant & McClements, 1998; Chapter 4). Therefore, the application of CaCl_2 , especially in the concentration used in the present study, tend to form less organized microstructures than the application of monovalent salts, such as the NaCl (Brito-Oliveira et al. 2020; Chapter 4).

Figure 6.1. Scanning electron micrographs and visual aspects of non-filled gels at days 1 (A, B) and 10 (C, D) of storage.



By the analysis of the microstructural organizations of gels it is possible to understand other important properties of the systems, including its water holding capacities (WHCs). In general, matrices with particulate and porous microstructures tend to present low WHC, due to the lower capacities to retain water by capillary forces (Kuhn et al., 2011). In fact, at the first day of storage, NFG presented WHC of only 46.5%. More than only porosity and permeability, other factors may explain the low WHC of such systems, including the relatively low solubility of the SPI at pH 7 (Brito-Oliveira et al., 2018) and also the application of CaCl_2 as gelling agent (Kuhn et al., 2011). According to Kuhn et al, (2011) divalent cations tend to form bridges between biopolymers chains decreasing the hydrophilic groups available to interact with water, which is kept free between the pores of the network.

Even with this low WHC, the NFG could be adequately analyzed at day 01 through frequency sweep tests, creep/recovery tests and uniaxial compression tests in the previous study of our group (Chapter 4). After 10 days, however, the systems could not be adequately analyzed

using a rheometer, due to the excessive syneresis verified in Figure 6.1(C), which compromised the accommodation of the samples in the equipment and, thus, the reliability of the data obtained.

For this reason, the properties of NFG at the 10th day of storage were only analyzed regarding the visual aspect (Figure 6.1C) and microstructural organization (Figure 6.1D). The micrograph available in Figure 6.1D evidenced that the alterations resulting from the aging of the matrices led to a significant microstructural compaction. Such compaction led to the expulsion of the water initially trapped in the gelled network, but free between the pores, as previously cited, explaining the extensive syneresis shown in Figure 6.1C. This syneresis prevented the development of any characterizations in the subsequent days of storage.

According to Alting, Hamer, Kruif & Visschers (2003), open clusters of aggregates, such as the ones verified at the first day of storage (Figure 6.1B), are thermodynamically unstable and can be partly stabilized by the formation of additional bonds, which causes the compaction verified in Figure 6.1D.

The microstructural alterations of the NFG may also be seen as the result of a sequence of microcollapses and formation of more stable bonds within the matrix. These events caused the large expulsion of water but did not lead to the failure of the systems due to the effectiveness of the protein-protein interactions/ salt bridges formed by CaCl₂.

According to the literature, the most dramatic manifestation of aging of gels is the sudden network collapse (Chang & Leong, 2014; Renard et al., 2006; Teece et al., 2011; Barlett et al., 2012). In their study, Barlett et al. (2012) explained that the collapse of the gel network occurs as a result of spatially heterogeneous process of localized microcollapses which leads to a buildup of internal stress within the gel and its ultimate failure. According to the authors, a gel is a metastable phase with a high free-energy density whose consolidation is driven by a force for phase separation. When the network is formed, however, the dynamics of phase separation is slowed down. With the ageing, the network lowers its free energy via structural reorganizations which, according to Barlett et al (2012) proceed through the rupture of single particle bonds. The authors explained that the breakup of an energetic bond between particles, diffusion to dense region of the network, and a reformation of the broken bond allows a net increase in the number of nearest-neighboring particles with a concomitant lowering of the free energy of the system. Such process tends to make the network to coarsen, as verified in the present investigation.

Even though the tendency of the gelled systems is to suffer microstructural rearrangements to low its free energy, it is known that the velocity through which these

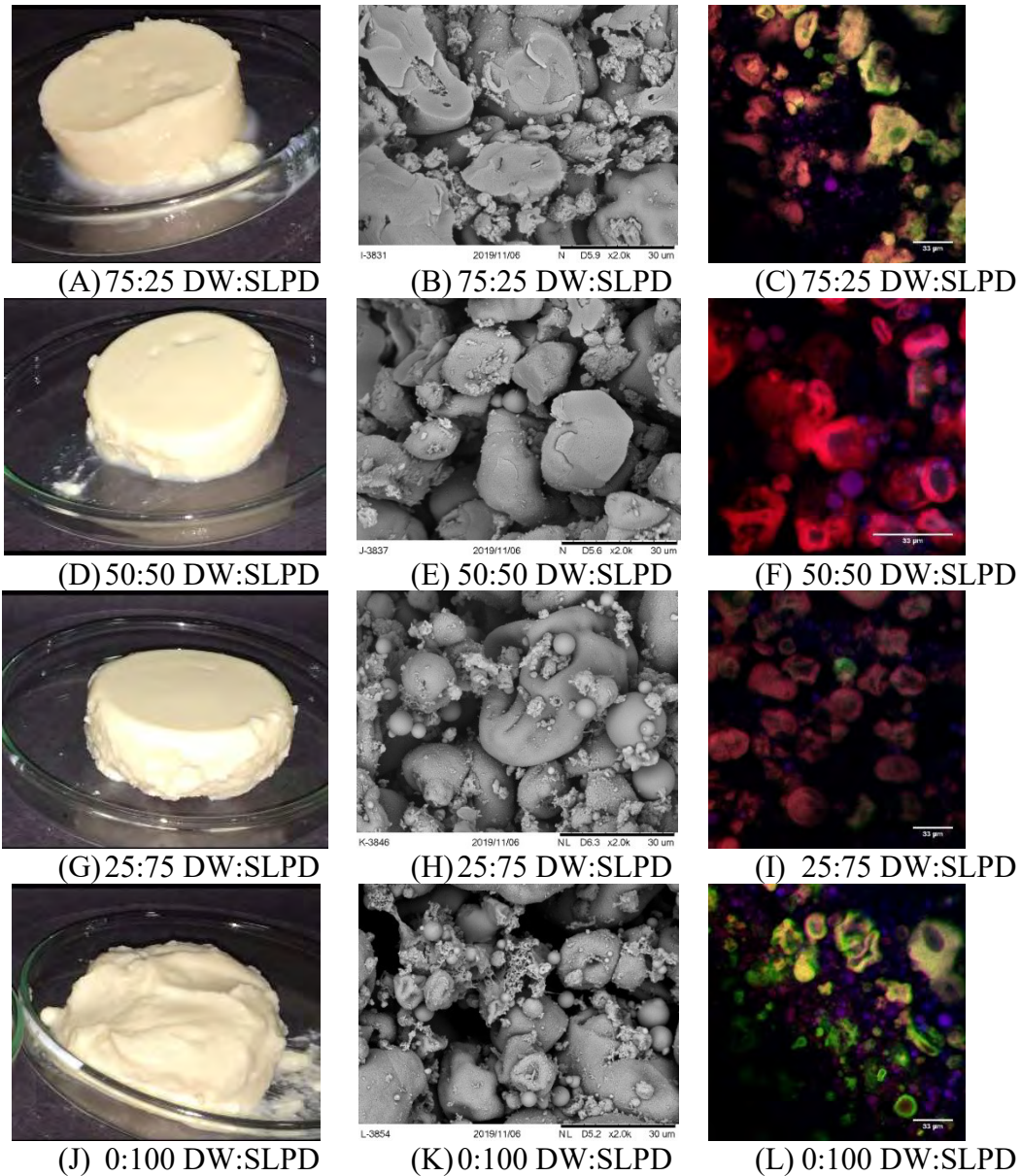
alterations will occur up to a point of compromising a food products acceptability can be altered by formulation changes. For this reason, SLP were incorporated to the NFG as a possible strategy to improve the stability of the systems, decreasing the undesirable changes, which led to the excessive water loss from the matrices.

6.4.2 Incorporation of different SLP concentrations to CaCl₂-induced gels

In order to understand the best conditions for producing self-supported (stronger) EFGs, different SLP concentrations were incorporated to the systems and characterized regarding their visual aspects and microstructural organizations, and the obtained results are shown in Figures 6.2 and 6.3. From the visual aspects, it was verified that the increase in SLP concentration decreased the strength of the systems. The weakening of the gels was especially evident in samples produced by the complete replacement of DW by SLPD, which presented aspect of non-self-supported gels (Figure 6.2I).

Whereas NFG presented microstructures formed by the small protein aggregates (Figure 6.1B), with a very particulate aspect, the EFG were formed by larger aggregates/structures which resembled capsules or microgels (Figure 6.2). Similar capsule-like structures were verified in the last study of our research group in micrographs of CaCl₂-induced gels of SPI, in the absence of LBG (Chapter 4). In such investigation, the formation of these capsules was explained by the different aggregation behavior of the distinct protein fractions of the SPI (i.e. β - conglycinin and the glycinin) during the preheating. According to the literature, when such fractions are heated together at pH 7 the hydrophilic groups brought by the β -conglycinin tend to occupy the surface of the complex aggregates formed by glycinin, leading to the initial formation of the “capsule-like” structures (Chapter 4; Guo et al., 2012).

Figure 6.2. Visual aspects and micrographs of CaCl_2 -induced gels produced with different deionized water (DW): solid lipid particle dispersion (SLPD) ratios. In scanning electron micrographs, the magnification of 2000 x was used, and the scale bar corresponds to 30 μm . In confocal laser scanning micrographs, the scale bar corresponds to 33 μm and the colors red, green and purple were used to identify the protein, polysaccharide, and lipid-rich phases of the systems, respectively.



As verified in Figure 6.1(B), the presence of LBG compromised the ability of the β -conglycinin to migrate and occupy the surface of the capsules, as consequence of the incomplete demixing caused by the excessively fast gelation process resulted from the direct CaCl_2

addition, largely discussed in our previous study (Chapter 4). The incomplete demixing, however, was minimized with the incorporation of SLP, as verified from the clear microphase separations in the micrographs presented in Figure 6.3.

It is known that the microstructural organizations of gels formed by protein ingredients and neutral polysaccharides, such as the LBG, result from the competition between gelation and the phase separation process (Jong & Van de Velde, 2007). Considering that the salt concentration and method of salt incorporation are the same for NFG and EFG, it is hardly possible that the SLP affected the gelation rate, however, it probably increased the rate of phase separation.

Such effect may be justified by the low chemical affinity between the protein ingredient and the surfactants applied (Tween 80 and Span 80), which probably increased the thermodynamical incompatibility within the gels and accelerated the phase separation process (Brito-Oliveira et al., 2017, 2018; Sala et al., 2007). According to the literature, phase separations tend to increase local biopolymer concentration in each phase, which favors a reduction of the excluded volume and a more extensive polymer self-association (Monteiro et al., 2013). In some studies, this extensive polymer self-association within each phase, led increases of gels' strength (Monteiro et al., 2013), however, this effect was not verified in the EFGs characterized here.

As shown in Table 6.1, the incorporation of SLP to the gels decreased the strength of the systems, as EFG presented lower E_g and rupture parameters than NFG. Such decreases were more pronounced in EFG with higher SLP content, which may be explained by the microstructural organizations of the systems.

Table 6.1. Uniaxial compression tests parameters and water holding capacities of non-filled gels and emulsion filled gels produced with different deionized water (DW):solid lipid particles dispersion (SLPD).

Formulation	E_g (Pa)	σ_H (Pa)	ϵ_H	WHC (%)
Non-filled gel	4063 ^a ± 82*	1519.0 ^a ± 199.2*	0.346 ^a ± 0.056*	51.1 ^b ± 1.0
75:25 DW:SLPD	3404 ^{ab} ± 298	1164.8 ^b ± 170.2	0.239 ^b ± 0.057	49.7 ^b ± 1.0
50:50 DW:SLPD	3161 ^b ± 420	1092.6 ^{bc} ± 72.7	0.240 ^b ± 0.010	65.0 ^a ± 4.6
25:75 DW:SLPD	1512 ^c ± 61	760.5 ^{cd} ± 107.7	0.259 ^{ab} ± 0.020	69.8 ^a ± 1.9
0:100 DW:SLPD	1125 ^c ± 71	650.2 ^d ± 28.2	0.223 ^b ± 0.008	64.1 ^a ± 1.7

Averages followed by different lowercase letters in the same column are statistically different

($p < 0.05$) for gels produced with different DW:SLPD ratios. *Chapter 4

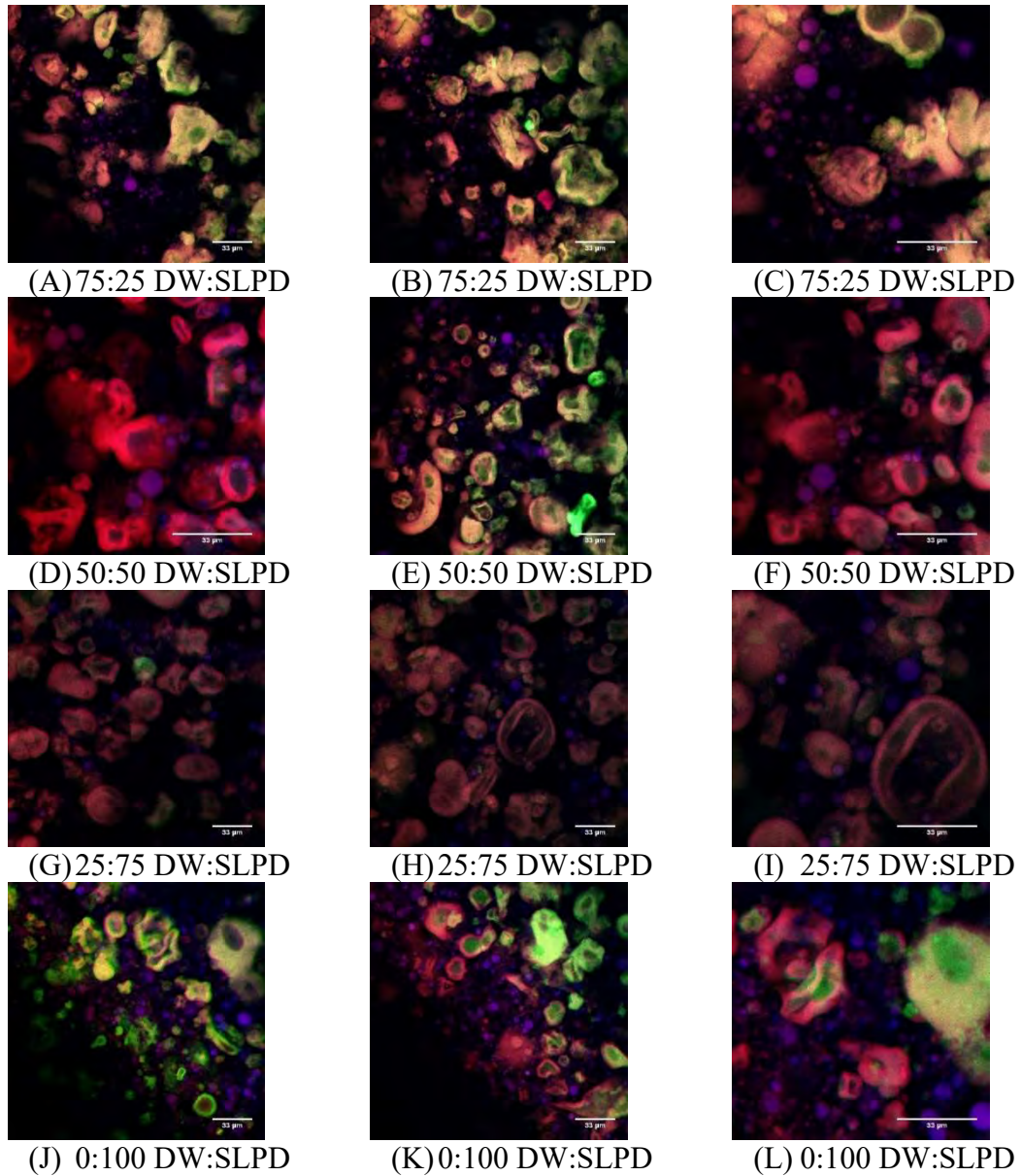
Due to the repulsive interactions between the SLP stabilized with Tween 80/Span 80 and the biopolymers, the molecules of protein and polysaccharide were confined in some regions of the samples before the gelation process. After the CaCl_2 -incorporation, there was an extensive polymer self-association concentrated in punctual regions of the systems (in which the biopolymers were concentrated), leading to the formation of the “capsules/microgel”-like structures. Even though the microphase separations were higher within the microgels, the presence of the SLP compromised the connections among these individual structures, causing the weakening of the matrices previously cited.

As verified in Figures 6.2 and 6.3, SLPs were located in the spaces among the microgels and affected the distance among these structures. It was verified that increases of DW replacement by SLPD increased the distance among the microgels, making the matrix more heterogeneous and discontinuous.

The presence of SLP in systems produced with at least 50% replacement of DW by SLPD, on the other hand, increased the WHC of the gels, as verified in Table 6.1. The increase of WHC is related to the microstructural organization of the EFGs composed by the microgels. According to Nicolai and Durand (2013), microgels are generally formed by a crosslinked network and contains a relatively large fraction of solvent inside. Considering that the systems produced by the replacement of 50%, 75% and 100% DW by SLPD presented statistically the same WHC, the increase of water retention was more related to the amount of liquid entrapped within the microgels than among in the spaces among them. If the higher amount of water were present among the microgels, the different spaces among these structures would have caused higher variations on WHC, due to distinct capillarity forces.

From the obtained results, the formulation produced with 50:50 DW:SLPD was selected as the best concentration for producing EFG for presenting the most adequate balance between WHC and gels' strength. For this reason, these EFG had their stability evaluated.

Figure 6.3. Confocal laser scanning micrographs of CaCl_2 -induced gels produced with different deionized water (DW): solid lipid particle dispersion (SLPD) ratios. In these micrographs, the scale bar corresponds to 33 μm and the colors red, green and purple were used to identify the protein, polysaccharide, and lipid-rich phases of the systems, respectively.

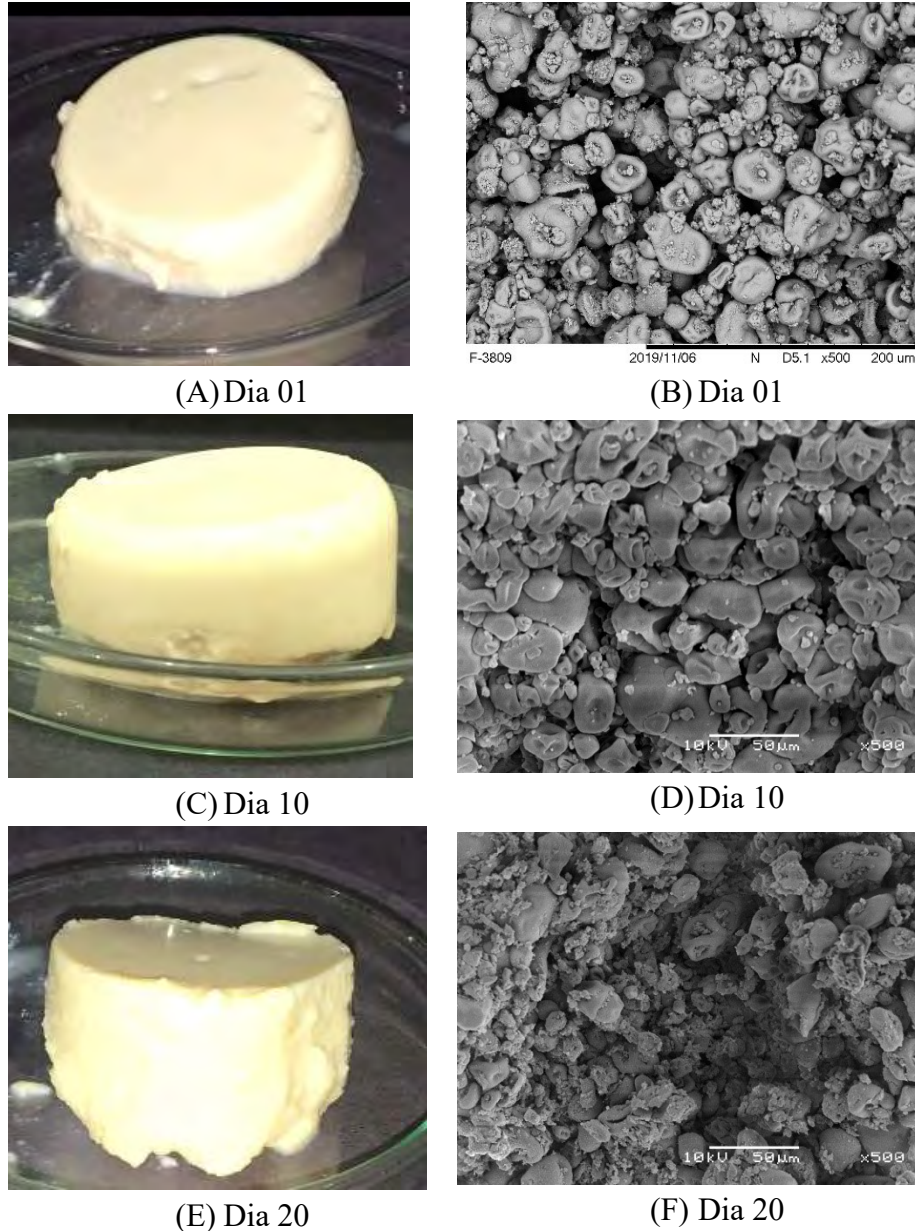


6.4.3 Stability of emulsion-filled gels (EFG)

EFGs were also evaluated in different days of storage regarding its visual aspects and microstructural organizations and the obtained results are shown in Figure 6.4. From the visual aspects, it was evident that the presence of SLP decreased the loss of water throughout the storage period in comparison to the NFG. The systems did not present syneresis during the 20

days analyzed. After this period, however, the EFG started to lose water and presented microbial growth (data not shown), which limited the analyzes in subsequent days of storage.

Figure 6.4. Visual aspects and scanning electron micrographs of emulsion filled gels at different days of storage.



As verified in the micrographs (Figure 6.4), the ageing process of EFG also led to a microstructural compaction of the systems, as the microgels were closer to each other after 10 days of storage. However, such compaction was much more subtle than that observed in NGF. The comparison of the micrographs of the systems between days 10 and 20 of storage showed only small alterations (if any).

Such results indicated that the free energy of the systems organized as microgels (EFG) was lower than that of particulate NFG. Considering that the microgels were very similar in all days of storage, only closer to each other, it is possible that the alterations have only led to the formation of new bonds between the microgels, not involving the breakup of existing bonds within the microgels. As previously cited, in gels with high free energy, such as the NFG, the ageing process may lead to breakup of an energetic bond between particles, diffusion to dense region of the network, and reformation of the broken bonds, causing higher alterations (Barlett et al., 2012).

The increase in the stability and subtlety of the microstructural changes was confirmed through the WHC values, which remained statistically the same throughout the 20 days analyzed, as verified in Table 6.2. Such fact reinforced the idea that the larger amount of liquid of the EFG was entrapped inside the microgels and not among them. So, the compaction of the systems, which brought the microgels closer to each other, did not cause higher expulsion of the water, as verified from the compaction of NFG.

Due to the higher WHC, the accommodation of the gels in the rheometer was possible in the different days of storage, so the systems were analyzed through frequency sweep tests and creep recovery tests at days 01, 10 and 20. The obtained results are shown in Figure 6.5 and Table 6.2.

Table 6.2. Parameters of Power Law model (frequency sweep data), Burger's model (creep/recovery data) and uniaxial compression data of emulsion filled gels (EFG) at different days of storage.

Analysis	Parameter	Day 01	Day 10	Day 20
Water holding capacity	WHC (%)	65.0 ^a ± 4.6	61.7 ^a ± 3.1	63.3 ^a ± 0.5
Frequency sweep tests	K' (Pa)	8103.47 ^c ± 318.38	10678.33 ^b ± 569.26	20113.33 ^a ± 562.79
	n'	0.1367 ^a ± 0.0023	0.1238 ^b ± 0.0018	0.1229 ^b ± 0.0038
	R ²	0.99	0.99	0.99
	K'' (Pa)	1698.67 ^c ± 50.20	2192.67 ^b ± 131.21	4060.33 ^a ± 92.74
	n''	0.0754 ^a ± 0.0042	0.0710 ^a ± 0.0074	0.0805 ^a ± 0.0035
	R ²	0.86	0.82	0.91
Creep/recovery tests	J ₀ (%/Pa)	0.0255 ^a ± 0.0022	0.0123 ^b ± 0.0003	0.0109 ^b ± 0.0017
	J ₁ (%/Pa)	0.0231 ^a ± 0.0013	0.0084 ^b ± 0.0009	0.0101 ^b ± 0.0021
	λ _{ret} (s)	99.06 ^{ab} ± 5.21	89.26 ^b ± 9.10	107.73 ^a ± 4.67
	η ₀ (Pa.s/%)	30914.5 ^b ± 4674.7	34352.4 ^b ± 2886.5	110475.2 ^a ± 29707.1
	R ²	0.91	0.93	0.89
	Recovery (%)	65.7 ^a ± 4.8	42.4 ^b ± 5.8	78.0 ^a ± 11.6
Uniaxial compression tests	E _g (Pa)	3161.7 ^b ± 419.8	7533.3 ^a ± 436.7	7857.7 ^a ± 537.30
	σ _H (Pa)	1092.6 ^b ± 72.7	2115.2 ^a ± 209.5	2348.7 ^a ± 240.8
	ε _H	0.2398 ^b ± 0.0097	0.2751 ^{ab} ± 0.0220	0.2956 ^a ± 0.0191

Averages followed by different lowercase letters in the same line are statistically different (p < 0.05) for EFG at different days of storage.

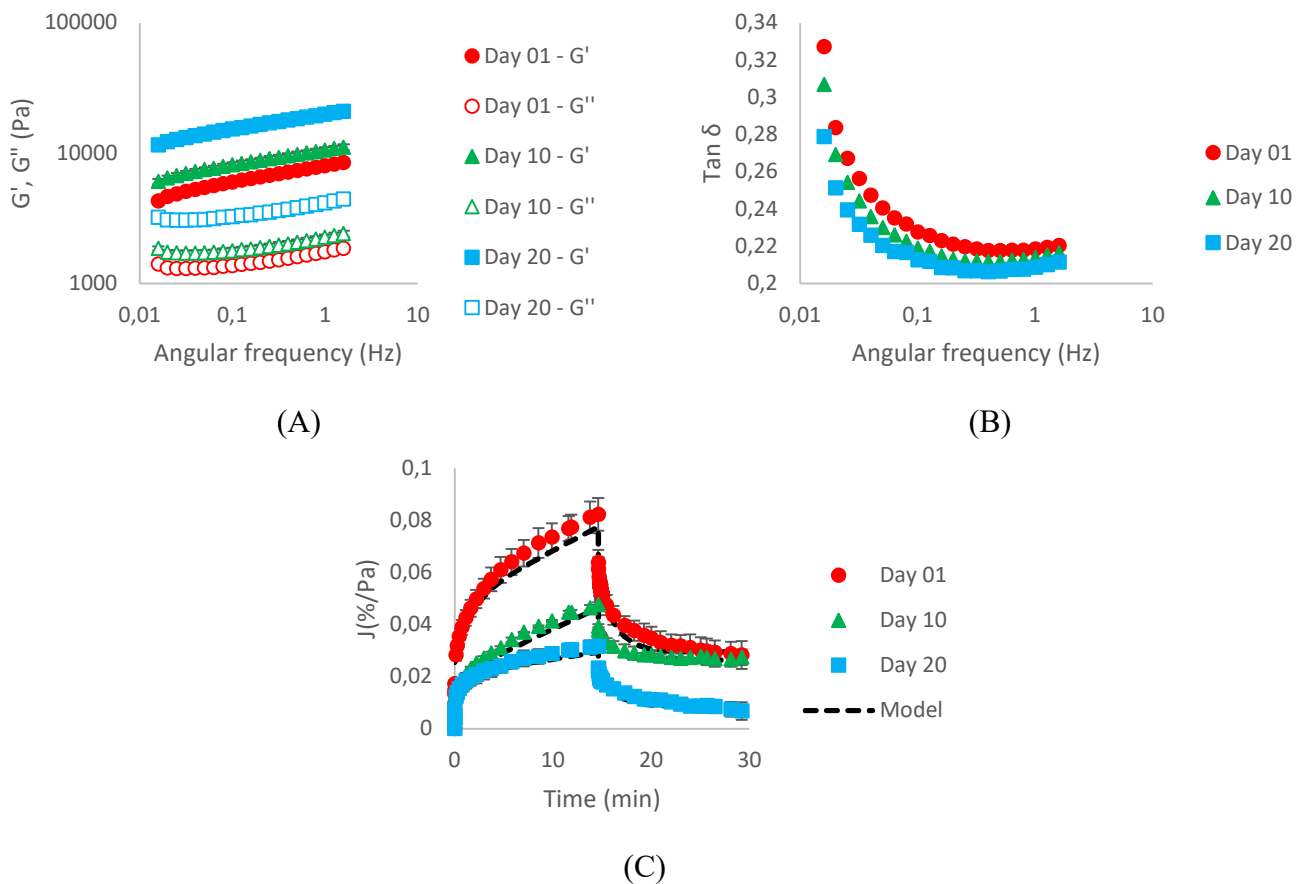
From frequency sweep tests it was verified a continuous increase of G', G'', and, consequently, K' and K'', and a decrease of n' during the 20 days. The strengthening of the gels indicated that, for EFG, the ageing process resulted in the formation of more stable bonds between protein groups which reduced the free energy of the system and increased the microstructural compaction. In addition, it was verified a continuous decrease in the values of tan δ, as verified in Figure 6.5(B), indicating an increase in the elastic responses of the EFG, possibly due to the more effective interactions of the biopolymers after the compaction of the microstructures.

The greater effectiveness of the new bonds and interactions resulted from the ageing process also led to decreases of compliance (Figure 6.5C), J₀ and J₁, and increases of η₀ (Table 6.2). Interestingly, on the 10th day of storage, the systems had the lowest values of λ_{ret} and recovery capacity. These results indicated that, although new connections and interactions were established (resulting in higher G' and G'' and lower compliance values), they were still fragile. At the 20th day, however, such interactions have become more stable, resulting in the further increases of λ_{ret} and recovery capacity.

The strengthening of the gels with the ageing process was also verified from the uniaxial compression parameters, which increased significantly after the 10th day of storage.

Such results confirmed that the incorporation of SLP was beneficial to the gels stability as it decreased the microstructural alterations, however, the rheological properties of the gels were very altered. The influences of these changes in the sensory perception of a future food originated from this EFG difficult to predict. However, these data allow us to affirm that the incorporation of SLP was an important step towards the reduction of water loss from NFG.

Figure 6.5. Results of frequency sweep tests (A, B) and creep/recovery tests (C) of emulsion filled gels (EFG) in different days of storage.



6.5 Conclusions

NFG presented a very particulate, disorganized, and porous microstructure. Such opened clusters of aggregates presented a high thermodynamical instability which caused the systems to change abruptly in less than 10 days. At the 10th day of storage, the NFG presented a great microstructural compaction due to the formation of additional bonds within the systems. Such

compaction led the systems to expulse a great amount of water from the matrix. Due to this large syneresis, the NFG could not be analyzed regarding its rheological properties. The incorporation of SLP, however, increased the WHC of the systems and altered its microstructural organizations to microgels-composed matrices. Such matrices were much more stable than the ones of NFG and did not present syneresis during the 20 days analyzed. During this period, the EFG presented a more subtle microstructural compaction, which led to increases of G' , G'' , E_g and rupture parameters and decreases of compliance values. These results confirmed that the incorporation of SLP was an interesting strategy to improve gels stability as it decreased the microstructural alterations and the water loss, even though the rheological properties of the gels have been changed during the 20 days analyzed.

Acknowledgments

This study was funded by Fundação de Amparo à Pesquisa do Estado de São Paulo (FAPESP) (grant number 2017/06224-9). We also thank the access to equipment and assistance provided by the Electron Microscope Laboratory (LME/UNICAMP).

Conflict of Interest: The authors declare that they have no conflict of interest.

6.6 References

- Alting, A.C., Hamer, R.J., Kruif, C.G. & Visschers, R.W. (2003). Cold-Set Globular Protein Gels: Interactions, Structure and Rheology as a Function of Protein Concentration. *Journal of Agricultural and Food Chemistry*, 51, 3150-3156
- Bartlett, P., Teece, L.J., & Faers, M.A. (2012) Sudden collapse of a colloidal gel. *Physical Review E*, 85 (2), 021404.
- Brito-Oliveira, T.C., Bispo, M., Moraes, I.C.F., Campanella, O.H, & Pinho, S.C. (2017). Stability of curcumin encapsulated in solid lipid microparticles incorporated in cold-set emulsion filled gels of soy protein isolate and xanthan gum. *Food Research International*, 102, 759–767.
- Beuschel, B. C., Culbertson, J.D., Partridge, P.A., & Smith, D. M. (1992). Gelation and emulsification properties of partially insolubilized whey protein concentrates. *Journal of Food Science*, 57, 605-609.
- Brito-Oliveira, T.C., Bispo, M., Moraes, I.C.F., Campanella, O.H., & Pinho, S.C. (2018). Cold-set gelation of commercial soy protein isolate: effects of the incorporation of locust bean gum and solid lipid microparticles on the properties of gels. *Food Biophysics*, 13, 226-239.

- Brito-Oliveira, Cavini, Ferreira, Moraes & Pinho (2020). Microstructural and rheological characterization of NaCl-induced gels of soy protein isolate and the effects of incorporating different galactomannans. *Food Structure*, 26, 100158.
- Brito-Oliveira, Cavini, Ferreira, Moraes & Pinho. Microstructural and rheological characterization of CaCl₂-induced gels of soy protein isolate and the effects of incorporating different galactomannans. *Chapter 4*.
- Bryant, C.M., & McClements, D.J. (1998). Molecular basis of protein functionality with special consideration of cold-set gels derived from heat denatured whey. *Trends in Food Science and Technology*, 9 (4), 143–151
- Buscall, R., Choudhury, T.H., Faers, M.A., Goodwin, J.W., Luckham, P.A., & Partridge, S.J. (2009). Towards rationalising collapse times for the delayed sedimentation of weakly-aggregated colloidal gels. *Soft Matter*, 5, 1345–1349.
- Cavallieri, A.L.F. & Cunha, R. L. (2008). The effects of acidification rate, pH and ageing time on the acidic cold set gelation of whey proteins. *Food Hydrocolloids*, 22(3), 439–448.
- Chang, W., & Leong, Y. (2014). Ageing and collapse of bentonite gels—effects of Li, Na, K and Cs ions. *Rheologica Acta*, 53, 109–122
- Chang, Y., Li, D., Wang, L., Bi, C., & Adhikari, B. (2014). Effect of gums on the rheological characteristics and microstructure of acid-induced SPI-gum mixed gels. *Carbohydrate Polymers*, 108, 183–191.
- Guo, J., Yang, X., He, X., Wu, N., Wang, J., Gu, W. & Zhang, Y. (2012). Limited Aggregation Behavior of β -Conglycinin and Its Terminating Effect on Glycinin Aggregation during Heating at pH 7.0. *Journal of Agricultural and Food Chemistry*, 60, 3782–3791.
- Jong, S., & van de Velde, F. (2007). Charge density of polysaccharide controls microstructure and large deformation properties of mixed gels. *Food Hydrocolloids*, 21, 1172–1187
- Kuhn, K. R., Cavallieri, A.L.F. & Cunha, R.L. (2010) Cold-set whey protein gels induced by calcium or sodium salt addition. *International Journal of Food Science Technology*, 45, 348–357.
- Kuhn, K. R., Cavallieri, A.L.F., & Cunha, R.L. (2011). Cold-set whey protein-flaxseed gum gels induced by mono or divalent salt addition. *Food Hydrocolloids*, 25, 1302-1310.
- Le, X.T., Rioux, L. & Turgeon, S.L. (2017). Formation and functional properties of protein–polysaccharide electrostatic hydrogels in comparison to protein or polysaccharide hydrogels. *Advances in Colloid and Interface Science*, 239, 127–135.
- Lee, K.H., Ryu, H.S. & Rhee, K.C. (2003). Protein Solubility Characteristics of Commercial Soy Protein Products. *JAOCs*, 80(1), 85 – 90.

- Lorenzo, G., Zaritzky, N., & Califano, A. (2013). Rheological analysis of emulsion-filled gels based on high acyl gellan gum. *Food Hydrocolloids*, 30, 672-680.
- Marangoni, A.G., Barbut, S., McGauley, S.E., Marcone, M. & Narine, S.S. (2000). On the structure of particulate gels – the case of salt-induced cold gelation of heat-denatured whey protein isolate. *Food Hydrocolloids*, 14, 61–74.
- Monteiro, S.R., Rebelo, S., Silva, O.A.B.C., & Lopes-da-Silva, J.A. (2013). The influence of galactomannans with different amount of galactose side chains on the gelation of soy proteins at neutral pH. *Food Hydrocolloids*, 33, 349-360.
- Monteiro, S.R. & Lopes-da-Silva, J.A. (2017). Effect of the molecular weight of a neutral polysaccharide on soy protein gelation. *Food Research International*, 102, 14–24.
- Nicolai, T. & Chassenieux, C. (2019). Heat-induced gelation of plant globulins. *Current Opinion in Food Science*, 27, 18–22
- Nicolai, T. & Durand, D. (2013). Controlled food protein aggregation for new functionality. *Current Opinion in Colloid Interface Science*, 18, 249–256.
- Oliver, L., Scholten, E., & van Aken, G.A. (2015). Effect of fat hardness on large deformation rheology of emulsion-filled gels. *Food Hydrocolloids*, 43, 299-310.
- Picone, C. S. F., Takeuchi, K. P. & Cunha, R. L. (2011). Heat-induced whey protein gels: Effects of pH and the addition of sodium caseinate. *Food Biophysics*, 6, 77–83.
- Renard, D., van de Velde, F., & Visschers, R.W. (2006). The gap between food gel structure, texture and perception. *Food Hydrocolloids*, 20(4), 423–431.
- Sala, G., van Aken, G.A., Stuart, M.A.C., & van de Velde, F. (2007). Effect of droplet–matrix interactions on large deformation properties of emulsion-filled gels. *Journal of Texture Studies*, 38, 511–535.
- Spotti, M.J., Tarhan, O., Schaffter, S., Corvalan, C., & Campanella, O.H. (2016) Whey protein gelation induced by enzymatic hydrolysis and heat treatment: Comparison of creep and recovery behavior. *Food Hydrocolloids*, 63, 696–704.
- Teece, L.J., Faers, M.A., & Bartlett, P. (2011) Ageing and collapse in gels with long-range attractions. *Soft Matter*, 7, 1341–1351.
- Tripathi, A.D., Mishra, R., Maurya, K.K., Singh, R.B., & Wilson, D.W. - Estimates for world population and global food availability for global health in Singh, R.B., Watson, R.R., & Takahashi, T. (Eds.), *The role of functional food security in global health*, Academic Press (2019)

Vilela, J.A.P., Cavallieri, A.L.F., & Cunha, R.L. (2011). The influence of gelation rate on the physical properties/structure of salt-induced gels of soy protein isolate-gellan gum. *Food Hydrocolloids*, 25(7), 1710-1718

**CHAPTER 7 : COLD-SET NACL-INDUCED GELS OF SOY PROTEIN ISOLATE
AND LOCUST BEAN GUM: HOW THE AGEING PROCESS AFFECT THEIR
MICROSTRUCTURE AND THE STABILITY OF INCORPORATED BETA-
CAROTENE**

Cold-set NaCl-induced gels of soy protein isolate and locust bean gum: how the ageing process affect their microstructure and the stability of incorporated beta-carotene

Thais C. Brito-Oliveira, Camila P.S. Cazado, Ana Clara M. Cavini,
Lorena M.F. Santos, Izabel C.F. Moraes and Samantha C. Pinho^{1*}

Department of Food Engineering, School of Animal Science and Food Engineering,
University of São Paulo (USP), Pirassununga, SP, Brazil

* Corresponding author: S.C. Pinho, Department of Food Engineering, School of Animal Science and Food Engineering (FZEA), University of São Paulo (USP), Av. Duque de Caxias Norte 225, Jd. Elite, Pirassununga, SP, Brazil 13635-900. Tel: +55-19-35654288; fax: +55-19-3565-4284.

E-mail address: samantha@usp.br

7.1 Abstract

This study aimed to evaluate the effects of solid lipid particles (SLP) incorporation on the ageing process of NaCl-induced gels of soy protein isolate and locust bean gum. The feasibility of incorporating beta-carotene (BC) in the emulsion-filled gels (EFGs) was evaluated and the stability of the carotenoid in two systems, SLP and NaCl-induced EFG, was determined. Non-filled gels (NFG) and EFG were characterized regarding their microstructural organization, rheological properties and water holding capacities (WHCs) along the storage. Also, the amount of BC present in SLP and EFG was quantified for 30 days. SLP dispersions were stable and preserved about 57% of the encapsulated bioactive after 30 days. As they presented good stability, they were suitable to be incorporated in the gels and produce EFG. Their incorporation increased the gelled systems' stability. Whereas the ageing of NFG decreased the strength and WHC of the systems, EFG were strengthened had higher values of WHC. In comparison to SLP, EFG presented a higher capacity to protect the encapsulated beta-carotene (about 90% of retention after 30 days of storage), indicating the gelation of the continuous phase was a good strategy to avoid the degradation of the encapsulated bioactive.

Keywords: Soy protein isolate; Solid lipid particles; Emulsion filled gels; Stability; beta-carotene.

7.2 Introduction

New formulations of protein gels have been developed due to various requirements of food industry, as fat replacement, and improvement of nutritional and functional sensory properties of foods (Chen et al., 2019; Guo et al., 2018; Niu, Xia, Wang, Kong, & Liu, 2018). In the last years, the interest about the investigation of gelling capacities of plant proteins, including soy protein isolates (SPIs), has significantly increased (Brito-Oliveira et al., 2020; Ingrassia et al., 2019; Monteiro et al., 2017; Zhao et al., 2020). Such growing interest in these proteins is mainly due to, new consumers' concerns, as environmental issues related to food production, which are more serious for ingredients obtained from animal sources. Due to this type of concern, as well as health issues, a significant number of consumers have been reevaluating their diets and giving preference to plant-based ingredients, including proteins (Loveday, 2019; Monteiro et al., 2013; Monteiro et al., 2017).

Even though efforts have been made for the development of new formulations of plant-based protein gels, most of the investigations are focused on the comprehension of the gelation process and characterization of the systems right after its production. It is known, however, that gels present highly transient characteristics, as they are at a thermodynamically metastable state. Therefore, their structural organization tends to change over time, due to spontaneous/aging processes and/or external forces (Renard et al., 2006; Teece et al., 2011).

Considering that the stability of food products is very important for its acceptability and for the determination of its shelf-life, understand how the properties of protein gels change over time is required for the development of new gelled foods. This is especially true when these gels are supposed to deliver bioactive compounds.

In a recent study of our research group (Brito-Oliveira et al., 2017a), for example, curcumin was encapsulated in solid lipid particles (SLP) incorporated to emulsion-filled gels (EFGs) and the results revealed that the encapsulated bioactive exhibited high stability for 15 days. However, color alterations were observed after this period, probably due to the structural rearrangement of the gelled systems, which led to the collapse of the structures after 30 days (Brito-Oliveira et al., 2017a).

Even though many food products classified as EFGs are already produced and commercialized by the food industry (eg yoghurts, cheeses, processed meats), the development of new formulations are of great interest, as such combination of lipids and gelling agents may enable reductions in the lipid content of products, without compromising its sensory quality (Dickinson, 2012; Farjami & Madadlou, 2019; Liu et al., 2015; Lu et al., 2019; Lu et al., 2020;

Mao et al., 2018; Oliver, Scholten & Van Aken, 2015; Sala et al., 2009a, b).

In addition to their textural and structural importance, EFGs may improve the oxidative stability of encapsulated systems. According to Sato et al. (2014), the increase of viscosity of the continuous phase of emulsions may retard the oxygen diffusion within the protein network and, consequently, increase its oxidative stability. In fact, different studies found in the literature have shown the emulsion gels are suitable carriers for lipid-soluble food bioactives, such as beta-carotene, especially because strong gels may be able to provide effective protection against deterioration (McClements, 2010; Lu et al., 2019; Lu et al., 2020; Torres, Murray, & Sarkar, 2016).

Even though beta-carotene is a very important and extensively used lipophilic bioactive, its incorporation for the production of functional foods is still challenging, due to its poor stability and high lipophilicity, which often require the application of encapsulation techniques (Mahalakshmi et al., 2020).

In this context, this study aimed to evaluate the effects of solid lipid particles (SLP) incorporation on the stability of NaCl-induced gels, in order to understand how these structures alter the effects of the gelled systems' ageing. Besides, the feasibility of incorporating beta-carotene in such EFGs was analyzed, by comparing the stability of the bioactive in two different systems: SLP dispersions and NaCl-induced EFG.

7.3 Materials and methods

7.3.1 Chemicals and reagents

For the production of SLP, palm stearin (PS) was donated by Agropalma (Belém, PA, Brazil), and Tween 80, Span 80 and beta-carotene were obtained from Sigma-Aldrich (St. Louis, MO, USA). For the production of the gels, the SPI (Protimarti M-90, 84.3% protein) was obtained from Marsul (Montenegro, RS, Brazil), LBG (Viscogum LBG ®) was donated by Cargill (Campinas, SP, Brazil) and sodium chloride was purchased from Synth (Diadema, SP, Brazil). Ultrapure water (Millipore system Direct Q3®, Billerica, MA, USA) was used throughout the experiments.

7.3.2 Production of solid lipid particles

The solid lipid particles were produced according to protocol adapted from Brito-Oliveira et al. (2017a, 2017b). The lipid phase, composed by palm stearin (4.5% w/w) and Span 80 (2.7%, w/w), was kept at 80°C for 30 min to eliminate the thermal memory. Afterwards, beta-carotene (0.023%, w/w) was added to the lipid phase. Subsequently, the aqueous phase, composed by Tween 80 (1.8 %, w/v) and deionized water, was dispersed in the lipid phase, at 80° C, using a rotor–stator device (T25, IKA, Staufen, Germany) at 18.000 rpm for 5 min. Sodium benzoate (0.02%, w/w) was added to the samples to avoid microbiological contamination. The SLP were kept overnight at 10 °C before its application to produce the emulsion filled gels (EFG). The SLP were characterized in terms of average particle size using a ZetaPlus analyzer (Brookhaven Instruments Company, Holtsville, NY, USA)

7.3.3 Production of cold-set non-filled gels (NFG) and emulsion-filled gels (EFG)

Non-filled gels were produced according to Brito-Oliveira et al. (2020). SPI powder (14%, w/v) and LBG (0.1 %, w/v) were hydrated in deionized water, at pH 7, and the resulting mixture was preheated in a water bath at 80 °C for 30 min. Afterwards, NaCl (300 mM) was incorporated to the systems at room temperature. For EFGs production, the same protocol was applied, however, the deionized water used to hydrate the SPI/LBG was replaced by SLP. The samples were stored at 10°C before further characterization.

7.3.4 Water holding capacity

Water-holding capacity (WHC) of the gels was determined according to Beuschel, Culbertson, Partridge & Smith (1992). The samples were initially weighed on Whatman paper No. 1, placed in Falcon tubes, and centrifuged at 2500 rpm for 10 min at 6° C (Z-216 MK, Hermle Labortechnik GmbH, Wehingen, Germany). Afterwards, the gels were removed from the filters and the papers weights were determined. WHCs calculated using Equation 7.1.

$$WHC(\%) = \left(1 - \frac{mf-m}{ms}\right) * 100 \quad (7.1)$$

where mf is the weight of the wet filter (g), mi is the initial weight of the dry filter (g), and ms is the weight of the SPI sample (1–2 g). Each experiment was performed in triplicate.

7.3.5 Scanning electron microscopy

For scanning electron microscopy (SEM), the samples were prepared according to Picone, Takeuchi & Cunha (2011). The samples (1.0 × 0.5 × 0.5 cm) were, initially, fixed in 2.5 g/100 g glutaraldehyde in a cacodylate buffer (16 g/L) at pH 7.2 and stored at 7°C for 24 h. Subsequently, they were rinsed twice in a cacodylate sodium buffer (16 g/L, pH 7.2), fractured in liquid nitrogen, subjected to post-fixation using osmium tetroxide 1 g/100 g in a cacodylate buffer (16 g/L, pH 7.2) for 120 min, and rinsed twice in deionized water. Afterwards, they were dehydrated in a graded ethanol series (30, 50, 70, and 90 mL/100 mL) for 20 min in each. Dehydration was continued in 100% ethanol (three changes in 1 h) and completed by critical point drying (CPD03 Balzers Critical Point Dryer, Alzenau, Germany). The obtained samples were fractured, placed in aluminum stubs, coated with gold (200 s/40 mA) in a Balzers SCD 050 Sputter Coater (Alzenau, Germany), and analyzed using a TM 3000 tabletop microscope (Hitachi, Tokyo, Japan).

7.3.6 Uniaxial compression tests

Uniaxial compression tests were performed in a texturometer (TA-XT.plus Texture Analyser, Godalming, Surrey, UK), according to protocol adapted from Oliver, Scholten & van Aken (2015). For this purpose, the samples with cylindrical shape were compressed to 80% of their original height using an aluminum probe lubricated with silicone oil to minimize friction, with a deformation speed of 1 mm/s. The formulations were tested using five replicates. The values of Hencky stress (σ_H) and Hencky strain (ε_H) were obtained from the force-deformation data according to Equations (7.2) and (7.3), respectively:

$$\sigma_H = F(t) \cdot \frac{H(t)}{H_0 \cdot A_0} \quad (7.2)$$

$$\varepsilon_H = \ln \frac{H(t)}{H_0} \quad (7.3)$$

where $F(t)$ is the force at time t , A_0 is the initial area, H_0 is the initial height, and $H(t)$ is the height at time t . The rupture parameters were associated with the maximum value of the stress-strain curve. The values of the apparent Young's modulus (E_g) of the systems were determined by the slope of the first linear interval in the Hencky stress (σ_H) versus Hencky strain (ε_H) curves, up to rupture.

7.3.7 Small strain oscillatory tests

Small strain oscillatory tests were performed according to a protocol adapted from Chang, Li, Wang, Bi & Adhikari (2014), in an AR2000 rheometer (TA Instruments, New Castle, DE, USA), using an aluminum parallel plate geometry (60 mm diameter, 1 mm gap), at 10°C. To avoid water evaporation, silicone oil was added at the edge of the samples and before the experiments, a 2 min resting period was respected. Strain sweep tests (data not shown) were developed in the range 0.01–100%, at a constant frequency of 1 Hz, for the determination of the linear viscoelastic regions (LVRs) of the samples. Frequency sweep tests were carried out over an angular frequency range of 0.016–1.6 Hz, using a strain amplitude of 2% (within the LVRs).

7.3.8 Creep/recovery tests

Creep/recovery tests were developed according to Brito-Oliveira et al. (2020) in an AR2000 rheometer (TA Instruments, New Castle, PN, EUA), using an aluminum parallel plate geometry (60 mm diameter, 2 mm gap), at 10°C. For this purpose, a resting time of 10 minutes was applied for the elimination of loading effects. Afterwards, a constant stress of 5 Pa was applied for 15 min (creep) and then removed for the evaluation of the recovery behavior of the samples for more 15 min. Silicone oil was added on the edges of the samples in order to avoid water evaporation. Creep and recovery data were analyzed using the four-parameter Burger's model represented by Equation 7.4 (Chang et al., 2014).

$$J(t) = \begin{cases} J_0 + J_1 \left(1 - \exp \left(\frac{-t}{\lambda_{ret}} \right) \right) + \frac{t}{\eta_0}, & t \leq t_1 \\ J_1 \left(\exp \left(\frac{t_1-t}{\lambda_{ret}} \right) - \exp \left(\frac{-t}{\lambda_{ret}} \right) \right) + \frac{t_1}{\eta_0}, & t > t_1 \end{cases} \quad (7.4)$$

where J_0 is the instantaneous compliance in %/Pa, η_0 is the viscosity of the Maxwell dashpot in Pa.s/%, J_1 is the compliance associated with the Kelvin–Voigt element in %/Pa, λ_{ret} is the retardation time associated with the Kelvin–Voigt element in s, and t_1 is the time when the stress was removed.

The recovery rates were calculated using Equation 7.5, where ε_{max} is the maximum strain at the end of the creep test and ε_f is the final strain (Chang et al., 2014).

$$Recovery (\%) = \left(\frac{\varepsilon_{max} - \varepsilon_f}{\varepsilon_{max}} \right) * 100 \quad (7.5)$$

7.3.9 Quantification of beta-carotene in solid lipid particles

beta-carotene quantification was performed according to protocol described by Brito-Oliveira et al. (2017b). Initially, the SLP were diluted 50 times in ultra-pure water. Afterwards, 1.5 mL of ethanol and 1 mL of methanol with potassium hydroxide were added to 2 mL of the prepared dilutions. The mixtures were then stirred for 10 s and heated to 45 °C for 30 min. After this process, 2 mL of hexane containing butylated hydroxytoluene was added to the heated mixtures, which were then stirred for 30 s. This extraction with hexane was repeated 3 times. The organic phase was obtained and removed after 10 min. Anhydrous sodium sulfate was added to the obtained samples to absorb any residual water. The absorbance of hexane phase was measured at 450 nm (Genesys 10S UV-Vis, Thermo Scientific, Waltham, Massachusetts, USA) and the BC was quantified using a calibration curve of pure BC in hexane.

7.3.10 Quantifications of beta-carotene in EFG

For the quantification of beta-carotene in the EFG, initially 0.25 g gel were mixed with 4 mL of ethanol and 4 mL of methanol with potassium hydroxide. The mixture were subsequently stirred using a rotor–stator device (T25, IKA, Staufen, Germany) at 15,000 rpm for 1 min, and then heated to 45 °C for 30 min. Afterwards, 3 mL of hexane containing butylated hydroxytoluene were added to the mixture, which were stirred for 30 s. This extraction with hexane was repeated twice. The samples were, then, centrifuged at 7,100g for 10 min at 10° C (Z-216 MK, Hermle Labortechnik GmbH Wehingen, Germany). The organic phase was removed, diluted 10 times in hexane, the absorbance was measured at 450 nm (Genesys 10S UV-Vis, Thermo Scientific, Waltham, Massachusetts, USA) and the BC was quantified using a calibration curve of pure BC in hexane.

7.3.11 Evaluation of gels stability

Gelled systems were characterized in terms of their visual aspects, WHCs, microstructural properties (scanning electron microscopy) and rheological parameters (uniaxial compression tests, small strain oscillatory tests and creep/recovery tests) in different days of storage in order to investigate the stability of the systems.

7.3.12 Statistical analyses

All measurements were performed at least in triplicate, and mean values and corresponding errors were calculated. For the statistical treatment of data, an analysis of variance (ANOVA) was conducted, followed by Tukey's tests with a 5% significance level using SAS software version 9.2 (SAS Institute Inc, Cary, NC).

7.4 Results and Discussion

7.4.1 Production of solid lipid particles encapsulating beta-carotene and incorporation in emulsion-filled gels EFG

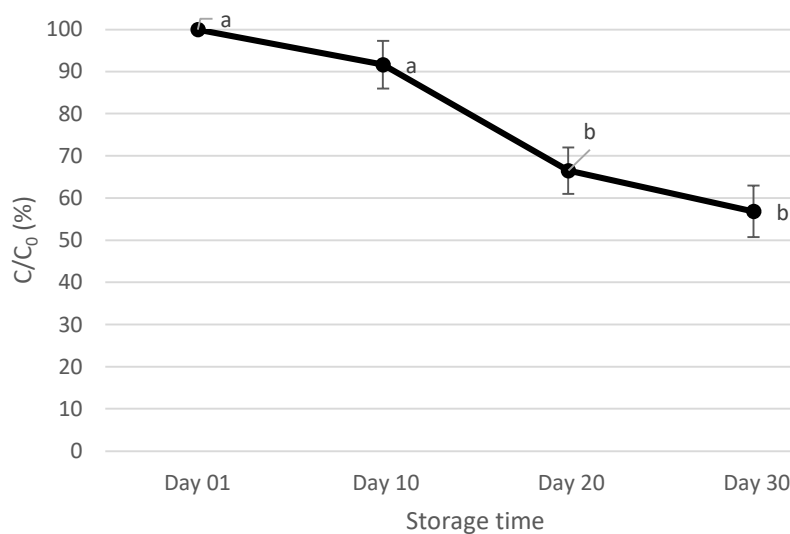
After the production, the SLP encapsulating beta-carotene (shown in Figure 7.1A) were characterized regarding its average particle size along the storage period. The results are presented in Table 7.1 and indicated a relative stability of the SLP during the 30 days of storage.

Such good stability is fundamental for the protection of the encapsulated bioactive. As shown in Figure 7.1B, the retention ratio of beta-carotene was constant for the first 10 days of storage. After that, beta-carotene started to degrade, with a decrease of retention from 91.6%, on day 10, to 66.5%, on day 20. At the end of 30 days, 56.8% of the beta-carotene initially present in the systems were retained in the SLP.

Figure 7.1. Visual aspects of SLP dispersions containing β -carotene after production (A) and retention ratios of β -carotene in SLP dispersions at different days of storage.



(A)



(B)

Even though some degradation was verified, the ability of the particles to protect more than 50% of the encapsulated bioactive for 30 days can be considered as noticeable, considering the high sensitivity of the beta-carotene to light, temperature and the presence of oxygen (Mahalakshmi et al., 2020). In a previous study of our research group, for example, SLP of palm stearin stabilized with hydrolyzed soy protein isolate (HSPI) was used to encapsulate beta-carotene, and the systems presented a lower retention capacity than the SLPs produced here (Brito-Oliveira et al., 2017b). The results showed that the HSPI-stabilized SLP protected only about 35% of the bioactive after 30 days of storage (Brito-Oliveira et al., 2017b). Similar retentions were verified by Liu et al. (2018), who encapsulated beta-carotene in two systems: biopolymer microparticles formed by electrostatic complexation and in caseinate emulsions. The authors verified that around 32% carotenoid was retained after 42 days storage in the microparticles, whereas <10% was retained in the emulsions (Liu et al., 2018).

In addition to affecting the capacity of the SLP to protect the encapsulated beta-carotene, the high stability of the systems, as can be seen in Table 7.1, was important for their incorporation in the emulsion-filled gels. This is due to the fact that, according to the literature, EFG may only be produced from a stable emulsion/SLP dispersion, through the gelation of the continuous phase, or by aggregation of the emulsion droplets (Dickinson, 2012; Farjami & Madadlou, 2019; Lu et al., 2019; Lu et al., 2020).

Table 7.1 Average particle sizes of solid lipid particles along the storage

Day of storage	Average particle size (nm)
01	309.5 ^a ± 22.80
10	362.2 ^a ± 55.2
20	375.0 ^a ± 53.6
30	348.2 ^a ± 48.9

Averages followed by different lowercase letters in the same column are statistically different ($p < 0.05$).

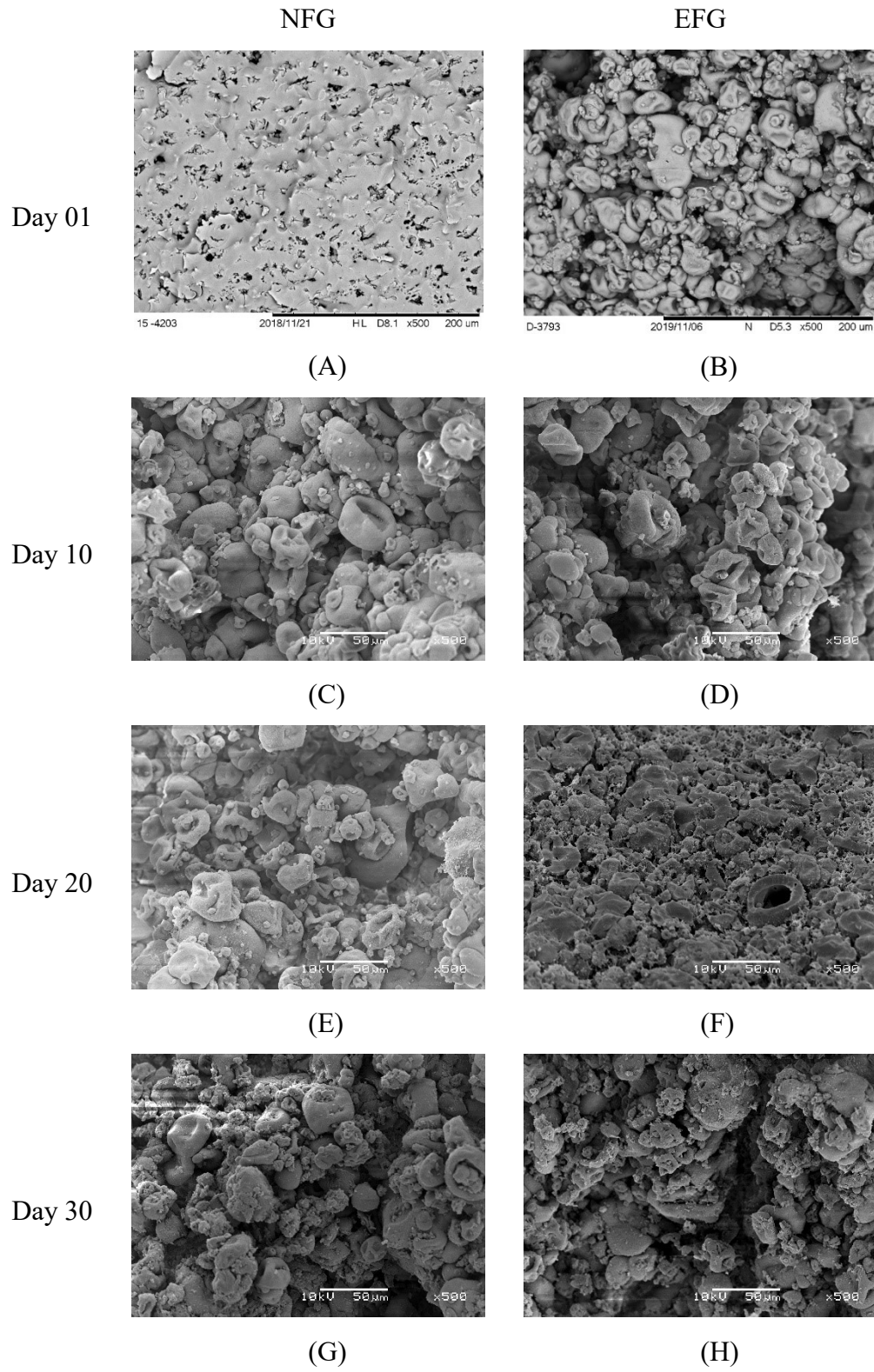
7.4.2 Stability of the gelled systems

The formulation applied for producing NFG in the present study was selected in a previous study published by Brito-Oliveira et al. (2020). In that study, this gel formulation was characterized in terms of microstructure on the 1st day after production, but no information was

obtained regarding the systems' stability along the storage time. On the other hand, in the present study, NFG and EFG were characterized in different days of storage regarding their morphology, rheological properties and WHC, in order to assess changes in their microstructure which may have been occurred due to an ageing process. Such ageing process was evaluated in both types of gels (non-filled and filled) in order to evaluate in what extent the presence of the particles would have influence on the modifications of the protein network.

Regarding non-filled gels, according to the micrographs shown in Figure 7.2, they apparently became more porous and particulate along the time of storage. On the first day of storage (Figure 7.2A), the NFG presented a continuous matrix with small pores, whereas after 10 days, these gels seemed to be formed by particulate structures, similar to microgels, with heterogeneous sizes. On the 10th day (Figure 7.2C), these structures were, apparently, very close, whereas on the 20th (Figure 7.2E) and on the 30th day (Figure 7.2G) they seemed to have moved relatively apart from each other.

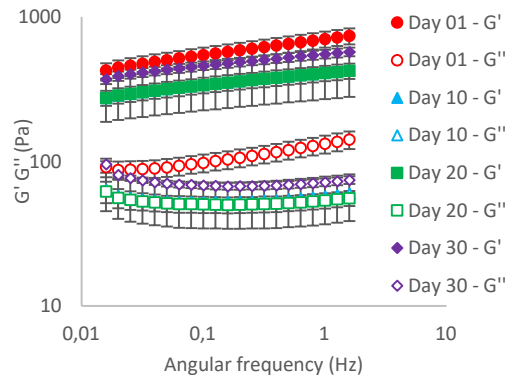
Figure 7.2 Scanning electron micrographs of non-filled gels (NFG) and emulsion-filled gels (EFG) at different days of storage, with the magnification of 500 x.



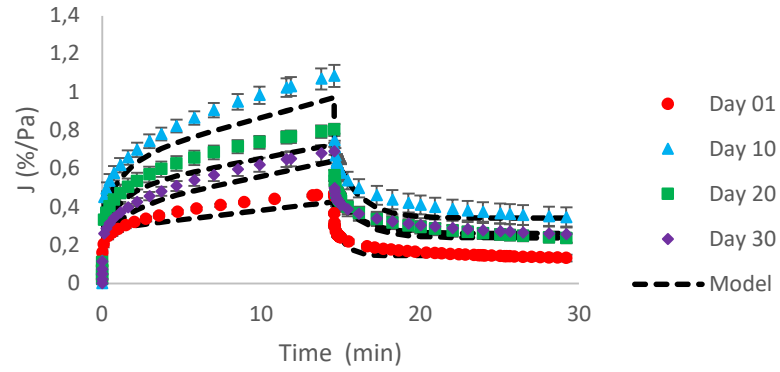
This behavior is possibly related to the relative fragility of the protein interactions within the NaCl-induced gels. As reported in previous studies, during the production of the gels, monovalent ions act by neutralizing negatively charged residues in biopolymers, decreasing the electrostatic repulsion of the carboxylate groups, and then promoting indirect crosslinking in double helices or other linkages (Vilela et al., 2011; Brito-Oliveira et al., 2020). Possibly, during the storage, these indirect crosslinks were weakened and/or broken, causing the matrix to reorganize in a more discontinuous way and present a less compact organization, up to the 30th day of storage. Such phenomenon would be a characteristic of the ageing process of this type of gel.

This weakening and rupture of protein-protein interactions were confirmed by the rheological data obtained for NGF, presented in Figure 7.3. It was verified that the ageing process decreased G' and G'' and increased compliance values, indicating that the microstructural alterations, previously discussed, weakened the gels.

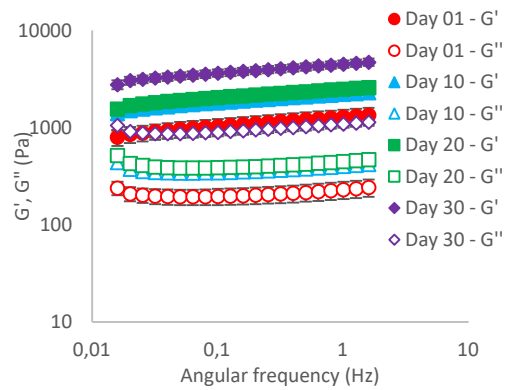
Figure 7.3 Results of frequency sweep tests (A, C) and creep/recovery tests (B, D) of non-filled gels (NFG) (A, B) and emulsion filled gels (EFG) (C, D) at different days of storage.



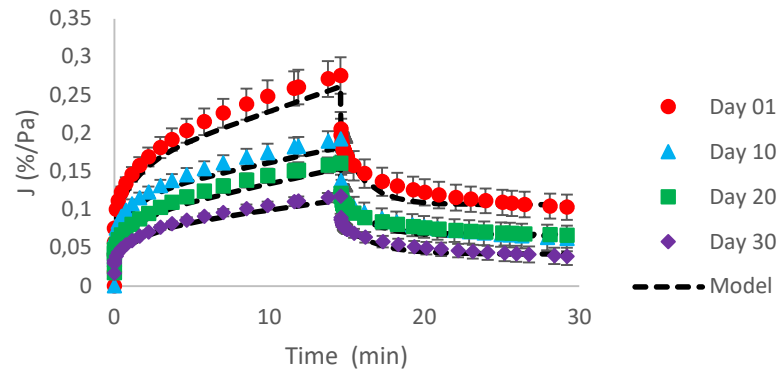
(A) NFG



(B) NFG



(C) EFG



(D) EFG

As expected, the increases of compliance reflected in the Burger's model parameters, shown in Table 7.2, which satisfactorily represented the experimental data ($R^2 > 0.80$). The results revealed that the alterations caused by the ageing process from days 01 to 10, led to an extensive increase of J_0 and J_1 , indicating a drastic decrease of strength. From days 10 to 30, however, a decrease of these parameters was detected, indicating that the reorganizations within the system, which happen in order to lower its free energy, possibly allowed the formation of new protein interactions, increasing the systems strength.

Table 7.2 Parameters of Burger's model (creep/recovery data) for non-filled and emulsion-filled gels along the storage

Day of storage	J_0 (%/Pa)	J_1 (%/Pa)	λ_{ret} (s)	η_0 (Pa.s/%)	R^2	Recovery (%)
NFG						
1	$0.1890^c \pm 0.0110$	$0.0954^d \pm 0.0046$	$32.28^b \pm 0.81$	$6213.7^a \pm 686.3$	0.83	$71.68^a \pm 3.89$
10	$0.3770^a \pm 0.0226$	$0.2625^a \pm 0.0143$	$85.80^a \pm 4.99$	$2676.0^b \pm 4.99$	0.80	$67.77^b \pm 4.17$
20	$0.2841^b \pm 0.0296$	$0.2111^b \pm 0.0136$	$87.16^a \pm 8.14$	$3808.4^b \pm 473.9$	0.82	$70.23^b \pm 3.79$
30	$0.2230^c \pm 0.0119$	$0.1638^c \pm 0.0139$	$91.93^a \pm 3.23$	$3502.2^b \pm 534.7$	0.86	$62.40^b \pm 5.09$
EFG						
1	$0.0913^a \pm 0.0048$	$0.0663^a \pm 0.0046$	$93.90^b \pm 1.20$	$8581.0^b \pm 1355.6$	0.90	$62.72^a \pm 2.87$
10	$0.0695^b \pm 0.0035$	$0.0484^b \pm 0.0051$	$97.82^b \pm 0.60$	$14119.9^b \pm 2879.1$	0.89	$67.75^a \pm 7.05$
20	$0.0528^c \pm 0.0044$	$0.0360^c \pm 0.0035$	$100.14^{ab} \pm 0.70$	$13357.7^b \pm 1126.7$	0.91	$58.57^a \pm 3.31$
30	$0.0377^d \pm 0.0022$	$0.0341^c \pm 0.0046$	$119.90^a \pm 15.00$	$22185.9^a \pm 4569.0$	0.93	$67.15^a \pm 7.81$

Averages followed by different lowercase letters in the same column are statistically different ($p < 0.05$).

According to Barlett et al (2012), during the ageing of gels, the process that generally takes place involves the breakup of energetic bonds among particles, their diffusion to dense regions of the network, and reformations of the broken bond, which allow a net increase in the number of nearest-neighboring particles with a concomitant lowering of the free energy of the system. Such process tends to make the network to coarsen, which was not observed for NFG.

It is possible that between the 1st and 10th days, the dominant process in the gelled network was the breakup of energetic bonds, which caused the systems to show more microstructural discontinuous and weak, presenting increases of J_0 and J_1 . From days 10 to 30, the particles/protein molecules were not able to migrate to denser regions of the network, possibly due to the presence of LBG, which restricted movements within the matrix, however,

reformations of some broken bonds made the systems stronger, as verified from the decreases of J_0 and J_1 .

The alterations caused by the ageing process in the NFG gels during the 30 days of storage, however, caused continuous increases of λ_{ret} and decreases of η_0 and recovery capacity. According to the literature, λ_{ret} is the retardation time required for the strain of structural elements to decrease to approximately 63% of their maximum strain, whereas η_0 reflects the viscous behavior of the systems (Wu et al., 2010; Chang et al., 2014). These results indicated that the alterations decreased the viscous component of the gels and made the systems more sensitive during the deformation process (creep), causing more permanent changes in the structure of older samples.

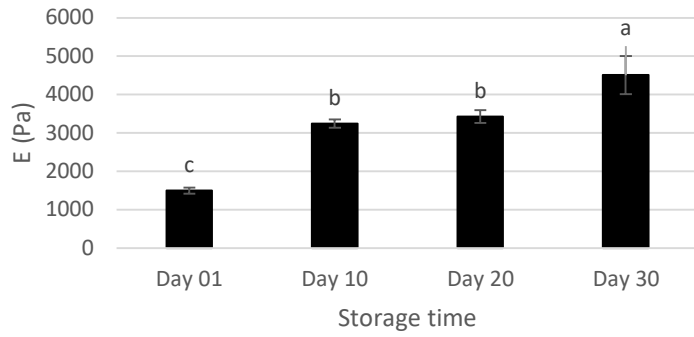
Even though frequency sweep tests and creep/recovery tests could be adequately performed in NFG, the systems were not strong enough to be subjected to uniaxial compression tests.

On the other hand, EFG were strong enough for the development of uniaxial compression tests (Figure 7.4) and the results confirmed the strengthening of the systems with the ageing process, with increases of Young's modulus and rupture parameters.

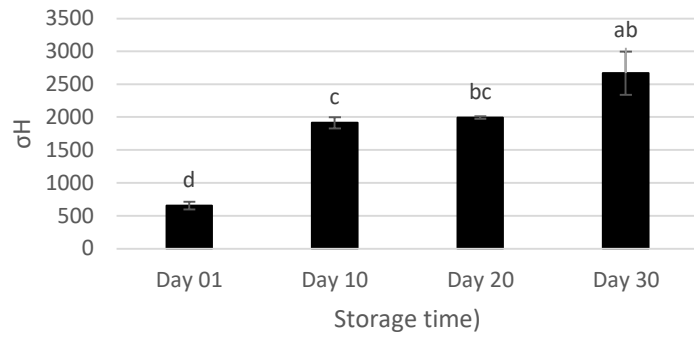
As expected, the alterations in the microstructural organization of the NFG caused decreases in the WHC of the systems (Figure 7.5). According to the literature, gels with particulate and porous microstructures, such as the ones presented by NFG after the 10th day of storage, tend to present low WHC, due to the lower capacities to retain water by capillary forces.

A different behavior, however, was verified in the EFG, in which the aging process led to a microstructural compaction of the matrices (Figure 7.2). According to the literature, the relatively "open clusters" of aggregates observed on the first day of storage (Figure 7.2B) are thermodynamically unstable and can be partly stabilized by the formation of additional bonds (Alting, Hamer, Kruif & Visschers, 2003). Probably, the formation of these additional bonds caused the compaction verified especially from days 01 to 20.

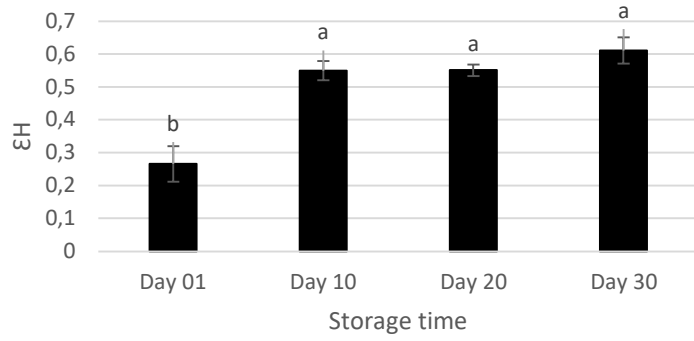
Figure 7.4 Results of uniaxial compression tests of emulsion-filled gels (EFG) at different days of storage.



(A)

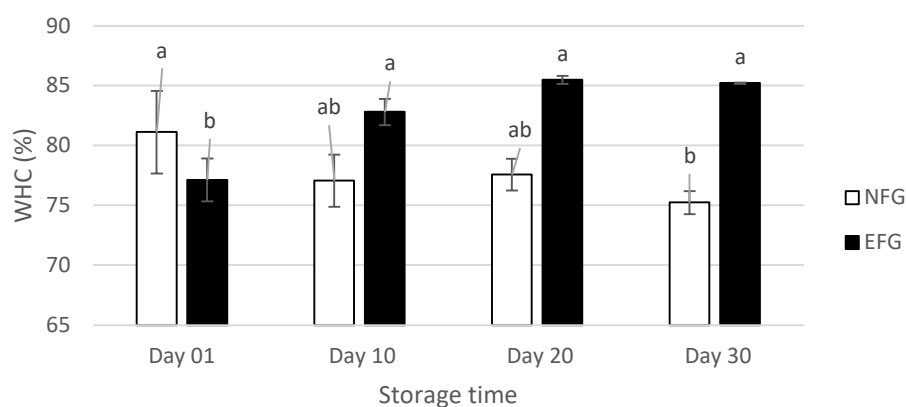


(B)



(C)

Figure 7.5 Water holding capacities (WHC) of non-filled gels (NFG) and emulsion-filled gels (EFG) along the storage.



Averages followed by different lowercase letters are statistically different ($p < 0.05$) for the same systems at different days of storage.

Such formation of additional bonds and microstructural compaction increased the gels' strength, as verified from the continuous increases of G' and G'' (Figure 7.3C) and decreases of compliance (Figure 7.3D). In this case, the decreases in compliance also caused decreases of J_0 and J_1 and increases of λ_{ret} and η_0 , as verified in Table 7.2. The recovery capacity of the EFG, however, were not affected by the ageing process.

Also, the microstructural compaction and formation of new bonds within the matrices increased the WHC of the EFG (Figure 7.5), probably for increasing the capillary forces (Kuhn et al., 2011). According to Kuhn et al. (2011), gels formed by monovalent cation salts tend to present good water-holding capacities due to the number of sites available to interact with the water. These available sites result from electrostatic screening on charges, which reduce the electrostatic repulsion and attract the water molecules, forming hydration layers (Kuhn et al., 2011).

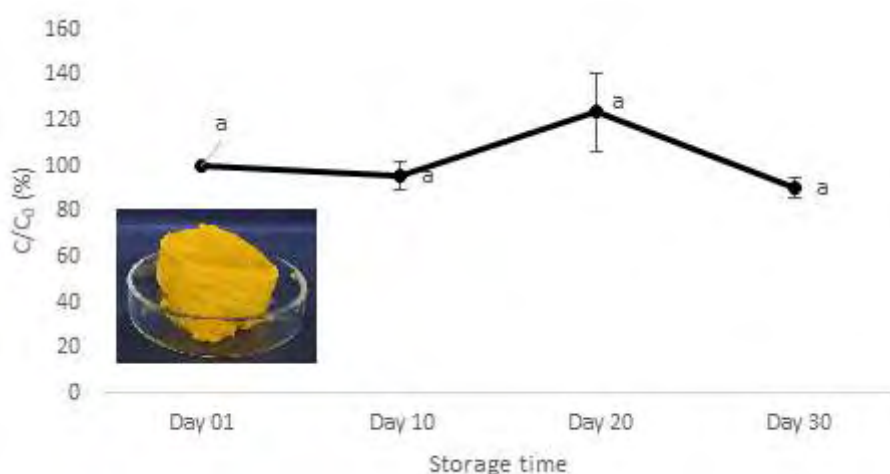
These results evidenced that the incorporation of SLP to the SPI/LBG cold-set gels was an interesting strategy to decrease the weakening and the undesirable effects of the ageing processes in the protein network. Brito-Oliveira et al. (2017a, 2018) had already shown that SLPs stabilized with Tween 80/Span 80 appeared to be physically connected to the SPI matrices, and the conclusion obtained was that this physical interactions among the gelled matrix and the SLP may have been a result from the different sizes of the polar heads of the mixture of surfactants. Such a difference in size may have caused inhomogeneities on in the interface (like the presence of "voids"), in which some groups of the protein and/or

polysaccharide chains were able to anchor (Brito-Oliveira et al., 2017a, 2018). Possibly, in the present study, this same anchoring made the SLP act as junction zones within the matrices, preventing the weakening of the protein cross-links caused by the aging of NFG, but allowing the compaction of the structures verified with the ageing of EFGs.

7.4.3 Quantification of beta-carotene in EFG

In addition to the characterization regarding its microstructural and rheological properties at different days of storage, EFGs were subjected to beta-carotene quantification in order to evaluate the ability of such systems to protect the encapsulated bioactive. The results shown in Figure 7.6 indicated the beta-carotene concentration within the systems was constant over the 30 days of storage.

Figure 7.6 Concentration of β -carotene in emulsion filled gels (EFG) along the storage.



Averages followed by different lowercase letters are statistically different ($p < 0.05$).

Considering that, in the same period, SLPs in dispersion were capable of protecting round 57% of the encapsulated bioactive (Figure 7.1B), the data obtained for the EFG showed the gelation of the continuous phase was extremely efficient to protect the encapsulated beta-carotene.

These results are probably related to the retardation of the oxygen diffusion within the gels caused by the increase of the viscosity of the continuous phase, already verified by other authors in different systems (McClements, 2010; Torres, Murray, & Sarkar, 2016; Lu et al., 2019; Lu

et al., 2020). And also important, the structural modifications due to the ageing process did not affect the EFG ability to protect the encapsulated bioactive.

7.5 Conclusions

The incorporation of beta-carotene-loaded SLP to the gels of SPI and locust beam gum altered their microstructural characteristics, and also affected their rheological properties. Small strain oscillatory shear and uniaxial compression tests revealed the SLP stabilized with behaved as active fillers in the protein/polysaccharide matrix, increasing its strength. The comparison between EFG with encapsulated beta-carotene and beta-carotene-loaded SLP pointed out there is a substantial improvement of the stability of the carotenoid in the case of EFG. The results indicated that the encapsulation of beta-carotene in SLP incorporated in EFG may be considered a potential alternative for a future enrichment of this type of protein matrix with this carotenoid. However, some aspects related to the ageing of the gel needed to be more investigated, in order to increase its shelf-life.

Acknowledgments

This study was funded by Fundação de Amparo à Pesquisa do Estado de São Paulo (FAPESP) (grant number 2017/06224-9). We also thank the access to equipment and assistance provided by the Electron Microscope Laboratory (LME/UNICAMP).

Conflict of Interest: The authors declare that they have no conflict of interest.

7.6 References

- Alting, A.C., Hamer, R.J., Kruij, C.G. & Visschers, R.W. (2003). Cold-Set Globular Protein Gels: Interactions, Structure and Rheology as a Function of Protein Concentration. *Journal of Agricultural and Food Chemistry*, 51, 3150-3156
- Bartlett, P., Teece, L.J., & Faers, M.A. (2012) Sudden collapse of a colloidal gel. *Physical Review E*, 85 (2), 021404.
- Beuschel, B. C., Culbertson, J.D., Partridge, P.A., & Smith, D. M. (1992). Gelation and emulsification properties of partially insolubilized whey protein concentrates. *Journal of Food Science*, 57, 605-609.
- Brito-Oliveira, T.C., Bispo, M., Moraes, I.C.F., Campanella, O.H, & Pinho, S.C. (2017a). Stability of curcumin encapsulated in solid lipid microparticles incorporated in cold-set

emulsion filled gels of soy protein isolate and xanthan gum. *Food Research International*, 102, 759–767.

Brito-Oliveira, T.C., Molina, C.V., Netto, F.M. & Pinho, S.C. (2017b). Encapsulation of beta-carotene in lipid microparticles stabilized with hydrolyzed soy protein isolate: production parameters, alpha-tocopherol coencapsulation and stability under stress conditions. *Journal of Food Science*, 82(3), 659-669.

Brito-Oliveira, T.C., Bispo, M., Moraes, I.C.F., Campanella, O.H., & Pinho, S.C. (2018). Cold-set gelation of commercial soy protein isolate: effects of the incorporation of locust bean gum and solid lipid microparticles on the properties of gels. *Food Biophysics*, 13, 226-239.

Brito-Oliveira, Cavini, Ferreira, Moraes & Pinho (2020). Microstructural and rheological characterization of NaCl-induced gels of soy protein isolate and the effects of incorporating different galactomannans. *Food Structure*, 26, 100158.

Chang, Y., Li, D., Wang, L., Bi, C., & Adhikari, B. (2014). Effect of gums on the rheological characteristics and microstructure of acid-induced SPI-gum mixed gels. *Carbohydrate Polymers*, 108, 183–191.

Chen, X., Yuan, J, Li, R. & Kang, X. (2019). Characterization and embedding potential of bovine serum albumin cold-set gel induced by glucono- δ -lactone and sodium chloride. *Food Hydrocolloids*, 95, 273–282.

Cornacchia, L & Roos, Y.H. (2011). Stability of beta-carotene in protein-stabilized oil-in-water delivery systems. *Journal of Agricultural and Food Chemistry*, 59, 7013-702.

Dickinson, E. (2012). Emulsion gels: The structuring of soft solids with protein-stabilized oil droplets. *Food Hydrocolloids*, 28(1), 224-241.

Farjami, T. & Madadlou, A. (2019). An overview on preparation of emulsion-filled gels and emulsion particulate gels. *Trends in Food Science & Technology*, 86, 85–94.

Guo, Y. et al. (2018). Nano-bacterial cellulose/soy protein isolate complex gel as fat substitutes in ice cream model. *Carbohydrate Polymers*, 198, 620–630.

Ingrassia, R. et al. (2019). Microstructural and textural characteristics of soy protein isolate and tara gum cold-set gels. *LWT - Food Science and Technology*, 113, 108286.

Kuhn, K.R., Cavallieri, A.L.F & Cunha, R.L. (2011). Cold-set whey protein-flaxseed gum gels induced by mono or divalent salt addition. *Food Hydrocolloids*, 25(5), 1302 – 1310, 2011.

Liu, K. et al. (2015). Fat droplet characteristics affect rheological, tribological and sensory properties of food gels. *Food Hydrocolloids*, 44, 244-259.

- Liu, W. et al. (2018). Encapsulation of β -carotene-loaded oil droplets in caseinate/alginate microparticles: Enhancement of carotenoid stability and bioaccessibility. *Journal of Functional Foods*, 40, 527-535.
- Loveday, S. M. (2019). Food Proteins: Technological, Nutritional, and Sustainability Attributes of Traditional and Emerging Proteins. *Annual Review of Food Science and Technology*, 10, 311–39.
- Lu, Y. et al. (2019). Development of Emulsion Gels for the Delivery of Functional Food Ingredients: from Structure to Functionality. *Food Engineering Reviews*, 11, 245–258.
- Lu, Y. et al. (2020). Characterization of beta-carotene loaded emulsion gels containing denatured and native whey protein. *Food Hydrocolloids*, 102, 105600.
- Mahalakshmi, L., Leena, M.M., Moses, J.A. & Anandharamakrishnan, C. (2020). Micro- and nano-encapsulation of beta-carotene in zein protein: size-dependent release and absorption behavior. *Food & Function*, 11, 1647-1660.
- Mao, L., Miao, S., Yuana, F. & Gao, Y. (2018). Study on the textural and volatile characteristics of emulsion filled protein gels as influenced by different fat substitutes. *Food Research International*, 103, 1–7.
- McClements, D. J. (2010). Emulsion design to improve the delivery of functional lipophilic components. *Annual Review of Food Science and Technology*, 1, 241–269.
- Monteiro, S.R., Rebelo, S., Silva, O.A.B.C., & Lopes-da-Silva, J.A. (2013). The influence of galactomannans with different amount of galactose side chains on the gelation of soy proteins at neutral pH. *Food Hydrocolloids*, 33, 349-360.
- Monteiro, S.R. & Lopes-da-Silva, J.A. (2017). Effect of the molecular weight of a neutral polysaccharide on soy protein gelation. *Food Research International*, 102, 14–24.
- Oliver, L., Scholten, E., & van Aken, G.A. (2015). Effect of fat hardness on large deformation rheology of emulsion-filled gels. *Food Hydrocolloids*, 43, 299-310.
- Picone, C. S. F., Takeuchi, K. P. & Cunha, R. L. (2011). Heat-induced whey protein gels: Effects of pH and the addition of sodium caseinate. *Food Biophysics*, 6, 77–83.
- Renard, D., Van De Velde, F. & Visschers, R.W. (2006). The gap between food gel structure, texture and perception. *Food Hydrocolloids*, 20(4), 423–431.
- Sala, G. et al. (2009a). Deformation and fracture of emulsion-filled gels: Effect of gelling agent concentration and oil droplet size. *Food Hydrocolloids*, 23(7), 1853–1863.
- Sala, G. et al. (2009b). Deformation and fracture of emulsion-filled gels: Effect of oil content and deformation speed. *Food Hydrocolloids*, 23(7), 1381–1393.
- Sato, A.C.K., Moraes, K.E.F.P. & Cunha, R.L. (2014). Development of gelled emulsions with

- improved oxidative and pH stability. *Food Hydrocolloids*, 34, 184-192.
- Teece, L.J., Faers, M.A., & Bartlett, P. (2011) Ageing and collapse in gels with long-range attractions. *Soft Matter*, 7, 1341–1351.
- Torres, O., Murray, B., & Sarkar, A. (2016). Emulsion microgel particles: Novel encapsulation strategy for lipophilic molecules. *Trends in Food Science & Technology*, 55, 98–108.
- Vilela, J.A.P., Cavallieri, A.L.F., & Cunha, R.L. (2011). The influence of gelation rate on the physical properties/structure of salt-induced gels of soy protein isolate-gellan gum. *Food Hydrocolloids*, 25(7), 1710-1718
- Wu, M., Li, D., Wang, L., Özkan, N., & Mao, Z. (2010). Rheological properties of extruded dispersions of flaxseed–maize blend. *Journal of Food Engineering*, 98(4),480–491.
- Zhao, H. et al. (2020). Improvement of calcium sulfate-induced gelation of soy protein via incorporation of soy oil before and after thermal denaturation. *LWT - Food Science and Technology*, 117, 108690.

**CHAPTER 8 : EVALUATING THE STABILITY OF COLD-SET GELS USING SMALL-
ANGLE X-RAY SCATTERING (SAXS)**

Evaluating the stability of cold-set gels using small-angle x-ray scattering (SAXS)

Thais C. Brito-Oliveira¹, Pedro L.F. Oseliero², Cristiano L.P. Oliveira²
and Samantha C. Pinho^{1*}

¹Department of Food Engineering, School of Animal Science and Food Engineering,
University of São Paulo (USP), Pirassununga, SP, Brazil

²Institute of Physics, University of São Paulo (USP), São Paulo, SP, Brazil

* Corresponding author: S.C. Pinho, Department of Food Engineering, School of Animal Science and Food Engineering (FZEA), University of São Paulo (USP), Av. Duque de Caxias Norte 225, Jd. Elite, Pirassununga, SP, Brazil 13635-900. Tel: +55-19-35654288; fax: +55-19-3565-4284.

E-mail address: samantha@usp.br

8.1 Abstract

The objective of this study was to evaluate the stability of cold-set non-filled gels (NFG) and emulsion-filled gels (EFG) produced with SPI and locust bean gum, induced by different salts (CaCl_2 and NaCl), using small-angle x-ray scattering (SAXS). For this purpose, the systems were characterized at days 01 and 10 of storage. Data indicated the incorporation of solid lipid particles (SLP) to both formulations tested (using CaCl_2 and NaCl) caused a higher ordering of the systems. These results are associated to microstructural organizations of EFGs, which has been reported to be composed by microgels. NaCl -induced gels presented a more intense peak at $q = 0.1443 \text{ \AA}^{-1}$ than CaCl_2 , indicating a higher ordering for the first salt. Such behavior is associated to the higher concentration of SLP within the gels produced with NaCl and the different abilities of the distinct salts. Regarding the stability of the systems in the period evaluated (within 10 days), the gels produced with NaCl were more stable than the ones induced by CaCl_2 , confirming the results reported in previous investigations.

Keywords: Gels; Stability; Soy protein Isolate; Cold-set gelation; SAXS.

8.2 Introduction

The interest of the food industry in decreasing fat content and improving nutritional, functional and sensory characteristics of products has been increasing the necessity of the development of new plant protein gels formulations (Chen et al., 2019; Guo et al., 2018). Plant protein ingredients has been gaining the attention of researchers due to the new consumers' concerns, especially related to environmental issues of food production using ingredients of animal sources (Loveday, 2019; Monteiro et al., 2013; Monteiro et al, 2017).

Among the most important plant protein ingredients available for commercial applications is the soy protein isolate (SPI), which has been applied in different research for the production of gelled systems (Brito-Oliveira et al., 2020; Ingrassia et al., 2019; Monteiro et al., 2017; Zhao et al., 2020). Such investigations, however, are generally focused on the comprehension of the gelation process and characterization of the systems right after its production. Little is known about properties alterations throughout a storage period, due to spontaneous/aging processes and/or external forces (Brito-Oliveira et al., 2017; Renard et al., 2006; Teece et al., 2011).

In this context and considering the importance of food products' stability for researchers and industry, in previous studies of our research group, cold-set non-filled gels and emulsion-filled gels produced with SPI and locust bean gum, using different salts (CaCl_2 and NaCl), were characterized regarding its microstructural and rheological properties in different days of storage (Chapters 6 and 7). Even though the results obtained were interesting and conclusive, it is known that the application of different techniques for gels characterization is fundamental for a more complete understanding of the systems' properties.

In addition to the techniques cited above, other tests can be used to develop complete characterizations of gelled systems, such as small-angle X-ray scattering (SAXS) scattering tests. Although they are less applied than rheological and microscopic tests, SAXS tests are used to obtain information about the size and characteristic of protein aggregates, the properties and structural organization of gels, as well as for the description of mechanisms involved in the process gelation (Alting et al., 2004; Oca-Ávalos et al., 2016). In addition, according to Alting et al. (2004), SAXS tests can be used to evaluate structural rearrangements of the samples after the gelation process.

In this context, the objective of this study was to evaluate the stability of cold-set non-filled gels and emulsion-filled gels produced with SPI and locust bean gum, induced by different salts (CaCl_2 and NaCl), using small-angle x-ray scattering (SAXS).

8.3 Materials and methods

8.3.1 Chemicals and reagents

For the production of SLP, palm stearin (PS) was donated by Agropalma (Belém, PA, Brazil), and Tween 80, Span 80 and beta-carotene were obtained from Sigma-Aldrich (St. Louis, MO, USA). For the production of the gels, the SPI (Protimarti M-90, 84.3% protein) was obtained from Marsul (Montenegro, RS, Brazil), LBG (Viscogum LBG ®) was donated by Cargill (Campinas, SP, Brazil), sodium chloride was purchased from Synth (Diadema, SP, Brazil) and Calcium chloride dihydrate was purchased from Kyma (Americana, SP, Brazil). Ultrapure water (Millipore system Direct Q3®, Billerica, MA, USA) was used throughout the experiments.

8.3.2 Production of cold-set gels

8.3.2.1 Production of solid lipid particles (SLP)

SLP were produced according to Brito-Oliveira et al. (2017). For this purpose, the lipid phase, composed by palm stearin (4.5% w/w) and Span 80 (2.7%, w/w), was kept at 80°C for 30 min to eliminate the thermal memory. Subsequently, the aqueous phase, composed by Tween 80 (1.8 %, w/v) and deionized water, was dispersed in the lipid phase, at 80°C, using a rotor–stator device (IKA T25, IKA, Staufen, Germany) at 18.000 rpm for 5 min. Sodium benzoate (0.02%, w/w) was added to the samples to avoid microbiological contamination. The solid lipid particles dispersions (SLPD) were kept overnight at 10 °C before its application to produce EFGs.

8.3.2.2 Production of cold-set gels: non-filled gels and emulsion filled gels

Non-filled gels were produced according to Brito-Oliveira et al. (2020). For this purpose, SPI powder (14%, w/v) with LBG (0.1%, w/v) was hydrated using deionized water at pH 7, and the systems were preheated in a water bath at 80 °C for 30 min. Subsequently, CaCl₂ (100 mM) or NaCl (300 mM) was incorporated to the systems at room temperature. For EFGs production, the same protocol was applied, however, the deionized water used to hydrate the SPI/LBG were replaced (fully or partially) by solid lipid particles dispersions (SLPD). While for systems produced with NaCl, 100% of the water was replaced by SLPD, for gels with CaCl₂

the replacement was only of 50%. These ratios were determined in previous investigations (chapters 5 and 6 of this thesis).

8.3.3 Small-angle X-ray scattering (SAXS)

Non-filled gels and emulsion-filled gels were characterized in different days of storage by Small-angle X-ray scattering (SAXS). SAXS measurements were performed using a Xeuss instrument equipped with a microfocus Genix 3D system (Xenocs), according to Oliveira et al. (2009). The samples were maintained between two sheets of Kapton in a sample holder suitable for gel-like materials. All measurements were carried out in air and the scattered intensity was collected on a Pilatus detector (Dectris). The sample-to-detector distance was ~ 0.66 m, which provided an effective range of the modulus of the transfer moment vector q experimentally accessible of 0.015 – 0.32 \AA^{-1} , with $q = 4\pi \sin(\theta)/\lambda$ (where 2θ is the scattering angle and $\lambda = 1.54$ \AA is the X-ray wavelength from the copper K_{α} radiation). For the treatment of 1D data, obtained through azimuthal integration of the 2D data, the SUPERSAXS package¹ was used and consisted of normalization by the measuring time (900 s) and sample transmission, followed by correction using the scattering from the Kapton sheets, taken as the background.

8.4 Results and Discussion

8.4.1 Small-angle X-ray scattering (SAXS) of non-filled gels and emulsion-filled gels

From the obtained results, shown in Figures 8.1 and 8.2, it is evident that the incorporation of SLP to both, NaCl and CaCl_2 -induced gels caused a higher ordering of the systems, having seen the peak at $q = 0.1443$ angs^{-1} . This is associated with a repetition distance of $2 * \pi / q \sim 4.4$ nm.

Such data is associated to the results discussed in Chapters 5 and 6, in which it was possible to verify the differences between the microstructural organizations of NFG and EFG. For both salts, it was clear that the presence of SLP influenced the aggregation and gelling behavior of the SPI/LBG system. In general, the EFG matrices were composed by structures that resemble microgels (Vincent & Saunders, 2011; Schmitt et al., 2009). As previously discussed in this thesis, the formation of these capsule-like microstructures was associated to two factors: (I) the behavior of the protein fractions of the SPI and (II) the effect of the SLP over the protein aggregation.

It is known that, when heated together (in the present study, during the preheating), the β -conglycinin and the glycinin present different aggregation behavior, and the β -conglycinin tend to occupy the surface of the complex aggregates formed by glycinin, resulting in the initial formation of the “capsule-like” structures (Brito-Oliveira et al., 2020; Guo et al., 2012).

Also, according to the literature, microgel-like organizations result from a self-limited aggregation controlled by the protein net charge and hydrophobic regions exposed to heat denaturation (Vincent & Saunders, 2011; Schmitt et al., 2009). In the present study, the presence of the SLP restricted the continuous aggregation of the structures and influenced the the charge distribution through the medium, collaborating to the formation of the ordered systems composed by the capsule-like estructures.

The comparison of the SAXS data of NaCl-induced gels (Figure 8.1) and CaCl₂-induced gels (Figure 8.2), indicated that the peak at $q = 0.1443 \text{ \AA}^{-1}$ was more intense for NaCl than for CaCl₂, suggesting a higher ordering for the first salt.

These differences are associated to the higher concentration of SLP within the gels produced with NaCl, which, obviously, affected the organization of the systems, and also to the different actions of the distinct salts. As previously cited, it is known that divalent salts cause much faster and effective interactions among protein aggregates than monovalent salts, due to its higher capacity to screen electrical charges and to cross-link negatively charged carboxyl groups (Bryant & McClements, 1998; Brito-Oliveira et al., 2020). For this reason, the incorporation of CaCl₂ to protein gels tend to form less organized microstructures than the application of monovalent salts, such as the NaCl (Brito-Oliveira et al., 2020).

Figure 8.1. Results obtained from non-filled gels (NFG) and emulsion-filled gels (EFG) induced by NaCl, in different days of storage.

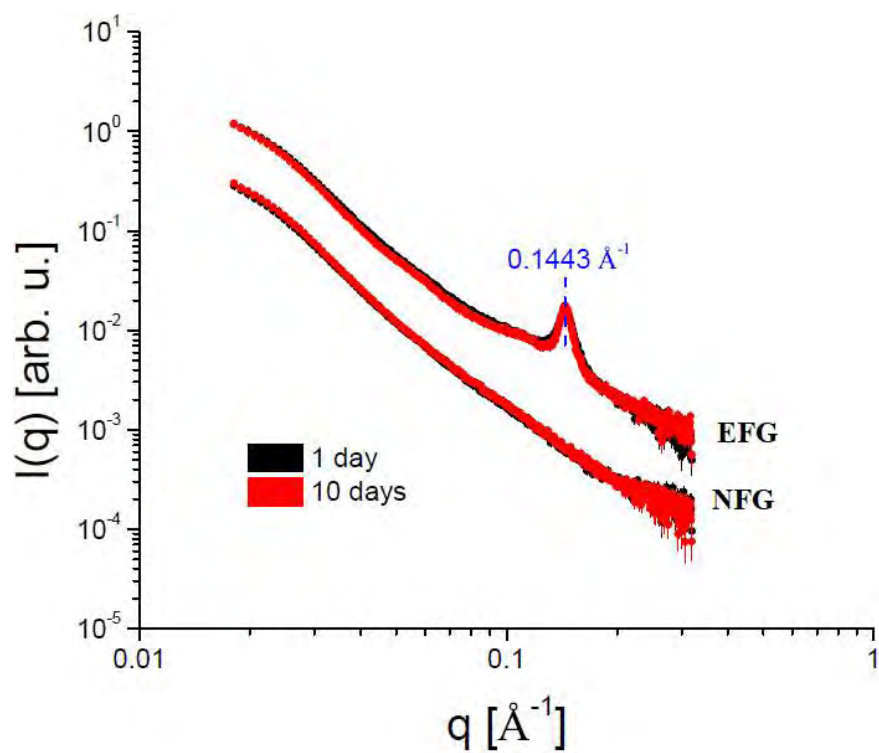
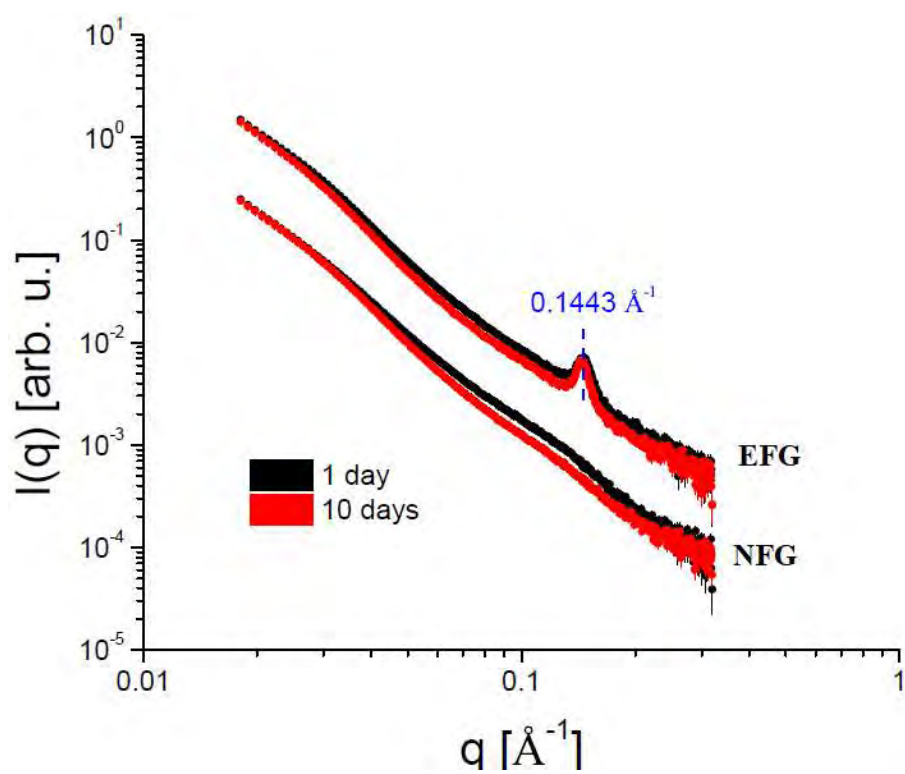


Figure 8.2. Results obtained from non-filled gels (NFG) and emulsion-filled gels (EFG) induced by CaCl_2 , in different days of storage.



Regarding the stability of the systems, the results shown in Figures 8.1 and 8.2, revealed that, in the period evaluated (within 10 days), the gels produced with NaCl were more stable than the ones induced by CaCl₂, confirming the results presented in Chapters 6 and 7.

Unfortunately, due to equipment problems and the interruption of research activities at the University of São Paulo due to the coronavirus pandemic, evaluations in the subsequent days of storage (20 and 30) were not possible, which limits further discussions. But to all appearances, the answers obtained from the SAXS confirm the stability data obtained from rheological and microstructural evaluations of gels during storage.

8.5 Conclusions

The results obtained in the present investigation revealed that the incorporation of SLP to both, NaCl and CaCl₂-induced gels, caused a higher ordering of the systems, having seen the peak at $q = 0.1443 \text{ \AA}^{-1}$, which is associated with a repetition distance of $2 * \pi / q \sim 4.4 \text{ nm}$. Such data is associated to the microstructural organizations of EFGs, which has been reported to be composed by microgels. NaCl-induced gels presented a more intense peak at $q = 0.1443 \text{ \AA}^{-1}$ than CaCl₂, indicating a higher ordering for the first salt. Such results are associated to the higher concentration of SLP within the gels produced with NaCl and the different abilities of the distinct salts. Regarding the stability of the systems in the period evaluated (within 10 days), the gels produced with NaCl were more stable than the ones induced by CaCl₂, confirming the results reported in previous investigations.

8.6 References

- Alting, A.C. et al. (2004). Acid-Induced Cold Gelation of Globular Proteins: Effects of Protein Aggregate Characteristics and Disulfide Bonding on Rheological Properties. *Journal of Agricultural and Food Chemistry*, 52, 623-631.
- Brito-Oliveira, T.C., Bispo, M., Moraes, I.C.F., Campanella, O.H, & Pinho, S.C. (2017). Stability of curcumin encapsulated in solid lipid microparticles incorporated in cold-set emulsion filled gels of soy protein isolate and xanthan gum. *Food Research International*, 102, 759–767.
- Brito-Oliveira, Cavini, Ferreira, Moraes & Pinho (2020). Microstructural and rheological characterization of NaCl-induced gels of soy protein isolate and the effects of incorporating different galactomannans. *Food Structure*, 26, 100158.

- Bryant, C.M. & McClements, D.J. (1998). Molecular basis of protein functionality with special consideration of cold-set gels derived from heat-denatured whey. *Trends Food Science Technology*, 9, 143–151.
- Chen, X., Yuan, J, Li, R. & Kang, X. (2019). Characterization and embedding potential of bovine serum albumin cold-set gel induced by glucono- δ -lactone and sodium chloride. *Food Hydrocolloids*, 95, 273–282.
- Guo, Y. et al. (2018). Nano-bacterial cellulose/soy protein isolate complex gel as fat substitutes in ice cream model. *Carbohydrate Polymers*, 198, 620–630.
- Guo, J. et al. (2012). Limited Aggregation Behavior of β -Conglycinin and Its Terminating Effect on Glycinin Aggregation during Heating at pH 7.0. *Journal of Agricultural and Food Chemistry*, 60, 3782–3791.
- Ingrassia, R. et al. (2019). Microstructural and textural characteristics of soy protein isolate and tara gum cold-set gels. *LWT - Food Science and Technology*, 113, 108286.
- Loveday, S. M. (2019). Food Proteins: Technological, Nutritional, and Sustainability Attributes of Traditional and Emerging Proteins. *Annual Review of Food Science and Technology*, 10, 311–39.
- Monteiro, S.R., Rebelo, S., Silva, O.A.B.C., & Lopes-da-Silva, J.A. (2013). The influence of galactomannans with different amount of galactose side chains on the gelation of soy proteins at neutral pH. *Food Hydrocolloids*, 33, 349-360.
- Monteiro, S.R. & Lopes-da-Silva, J.A. (2017). Effect of the molecular weight of a neutral polysaccharide on soy protein gelation. *Food Research International*, 102, 14–24.
- Oca-Ávalos, J.M.M., Huck-Iriart, C., Candal, R.J., & Herrera, M.L. (2016). Sodium Caseinate/Sunflower Oil Emulsion-Based Gels for Structuring Food. *Food Bioprocess Technology*, 9, 981–992.
- Oliveira, C.L.P et al. (2009). A SAXS Study of Glucagon Fibrillation. *Journal of Molecular Biology*, 387, (1).
- Renard, D., Van De Velde, F. & Visschers, R.W. (2006). The gap between food gel structure, texture and perception. *Food Hydrocolloids*, 20(4), 423–431.

Schmitt, C., Bovay, C., Vuillomenet, A.-M., Rouvet, M., Bovetto, L., Barbar, R., et al. (2009). Multiscale characterization of individualized b-lactoglobulin microgels formed upon heat treatment under narrow pH range conditions. *Langmuir*, 25, 7899–7909.

Teece, L.J., Faers, M.A., & Bartlett, P. (2011) Ageing and collapse in gels with long-range attractions. *Soft Matter*, 7, 1341–1351.

Vincent, B. & Saunders, B. R. (2011). Interactions and colloid stability of microgel particles. In A. Fernandez-Nieves, H. Wyss, J. Mattsson, & D. A. Weitz (Eds.), *Microgel suspensions*. Weinheim: WileyVCH, Chap. 6.

Zhao, H. et al. (2020). Improvement of calcium sulfate-induced gelation of soy protein via incorporation of soy oil before and after thermal denaturation. *LWT - Food Science and Technology*, 117, 108690.

GENERAL CONCLUSIONS

The results obtained in this Ph.D. Thesis showed the ability of the soy protein isolate to form cold-set gels by incorporating NaCl or CaCl₂, but also confirmed the challenging properties of the commercial ingredient used (e.g. low solubility at pH 7). Due to this fact, the lowest SPI concentration in which it was possible to obtain self-supported gels with the two types of salts tested was 14% (w/v). In such protein concentration, the strongest gels (*i.e.* with higher G' and G'', lower values of compliance and higher values of Young's modulus) were those produced using ionic strength equal to 300, for both salts tested (*i.e.* 300 mM NaCl and 100 mM CaCl₂). This ionic strength was, therefore, selected for the further development of the project.

Under these conditions, however, gels produced with NaCl were still weak, with relative structural instability when subjected to room temperature for approximately 10 minutes. Gels produced with CaCl₂, on the other hand, presented low water holding capacities (WHC), presenting syneresis after one day of storage. Such problems evidenced the importance of studying the effects of the incorporation of different galactomannans on the properties of the gels produced with the different salts.

In this context, the formulations G_{CaCl₂} (14% SPI, 100 mM CaCl₂) and G_{NaCl} (14% SPI, 300 mM NaCl) were used to produce mixed gels using locust bean gum (LBG) or guar gum (GG), in different concentrations. The results of WHC, rheological tests and CLSM revealed that the incorporation of polysaccharides in different concentrations had different effects on the properties of the gels. Such effects depended not only on the type of salt, but also on the characteristics of the galactomannans used, which influenced the extent of demixing in the systems (*i.e.*, the degree of microstructural phase separation). Such processes affected the protein-protein interactions and, consequently, influenced the rheological properties of the gels.

The results obtained allowed the selection of two formulations for the production of emulsion-filled gels (EFG): G_{NaCl}^{MIX} (14% SPI 300 mM NaCl, 0.1% LBG) and G_{CaCl₂}^{MIX} (14% SPI, 100 mM CaCl₂, 0.1% LBG). The incorporation of LBG to the samples produced with both types of salt resulted in stronger and more stable systems, with higher WHC, in comparison to the incorporation of GG. In addition, among the gels produced with different concentrations of LBG, the ones with 0.1%, for both salts, resulted in stronger systems with higher WHC.

These two formulations for mixed gels were used for the incorporation of solid lipid particles (SLP) stabilized with different surfactants (WPI and Tween 80/Span 80 - TS). The incorporation of SLP stabilized with WPI resulted in the formation of heat-induced gels, and,

therefore, such formulations were eliminated from the study. The incorporation of SLP stabilized with Tween 80/Span 80, on the other hand, allowed the production of cold-set EFG.

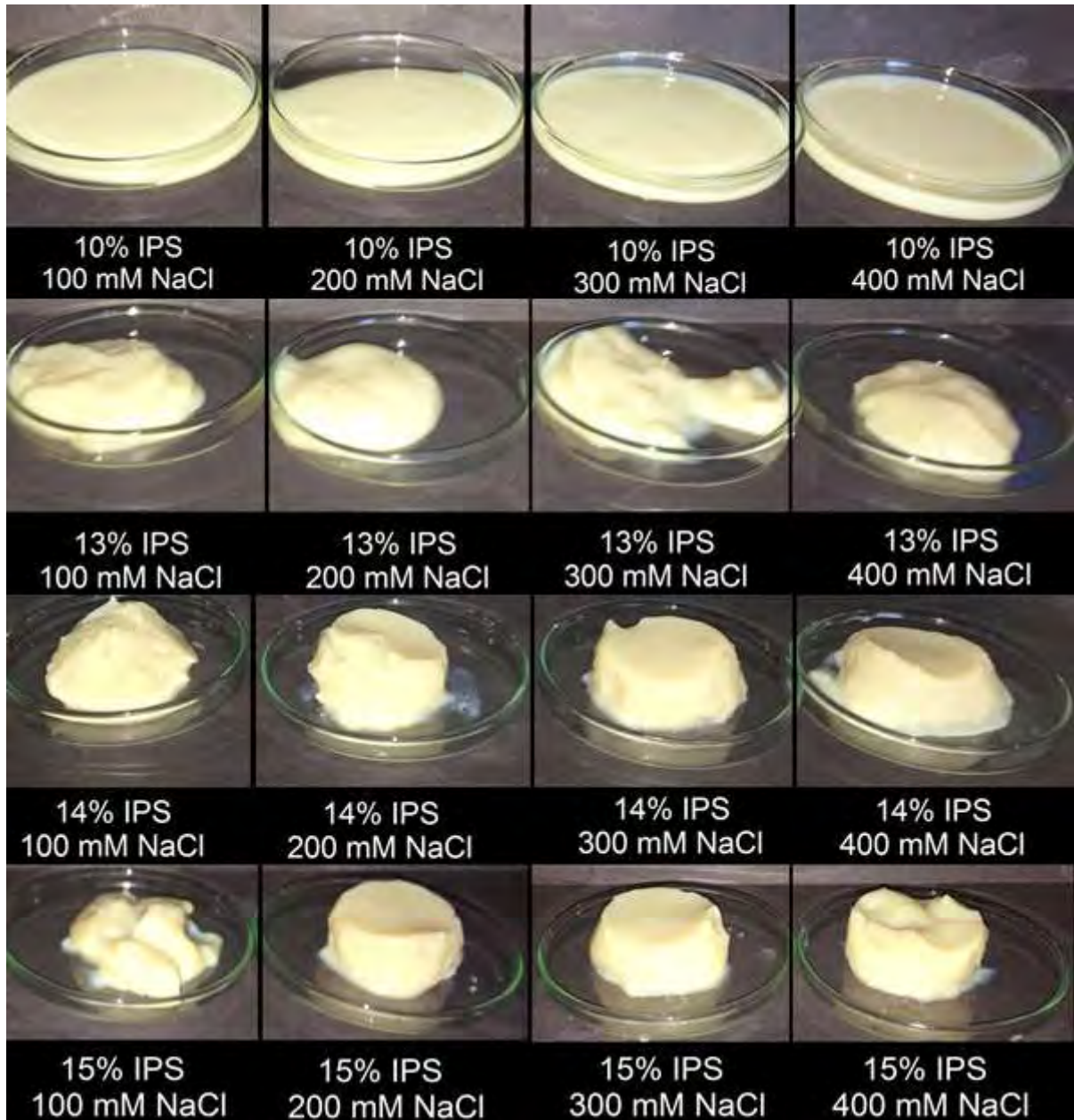
For NaCl-induced gels, the presence of SLP reduced WHC, altered the microstructures of the gels (resulting in “microgel-like” organizations), and decreased E_g , σ_H , and ϵ_H , in comparison to compared to NFG. However, increases in the SLP content caused different effects over E_g , σ_H , and ϵ_H , possibly due to the heterogeneity of the samples. These results suggested that, even though TS-stabilized SLP were “unbound” to the matrix, due to the low chemical affinity between surfactants and gelled matrix (unbound fillers), they were “active”, interacting with the gelled matrices, changing their aggregation patterns and microstructural organizations.

For CaCl_2 -induced systems, the incorporation of SLP increased the WHC of the systems and altered its microstructural organizations to microgels-composed matrices. Besides, wuch incorporation altered the systems stability. NFG presented a very particulate, disorganized, and porous microstructure, with low WHC. Such opened clusters of aggregates presented a high thermodynamical instability which caused the systems to change abruptly in less than 10 days. At the 10th day of storage, the NFG presented a great microstructural compaction due to the formation of additional bonds within the systems. Such compaction led the systems to expulse a great amount of water from the matrix. Due to this large syneresis, the NFG could not be analyzed regarding its rheological properties. EFG, however, were much more stable and did not present syneresis during the 20 days analyzed. During this period, the EFG presented a more subtle microstructural compaction, which led to increases of G' , G'' , E_g and rupture parameters and decreases of compliance values. These results confirmed that the incorporation of SLP was an interesting strategy to improve gels stability as it decreased the microstructural alterations and the water loss, even though the rheological properties of the gels have been changed during the 20 days analyzed.

Regarding the NaCl-induced gels' stability, the results revealed that while the ageing process of NFG caused a decrease of strength and WHC of the systems, EFG presented a strengthening and an increased ability to retain water during the 30 days analyzed. Due to this interesting stability, the NaCl-induced EFG could be adequately applied for the encapsulation of beta-carotene. In comparison to the SLP dispersion, which were capable of retaining around 57% of the bioactive iniatilly encapsulated for 30 days, the EFG presented a higher capacity to protect the encapsulated beta-carotene, presenting around 90% of retention. Such results indicated that the gelation of the continuous phase was a good strategy to improve the stability of the encapsulated bioactive.

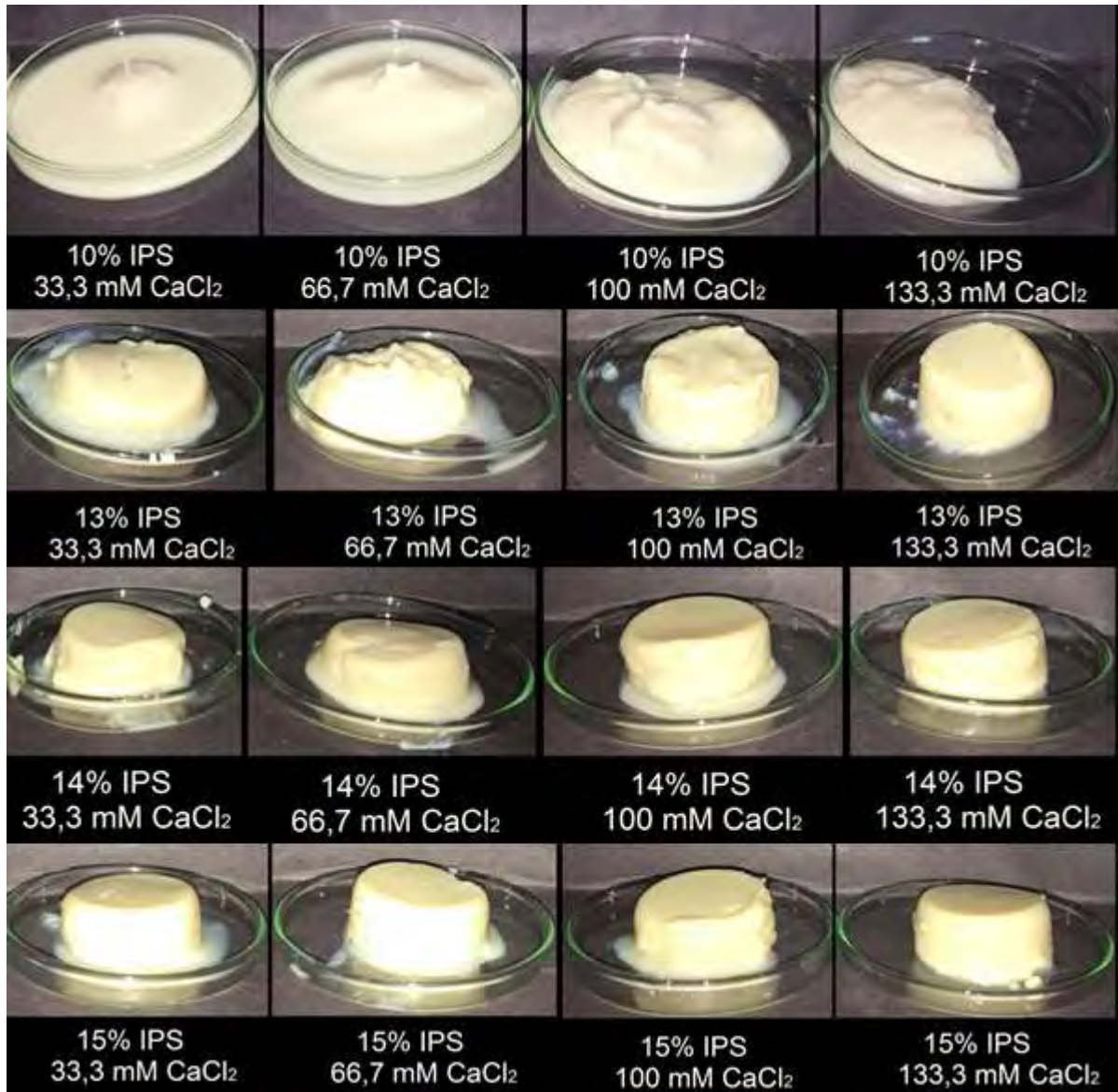
APPENDICES

APPENDIX A – Visual aspects of systems produced with SPI and NaCl



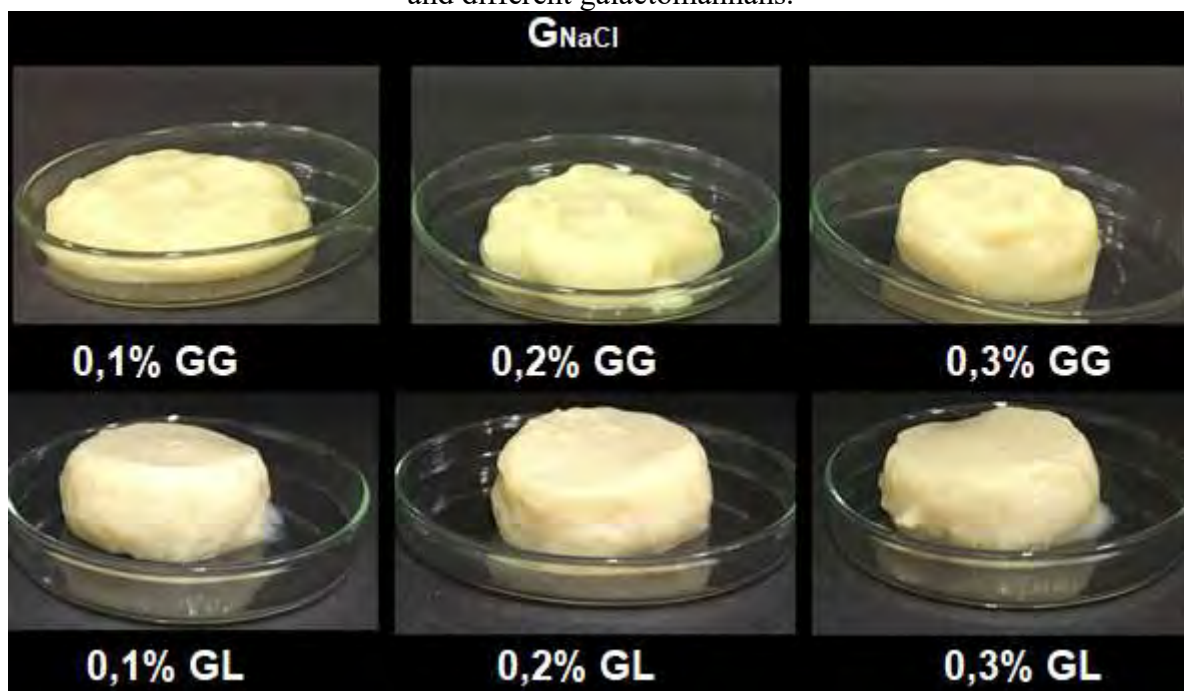
Source: Own authorship.

APPENDIX B – Visual aspects of systems produced with SPI and CaCl₂



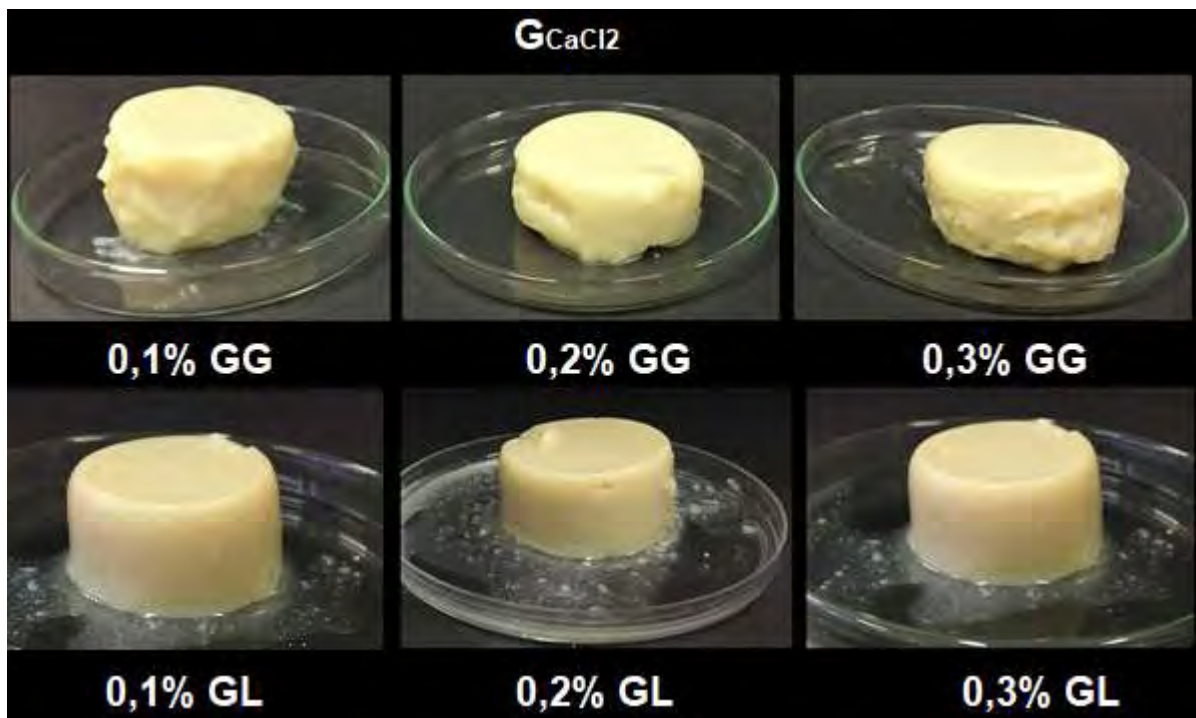
Source: Own authorship.

APPENDIX C - Visual aspect of mixed biopolymeric gels produced using formulation G_{NaCl} and different galactomannans.



Source: Own authorship.

APPENDIX D - Visual aspect of mixed biopolymeric gels produced using formulation G_{CaCl_2} and different galactomannans.



Source: Own authorship.

ANNEXES

ANNEX A – Specification sheet of commercial soy protein isolate, provided by the supplier (Marsul Proteínas LTDA).

PROTIMARTI M-90 - PROTEÍNA ISOLADA DE SOJA

DESCRIÇÃO DO PRODUTO:

Protimarti M-90, proteína isolada de soja, caracteriza-se por suas propriedades funcionais, muito importantes na produção de alimentos: retenção de líquidos, poder estabilizante, melhorias na coloração e na textura, grande poder emulsificante; sua neutralidade não interfere no sabor do produto final. É capaz de manter sua estabilidade funcional em condições adversas (sistemas com alto teor de gordura ou umidade). Além disso, o produto apresenta alto teor proteico, baixo teor de açúcar e ótima digestibilidade. Apresenta capacidade de hidratação, de 1:5, e de emulsão, de 1:6:6.

APLICAÇÃO DO PRODUTO:

Indicado para utilização no processo de fabricação de uma grande variedade de produtos alimentícios, como: pães, bolos, biscoitos, suplementos proteicos, sopas desidratadas, alimentos infantis, massas, alimentos especiais (funcionais e/ou dietéticos). Também, é indicado para utilização em produtos cárneos frescos ou cozidos, embutidos ou não, misturados ou injetados; pode ser adicionado diretamente na massa ou após prévia hidratação ou emulsão, em concentração de 2,0% a 4,0% sobre a massa cárnea, conforme o Regulamento Técnico de Identidade e Qualidade do produto (se aplicado diretamente na massa, é indicado adicionar o produto após a mistura das carnes, do sal e parte do gelo ou água).

CARACTERÍSTICAS DE QUALIDADE:

PARÂMETRO	PADRÃO	METODOLOGIA
Aspecto	pó fino, cor natural	observação visual
Proteína (base seca)	mín. 88,0%	Normas Analíticas - Instituto Adolfo Lutz
Umidade	máx. 8,0%	Normas Analíticas - Instituto Adolfo Lutz
Gordura	máx. 2,0%	Normas Analíticas - Instituto Adolfo Lutz
pH (solução 1%)	6,0 – 8,5	Normas Analíticas - Instituto Adolfo Lutz
Granulometria (retido #100)	máx. 5,0%	Normas Analíticas - Instituto Adolfo Lutz
<i>E. coli</i>	máx. 10 UFC/g	APHA
<i>Bacillus cereus</i> *	máx. 5 x 10 ² UFC/g	EMBRAPA
<i>Salmonella sp.</i> *	ausência em 25g	APHA
* Conforme Resolução RDC nº 12 de 02/01/2001.		

EMBALAGEM:

Embalado em saco de polietileno, revestido por saco de papel multifolhado; peso líquido de 5kg ou 20kg. Também, disponível embalado em saco de polietileno, revestido por saco plástico leitoso; peso líquido de 20kg.

VALIDADE:

Doze meses, a contar da data de fabricação.

ARMAZENAMENTO:

O produto deve ser armazenado em local seco e ventilado, protegido contra roedores e insetos e ao abrigo de luz solar